This electronic thesis or dissertation has been downloaded from the King's Research Portal at https://kclpure.kcl.ac.uk/portal/

KING'S College LONDON

Development of a voxel-based meta-analytic method for neuroimaging studies

Radua, Joaquim

Awarding institution:
King's College London

The copyright of this thesis rests with the author and no quotation from it or information derived from it may be published without proper acknowledgement.

END USER LICENCE AGREEMENT

Unless another licence is stated on the immediately following page this work is licensed

under a Creative Commons Attribution-NonCommercial-NoDerivatives 4.0 International

licence. https://creativecommons.org/licenses/by-nc-nd/4.0/

You are free to copy, distribute and transmit the work

Under the following conditions:

- Attribution: You must attribute the work in the manner specified by the author (but not in any way that suggests that they endorse you or your use of the work).
- Non Commercial: You may not use this work for commercial purposes.
- No Derivative Works - You may not alter, transform, or build upon this work.

Any of these conditions can be waived if you receive permission from the author. Your fair dealings and other rights are in no way affected by the above.

Take down policy

If you believe that this document breaches copyright please contact librarypure@kcl.ac.uk providing details, and we will remove access to the work immediately and investigate your claim.

Download date: 05. May. 2023

This electronic theses or dissertation has been downloaded from the King's Research Portal at https://kclpure.kcl.ac.uk/portal/

KING'S College LONDON

Title: Development of a voxel-based meta-analytic method for neuroimaging studies

Author: Joaquim Radua

The copyright of this thesis rests with the author and no quotation from it or information derived from it may be published without proper acknowledgement.

END USER LICENSE AGREEMENT

This work is licensed under a Creative Commons Attribution-NonCommercial-NoDerivs 3.0 Unported License. http://creativecommons.org/licenses/by-nc-nd/3.0/

You are free to:

- Share: to copy, distribute and transmit the work

Under the following conditions:

- Attribution: You must attribute the work in the manner specified by the author (but not in any way that suggests that they endorse you or your use of the work).
- Non Commercial: You may not use this work for commercial purposes.
- No Derivative Works - You may not alter, transform, or build upon this work.

Any of these conditions can be waived if you receive permission from the author. Your fair dealings and other rights are in no way affected by the above.

Take down policy

If you believe that this document breaches copyright please contact librarypure@kcl.ac.uk providing details, and we will remove access to the work immediately and investigate your claim.

DEVELOPMENT OF A VOXEL-BASED META-ANALYTIC METHOD FOR NEUROIMAGING STUDIES

Thesis submitted for the degree of Doctor of Philosophy

Institute of Psychiatry

King's College London

Joaquim Radua

October 2012

ABSTRACT

The number of neuroimaging studies has grown exponentially in recent years and their results are not always consistent. Meta-analyses are helpful to summarize this vast literature and also offer insights that are not apparent from the individual studies. While a number of suitable voxel-based meta-analytic methods for neuroimaging data had been developed at the time this thesis was conceived, they also suffered from a series of important drawbacks such as the separate analyses of positive (e.g. grey matter volume increases) and negative (e.g. grey matter volume reductions) findings, not accounting for the effect size, not taking sample size, intra-study variance or between-study heterogeneity into account, and not allowing combination of reported peak coordinates and statistical parametric maps.

The aim of this thesis was the development of a series of voxel-based meta-analytic methods and software tools for neuroimaging studies, which overcame some of the limitations of previous methods. Specifically, this thesis includes: a) the development of a new voxel-based meta-analytic method, named *signed differential mapping* (SDM), which adopted and combined the various positive features of previous methods and also introduced a series of improvements and novel features; b) the subsequent development and adaptation of the method to allow addressing additional research questions, such as meta-analyses comparing several disorders, meta-analyses of white matter volume or fractional anisotropy studies, and combination of various imaging modalities; and c) examples of applications of these methods.

The methods and software derived from this thesis have been well received by the field. As of September 2012, more than thirty meta-analyses using SDM have been published, and the first study introducing the methods has been cited more than a hundred times. Suggestions for future research and further methodological development are discussed.

TABLE OF CONTENTS

LIST OF FIGURES

LIST OF TABLES

LIST OF ACRONYMS

ACG	Anterior Cingulate Gyrus
ALE	Activation Likelihood Estimation
ALIC	Anterior Limb of the Internal Capsule
APA	American Psychiatric Association
ASD	Autism Spectrum Disorder
ATR	Anterior Thalamic Radiation
BOLD	Blood Oxygen Level-Dependent
CC	Corpus Callosum
CST	Cortico-Spinal Tract
dMFG	Dorso-Medial Frontal Gyrus
DSM	Diagnostic and Statistical Manual of Mental Disorders
DTI	Diffusion Tensor Imaging
ES-SDM	Effect-Size Signed Differential Mapping
FA	Fractional Anisotropy
FDR	False Discovery Rate
FEP	First Episode of Psychosis
fMRI	Functional Magnetic Resonance Imaging
FSL	FMRIB Software Library
FWE	Family-Wise Error
FWHM	Full Width at Half Maximum
GM	Grey Matter
GMV	Grey Matter Volume
GRF	Gaussian Random Fields
IFOF	Inferior Fronto-Occipital Fasciculus
ILF	Inferior Longitudinal Fasciculus
IPL	Inferior Parietal Lobule
KDA	Kernel Density Analysis
MKDA	Multilevel Kernel Density Analysis
MNI	Montreal Neurological Institute

MOOSE	Meta-analysis Of Observational Studies in Epidemiology
MRI	Magnetic Resonance Imaging
MTG	Middle Temporal Gyrus
NOS	Not Otherwise Specified
OADs	Other Anxiety Disorders
OCD	Obsessive-Compulsive Disorder
PET	Positron Emission Tomography
PDD	Pervasive Developmental Disorder
PLIC	Posterior Limb of the Internal Capsule
PRISMA	Preferred Reporting Items for Systematic reviews and Meta-Analyses
PTSD	Posttraumatic Stress Disorder
PVM	Parametric Voxel-based Meta-analysis
ROI	Region of Interest
sCR	Superior Corona Radiata
SDM	Signed Differential Mapping
SLF	Superior Longitudinal Fasciculus
SPECT	Single Photon Emission Computed Tomography
SPM	Statistical Parametric Mapping
SPSS	Statistical Package for the Social Sciences
SVC	Small Volume Correction
TBSS	Tract-Based Spatial Statistics
UHR	Ultra High Risk (for psychosis)
VBA	Voxel-Based Analysis
VBM	Voxel-Based Morphometry
WASI	Wechsler Abbreviated Scale of Intelligence
WHO	World Health Organization
WM	White Matter
WRAT	Wide Range Achievement Test
YBOCS	Yale–Brown Obsessive–Compulsive Scale

LIST OF PUBLICATIONS DERIVED FROM THIS THESIS

- **Radua J** and Mataix-Cols D. **Meta-analytic methods for neuroimaging data explained**. *Biology of Mood and Anxiety Disorders* 2012; 2:6.

- **Radua J** and Mataix-Cols D. **Voxel-wise meta-analysis of gray matter changes in obsessive-compulsive disorder**. *British Journal of Psychiatry* 2009; 195:391-400.

- **Radua J** and Mataix-Cols D. **Authors' reply: Heterogeneity of coordinate-based meta-analyses of neuroimaging data: an example from studies in OCD**. *British Journal of Psychiatry* 2010; 197:77.

- **Radua J**, Van den Heuvel OA, Surguladze SA and Mataix-Cols D. **Meta-analytical comparison of voxel-based morphometry studies in obsessive-compulsive disorder vs. other anxiety disorders**. *Archives of General Psychiatry* 2010; 67:701-711.

- **Radua J**, Mataix-Cols D, Phillips ML, El-Hage W, Kronhaus DM, Cardoner N and Surguladze S. **A new meta-analytic method for neuroimaging studies that combines reported peak coordinates and statistical parametric maps**. *European Psychiatry* 2012, 27:605-611.

- **Radua J**, Via E, Catani M and Mataix-Cols D. **Voxel-based meta-analysis of regional white-matter volume differences in autism spectrum disorder versus healthy controls**. *Psychological Medicine* 2011; 41:1539-1550.

- Peters BD, Szeszko PR, **Radua J**, Ikuta T, Gruner P, Derosse P, Zhang JP, Giorgio A, Qiu D, Tapert SF, Brauer J, Asato MR, Khong PL, James AC, Gallego JA and Malhotra AK. **White matter development in adolescence: diffusion tensor imaging and meta-analytic results**. *Schizophrenia Bulletin* 2012, 38:1308-1317.

- **Radua J**, Romeo M, Mataix-Cols D, Fusar-Poli P. **A general approach for combining voxel-based meta-analyses conducted in different neuroimaging modalities**. *Current Medicinal Chemistry* 2012; in Press.

- **Radua J**, Borgwardt S, Crescini A, Mataix-Cols D, Meyer-Lindenberg A, McGuire PK, Fusar-Poli P. **Multimodal meta-analysis of structural and functional brain changes in first episode psychosis and the effects of antipsychotic medication**. *Neuroscience and Biobehavioral Reviews* 2012; 36:2325:2333.

LIST OF PUBLISHED STUDIES EMPLOYING SIGNED DIFFERENTIAL MAPPING (CO-AUTHORED BY THE CANDIDATE)

- Bora E, Fornito A, **Radua J**, Walterfang M, Seal M, Wood S, Yucel M, Velakoulis D and Pantelis C. **Neuroanatomical abnormalities in schizophrenia: a multimodal voxelwise meta-analysis and meta-regression analysis**. *Schizophrenia Research* 2011, 127:46-57.

- Via E, **Radua J**, Cardoner N, Happe F and Mataix-Cols D. **Meta-analysis of gray matter abnormalities in Autism Spectrum Disorder**. *Archives of General Psychiatry* 2011, 68:409-418.

- Nakao T, **Radua J**, Rubia K and Mataix-Cols D. **Gray matter volume abnormalities in ADHD: Voxel-based meta-analysis exploring the effects of age and stimulant medication**. *American Journal of Psychiatry* 2011, 168:1154-1163.

- Fusar-Poli P, **Radua J**, McGuire P and Stefan B. **Neuroanatomical maps of psychosis onset: Voxel-wise meta-analysis of antipsychotic-naive VBM studies**. *Schizophrenia Bulletin* 2012; 38:1297:1307.

- Palaniyappan L, Balain V, **Radua J** and Liddle PF. **Structural correlates of auditory hallucinations in schizophrenia: a meta-analysis**. *Schizophrenia Research* 2012; 137:169-73.

- Hart H, **Radua J**, Nakao T, Mataix-Cols D, Rubia K. **Meta-analysis of fMRI studies of inhibition and attention in ADHD: exploring task-specific, stimulant medication and age effects**. *Archives of General Psychiatry* 2012; in Press.

- Hart H, **Radua J**, Mataix-Cols D, Rubia K. **Meta-analysis of fMRI studies of timing in attention deficit hyperactivity disorder (ADHD)**. *Neuroscience and Biobehavioral Reviews* 2012; 36:2248:2256.

LIST OF OTHER PUBLISHED STUDIES USING SIGNED DIFFERENTIAL MAPPING (NOT CO-AUTHORED BY THE CANDIDATE)

- Bora E, Fornito A, Yücel M and Pantelis C. **Voxelwise meta-analysis of gray matter abnormalities in bipolar disorder**. *Biological Psychiatry* 2010; 67:1097-1105.

- Chen Z and Ma L. **Grey matter volume changes over the whole brain in amyotrophic lateral sclerosis: A voxel-wise meta-analysis of voxel based morphometry studies**. *Amyotrophic Lateral Sclerosis* 2010; 11:549-554.

- Richlan F, Kronbichler M and Wimmer H. **Meta-analyzing brain dysfunctions in dyslexic children and adults**. *Neuroimage* 2011; 56:1735-42.

- Lai CH. **Gray matter deficits in panic disorder: a pilot study of meta-analysis**. *Journal of Clinical Psychopharmacology* 2011; 31:287-93.

- Bora E, Fornito A, Pantelis and Yücel M. **Gray matter abnormalities in Major Depressive Disorder: a meta-analysis of voxel based morphometry studies**. *Journal of Affective Disorders* 2011; 138:9-18.

- Li J, Pan P, Song W, Huang R, Chen K and Shang H. **A meta-analysis of diffusion tensor imaging studies in amyotrophic lateral sclerosis**. *Neurobiology of Aging* 2011; 33:1833-8.

- Pan PL, Song W and Shang HF. **Voxel-wise meta-analysis of gray matter abnormalities in idiopathic Parkinson's disease**. *European Journal of Neurology* 2011; 19:199-206.

- Bora E, Fornito A, Yücel M and Pantelis C. **The effects of gender on grey matter abnormalities in major psychoses: a comparative voxelwise meta-analysis of schizophrenia and bipolar disorder**. *Psychological Medicine* 2011; 42:295-307.

- Murphy ML and Frodl T. **Meta-analysis of diffusion tensor imaging studies shows altered fractional anisotropy occurring in distinct brain areas in association with depression**. *Biology of Mood and Anxiety Disorders* 2011; 1:3.

- Frodl T and Skokauskas N. **Meta-analysis of structural MRI studies in children and adults with attention deficit hyperactivity disorder indicates treatment effects**. *Acta Psychiatrica Scandinavica* 2012; 125:114-26.

- Fusar-Poli P. **Voxel-wise meta-analysis of fMRI studies in patients at clinical high risk for psychosis**. *Journal of Psychiatry and Neuroscience* 2012; 37:106-12.

- Li J, Pan P, Huang R and Shang H. **A meta-analysis of voxel-based morphometry studies of white matter volume alterations in Alzheimer's disease**. *Neuroscience and Biobehavioral Reviews* 2012; 36:757-63.

- Fusar-Poli P, Smieskova R, Serafini G, Politi P and Borgwardt S. **Neuroanatomical markers of genetic liability to psychosis and first episode psychosis: A voxelwise meta-analytical comparison**. *World Journal of Biological Psychiatry* 2012; in Press, available online 27 January 2012, doi: 10.3109/15622975.2011.630408.

- Richlan F, Kronbichler M and Wimmer H. **Structural abnormalities in the dyslexic brain: A meta-analysis of voxel-based morphometry studies**. *Human Brain Mapping* 2012; in Press, available online 19 June 2012, doi: 10.1002/hbm.22127.

- Pan PL, Song W, Yang J, Huang R, Chen K, Gong QY, Zhong JG, Shi HC and Shang HF. **Gray matter atrophy in behavioral variant frontotemporal dementia: a meta-analysis of voxel-based morphometry studies**. *Dementia and Geriatric Cognitive Disorders* 2012; 33:141-8.

- Palaniyappan L, Balain V and Liddle PF. **The neuroanatomy of psychotic diathesis: A meta-analytic review**. *Journal of Psychiatric Research* 2012; 46:1249-56.

- Bohrn IC, Altmann U and Jacobs AM. **Looking at the brains behind figurative language - A quantitative meta-analysis of neuroimaging studies on metaphor, idiom, and irony processing**. *Neuropsychologia* 2012; 50:2669-83.

ACKNOWLEDGEMENTS

Most importantly, I would like to thank my first supervisor, Professor David Mataix-Cols, as well as to the other researchers who also guided me through the different stages of my PhD study, Drs Alberto Pertusa, Simon Surguladze, Narcís Cardoner and Edith Pomarol-Clotet. It is only through their help that this PhD project has been possible. David, you have been the best supervisor anyone could ever wish, and I will always be indebted with you for that. Thank you with all my heart.

Also, this thesis would not have been possible without the help and support of my beloved wife Marga, my brother Roger, my sister-in-law Angeliki and my parents Josep and Mercè.

My thanks also go to my colleagues and fellow researchers (Drs Alonso, Alonso-Lana, Alonso-Villaverde, Alvarez, Amann, Andreo, Anguera-Camós, Artigas, Asato, Balain, Bañeras, Bora, Borgwardt, Bosch, Brammer, Bramon, Brauer, Brittain, Bullich, Canales-Rodríguez, Carulla, Casas, Cases-Viedma, Castellanos, Catani, Collier, Cooper, Crescini, Crow, Dalgleish, David, de Diego-Adeliño, de Quintana, Derosse, El-Hage, Ellison-Wright, Farré, Fernandez de la Cruz, Fernandez-Villar, Fornito, Frascarelli, Fullana, Fung, Fusar-Poli, Gallego, Garcia, García-Luján, Garcia-Olivé, Giampietro, Giorgio, Gironell, Gispert, Gohier, Goikolea, Gomar, Gómez-Ansón, Grau, Gruner, Gutiérrez, Happe, Hart, He, Herance, Ikuta, Jaafari, James, Kalidindi, Khong, Knowles, Kronhaus, Landín-Romero, Lansley, Lawrence, Lawrie, Liddle, López-

Vilanova, Madre, Malhotra, Marshall, McDonald, McGuire, Mckenna, Mechelli, Meléndez, Menchón, Meyer-Lindenberg, Milham, Molet, Monsó, Monté, Moreno, Morera, Murray, Nakao, Núñez-Delgado, Ortiz-Gil, Palaniyappan, Palomar, Pan, Panicali, Pantelis, Pérez, Pérez-Egea, Peters, Phillips, Porta, Portella, Powell, Prata, Proitsi, Puigdemont, Qiu, Quidé, Quintana, Ramos-Quiroga, Reichenberg, Ribasés, Rodríguez, Romeo, Rosell, Rubia, Ruiz-Manzano, Ruiz-Ripoll, Russell, Salavert, Salgado-Pineda, Salvador, Sanz-Santos, Sarró, Sastre-Garriga, Sato, Seal, Segalas, Serra, Stephan-Otto, Szeszko, Tapert, Vallejo, Valls, van den Eynde, van den Heuvel, Velakoulis, Via, Vicens, Vieta, Villalta-Gil, Walshe, Walterfang, Wood, Wooderson, Yücel, Zelaya, Zhang), and to anyone else who has helped me along the way but whom I have failed to mention.

CHAPTER 1

Introduction:

Meta-analytic methods for neuroimaging data

The number of neuroimaging studies has grown exponentially in recent years. However, findings from different studies may sometimes be difficult to integrate into a coherent picture. Inconsistent results are not uncommon. Furthermore, a few influential studies might often eclipse robust findings from other studies. In other words, we may at times not see the forest for the trees. In this context, meta-analyses are helpful to combine and summarize the data of interest and potentially offer insights that are not immediately apparent from the individual studies.

This introductory chapter aims to describe the main methods which have been used to summarize the results of neuroimaging studies, as well as their advantages and drawbacks. Section 1.1 introduces how a standard meta-analysis is conducted, that is, when there is only one variable of interest, with an example from a meta-analysis of global brain volumes. This is important for a better appreciation of the pros and cons of the meta-analytic methods

reviewed later. Section 1.2 describes the meta-analyses of neuroimaging studies based on regions of interest (ROI) and their particular issues. Finally, section 1.3 introduces the various available voxel-based meta-analytic methods, which aim to overcome some of the limitations of the ROI-based methods but have, in turn, their own limitations. Note that this review includes methods available up to the point this thesis was conceived. Other methods have since become available and will be exposed later, in the final chapter.

Chapters 1 and 8 were partially published in *Biology of Mood & Anxiety Disorders* under the title '*Meta-analytic methods for neuroimaging data explained*' (Joaquim Radua and David Mataix-Cols 2012; 2:6).

The definitive publisher-authenticated version is available online at http://www.biolmoodanxietydisord.com/content/2/1/6 License is appended at the end of this Chapter.

1.1 STANDARD META-ANALYSES

Prior to any meta-analytic calculation, researchers conduct an exhaustive and critical literature search, often including contact with the authors of the original studies in order to retrieve important pieces of missing information. Then, researchers conduct a mathematical summary of the findings of the included studies (that is, the meta-analysis proper). Finally, researchers apply a series of tests, plots and subgroup analyses to assess the heterogeneity and robustness of the results. The latter step, along with the exhaustive and critical inclusion of studies, is of utmost importance in order to obtain unbiased meta-analytic conclusions.

With the aim of introducing the logics of a standard meta-analysis, a meta-analysis of global grey matter volumes in patients with obsessive-compulsive disorder (OCD) is used in this section as an example (see **Table 1.1**). The included studies correspond to seven publications reporting global grey matter volume, which would be included in a published meta-analysis of voxel-based morphometry studies in OCD (see Chapter 2).

1.1.1 Weighting of the studies

In order to summarize these 7 studies, a simple meta-analysis could consist of calculating the *mean difference* in global grey matter volume between patients

Table 1.1 Global grey matter volumes in seven studies on OCD.

	Patients		Controls		Patients + controls		Difference		Effect size	
	N	Volume ± SD	N	Volume ± SD	N	Variance	Estimate	Variance	Estimate	Variance
Study 1	18	773 ± 56	18	822 ± 56	36	3,114	-49	346	-0.854	0.122
Study 2	55	685 ± 74	50	708 ± 72	105	5,323	-23	203	-0.313	0.039
Study 3	25	850 ± 83	25	834 ± 71	50	5,997	+16	480	0.196	0.080
Study 4	72	739 ± 82	72	763 ± 78	144	6,404	-24	178	-0.298	0.028
Study 5	37	776 ± 69	26	747 ± 68	63	4,680	+29	307	0.418	0.067
Study 6	19	827 ± 44	15	836 ± 63	34	3,041	-9	363	-0.179	0.120
Study 7	71	740 ± 66	71	738 ± 63	142	4,119	+2	116	0.035	0.028

All volumes are in milliliters. Study 1: by Carmona *et al.* (2007). Study 2: by van den Heuvel *et al.* (2009). Study 3: by Kim *et al.* (2001). Study 4: by Pujol *et al.* (2004). Study 5: by Szeszko *et al.* (2008). Study 6: by Valente *et al.* (2005). Study 7: by Yoo *et al.* (2008)

and controls as reported in the original studies (Mulrow and Oxman 1996). Thus, **Table 1.1** could be summarized by saying that the mean global grey matter volume is 8.4 mL smaller in patients than in healthy controls – this number is just the arithmetic mean of the differences shown in the table.

The use of the arithmetic mean, however, may be too simplistic, because the different studies should have different weights. For example, the number of patients in study 4 is four times larger than the number of patients in study 1. Clearly, more weight should be given to study 4. Probably, it should be given about four times more weight, as it includes four times as many patients.

Weighting the mean difference by the sample sizes of the studies, one would conclude that the mean global grey matter volume is 8.8 mL smaller in patients than in controls. Note that when we previously calculated the mean difference as the simple arithmetic mean, we were indeed assuming that all the studies had the same sample size. This erroneous assumption had only a minor effect here (we thought that the difference was about 5% smaller than what we

think now), but it could have important effects in other meta-analyses, especially if studies with smaller sample sizes *inexplicably* find more differences than studies with larger sample sizes – methods for detecting this kind of bias are introduced later.

Unfortunately, weighting the calculations *only* by sample size would still be too simplistic, because the weight of a study should also include its precision. For example, study 1 included fewer patients than study 4, but its volume estimates seem more precise, as its sample variance is approximately the half than that in study 4 (see *Patients + controls* column in **Table 1.1**). The reason for this higher precision is usually unknown (maybe the sample was more homogenous; maybe the technical procedures were cleaner; maybe it was just chance); however, this precision must be taken into account by weighting by the inverse of the *variance of the difference* – which also includes the sample size.

Weighting the mean difference by the inverse of the variance of the difference, one would conclude that the mean global grey matter volume is 8.9 mL smaller in patients than in controls (z-value = -1.55, P = 0.121). When previously we did not weight by sample variance we were assuming that all the studies had the same variance, though in this case this assumption was acceptable because the variance of the studies is rather homogeneous.

However, as explained in the next section, weighting the calculations *only* by the inverse of the variance of the difference may *still* be too simplistic.

1.1.2 Heterogeneity within studies

Healthy individuals have different global grey matter volumes, that is, some have larger brains, some have thicker cortices, and so on. When conducting an analysis with original data, researchers are usually able to explain or model a part of this variability, but there is also a part of this variability that remains unexplained. This residual error may be due to unobserved variables, etiological heterogeneity within particular diagnoses, poor model fitting, or maybe just pure chance. This individual-based *within-study* variability cause the sample means to be variable, so that different studies obtain different results.

However, *within-study* variability is not the only source of the *between-study* variability or heterogeneity. Given the relatively small amount of robust findings in neuroimaging, it would be highly desirable that all researchers conducted their studies using the exact same inclusion criteria and methods so that all *between-study* variability was only related to the *within-study* variability. However, the fact is that clinical and methodological differences between studies are often substantial.

On the one hand, patients included in the individual studies may have been sampled from clinically different populations; for example, one study of major depressive disorder may include outpatients with mild reactive depressive episodes while another study may be focused on inpatients suffering from severe endogenous depressions with melancholic symptoms. Similarly, patients in different studies may be receiving different treatments, or be in different

phases of the disorder (for example, having a first episode or having a history of multiple episodes).

On the other hand, researchers may have been investigated similar but still different aspects of a disorder; for example, one study may have described the *blood oxygen level-dependent* (BOLD) brain response to a task involving a high memory load, while another study may be interest in the BOLD response to a task related to decision-making. Or even if studying the same particular cognitive function, each study may employ a particular statistical package, and its large set of associated assumptions.

Finally, there may be a relevant part of the between-study heterogeneity which can be neither related to the within-study variability, nor explained by known clinical or methodological differences between studies. This is called residual heterogeneity.

It is highly recommended to study the between-study variability or heterogeneity in any meta-analysis. For example, if the main analysis detects differences between patients and controls, it may be of interest to explore whether these differences depend on the severity of the disorder, or if they are related to special subtypes of the disorder. These questions may be assessed with meta-regressions. But even if the meta-analysis does not aim to explore the modulating effects of clinical variables on the main outcomes, heterogeneity should *still* be taken into account.

Indeed, there is agreement on always including the residual heterogeneity in the weighting of the calculations (DerSimonian and Laird 1986;

Figure 1.1 Forest (left) and funnel (right) plots of the mean differences in global grey matter volume between patients with obsessive-compulsive disorder and healthy controls (using a random-effects model).

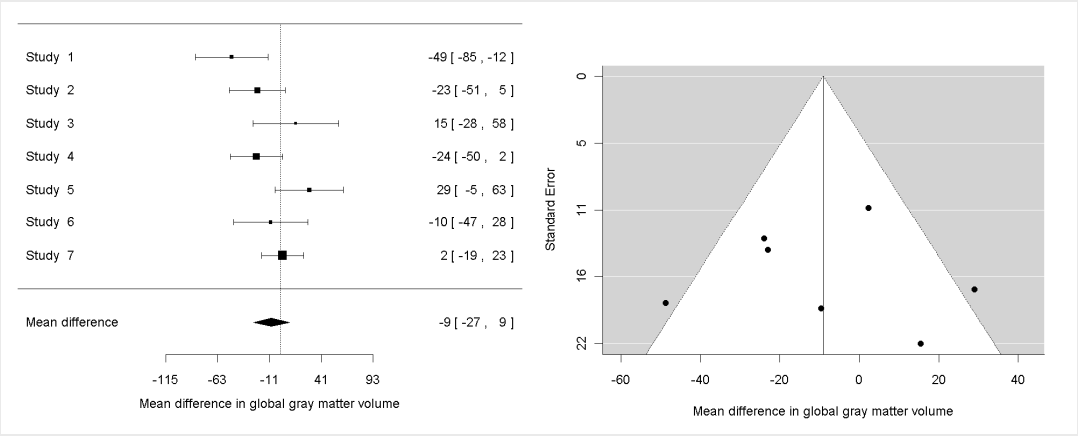

On the funnel plot, the included studies appear to be symmetrically distributed on either side of the mean difference, suggesting no publication bias towards positive or negative studies.

Fleiss and Gross 1991; Ades and Higgins 2005; Viechtbauer 2005). Meta-analyses conducted this way are said to follow *random-effects* models, in opposition to the *fixed-effects* models presented in the previous section, which did not include heterogeneity. In the example of **Table 1.1**, the use of a random-effects model would lead us to conclude that the mean global grey matter volume is 9.0 mL smaller in patients than in controls (*z*-value = -0.98, *P* = 0.328; see **Figure 1.1, left**). Note the increase of *P*-value in the random-effects model (from 0.121 to 0.328), thus better controlling the false positive rate.

1.1.3 Other complementary analyses

Some complementary plots and tests are recommended to help the reader assess the reliability and robustness of the findings (Elvik 1998).

On the one hand, the meta-regressions may be useful for assessing if the findings are predominantly (or only) present in one group of patients, for example, in those with more severe forms of OCD. In this regard, specific meta-analyses of subgroups of patients may further confirm these hypotheses or, also important, may state that the abnormalities are present in all subgroups of patients, increasing the robustness of the findings. Similarly, sensitivity analyses consisting of repeating the meta-analysis many times, each time with a different combination of studies, may be useful to assess whether the findings are driven by one or few studies. Finally, funnel plots (see **Figure 1.1, right**) may be useful for appraising whether studies with small samples report more statistically significant findings than studies with larger samples. This is typical of study areas that are prone to publication bias, where studies with small samples are only published if their results match *a priori* hypotheses.

It is important to note that these kinds of tests and graphical aids are necessary but do not provide conclusive information, and should only be interpreted in the context of the field under investigation. A symmetrical funnel plot, for example, is not an amulet against publication bias, especially in some types of meta-analysis. ROI-based studies, for instance, may be more prone to be affected by publication biases, as the authors may decide which brain regions are reported and which are not. Conversely, an asymmetrical funnel plot would not necessarily invalidate a meta-analysis if publication bias appears unlikely. This may be the case of voxel-based studies, where the whole brain is included in the analysis.

Figure 1.2 Forest (left) and funnel (right) plots of the effect size of the differences in global grey matter volume between patients with obsessive-compulsive disorder and healthy controls (using a random-effects model).

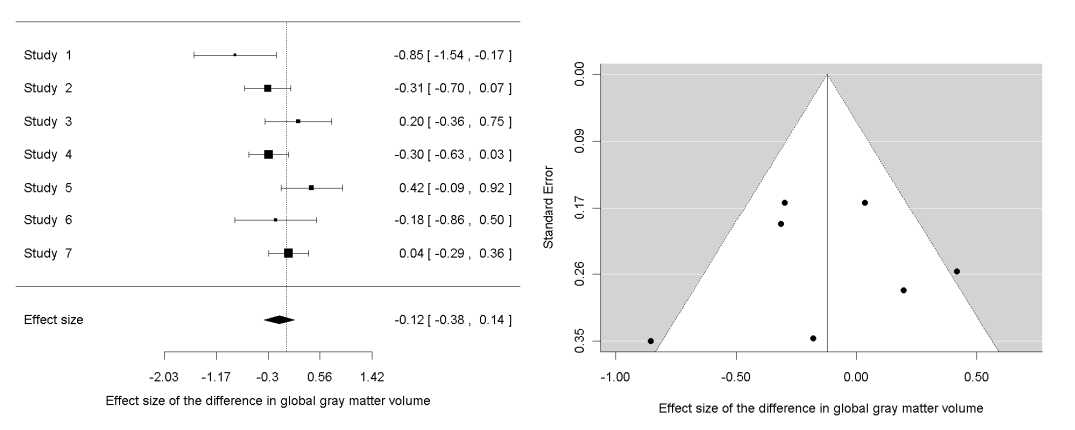

On the funnel plot, the included studies appear to be symmetrically distributed on either side of the mean difference, suggesting no publication bias towards positive or negative studies.

1.1.4 Use of effect sizes

Most meta-analyses do not use the *raw* volume differences as in the OCD example but, rather, they use *standardized* volume differences, that is, *effect sizes* (Hedges and Olkin 1985). Briefly, in structural neuroimaging studies, a *raw* difference is the difference in millilitres between patients' and controls' global grey matter volume, while a *standardized* difference is the difference in standard deviations – usually corrected for small sample size bias.

This subtle difference has a series of consequences. First, the unit of measure (millilitres, in this case) is lost, which makes the interpretation of the findings less straightforward but indeed more comparable with other measures, for example, an effect size of d = 0.5 is considered 'medium' independently of whether it refers to a difference in grey matter volume, in BOLD response or in

a questionnaire score. Using the data from **Table 1.1**, the effect size of the difference in global grey matter volume between patients and controls is d = -0.122 (*z*-value = -0.93, *P* = 0.354; see **Figure 1.2**), which is below the conventional range of 'small' effect (0.2 to 0.3) (Cohen 1988). Second, a study reporting a larger difference may be found to have a smaller effect size, or vice versa, depending on the sample variance. For instance in **Table 1.1**, the raw difference is slightly larger in study 4 than in study 3, whilst the effect size is slightly larger in study 3 than in study 4. Third, and very important, the effect size can be directly derived from many statistics like a *t*-value or a *P*-value, which are much more often reported than sample statistics; that is, meta-analytic researchers can often know the effect size but not the raw difference. This advantage usually allows a much more exhaustive inclusion of studies, thus clearly justifying the use of effect sizes in many meta-analyses.

1.2 META-ANALYSES BASED ON REGIONS OF INTEREST

A ROI is a part of the brain that the authors of the study wish to investigate, usually based on *a priori* hypotheses. ROI-based studies usually select a set of few ROIs and manually delimitate them on the raw images. Researchers then analyze the volume of these ROIs, their mean BOLD response to a stimulus, their positron emission tomography (PET) ligand volume of distribution, or any other measure of interest.

1.2.1 ROI-based meta-analyses

A typical ROI-based meta-analysis can be viewed as a set of different meta-analyses, each of them applied to a different ROI. These meta-analyses can usually be optimally conducted with all appropriate weightings and complementary analyses, as seen for example in the meta-analysis of regional brain volumes in OCD conducted by Rotge *et al.* (2009), in which the analyses are based on effect sizes and random-effects models and complemented with explicit assessments of the heterogeneity, several sensitivity analyses, funnel plots and meta-regressions. Unfortunately, each original study included in this meta-analysis only investigated a small set of brain regions, causing the meta-analyses to include only a very small number of studies for each brain region. Indeed, only three or four studies could be included for highly relevant regions in contemporary biological models of the disorder, such as the putamen or the

anterior cingulate cortex. Other brain regions could not be meta-analyzed because they had been investigated by too few or no studies. Needless to say, this would not be the case for those ROI studies reporting whole brain results in online supplements or similar, but this is seldom the case.

Moreover, it must be noted that some brain regions are more frequently studied than others, which causes the statistical power to differ depending on the brain region under study. In the example (Rotge, Guehl et al. 2009), while data from five studies or more were available for the orbitofrontal cortex, the thalamus and the caudate nuclei, some brain regions could not be meta-analyzed at all.

Ultimately, the authors of the original studies have a set of *a priori* hypotheses which influence their decision to investigate differences in a given brain region at the expense of other regions. These decisions determine the number of studies investigating that brain region, and thus the statistical power to detect that brain region as significantly different between patients and controls in a ROI-based meta-analysis. Publication bias is also a problem as studies failing to report statistically significant differences on hypothesized ROIs may be less likely to ever be become publicly available. A recent analysis of more than 450 ROI-based neuroimaging studies in psychiatry illustrates this point well (Ioannidis 2011). The author demonstrated that the number of studies reporting significant results was nearly the double than expected, suggesting strong publication biases in the ROI literature.

Another consideration is the heterogeneous definition or the boundaries of the ROIs, which may differ from one study to the other (Rotge, Guehl et al. 2009). However, this variability might have a relatively small impact on effect sizes, as boundary definitions are the same for the patients and controls included in each study. Furthermore, the spatial error may probably be counteracted by the higher anatomical accuracy achieved by the manual delimitation of the ROIs in the original studies (Uchida, Del-Ben et al. 2008; Bergouignan, Chupin et al. 2009).

1.2.2 Label-based reviews

Some authors have used a simplified type of ROI-based meta-analysis, consisting of just counting how many times a particular ROI is detected as significantly abnormal in patients versus healthy controls. This procedure has been called label-based review (Laird, McMillan et al. 2005). For example, in their functional neuroimaging meta-analysis of the brain's response to emotional tasks, Phan *et al.* (2002) represented each activation peak as a dot in an atlas of the brain. They then divided the brain into twenty ROIs and counted how many studies had one or more activation peaks in each ROI.

A fictitious example of such approach is shown in **Figure 1.3A**. Here, the studies would have reported that the patients with mood or anxiety disorders have increases of grey matter volume in the basal ganglia, extending to the anterior part of the right insula, as well as decreases of grey matter volume in the anterior cingulate and insular cortices. The authors of a label-based review

would have first plotted the peaks of the clusters of significant increase (red) or decrease (blue) of grey matter volume in a brain template. Then, they would divide the brain into several regions, for example, anterior cingulate gyrus, left and right inferior frontal gyri, insulas, superior temporal gyri, caudate nuclei, putamen nuclei, and so on. Finally, they would have counted how many peaks lay within each of these regions.

This method may be useful when other approaches are not feasible, for example when not enough information is available for conducting a ROI-based or a voxel-based meta-analysis. Its simplicity, however, may conceal a series of important drawbacks which must be taken into account. First, no weighting of the studies is performed, which means that all studies are assumed to have the same sample size and precision. This is a strong and unrealistic assumption which may be violated in most meta-analyses. Fortunately, sample size information is always available, and so label-based meta-analyses should at least be weighted by sample size. Second, the findings of the studies are binarized (significant versus not-significant), leading to a loss of information on the magnitude of the raw differences or on the effect sizes. Third, it is not clear whether studies reporting opposite findings in a particular ROI (for example, volume decrease in some studies and volume increase in others) are adequately dealt with. Finally, they may be also affected by the particular issues of ROI-based meta-analyses described above.

Figure 1.3 Summary of label-based reviews and the main voxel-based meta-analytic methods available at the time the current thesis was conceived.

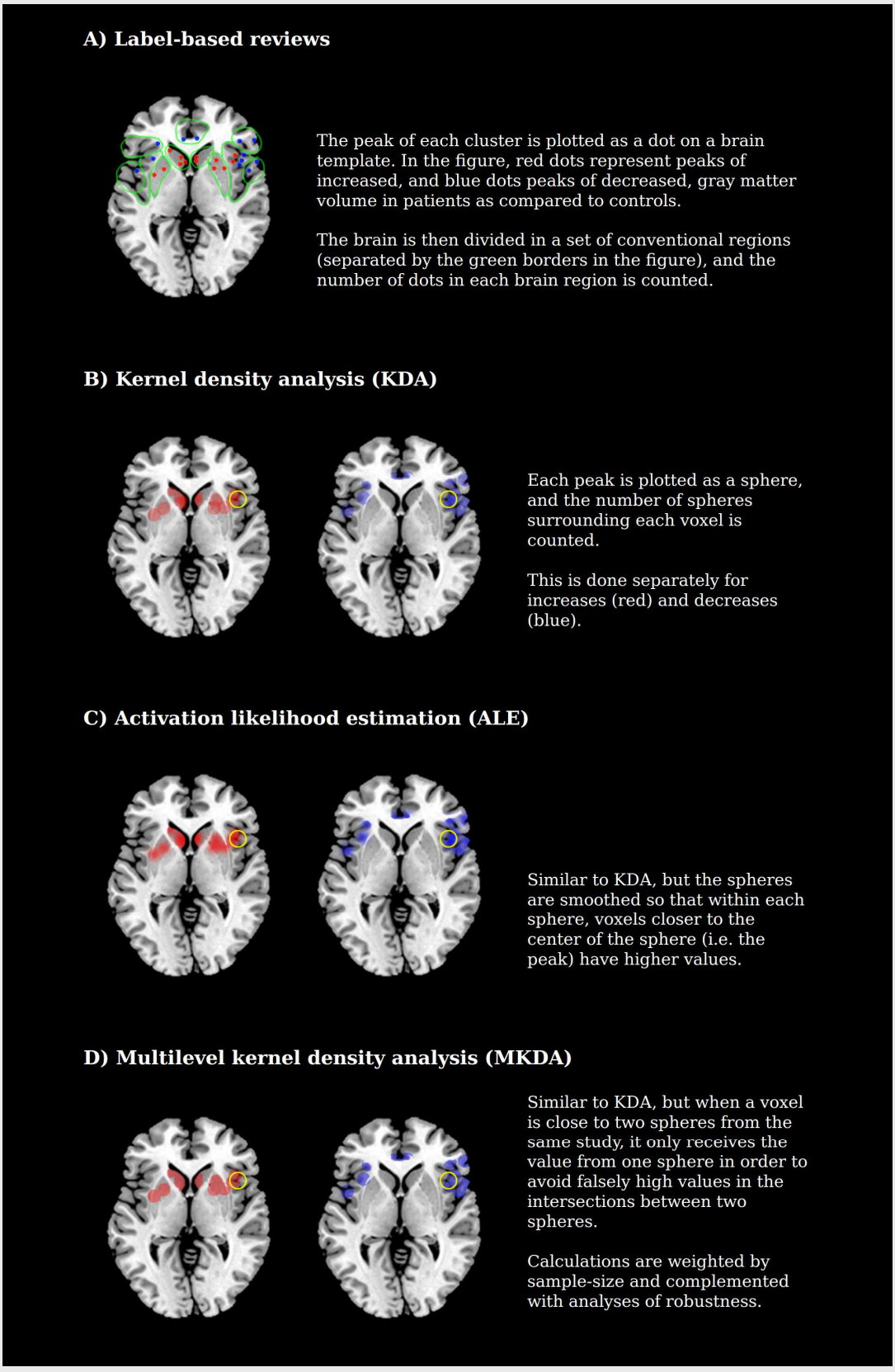

1.3 VOXEL-BASED META-ANALYSES

Scanner three-dimensional images are composed of thousands of tiny cubes (or rectangular cuboids) called voxels, in the same way that digital photographs are composed of thousands of tiny squares called pixels. Voxel-based methods consist of conducting the meta-analytic calculations separately in each voxel of the brain, thus freeing the meta-analysis from aprioristic anatomical definitions. There are two different types of voxel-based meta-analyses, including image-based and coordinate-based meta-analyses.

1.3.1 Image-based meta-analyses

An image-based meta-analysis should be understood as a voxel-based version of the standard meta-analysis, that is, it consists of thousands of standard meta-analyses, each of them applied to a different voxel (Lazar, Luna et al. 2002). The data of each study is retrieved from its statistical parametric maps (the three-dimensional images resulting from the comparison between patients and controls), and thus include the whole brain. This technique shares some limitations with any voxel-based analysis, mainly relating to the massive number of statistical tests (that is, one test for each voxel). The correction of multiple comparisons is an unsolved issue, with current methods being either too liberal or too conservative. For this reason, thresholds based on uncorrected *P*-values and cluster-size are usually preferred (Wager, Lindquist et al. 2007). Also, such

massive-scale testing prevents a careful visual inspection of the analyses (for example, to describe relevant non-significant trends).

However, the biggest drawback of image-based meta-analyses is that the statistical parametric maps of the original studies are seldom available, therefore seriously limiting the inclusion of studies.

1.3.2 Coordinate-based meta-analyses

Given the poor availability of statistical parametric maps, early meta-analyses of voxel-based studies consisted of label-based (rather than image-based) reviews, as discussed earlier. These methods quickly evolved to coordinate-based meta-analyses, which in their simplest form consisted of counting, for each voxel, how many activation peaks had been reported within its surroundings (Wager, Phan et al. 2003). In the fictitious example, the dots of the label-based review (**Figure 1.3A**) would be replaced with spheres (**Figure 1.3B**, **C**), and the brain would not be divided into conventional regions but rather the number of spheres touching each voxel would be counted, thus obtaining a count for each voxel. It must be noted that calculations in *activation likelihood estimate* (ALE) (Turkeltaub, Eden et al. 2002) are not exactly based on counting the number of spheres but on computing the probability of a union, though in practice, the latter behaves like the former.

The use of voxels rather than conventional divisions of the brain improved the anatomical localization of the findings. However, the first available

methods, namely ALE and *kernel density analysis* (KDA) (Wager, Phan et al. 2003), had some additional issues which enlarged the list of drawbacks of label-based reviews. Specifically, they only counted the total number of peaks, independently of whether they came from the same or different studies, and thus the analysis could not be weighted by sample size and a single study reporting many peaks in close proximity could drive the findings of the whole meta-analysis.

These drawbacks led to the creation of a second generation of coordinate-based meta-analytic methods, mainly evolved versions of KDA, such as *multilevel KDA* (MKDA) (Wager, Barrett et al. 2007), as well as evolved versions of ALE (Ellison-Wright, Ellison-Wright et al. 2008), which overcame these limitations by separating the peaks of each study. Moreover, some of these new methods weighted the studies by their sample size and included a series of complementary analyses to assess the reliability and robustness of the findings. However, as detailed in the next section, these methods still had several relevant issues.

1.4 LIMITATIONS OF EXISTING VOXEL-BASED METHODS

As shown in the previous section, there are two different types of voxel-based meta-analyses: those based on statistical parametric maps (i.e. images), and those based on the reported peak coordinates. Image-based meta-analyses are based on well-established statistical models and tests, but the images of the original studies are seldom available, therefore seriously limiting the inclusion of studies.

Coordinate-based meta-analyses are more feasible, as they only require the reported peak coordinates. However, these coordinate-based methods are statistically more limited.

First, it is not clear whether studies reporting opposite findings in a particular ROI (for example, volume decrease in some studies and volume increase in others) are adequately dealt with. This is an important limitation as a particular voxel may erroneously appear to be positive (e.g. increased volume or BOLD) and negative (e.g. decreased volume or BOLD) at the same time, as seen in some published meta-analyses (Menzies, Chamberlain et al. 2008).

Second, some methods do not perform weighting of the studies and may indeed only count the total number of peaks, which means that a single study reporting many peaks in close proximity may drive the findings of the whole analysis, and that all studies are assumed to have the same sample size and

precision. This is a strong and unrealistic assumption which may be violated in most meta-analysis.

Finally, the findings of the studies are binarized (“significant” versus “not-significant”), leading to a loss of information on the magnitude of the raw differences or on the effect sizes and preventing relevant complementary analyses such as meta-regression.

1.5 OVERALL AIM OF THE CURRENT THESIS

As discussed in the previous section, at the time this thesis was conceived, the available voxel-based meta-analytical methods had important limitations. The main drive for this thesis was the development of a new meta-analytical method named *signed differential mapping* (SDM), that would adopt and combine the various positive features of the existing methods, but also introduce a series of improvements and novel features. Thus, the main aim was to develop and validate a method that would overcome some of these limitations. Subsequently, the method evolved and progressively incorporated new features, culminating in a new version of SDM called *effect-size signed differential mapping* (ES-SDM). Each of these incremental steps is summarised in the next section and will constitute a separate chapter of this thesis.

1.6 STRUCTURE OF THE THESIS

This PhD thesis incorporates publications. This is an alternative route for submission of PhD thesis under new regulations of King's College London (revised July 2011). Each chapter of this thesis therefore corresponds to one (or two) published paper. The published papers in final pfd format appear in the **Appendix 3**. For the purpose of this thesis, each paper has been reformatted so that the methods are presented first and the practical application of each method is illustrated with the use of an example. Thus, the appearance of the thesis is similar to a traditional PhD thesis.

CHAPTER 2 details the development of the new voxel-based meta-analytic method, *signed differential mapping* (SDM). It also includes a practical application of the method to study the regional grey matter volume in patients with obsessive-compulsive disorder (OCD). This study was published in the *British Journal of Psychiatry* under the title *"Voxel-wise meta-analysis of grey matter changes in obsessive-compulsive disorder"* (Joaquim Radua and David Mataix-Cols 2009; 195:393-402). At the time of submission of this thesis, this paper has received 89 citations in Scopus and 116 in Google Scholar.

CHAPTER 3 describes the generalization of the method to allow more complex statistical models such as comparisons between more than two groups or inclusion of covariates. It also includes a practical application of these models to study the regional grey matter volume in various anxiety disorders. This study was published in the *Archives of General Psychiatry* under the title *"Meta-analytical comparison of voxel-based morphometry studies in obsessive-compulsive disorder vs. other anxiety disorders"* (Joaquim Radua, Odile A. van den Heuvel, Simon Surguladze and David Mataix-Cols 2010; 67:701-711). At the time of submission, this paper has received 35 citations in Scopus and 59 in Google Scholar.

CHAPTER 4 details an improved version of the method, *effect-size signed differential mapping* (ES-SDM), which can combine coordinates and statistical parametric maps and uses standard meta-analytic statistics. It also includes an empirical validation of the method. This study was published in *European Psychiatry* under the title *"A new meta-analytic method for neuroimaging studies that combines reported peak coordinates and statistical parametric maps"* (Joaquim Radua, David Mataix-Cols, Mary L. Phillips, Wissam El-Hage, Dina M. Kronhaus, Narcís Cardoner and Simon Surguladze 2012; 27:605-611). At the time of submission, this paper has received 14 citations in Google Scholar.

CHAPTER 5 describes the adaptation of the SDM method for meta-analyzing white matter images. It also includes a practical application of the adapted method to study the regional white matter volume in the autism spectrum disorders (ASD). This study was published in *Psychological Medicine* under the title *"Voxel-based meta-analysis of regional white matter volume differences in autism spectrum disorder vs. healthy controls"* (Joaquim Radua, Esther Via, Marco Catani and David Mataix-Cols 2011; 41:1539-1550). At the time of submission, this paper has received 10 citations in Scopus and 26 in Google Scholar.

CHAPTER 6 describes the adaptation of the ES-SDM method for meta-analyzing Tract-Based Spatial Statistics (TBSS) Fractional Anisotropy (FA) images. It also includes a practical application of the adapted method to study the regional white matter development in adolescence. This meta-analysis was published as a companion study of an analysis of original data in *Schizophrenia Bulletin* under the title *"White matter development in adolescence: diffusion tensor imaging and meta-analytic results"* (Bart D. Peters, Philip R. Szeszko, Joaquim Radua, Toshikuza Ikuta, Patricia Gruner, Pamela Derosse, et al 2012; 38:1308-1317).

CHAPTER 7 describes an approach for combining voxel-based meta-analyses involving different neuroimaging modalities, e.g. grey matter volume and functional response to attention tasks. It also includes an application of the

method to study such abnormalities in patients with a first episode of psychosis. The method for combining meta-analyses conducted in different modalities was accepted for publication in *Current Medicinal Chemistry* under the title "*A general approach for combining voxel-based meta-analyses conducted in different neuroimaging modalities*" (Joaquim Radua, Margarita Romeo, David Mataix-Cols and Paolo Fusar-Poli 2012; in Press). The application of the method was published in *Neuroscience & Biobehavioral Reviews* under the title *"Multimodal meta-analysis of structural and functional brain changes in first episode psychosis and the effects of antipsychotic medication"* (Joaquim Radua, Stefan Borgwardt, Alessandra Crescini, David Mataix-Cols, Andreas Meyer-Lindenberg, Philip K. McGuire, Paolo Fusar-Poli 2012; 36:2325:2333).

Finally, **CHAPTER 8** offers the general conclusions, as well as the strengths and limitations of the meta-analytic set of methods included in the thesis. This chapter also exposes other developments in the field since the time the thesis was first conceived. Suggestions for future research are also included.

The **APPENDICES 1, 2 and 3** include screenshots of the SDM software, an SDM tutorial, screenshots of the SDM Project website, and a copy of the published papers.

1.7 REFERENCES

Ades, A. E. and J. P. T. Higgins (2005). "The interpretation of random-effects meta-analysis in decision models." Medical Decision Making **25**(6): 646-654.

Bergouignan, L., M. Chupin, et al. (2009). "Can voxel based morphometry, manual segmentation and automated segmentation equally detect hippocampal volume differences in acute depression?" Neuroimage **45**(1): 29-37.

Carmona, S., N. Bassas, et al. (2007). "Pediatric OCD structural brain deficits in conflict monitoring circuits: a voxel-based morphometry study." Neurosci Lett **421**(3): 218-223.

Cohen, J. (1988). Statistical Power Analysis for the Behavioral Sciences, Lawrence Erlbaum Associates.

DerSimonian, R. and N. Laird (1986). "Meta-analysis in clinical trials." Control Clin Trials **7**(3): 177-188.

Ellison-Wright, I., Z. Ellison-Wright, et al. (2008). "Structural brain change in Attention Deficit Hyperactivity Disorder identified by meta-analysis." BMC.Psychiatry **8**: 51.

Elvik, R. (1998). "Evaluating the statistical conclusion validity of weighted mean results in meta-analysis by analysing funnel graph diagrams." Accid Anal Prev **30**(2): 255-266.

Fleiss, J. L. and A. J. Gross (1991). "Meta-analysis in epidemiology, with special reference to studies of the association between exposure to environmental tobacco smoke and lung cancer: A critique." Journal of Clinical Epidemiology **44**(2): 127-139.

Hedges, L. V. and I. Olkin (1985). Statistical Methods for Meta-Analysis. Orlando, Academic Press.

Ioannidis, J. P. A. (2011). "Excess significance bias in the literature on brain volume abnormalities." Arch Gen Psychiatry **68**(8): 773-780.

Kim, J. J., M. C. Lee, et al. (2001). "Grey matter abnormalities in obsessive-compulsive disorder: statistical parametric mapping of segmented magnetic resonance images." Br J Psychiatry **179**: 330-334.

Laird, A. R., K. M. McMillan, et al. (2005). "A comparison of label-based review and ALE meta-analysis in the Stroop task." Hum Brain Mapp **25**(1): 6-21.

Lazar, N. A., B. Luna, et al. (2002). "Combining Brains: A Survey of Methods for Statistical Pooling of Information." Neuroimage **16**(2): 538-550.

Menzies, L., S. R. Chamberlain, et al. (2008). "Integrating evidence from neuroimaging and neuropsychological studies of obsessive-compulsive disorder: the orbitofronto-striatal model revisited." Neurosci Biobehav Rev **32**(3): 525-549.

Mulrow, C. D. and A. D. Oxman (1996). Cochrane Collaboration Handbook. Oxford, Cochrane Collaboration.

Phan, K. L., T. Wager, et al. (2002). "Functional neuroanatomy of emotion: a meta-analysis of emotion activation studies in PET and fMRI." Neuroimage **16**(2): 331-348.

Pujol, J., C. Soriano-Mas, et al. (2004). "Mapping structural brain alterations in obsessive-compulsive disorder." Arch Gen Psychiatry **61**(7): 720-730.

Rotge, J. Y., D. Guehl, et al. (2009). "Meta-analysis of brain volume changes in obsessive-compulsive disorder." Biol Psychiatry **65**(1): 75-83.

Szeszko, P. R., C. Christian, et al. (2008). "Gray Matter Structural Alterations in Psychotropic Drug-Naive Pediatric Obsessive-Compulsive Disorder: An Optimized Voxel-Based Morphometry Study." Am J Psychiatry **165**(10): 1299-1307.

Turkeltaub, P. E., G. F. Eden, et al. (2002). "Meta-analysis of the functional neuroanatomy of single-word reading: method and validation." Neuroimage **16**(3 Pt 1): 765-780.

Uchida, R. R., C. M. Del-Ben, et al. (2008). "Correlation between voxel based morphometry and manual volumetry in magnetic resonance images of the human brain." An Acad Bras Cienc **80**(1): 149-156.

Valente, A. A., Jr., E. C. Miguel, et al. (2005). "Regional gray matter abnormalities in obsessive-compulsive disorder: a voxel-based morphometry study." Biol Psychiatry **58**(6): 479-487.

van den Heuvel, O. A., P. L. Remijnse, et al. (2009). "The major symptom dimensions of obsessive-compulsive disorder are mediated by partially distinct neural systems." Brain **132**(Pt 4): 853-868.

Viechtbauer, W. (2005). "Bias and efficiency of meta-analytic variance estimators in the random-effects model." Journal of Educational and Behavioral Statistics **30**(3): 261-293.

Wager, T. D., L. Barrett, et al. (2007). The neuroimaging of emotion. Handbook of Emotions. New York, Guilford. **3rd ed**.

Wager, T. D., M. Lindquist, et al. (2007). "Meta-analysis of functional neuroimaging data: current and future directions." Soc Cogn Affect Neurosci **2**(2): 150-158.

Wager, T. D., K. L. Phan, et al. (2003). "Valence, gender, and lateralization of functional brain anatomy in emotion: a meta-analysis of findings from neuroimaging." Neuroimage **19**(3): 513-531.

Yoo, S. Y., M. S. Roh, et al. (2008). "Voxel-based morphometry study of gray matter abnormalities in obsessive-compulsive disorder." J Korean Med Sci **23**(1): 24-30.

Creative Commons

Attribution 2.0

CREATIVE COMMONS CORPORATION IS NOT A LAW FIRM AND DOES NOT PROVIDE LEGAL SERVICES. DISTRIBUTION OF THIS LICENSE DOES NOT CREATE AN ATTORNEY-CLIENT RELATIONSHIP. CREATIVE COMMONS PROVIDES THIS INFORMATION ON AN "AS-IS" BASIS. CREATIVE COMMONS MAKES NO WARRANTIES REGARDING THE INFORMATION PROVIDED, AND DISCLAIMS LIABILITY FOR DAMAGES RESULTING FROM ITS USE.

License

THE WORK (AS DEFINED BELOW) IS PROVIDED UNDER THE TERMS OF THIS CREATIVE COMMONS PUBLIC LICENSE ("CCPL" OR "LICENSE"). THE WORK IS PROTECTED BY COPYRIGHT AND/OR OTHER APPLICABLE LAW. ANY USE OF THE WORK OTHER THAN AS AUTHORIZED UNDER THIS LICENSE OR COPYRIGHT LAW IS PROHIBITED.

BY EXERCISING ANY RIGHTS TO THE WORK PROVIDED HERE, YOU ACCEPT AND AGREE TO BE BOUND BY THE TERMS OF THIS LICENSE. THE LICENSOR GRANTS YOU THE RIGHTS CONTAINED HERE IN CONSIDERATION OF YOUR ACCEPTANCE OF SUCH TERMS AND CONDITIONS.

1. Definitions

a. **"Collective Work"** means a work, such as a periodical issue, anthology or encyclopedia, in which the Work in its entirety in unmodified form, along with a number of other contributions, constituting separate and independent works in themselves, are assembled into a collective whole. A work that constitutes a Collective Work will not be considered a Derivative Work (as defined below) for the purposes of this License.
b. **"Derivative Work"** means a work based upon the Work or upon the Work and other pre-existing works, such as a translation, musical arrangement, dramatization, fictionalization, motion picture version, sound recording, art reproduction, abridgment, condensation, or any other form in which the Work may be recast, transformed, or adapted, except that a work that constitutes a Collective Work will not be considered a Derivative Work for the purpose of this License. For the avoidance of doubt, where the Work is a musical composition or sound recording, the synchronization of the Work in timed-relation with a moving image ("synching") will be considered a Derivative Work for the purpose of this License.
c. **"Licensor"** means the individual or entity that offers the Work under the terms of this License.
d. **"Original Author"** means the individual or entity who created the Work.
e. **"Work"** means the copyrightable work of authorship offered under the terms of this License.
f. **"You"** means an individual or entity exercising rights under this License who has not previously violated the terms of this License with respect to the Work, or who has received express permission from the Licensor to exercise rights under this License despite a previous violation.

2. Fair Use Rights. Nothing in this license is intended to reduce, limit, or restrict any rights arising from fair use, first sale or other limitations on the exclusive rights of the copyright owner under copyright law or other applicable laws.

3. License Grant. Subject to the terms and conditions of this License, Licensor hereby grants You a worldwide, royalty-free, non-exclusive, perpetual (for the duration of the applicable copyright) license to exercise the rights in the Work as stated below:

a. to reproduce the Work, to incorporate the Work into one or more Collective Works, and to reproduce the Work as incorporated in the Collective Works;
b. to create and reproduce Derivative Works;
c. to distribute copies or phonorecords of, display publicly, perform publicly, and perform publicly by means of a digital audio transmission the Work including as incorporated in Collective Works;
d. to distribute copies or phonorecords of, display publicly, perform publicly, and perform publicly by means of a digital audio transmission Derivative Works.
e. For the avoidance of doubt, where the work is a musical composition:
    i. **Performance Royalties Under Blanket Licenses.** Licensor waives the exclusive right to collect, whether individually or via a performance rights society (e.g. ASCAP, BMI, SESAC), royalties for the public performance or public digital performance (e.g. webcast) of the Work.
    ii. **Mechanical Rights and Statutory Royalties.** Licensor waives the exclusive right to collect, whether individually or via a music rights agency or designated agent (e.g. Harry Fox Agency), royalties for any phonorecord You create from the Work ("cover version") and distribute, subject to the compulsory license created by 17 USC Section 115 of the US Copyright Act (or the equivalent in other jurisdictions).
f. **Webcasting Rights and Statutory Royalties.** For the avoidance of doubt, where the Work is a sound recording, Licensor waives the exclusive right to collect, whether individually or via a performance-rights society (e.g. SoundExchange), royalties for the public digital performance (e.g. webcast) of the Work, subject to the compulsory license created by 17 USC Section 114 of the US Copyright Act (or the equivalent in other jurisdictions).

The above rights may be exercised in all media and formats whether now known or hereafter devised. The above rights include the right to make such modifications as are technically necessary to exercise the rights in other media and formats. All rights not expressly granted by Licensor are hereby reserved.

4. Restrictions. The license granted in Section 3 above is expressly made subject to and limited by the following restrictions:

a. You may distribute, publicly display, publicly perform, or publicly digitally perform the Work only under the terms of this License, and You must include a copy of, or the Uniform Resource Identifier for, this License with every copy or phonorecord of the Work You distribute, publicly display, publicly perform, or publicly digitally perform. You may not

offer or impose any terms on the Work that alter or restrict the terms of this License or the recipients' exercise of the rights granted hereunder. You may not sublicense the Work. You must keep intact all notices that refer to this License and to the disclaimer of warranties. You may not distribute, publicly display, publicly perform, or publicly digitally perform the Work with any technological measures that control access or use of the Work in a manner inconsistent with the terms of this License Agreement. The above applies to the Work as incorporated in a Collective Work, but this does not require the Collective Work apart from the Work itself to be made subject to the terms of this License. If You create a Collective Work, upon notice from any Licensor You must, to the extent practicable, remove from the Collective Work any reference to such Licensor or the Original Author, as requested. If You create a Derivative Work, upon notice from any Licensor You must, to the extent practicable, remove from the Derivative Work any reference to such Licensor or the Original Author, as requested.

b. If you distribute, publicly display, publicly perform, or publicly digitally perform the Work or any Derivative Works or Collective Works, You must keep intact all copyright notices for the Work and give the Original Author credit reasonable to the medium or means You are utilizing by conveying the name (or pseudonym if applicable) of the Original Author if supplied; the title of the Work if supplied; to the extent reasonably practicable, the Uniform Resource Identifier, if any, that Licensor specifies to be associated with the Work, unless such URI does not refer to the copyright notice or licensing information for the Work; and in the case of a Derivative Work, a credit identifying the use of the Work in the Derivative Work (e.g., "French translation of the Work by Original Author," or "Screenplay based on original Work by Original Author"). Such credit may be implemented in any reasonable manner; provided, however, that in the case of a Derivative Work or Collective Work, at a minimum such credit will appear where any other comparable authorship credit appears and in a manner at least as prominent as such other comparable authorship credit.

5. Representations, Warranties and Disclaimer

UNLESS OTHERWISE MUTUALLY AGREED TO BY THE PARTIES IN WRITING, LICENSOR OFFERS THE WORK AS-IS AND MAKES NO REPRESENTATIONS OR WARRANTIES OF ANY KIND CONCERNING THE WORK, EXPRESS, IMPLIED, STATUTORY OR OTHERWISE, INCLUDING, WITHOUT LIMITATION, WARRANTIES OF TITLE, MERCHANTIBILITY, FITNESS FOR A PARTICULAR PURPOSE, NONINFRINGEMENT, OR THE ABSENCE OF LATENT OR OTHER DEFECTS, ACCURACY, OR THE PRESENCE OF ABSENCE OF ERRORS, WHETHER OR NOT DISCOVERABLE. SOME JURISDICTIONS DO NOT ALLOW THE EXCLUSION OF IMPLIED WARRANTIES, SO SUCH EXCLUSION MAY NOT APPLY TO YOU.

6. Limitation on Liability. EXCEPT TO THE EXTENT REQUIRED BY APPLICABLE LAW, IN NO EVENT WILL LICENSOR BE LIABLE TO YOU ON ANY LEGAL THEORY FOR ANY SPECIAL, INCIDENTAL, CONSEQUENTIAL, PUNITIVE OR EXEMPLARY DAMAGES ARISING OUT OF THIS LICENSE OR THE USE OF THE WORK, EVEN IF LICENSOR HAS BEEN ADVISED OF THE POSSIBILITY OF SUCH DAMAGES.

7. Termination

a. This License and the rights granted hereunder will terminate automatically upon any breach by You of the terms of this License. Individuals or entities who have received Derivative Works or Collective Works from You under this License, however, will not have their licenses terminated provided such individuals or entities remain in full compliance with those licenses. Sections 1, 2, 5, 6, 7, and 8 will survive any termination of this License.

b. Subject to the above terms and conditions, the license granted here is perpetual (for the duration of the applicable copyright in the Work). Notwithstanding the above, Licensor reserves the right to release the Work under different license terms or to stop distributing the Work at any time; provided, however that any such election will not serve to withdraw this License (or any other license that has been, or is required to be, granted under the terms of this License), and this License will continue in full force and effect unless terminated as stated above.

8. Miscellaneous

a. Each time You distribute or publicly digitally perform the Work or a Collective Work, the Licensor offers to the recipient a license to the Work on the same terms and conditions as the license granted to You under this License.

b. Each time You distribute or publicly digitally perform a Derivative Work, Licensor offers to the recipient a license to the original Work on the same terms and conditions as the license granted to You under this License.

c. If any provision of this License is invalid or unenforceable under applicable law, it shall not affect the validity or enforceability of the remainder of the terms of this License, and without further action by the parties to this agreement, such provision shall be reformed to the minimum extent necessary to make such provision valid and enforceable.

d. No term or provision of this License shall be deemed waived and no breach consented to unless such waiver or consent shall be in writing and signed by the party to be charged with such waiver or consent.

e. This License constitutes the entire agreement between the parties with respect to the Work licensed here. There are no understandings, agreements or representations with respect to the Work not specified here. Licensor shall not be bound by any additional provisions that may appear in any communication from You. This License may not be modified without the mutual written agreement of the Licensor and You.

Creative Commons is not a party to this License, and makes no warranty whatsoever in connection with the Work. Creative Commons will not be liable to You or any party on any legal theory for any damages whatsoever, including without limitation any general, special, incidental or consequential damages arising in connection to this license. Notwithstanding the foregoing two (2) sentences, if Creative Commons has expressly identified itself as the Licensor hereunder, it shall have all rights and obligations of Licensor.

Except for the limited purpose of indicating to the public that the Work is licensed under the CCPL, neither party will use the trademark "Creative Commons" or any related trademark or logo of Creative Commons without the prior written consent of Creative Commons. Any permitted use will be in compliance with Creative Commons' then-current trademark usage guidelines, as may be published on its website or otherwise made available upon request from time to time.

Creative Commons may be contacted at http://creativecommons.org/.

CHAPTER 2

Development of a novel coordinate-based meta-analysis method for neuroimaging studies

2.1 THEORY

2.1.1 The method of signed differential mapping

As we have seen in Chapter 1, neuroimaging studies report, from each cluster of significant differences, the coordinates of the 'voxel' (i.e. the 3-dimensional pixel) where the difference between the patients and the healthy controls is maximum. The basic idea behind early voxel-based meta-analytic methods was 'counting', for each voxel, how many times it is close 'enough' to the reported maxima and subsequently associating a probability to test the statistical significance. In other words, are there more studies reporting coordinates near that voxel than would be expected by chance? As reviewed in Chapter 1, at the time this thesis was conceived, two different methods were available to perform meta-analyses of neuroimaging data: *activation likelihood estimate* (ALE)

Figure 2.1 Main features of the signed differential mapping (SDM) method for voxel-based meta-analysis of neuroimaging data

Features adapted from the activation likelihood estimate (ALE) (Turkeltaub, Eden et al. 2002)

a. The value assigned to each voxel is higher as the voxel is closer to the original coordinate.

Features adapted from multilevel kernel density analysis (MKDA) (Wager, Lindquist et al. 2007)

a. Voxel values are limited to be as high as the voxel at the coordinate of a maximum in order to avoid biases towards studies reporting various coordinates in close proximity.
b. Meta-analytic values are estimates of the values in the population of studies, unlike previous mathematically inconsistent estimators.
c. Meta-analytic values are weighted by the sample size of the studies, i.e. large samples contribute more.

Novel features of SDM

a. Only those coordinates which are significant at the whole-brain level are included in order to avoid biases towards a priori brain regions.
b. Coordinates from analyses with correction for multiple comparisons are preferred.
c. The full-width at half maximum of the kernel is set at 25 mm in order to control for false-positive results.
d. Both positive and negative coordinates are reconstructed in the same map in order to avoid that a particular voxel can erroneously appear to be positive and negative at the same time.
e. The new descriptive analysis of quartiles overcomes the unclear contribution of studies reporting no differences in the standard randomisation test.
f. Analyses of subgroups are expanded and regression is introduced for clinical quantitative variables in order to better analyse the methodological and clinical heterogeneity of the included studies.

Limitations (of all existing methods)

a. Only summarised data (i.e. coordinates) are included from the studies – an analysis using all the raw data from the included studies would probably be more accurate.
b. The breakdown of a cluster should not be understood as 'all these regions are abnormal' but as 'one or more of these regions are abnormal', because normal brain regions close to abnormal brain regions may artificially appear to be abnormal.

(Turkeltaub, Eden et al. 2002) and *multilevel kernel density analysis* (MKDA) (Wager, Lindquist et al. 2007). These two methods differ in a number of important ways and each has their own strengths and limitations. This chapter describes a new approach, *signed differential mapping* (SDM), which adopts and combines the various positive features of these two methods. In addition, SDM introduces a series of improvements and novel features that are summarised in **Figure 2.1** and explained in detail below.

Figure 2.2 A fictitious example of meta-analytic bias due to inclusion of studies with regionally heterogeneous thresholds

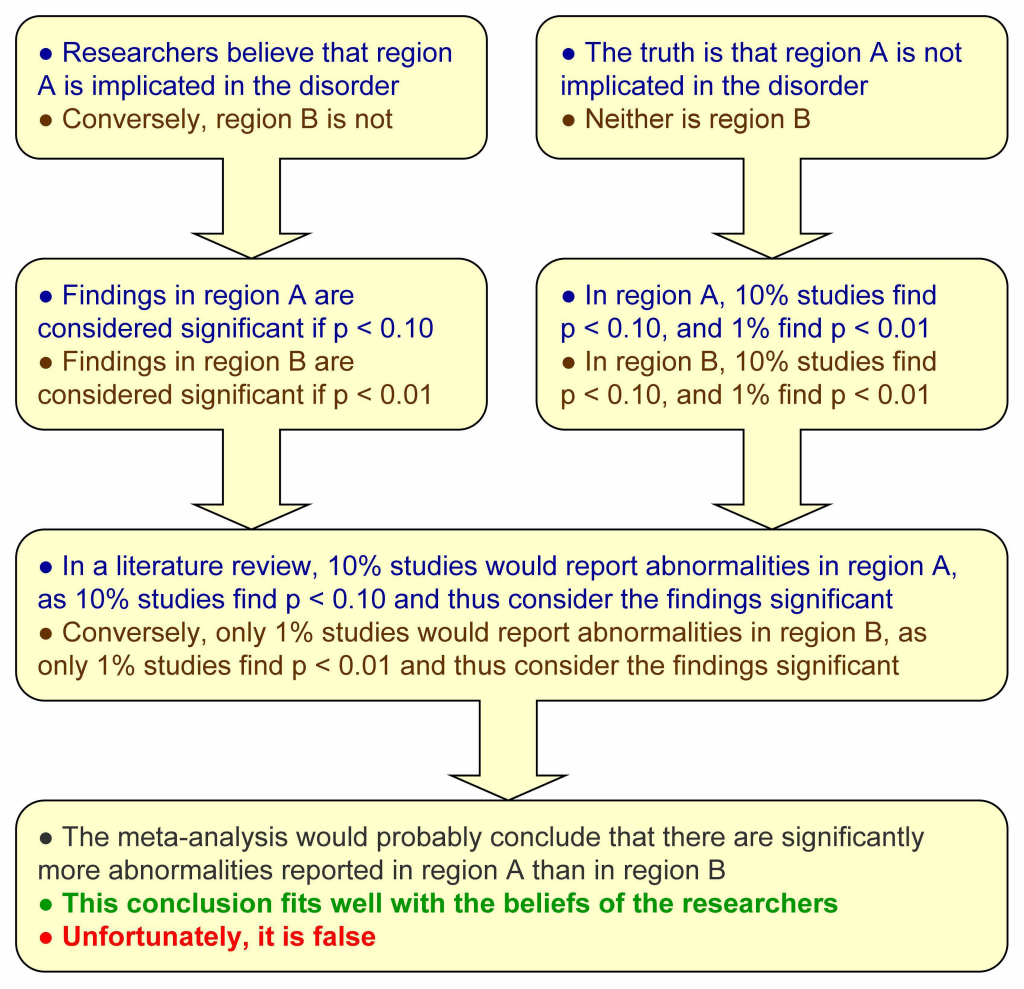

The first improvement introduced by SDM is a stricter selection of the reported peak coordinates to ensure that only regions that appear statistically significant at the *whole-brain* level are considered for inclusion in the meta-analysis. This strict criterion is intended to avoid biases towards liberally thresholded brain regions because it is not uncommon in neuroimaging studies that the statistical threshold for some *regions of interest* is rather more liberal than for the rest of the brain. A fictitious example of such a bias is shown in **Figure 2.2**.

Another improvement related to the selection of peak coordinates is the systematic preference for results that are corrected for multiple comparisons. SDM establishes the following order of preference: a) whole-brain analyses with correction for multiple comparisons and at least one statistically significant coordinate; b) whole-brain analyses without correction for multiple comparisons and at least one statistically significant coordinate; c) whole-brain analyses with no statistically significant coordinates; d) if none of (a)–(c) apply, the study is discarded.

Inclusion of analyses without correction for multiple comparisons does not bias the probability of finding significant results because the statistical analysis controls for the number of coordinates as described below. Coordinates reported in MNI (Montreal Neurological Institute) space are converted to Talairach space using the matrix transformations proposed by Lancaster (Lancaster, Tordesillas-Gutierrez et al. 2007), which have been shown to be more exact than earlier methods (Brett 1999). Coordinates reported in Talairach space which had been converted using earlier methods, are converted back to MNI space and subsequently converted to Talairach space using the matrix transformations.

Once the coordinates are selected and converted, a map of the differences in grey matter is separately recreated for each study. This consists of assigning a value to the voxels close to each of the reported coordinates within a grey matter map (based on the Talairach Daemon (Lancaster, Woldorff et al. 2000), voxel size 2 x 2 x $2m^3$). SDM uses a 25 mm full-width at half maximum (FWHM) un-normalised Gaussian kernel:

$$K(D_{ij}) = \exp\left(-\frac{4 \cdot \log(2)}{FWHM^2} \cdot D_{ij}^2\right)$$

where K is the un-normalized Gaussian kernel, *FWHM* is the full width at half maximum, and D_{ij} is the distance between the i^{th} voxel and the j^{th} peak (D_{ij} = 0 in the voxel containing the j^{th} peak).

It must be noted that this kernel is different in nature from the smoothing kernel used to smooth raw magnetic resonance images, since it is not intended to smooth any image but to assign indicators of proximity to reported coordinates. This kernel is adapted from that of ALE and preferred to that of MKDA because it assigns a higher value to the voxels closer to the reported coordinates. Full-width at half maximum is set at 25 mm because in previous simulations was found to have an excellent control of false positives – consistent with this simulation work, a study reported that the optimal FWHM for the previous methods was about 15-30mm (Salimi-Khorshidi, Smith et al. 2009).

When a voxel can be assigned values from more than one coordinate in the same study these values are summed. An important downside of the sum of values is a bias towards studies reporting various coordinates in close proximity, as voxels can achieve rather large values (Wager, Lindquist et al. 2007). Multilevel kernel density analysis elegantly overcomes this problem by limiting the values within one study to a maximum and SDM also incorporates

this feature. Thus, the value of each voxel is calculated as a restricted sum of the values given by the distances to its surrounding peaks:

$$SDM_{ik} = \sum_j S_j K(D_{ij}), \quad SDM_i \in [-1,1]$$

where SDM_{ik} is the SDM value of the ith voxel in the kth study, S_j is the sign of the jth peak (positive for increases, negative for decreases), D_{ij} is the distance between the ith voxel and the jth peak of the kth study, and K( ) is the un-normalized Gaussian kernel.

A novelty of the method is that both positive and negative coordinates (i.e. both increases and decreases of grey matter) are reconstructed in the same map, resulting in a signed differential map. This is an important feature that prevents a particular voxel erroneously appearing to be positive (i.e. increased volume or activation) and negative (i.e. decreased volume or activation) at the same time. This problem is often seen in published studies using previous methods, e.g. (Menzies, Chamberlain et al. 2008).

Once all the studies have their signed differential map created, a meta-analytic signed differential map is calculated. It must be noted that individual signed differential maps do not account for the variability within each study, indeed this is not reported, so that usual meta-analytic calculations are not applicable. However, MKDA overcomes this issue by defining the meta-analytic

value of a voxel as the proportion of studies reporting a coordinate around the voxel (weighted by the squared root of the sample size of each study so that studies with larger samples contribute more). Thus, the question to answer at each voxel is – *are there more studies reporting coordinates around that voxel than would be expected by chance?* SDM calculates the mean instead of the proportion of studies, although the meaning does not change:

$$SDM_i = \sum_k w_k \cdot SDM_{ik}, \quad w_k = \frac{\sqrt{n_k}}{\sum_{k'} \sqrt{n_{k'}}}$$

where SDM_i is the meta-analytic SDM value of the i^{th} voxel, SDM_{ik} is the SDM value of the i^{th} voxel in the k^{th} study, w_k is the weight of the k^{th} study, and n_k is the patient sample size of the k^{th} study.

Finally, a null distribution of the meta-analytic values is created to test which voxels have more studies reporting differences of grey matter around them than expected by chance. This is performed by means of Monte Carlo randomisations of the location of the coordinates (within a mask of grey matter plus 8 mm of white matter). The null distribution is generated at the whole-brain level to maximise statistical stability with relatively reduced computation time (almost 40 million values are obtained with 500 randomisations). It is recommended that researchers focus on results with uncorrected $p < 0.001$ because previous simulations showed that uncorrected $p < 0.001$ or even 0.002

was, in this method, empirically equivalent to FDR-corrected $p < 0.05$. However, researchers could also formally correct for multiple comparisons by means of the false discovery rate (Genovese, Lazar et al. 2002).

2.1.2 Descriptive analysis of quartiles

The standard randomisation test described above checks if there are more studies reporting coordinates in a particular region than in the rest of the brain. However, this information might be incomplete without describing the actual proportion of studies reporting coordinates in the region (e.g. it is not the same that half of the studies report changes in a particular region than if only 5% do). To overcome this issue, a descriptive analysis of quartiles is conducted, e.g. values higher than 0 in the second quartile (median) map mean that at least 50% of the studies found increases of grey matter near the voxel. Once again, the calculations are weighted by the square root of the sample size to make the studies with large samples contribute more.

2.1.3 Sensitivity analysis

In order to test the replicability of the results, a systematic whole-brain voxel-based jack-knife sensitivity analysis is conducted. This consists of repeating the main statistical analysis many times but discarding one different study each time, i.e. removing one study and repeating the analyses, then putting that study back and removing another study and repeating the analysis, and so on.

The rationale of this test is that if a previously significant brain region remains significant in all or most of the combinations of studies it can be concluded that this finding is highly replicable.

2.1.4 Analyses of subgroups

In order to control for any possible methodological differences observed between the studies, the analysis is repeated several times including only those studies which are methodologically homogenous.

2.1.5 Meta-regression

The potential effect of several relevant sociodemographic and clinical variables is examined by means of linear regression, weighted by the squared root of the sample size and restricted to only predict possible SDM values (i.e. from -1 to 1) in the observed range of values of the variable:

$$SDM_{i0} = -\frac{\sum_k w_k \cdot \left(x_k \cdot \overline{wX} - \overline{wX^2}\right) \cdot SDM_{ik}}{\overline{wX^2} - \overline{wX}^2}$$

$$SDM_{i\beta} = \frac{\sum_k w_k \cdot \left(x_k - \overline{wX}\right) \cdot SDM_{ik}}{\overline{wX^2} - \overline{wX}^2}$$

$$SDM_{i1} = SDM_{i0} + SDM_{i\beta}$$

$$\overline{wX} = \sum_k w_k x_k , \quad \overline{wX^2} = \sum_k w_k x_k^2$$

where SDM_{i0} is the meta-analytic SDM value of the ith voxel corresponding to the minimum value of the modulator (e.g. minimum age), SDM_{i1} is the meta-analytic SDM value of the ith voxel corresponding to the maximum value of the modulator (e.g. maximum age), $SDM_{i\beta}$ is the difference between SDM_{i0} and SDM_{i1}, w_k is the weight of the kth study, x_k is the value of the modulator in the kth study, and SDM_{ik} is the SDM value of the ith voxel in the kth study.

It must be noted that the statistical significance of the findings derived from meta-regressions may be sometimes overshadowed by the abnormalities revealed in the main between-group analysis, for what more conservative thresholds are strongly recommended (see section 2.2.2.3). This issue is further expanded in the context of the general linear model presented in Chapter 3.

2.1.6 Computational aspects

Software for all the computations was developed by means of a C language program with a GTK graphical interface (http://www.gtk.org/). The original Ubuntu GNU/Linux (http://www.ubuntu.com/) version, as well as other operative system adapted versions is freely available at http://www.sdmproject.com/software .

2.2 EXAMPLE: APPLICATION OF THE METHOD

To illustrate the practical uses of the new SDM method, this section describes a meta-analysis of voxel-based morphometry studies in *obsessive-compulsive disorder* (OCD).

This study was published in the *British Journal of Psychiatry* under the title '*Voxel-wise meta-analysis of grey matter changes in obsessive-compulsive disorder*' (Joaquim Radua and David Mataix-Cols 2009; 195:393-402). This is an author-produced electronic version of an article accepted for publication in the British Journal of Psychiatry. The definitive publisher-authenticated version is available online at http://bjp.rcpsych.org

2.2.1 Introduction

Current neuroanatomical models of OCD propose that specific cortico-striato-thalamic circuits are involved in the mediation of its symptoms, but structural neuroimaging studies have only produced mixed evidence to support these models. It is not uncommon for different studies to report increased or reduced grey matter volumes in the same brain regions. For example, the volume of caudate nucleus has been reported to be decreased (Robinson, Wu et al. 1995), normal (Aylward, Harris et al. 1996) or increased (Scarone, Colombo et al. 1992) in OCD patients vs. healthy controls. These inconsistencies can be partially attributed to the inclusion of small and heterogeneous samples of

participants with OCD, and also to substantial methodological differences between studies. Many morphometric studies in OCD have used manual (therefore subjective) or semi-automated methods to measure the volumes of brain regions defined *a priori* as being implicated in OCD, therefore preventing the exploration of other brain regions potentially implicated in the disorder. The recent development of fully-automated, whole-brain voxel-based morphometry methods (Ashburner and Friston 2000; Ashburner and Friston 2001; Mechelli, Price et al. 2005), which overcome some of the limitations of the region of interest approach, provide a powerful and unbiased tool to study the neural substrates of OCD. Unfortunately, recent applications of these novel methods to the study of OCD are often limited by relatively small sample sizes, resulting in insufficient statistical power. In this context, we considered it timely to conduct an exhaustive search of all published and unpublished voxel-based morphometry studies in OCD worldwide, and to perform a voxel-based quantitative meta-analysis using the SDM methods presented at the beginning of this chapter.

2.2.2 Methods

2.2.2.1 Inclusion of studies

Included articles were obtained from exhaustive searches by the investigators in the Medline, PubMed, ScienceDirect and Scopus databases using the keywords ‘obsessive-compulsive disorder’ plus ‘morphometry’, ‘voxel-based’ or ‘voxelwise’, as well as from hand searching in the reference lists of obtained

articles. In addition, the authors contacted 303 worldwide OCD experts by email (Mataix-Cols, Pertusa et al. 2007) requesting any unpublished voxel-based morphometry study in OCD that they wished to include in this meta-analysis. Studies comprising less than 10 individuals with OCD (Cecconi, Lopes et al. 2008) and studies that re-analyzed previously published data (Cardoner, Soriano-Mas et al. 2007; Soriano-Mas, Pujol et al. 2007) were not included. Twelve studies performing whole-brain voxel-based comparisons of grey matter between individuals with OCD and healthy controls and completed before 1 December 2008 were identified and included in the meta-analysis. These included 11 published papers and a previously unpublished analysis of a published paper (Soriano-Mas, Pujol et al. 2007) (new sample). The corresponding authors were contacted by email requesting any details not included in the original publications. After contacting the authors, no methodological ambiguities remained regarding the design or analysis of any of the studies. Meta-analysis Of Observational Studies in Epidemiology (MOOSE) guidelines (Stroup, Berlin et al. 2000) are followed in the study.

2.2.2.2 Global differences in grey matter volume

Meta-analytical estimates of the differences in *global* grey matter volumes between the participants with OCD and the controls were calculated using a random-effects model with RevMan version 5 for Linux (The Nordic Cochrane Centre, Copenhagen). A heterogeneity analysis was performed to test if the

observed variance across studies was larger than that resulting from sampling error alone.

2.2.2.3 Regional differences in grey matter volume

Differences in regional grey matter volume between participants with OCD and controls were assessed with the SDM methods presented at the beginning of this chapter, including the mean analysis, the descriptive analysis of quartiles, and the subgroup and meta-regression analyses.

It must be noted that the analysis of quartiles could be biased by the inclusion of studies that did not correct for multiple comparisons. Thus, only studies that performed such corrections are included (Pujol, Soriano-Mas et al. 2004; Riffkin, Yucel et al. 2005; Valente, Miguel et al. 2005; Carmona, Bassas et al. 2007; Soriano-Mas, Pujol et al. 2007; Christian, Lencz et al. 2008; Gilbert, Keshavan et al. 2008; Gilbert, Mataix-Cols et al. 2008; van den Heuvel, Remijnse et al. 2009).

The following analyses of subgroups were conducted: studies which acquired the images with a slice thickness of 1.2-1.5 mm, studies using a 12 mm smoothing kernel, studies performing parametric and voxel-based statistical tests, studies performing an additional modulation step (i.e. inference of absolute grey matter volume instead of grey matter density), studies reporting coordinates corrected for multiple comparisons, and studies that included adult participants; unfortunately, paediatric studies were too few to be analysed

separately. Subgroup analyses regarding the procedure used for controlling for global volumes were not possible, as there were not enough studies using the same approach. Separate analysis depending on the magnetic strength of the scanner was not required as all studies used 1.5 Tesla scanners.

Finally, variables explored by regression were the mean age, the mean Yale–Brown Obsessive–Compulsive Scale (YBOCS), the percentage of participants with a major depressive disorder, and the percentage of individuals receiving current antidepressant medication. The percentage of people receiving current antipsychotic medication was not considered because it was the same (0%) in all the studies. The following variables could not be studied because data was available for fewer than nine studies: mean years of education, mean age at onset, illness duration, percentage of participants with anxiety disorders other than OCD and percentage of participants having received past antidepressant or antipsychotic medication.

The main output for each meta-regression was a map of the regression slope (e.g. the amount of grey matter change per unit increase in mean YBOCS score). In order to reduce spurious results, only those clusters showing a significant trend across participants with OCD along with a predicted significant difference with healthy individuals in studies at one of the extremes (e.g. a predicted significant grey matter difference with healthy individuals in studies with maximum YBOCS) are reported. Because of the small number of studies included in this meta-analysis and the number of regression models tested (n = 6), a strict control of false positives is applied (Bonferroni correction: *P* =

0.001/6 = 0.00017). However, the meta-regression results should be taken with some caution because of the limited variability in the data.

2.2.3 Results

2.2.3.1 Included studies

Twelve studies were included comprising 401 individuals with OCD and 376 healthy controls. Of the 12 studies, 9 consisted of adult OCD samples and 3 of paediatric samples. The demographic and clinical characteristics of the participants are shown in **Table 2.1**. Further details and methodological aspects of each of the included studies can be found at http:/www.sdmproject.com/database .

2.2.3.2 Global grey matter volumes

Global grey matter volumes were obtained from seven studies including 297 individuals with OCD and 277 healthy controls with similar characteristics to those of the overall sample (Kim, Lee et al. 2001; Pujol, Soriano-Mas et al. 2004; Valente, Miguel et al. 2005; Carmona, Bassas et al. 2007; Szeszko, Christian et al. 2008; Yoo, Roh et al. 2008; van den Heuvel, Remijnse et al. 2009). Heterogeneity analysis revealed that variance across studies was not only a result of sampling error alone (χ^2 = 13.83, df = 6, *P* = 0.03). No

Table 2.1 Demographic and clinical characteristics of the 12 studies included in the meta-analysis.

	Sociodemographic characteristics of OCD participants (and controls)					Clinical characteristics (OCD participants only)					
	n	Mean age	Males	Right handed	Years education	Age at onset	Illness duration	Y-BOCS score	Major depressive disorder	Anxi-ety	Antide-pressant
Carmona *et al.* (2007)	18 (18)	12.9 (13.0)	72% (72%)	83% (83%)	N/A	N/A	N/A	21.4	0%	33%	56%
Christian *et al.* (2008)	21 (21)	38.0 (38.9)	71% (71%)	67% (76%)	14.6 (14.9)	N/A	N/A	27.0	33%	N/A	81%
Gilbert *et al.* (2008)	25 (20)	37.5 (29.8)	52% (45%)	N/A	N/A	29.5	8.0	26.9	36%	24%	80%
Gilbert *et al.* (2008)	10 (10)	12.9 (13.4)	60% (60%)	100% (100%)	N/A	N/A	N/A	26.5	0%	N/A	0%
van den Heuvel *et al.* (2009)	55 (50)	33.7 (31.4)	29% (40%)	89% (90%)	N/A	N/A	N/A	22.8	18%	N/A	0%
Kim *et al.* (2001)	25 (25)	27.4 (27.0)	68% (68%)	96% (96%)	14.2 (15.3)	19.0	8.4	24.2	16%	0%	0%
Pujol *et al.* (2004)	72 (72)	29.8 (30.1)	56% (56%)	85% (85%)	13.2 (14.0)	17.0	13.0	26.7	36%	19%	75%
Riffkin *et al.* (2005)	18 (18)	36.1 (34.6)	44% (44%)	94% (94%)	12.1 (13.4)	N/A	N/A	23.3	N/A	N/A	17%
Soriano-Mas *et al.* (2007)	30 (30)	31.9 (31.8)	70% (53%)	93% (90%)	12.2 (13.1)	19.7	11.3	21.0	13%	23%	87%
Szeszko *et al.* (2008)	37 (26)	13.0 (13.0)	38% (35%)	57% (65%)	N/A	9.4	3.6	24.9	0%	24%	0%
Valente *et al.* (2005)	19 (15)	32.7 (32.3)	53% (47%)	89% (73%)	11.7 (10.4)	14.4	18.3	24.6	47%	84%	58%
Yoo *et al.* (2008)	71 (71)	26.6 (26.7)	66% (66%)	96% (100%)	N/A	18.6	8.0	22.8	6%	4%	83%

N/A: not available

differences in global grey matter volume were found between individuals with OCD and healthy controls (Z = 1.00, P = 0.32).

2.2.3.3 Regional differences in grey matter

Coordinates for the SDM analyses were obtained from all the 12 studies representing 401 individuals with OCD and 376 healthy controls (**Figure 2.3**).

Figure 2.3 Plots of all the significant coordinates included in the meta-analysis (*n* = 12 studies).

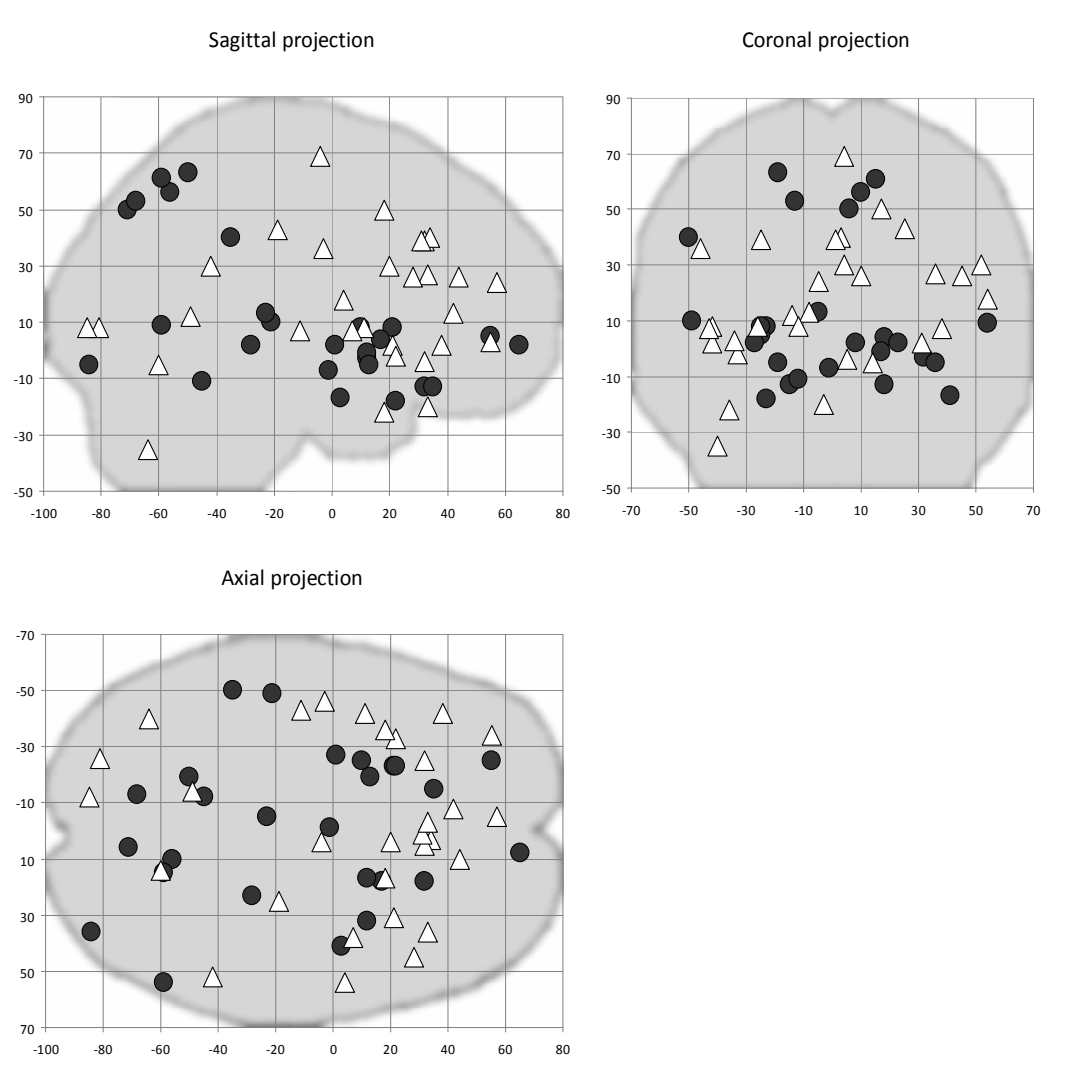

Reported peak coordinates of grey matter increases (OCD>controls; black circles) and decreases (OCD<controls; white triangles) have been projected to the sagittal, coronal and axial planes.

As shown in **Table 2.2** and **Figure 2.4**, individuals with OCD had significant bilateral (larger on the left) grey matter volume increases in the lenticular nucleus (mainly ventral anterior putamen) extending to the caudate nucleus, as well as in a small region in the right superior parietal lobule (Brodmann area 7). Participants with OCD also showed significant bilateral (larger on the right) grey matter volume decreases in dorsal medial

Table 2.2 Regional differences in grey matter volume between individuals with OCD and healthy controls.

	Maximum			Cluster	
	Talairach coordinates	SDM value	Uncorrected p-value	Number of voxels	Breakdown (number of voxels)
Clusters of increased grey matter					
Left lenticular nucleus (mainly anterior putamen)	-18, 8, 0	0.248	0.000005	506	Left lenticular nucleus (464 voxels) Left caudate nucleus (41 voxels) Left subcallosal gyrus (1 voxels)
Right superior parietal lobule and precuneus	14, -60, 62	0.210	0.00009	75	Right Brodmann area 7 (75 voxels)
Right lenticular nucleus (mainly anterior putamen)	14, 10, -2	0.187	0.0003	68	Right lenticular nucleus (54 voxels) Right caudate nucleus (14 voxels)
Clusters of decreased grey matter					
Right/left dMFG/ACG	4, 28, 36	-0.278	0.00002	385	Right Brodmann area 8 (93 voxels) Right Brodmann area 32 (96 voxels) Right Brodmann area 6 (34 voxels) Right Brodmann area 9 (22 voxels) Left Brodmann area 8 (59 voxels) Left Brodmann area 32 (41 voxels) Left Brodmann area 6 (26 voxels) Left Brodmann area 9 (14 voxels)

Notes: Brodmann area 6 = supplementary motor cortex; Brodmann area 7 = somatosensory association cortex; Brodmann area 8 = frontal eye fields; Brodmann area 9 = dorsal medial frontal gyrus; Brodmann areas 32 = dorsal anterior cingulate gyrus. All voxels with $p < 0.001$ uncorrected (SDM value thresholds of 0.163 for increases and of -0.183 for decreases). No significant voxels were found after FDR correction.

frontal/anterior cingulate gyri, extending to the supplementary motor area and frontal eye fields (Brodmann areas 8, 32, 6 and 9).

2.2.3.4 Descriptive analysis of quartiles

Decreases of grey matter in dorsal mediofrontal/anterior cingulate gyri were detected in the median analysis (maximum at Talairach (20,32,38), SDM -0.179), meaning that most of the studies had found some degree of decreased grey matter in the region.

Figure 2.4 Main increased (a) and decreased (b) grey matter regions in individuals with obsessive–compulsive disorder compared with healthy controls, and usual targets of capsulotomy / deep brain stimulation (c) and cingulotomy (d).

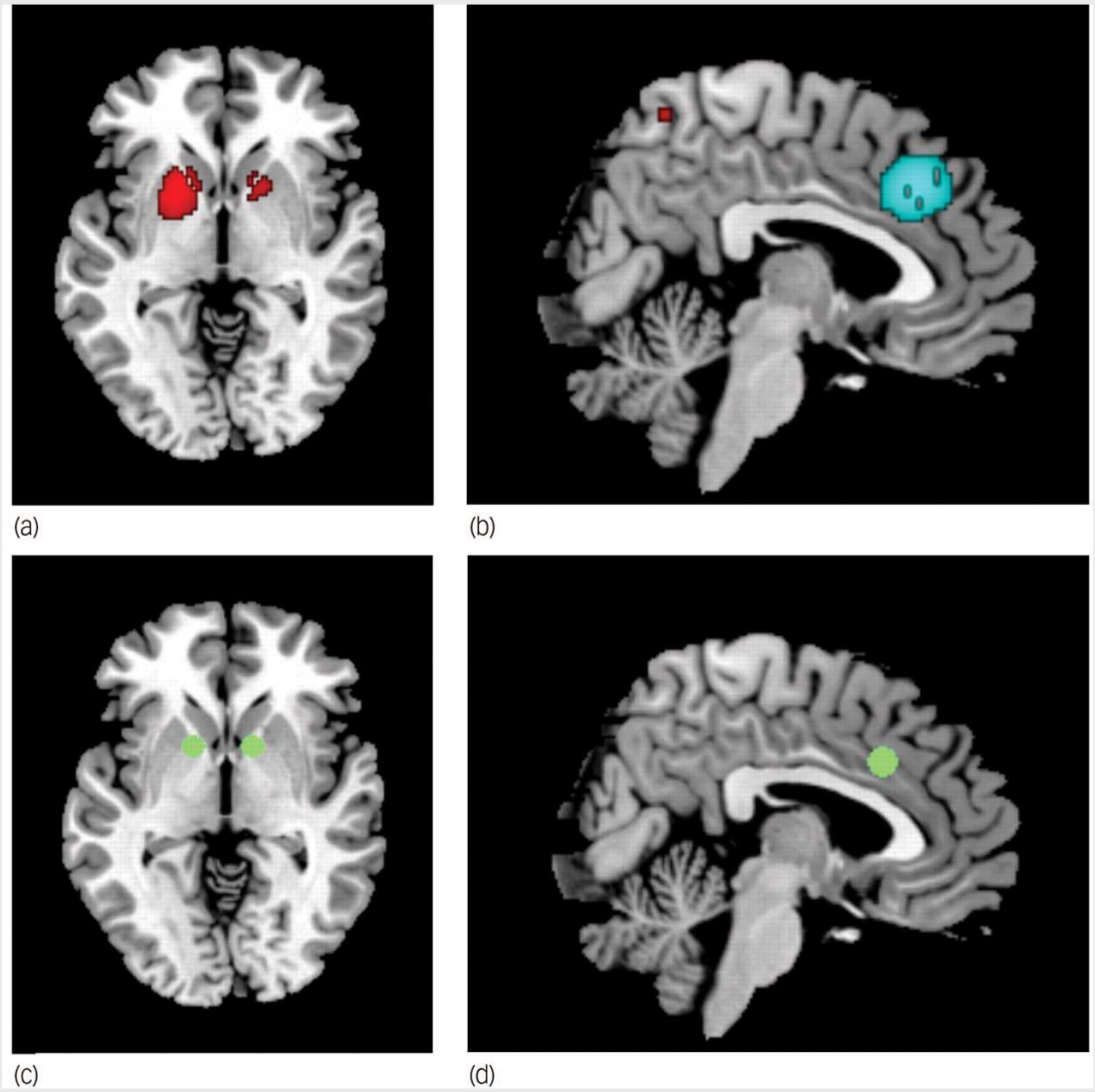

(a) Increased grey matter in lenticular nuclei and caudate, (b) decreased grey matter in dorsal mediofrontal/anterior cingulate gyri, (c) target of capsulotomy and deep brain stimulation, (d) target of cingulotomy. Images (a) and (c) are shown in the axial plane (Z = -2); images (b) and (d) are shown in the sagittal plane (X = 4). Note that the clusters of grey matter increase in bilateral lenticular nuclei include the usual targets of capsulotomy and deep brain stimulation. Similarly, the meta-analytic cluster of grey matter decrease in dorsal mediofrontal gyri/anterior cingulate gyri includes the usual target of cingulotomy. Significant clusters and surgery targets have been overlaid to an MRIcron template for Linux (http://www.mricro.com/mricron) for display purposes only.

These findings were rather larger as expected in the first quartile analysis (maximum at Talairach (2,32,40), SDM -0.978), including several nearby clusters.

Increases of grey matter in the left lenticular nucleus were only detected in the third quartile analysis (maximum at Talairach (-22,16,2), SDM 0.743), meaning that at least 25% but less than 50% of the studies had found some degree of increased grey matter in this region. In this analysis, no changes of grey matter were detected in the right lenticular nucleus.

2.2.3.5 Sensitivity analysis

As seen in **Table 2.3**, whole-brain jack-knife sensitivity analysis showed that the grey matter increase in left lenticular nucleus and grey matter decrease in bilateral dorsal mediofrontal/anterior cingulate gyri were highly replicable, as these findings were preserved throughout all the 12 combinations of 11 studies. Grey matter increases in right lenticular nucleus and superior parietal cortex failed to emerge in two of the study combinations. No additional significant clusters were found in any of the 12 study combinations.

2.2.3.6 Analyses of subgroups

The above results remained largely unchanged when the analyses were repeated and limited to methodologically homogenous groups of studies (**Table 2.3**). Only one additional significant cluster in the left cerebellum (maximum at Talairach (-12,-46,-12), SDM 0.179, $P = 0.0002$) emerged in the sub-analysis of studies reporting coordinates corrected for multiple comparisons.

Table 2.3 Analyses of subgroups and sensitivity analyses

		Increased grey matter			Decreased grey matter
		L lenticular nucleus	R sup. parietal lobule	R lenticular nucleus	R/L dMFG/ACG
Studies with slice thickness ≤ 1.5mm at acquisition (n=9) (Kim, Lee et al. 2001; Riffkin, Yucel et al. 2005; Valente, Miguel et al. 2005; Christian, Lencz et al. 2008; Gilbert, Keshavan et al. 2008; Gilbert, Mataix-Cols et al. 2008; Szeszko, Christian et al. 2008; Yoo, Roh et al. 2008; van den Heuvel, Remijnse et al. 2009)		Yes	Yes	No	No
Studies using a 12mm smoothing kernel (n=7) (Kim, Lee et al. 2001; Pujol, Soriano-Mas et al. 2004; Valente, Miguel et al. 2005; Carmona, Bassas et al. 2007; Gilbert, Mataix-Cols et al. 2008; Yoo, Roh et al. 2008; van den Heuvel, Remijnse et al. 2009)		Yes	No	No	Yes[(a)]
Studies with an additional modulation step (n=9) (Pujol, Soriano-Mas et al. 2004; Riffkin, Yucel et al. 2005; Valente, Miguel et al. 2005; Carmona, Bassas et al. 2007; Soriano-Mas, Pujol et al. 2007; Christian, Lencz et al. 2008; Gilbert, Mataix-Cols et al. 2008; Szeszko, Christian et al. 2008; van den Heuvel, Remijnse et al. 2009)		Yes[(b)]	No	Yes[(b)]	Yes
Studies performing parametric voxel-based statistics (n=11) (Kim, Lee et al. 2001; Pujol, Soriano-Mas et al. 2004; Valente, Miguel et al. 2005; Carmona, Bassas et al. 2007; Soriano-Mas, Pujol et al. 2007; Christian, Lencz et al. 2008; Gilbert, Keshavan et al. 2008; Gilbert, Mataix-Cols et al. 2008; Szeszko, Christian et al. 2008; Yoo, Roh et al. 2008; van den Heuvel, Remijnse et al. 2009)		Yes	Yes	Yes	Yes
Studies with correction for multiple comparison (n=9) (Pujol, Soriano-Mas et al. 2004; Riffkin, Yucel et al. 2005; Valente, Miguel et al. 2005; Carmona, Bassas et al. 2007; Soriano-Mas, Pujol et al. 2007; Christian, Lencz et al. 2008; Gilbert, Keshavan et al. 2008; Gilbert, Mataix-Cols et al. 2008; van den Heuvel, Remijnse et al. 2009)		Yes	No	Yes	Yes
Studies in adult individuals (n=9) (Kim, Lee et al. 2001; Pujol, Soriano-Mas et al. 2004; Riffkin, Yucel et al. 2005; Soriano-Mas, Pujol et al. 2007; Christian, Lencz et al. 2008; Gilbert, Mataix-Cols et al. 2008; Yoo, Roh et al. 2008; van den Heuvel, Remijnse et al. 2009)		Yes	No	No	Yes
Jack-knife sensitivity analysis discarded study:	Carmona *et al.* (2007)	Yes	Yes	Yes	Yes
	Christian *et al.* (2008)	Yes	Yes	Yes	Yes
	Gilbert *et al.* (2008)	Yes	Yes	Yes	Yes
	Gilbert *et al.* (2008)	Yes	Yes	Yes	Yes
	van den Heuvel *et al.* (2009)	Yes	Yes	Yes	Yes
	Kim *et al.* (2001)	Yes	Yes	Yes[(c)]	Yes
	Pujol *et al.* (2004)	Yes	Yes	No	Yes[(a)]
	Riffkin *et al.* (2005)	Yes	Yes	Yes	Yes
	Soriano-Mas *et al.* (2007)	Yes	Yes	Yes	Yes[(a)]
	Szeszko *et al.* (2008)	Yes	No	No	Yes
	Valente *et al.* (2005)	Yes	Yes	Yes	Yes
	Yoo *et al.* (2008)	Yes	No	Yes	Yes

R, right; L, left; dMFG, dorsal medial frontal gyri; ACG, anterior cingulate gyri. Yes = brain region remains significantly increased/decreased in the subgroup analysis or after exclusion of the study in the jack-knife analysis. No = brain region is no longer significantly increased/decreased in the subgroup analysis or after exclusion of the study in the jack-knife analysis. (a) Maximum of the dMFG/ACG cluster was displaced to right cingulate gyrus when only studies using a 12mm smoothing kernel were included, or when either S_7 or S_9 was not included in the analysis. (b) Increases in bilateral lenticular nuclei were significant after FDR correction in the analysis of studies performing an additional modulation step. (c) Maximum of the right lenticular nucleus cluster was displaced to right caudate nucleus when S_6 was not included in the analysis.

2.2.3.7 Meta-regression

Regression analyses showed that mean age (available in all the studies) was not associated with OCD-related grey matter changes, at least linearly (slope smallest *P* = 0.0004). Symptom severity (YBOCS scores, available in all the studies) was associated with increased grey matter volumes in bilateral lenticular nuclei (left maximum slightly displaced to claustrum, Talairach (-24,18,-6) and (20,14,0), SDM +0.106 and +0.116 per 1 point increase in mean YBOCS score, *P* = 0.0001 and *P* = 0.00004), with predicted grey matter increase in studies including individuals with more severe symptoms (maxima at Talairach (-20,14,-4) and (18,12,0), SDM 0.475 and 0.482, *P* = 0.000001 and *P* = 0.0000007) (**Figure 2.5**).

The reported percentage of participants with comorbid major depressive disorder (available in all the studies but one (Riffkin, Yucel et al. 2005)), was found to be negatively associated with grey matter volumes in the right superior parietal lobule (maximum at Talairach (14,-58,62), SDM -0.146 per 10% increase in the percentage of people with comorbid major depressive disorder, *P* = 0.00014), with predicted grey matter increase in studies reporting no individuals with comorbid major depressive disorder (maximum at Talairach (14,-60,62), SDM 0.502, *P* = 0.000004). No effect of current antidepressant medication (available in all the studies) was detected (slope smallest *P* = 0.003).

Figure 2.5 Meta-regression results showing an association between symptom severity (mean Yale–Brown Obsessive–Compulsive Scale (YBOCS) scores) and grey matter volume in left and right putamen

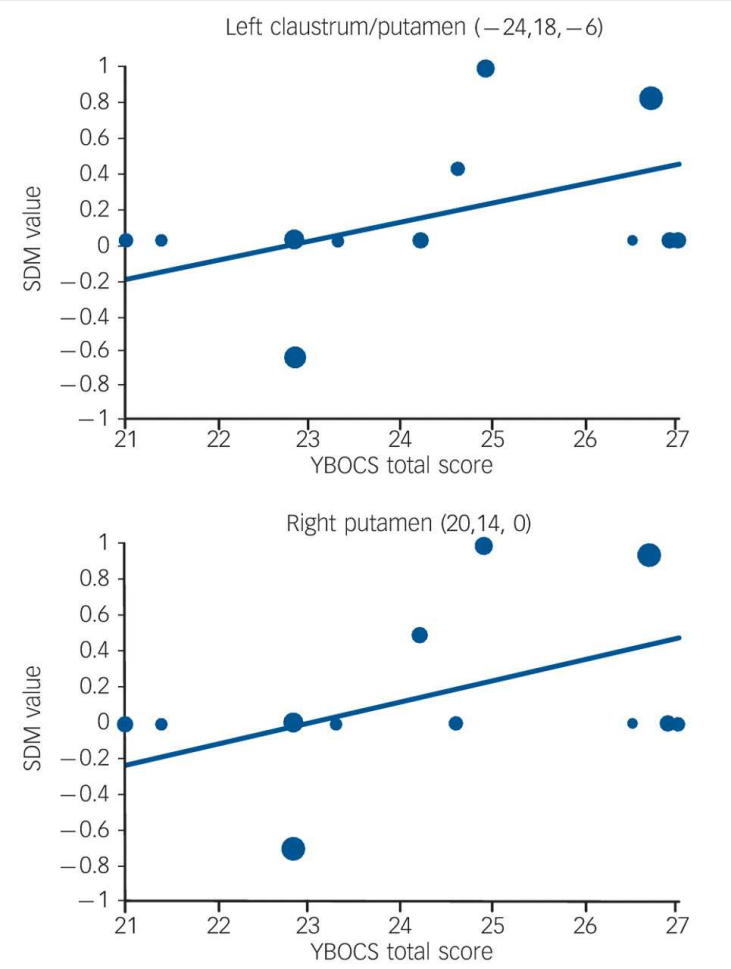

Each study is represented as a dot, with larger dots symbolising greater sample sizes. The regression line (meta-regression signed differential mapping (SDM) slope) is presented as a straight line. Note that the meta-regression SDM value is derived from the proportion of studies that reported grey matter changes near the voxel, so it is expected that the values of some of the studies are at 0 or near ±1 (instead of being close to the line).

2.2.4 Discussion

To our knowledge, this is the first meta-analysis of voxel-based morphometry studies of grey matter volume in OCD. The study is timely given that a sufficient number of high-quality studies have only recently become available. The main strengths of the study are the unbiased inclusion of published as well as unpublished studies, even if their results were negative (i.e. when no significant differences between people with OCD and controls were found), and the development and implementation of the voxel-wise meta-analytic method presented at the beginning of the chapter. In order to facilitate replication and further analyses by other colleagues, an online database, which contains all the data and methodological details from every study included in this meta-analysis, has also been developed and it is readily accessible at http://www.sdmproject.com/database .

The main findings were that individuals with OCD had increased bilateral regional grey matter volumes in the lenticular nucleus (mainly ventral anterior putamen) extending to the caudate nucleus, as well as decreased bilateral regional grey matter volumes in dorsal mediofrontal/anterior cingulate gyri, extending to the supplementary motor area and frontal eye fields (Brodmann area 8, 32, 6 and 9). Descriptive analysis of quartiles further revealed that most of the studies had found some degree of grey matter decrease in dorsal mediofrontal/anterior cingulate gyri and at least 25% of the studies had found some degree of grey matter increase in left lenticular region. The findings remained largely unchanged when each study was removed from the analyses 'only one at the time' (jack-knife sensitivity analysis), as well as

when methodologically homogeneous studies were analysed separately, thus adding to the robustness of the findings. Current use of antidepressant medication did not influence the results.

The basal ganglia have long been hypothesised to play a key role in the mediation of obsessive-compulsive symptoms (Rapoport and Wise 1988). Indirect evidence is available from focal lesion studies, disorders of known basal ganglia pathology and, more recently, from neuroimaging studies (Baxter, Saxena et al. 1996; Saxena, Brody et al. 1998; Mataix-Cols and van den Heuvel 2006). Structural neuroimaging studies have, however, been remarkably inconsistent, possibly because of the lack of sufficient sample sizes and methodological differences between the studies. This voxel-wise meta-analysis, which partially overcomes some of these problems, confirms that OCD is characterised by increased regional grey matter volumes in the basal ganglia, particularly the ventral, anterior part of the putamen, but also the caudate nucleus. Furthermore, meta-regression analyses showed that studies that included individuals with more severe OCD (YBOCS scores) were significantly more likely to report increased grey matter volumes in these regions.

The dorsal mediofrontal/anterior cingulate gyri region has also been implicated (usually hyperactive) in a wide range of functional neuroimaging studies in OCD, including resting state studies (Swedo, Schapiro et al. 1989; Perani, Colombo et al. 1995), symptom provocation studies (Rauch, Jenike et al. 1994; Breiter, Rauch et al. 1996; Mataix-Cols, Wooderson et al. 2004), and studies employing tasks requiring inhibitory control (Ursu, Stenger et al. 2003; Fitzgerald, Welsh et al. 2005; Maltby, Tolin et al. 2005; Yucel, Harrison et al.

2007). An important study by Yucel et al (2007) found reduced concentrations of neuronal N-acetylaspartate in the dorsal anterior cingulate gyri of people with OCD, which was inversely correlated with the level of activation in this region during a task of inhibitory control. The authors suggested that hyperactivations in the dorsal anterior cingulate gyri might therefore represent a secondary, compensatory response to neural abnormalities in this region. Our findings of reduced grey matter volume in this region are entirely consistent with this view and support current neuropsychological models of OCD whereby deficits in inhibitory processes would be primarily implicated in the disorder (Chamberlain, Blackwell et al. 2005).

It is striking that the regions identified in this meta-analysis are anatomically very close to the targets of surgical treatments for treatment-refractory OCD. Indeed, our maxima of grey matter increase in anterior putamen (**Figure 2.4A**) are situated only 2-13mm mainly laterorostrally from the usual targets of capsulotomy and deep brain stimulation (**Figure 2.4C**) (Nuttin, Gabriels et al. 2003; Rauch, Dougherty et al. 2006; Liu, Zhang et al. 2008; Greenberg, Gabriels et al. 2010). Similarly, our maxima of grey matter decrease in dorsal mediofrontal/anterior cingulate gyri (**Figure 2.4B**) are situated just 2-12mm mainly mediorostrally from the usual targets of cingulotomy (**Figure 2.4D**) (Ballantine, Bouckoms et al. 1987; Spangler, Cosgrove et al. 1996; Dougherty, Baer et al. 2002; Kim, Lee et al. 2002; Kim, Chang et al. 2003; Greenspan, Coghill et al. 2008).

Taken together, these converging lines of evidence suggest that the basal ganglia and the dorsal mediofrontal/anterior cingulate gyri are implicated

in OCD. Studies in animals have shown that these two structures have dense direct anatomical connections (Alexander, Crutcher et al. 1990; Kunishio and Haber 1994). The evidence in humans is more indirect. For example, in one study, individuals undergoing cingulotomy experienced significant reductions in the volume of the caudate nucleus several months post-operatively, suggesting that there are direct connections between these structures in the human brain (Rauch, Kim et al. 2000).

Some of the analyses also revealed increased grey matter volume in the right parietal cortex in people with OCD, although this finding was less robust. The meta-regression analyses further suggested that differences in this region may be particularly apparent in individuals with OCD but without comorbid depression. Although the parietal cortex is not a region traditionally implicated in OCD, recent reports suggest that its importance may have been overlooked (Menzies, Achard et al. 2007; Menzies, Chamberlain et al. 2008; Menzies, Williams et al. 2008; van den Heuvel, Remijnse et al. 2009). Our results would support this possibility, particularly in individuals without comorbid depression.

Interestingly, this meta-analysis did not reveal significant between-group differences in the orbitofrontal cortex, a region that has been consistently implicated in functional neuroimaging studies of OCD and constitutes the basis of the most widely accepted neurobiological model of OCD (Baxter, Saxena et al. 1996; Saxena, Brody et al. 1998; Mataix-Cols and van den Heuvel 2006). There are several plausible explanations, which are not necessarily mutually exclusive, for the lack of structural changes in this structure. First, only 3 of the

12 studies included in this meta-analysis identified changes in this region (Pujol, Soriano-Mas et al. 2004; Szeszko, Christian et al. 2008; Yoo, Roh et al. 2008). Although this may be partially a result of technical difficulties in obtaining high-quality images in this region, this seems unlikely since many functional neuroimaging studies, which are also susceptible to these same technical difficulties, have more frequently reported differences in activation in this region between participants with OCD and controls. Second, the precise location and direction of the changes in this region was heterogeneous across studies, with one study reporting grey matter reductions in lateral aspects of the orbitofrontal cortex (Yoo, Roh et al. 2008), one study reporting grey matter reductions in primarily medial aspects of the orbitofrontal cortex (Pujol, Soriano-Mas et al. 2004) and one paediatric study reporting increases rather than decreases of grey matter volume in this region (Szeszko, Christian et al. 2008). The orbitofrontal cortex is indeed heterogeneous both in structure and function, and the precise role of its subterritories in OCD or its subtypes is unclear. Third, it is also possible that the recruitment of the orbitofrontal cortex in functional neuroimaging studies in OCD reflects secondary, perhaps compensatory, neural responses to cognitive or emotional challenges, rather than being crucially implicated in the aetiopathogenesis of the disorder. Although our results would support a dorsal prefrontostriatal, rather than an orbitofrontal cortex-striatal model of OCD, the role of the orbitofrontal cortex in the aetiopathogenesis of OCD cannot be fully ruled out.

This meta-analysis is unable to answer whether the reported changes precede the onset of the symptoms; that is, whether they represent a

vulnerability factor for the development of OCD or whether they represent the consequence of a chronic illness. The fact that studies with participants with more severe OCD found greater changes in the basal ganglia could suggest the latter and some limited evidence supports this possibility. Indeed, some studies have reported volumetric reductions in subcortical brain structures following successful treatment with serotonin reuptake inhibitors in OCD (Gilbert, Moore et al. 2000; Rosenberg, MacMaster et al. 2000). On the other hand, recent reports of structural brain changes in unaffected first-degree relatives of people with OCD would suggest an underlying familial vulnerability that may be symptom-independent (Menzies, Achard et al. 2007; Menzies, Williams et al. 2008). Only large developmental studies that examine the association between brain structure and symptom onset longitudinally will be able to answer this question fully.

Another question unanswered by this meta-analysis is whether the reported changes are specific to OCD or whether they may be common to other psychiatric disorders (Mataix-Cols and van den Heuvel 2006). Of particular relevance to current discussions regarding the future classification of OCD in the next edition of the DSM is whether these changes are also seen in other anxiety disorders. Obsessive–compulsive disorder experts disagree on whether OCD should remain as one of the anxiety disorders or whether it should be classified separately in the DSM-V (Mataix-Cols, Pertusa et al. 2007). A voxel-based meta-analytical comparison of structural and functional neuroimaging studies in OCD vs. other anxiety disorders may shed some light on this contentious question.

It is important to highlight several limitations of this study, some of which are inherent to all meta-analytical approaches. First, voxel-based meta-analyses are based on summarised (i.e. coordinates from published studies) rather than raw data and this may result in less accurate results (Salimi-Khorshidi, Smith et al. 2009). However, obtaining and analysing the raw images from these studies is logistically and technically difficult. Second, despite our attempts to contact worldwide OCD experts and include as many unpublished voxel-based morphometry studies as possible, even if their results were negative, the possibility of publication bias cannot be entirely ruled out. Third, it must be noted that normal brain regions close to abnormal brain regions may artificially appear to be abnormal. Therefore, the breakdown of a cluster should not be understood as 'all these regions are abnormal' but as 'one or more of these regions are abnormal'. Fourth, most of the results were only significant before correction for multiple comparisons by the false discovery rate. However, previous simulation work established that uncorrected $p < 0.001$ or even 0.002 was, in SDM method, empirically equivalent to corrected $p < 0.05$. Fifth, as mentioned above, regression analyses should be taken cautiously because they included a small number of studies and variability in the data was limited. Similarly, subgroup analyses by specific symptom subtypes or dimensions could not be performed. This is important since OCD is likely to be aetiologically heterogeneous (Mataix-Cols, Rosario-Campos et al. 2005) and preliminary evidence suggests that each of the major symptom dimensions of OCD may have partially distinct neural substrates (Mataix-Cols, Wooderson et al. 2004; Saxena, Brody et al. 2004; An, Mataix-Cols et al. 2009; van den Heuvel, Remijnse et al. 2009).

2.2.5 Acknowledgements

We thank all the authors of the included studies and especially Drs Busatto, Kwon, Soriano-Mas and Szeszko for kindly sharing their unpublished data for inclusion in this meta-analysis.

2.3 OVERALL DISCUSSION

The number of neuroimaging studies has grown exponentially in recent years, making voxel-based meta-analytic methods useful to integrate a body of evidence which otherwise would be difficult to comprehend. However, previous voxel-based meta-analytic methods had a number of important limitations, such as including studies which employed spatially heterogeneous statistical thresholds, or not considering increases and decreases of grey matter volume or Blood Oxygen Level-Dependent (BOLD) response simultaneously.

This chapter has introduced a new voxel-based meta-analytic method, SDM, which adopts and combines the various positive features of the previous methods and introduces a series of improvements and novel features aimed to overcome these limitations. Also, an example of a successful application of this new approach has been offered yielding highly plausible results.

However, with all its innovations, the original SDM method still has a series of drawbacks that limit its utility. First, the original SDM method did not include the possibility of fitting more complex models such as multiple meta-regressions or addition of covariates. Second, its brain templates were only suitable for meta-analyses of grey matter measures (either volume or function), but not white matter or *tract-based spatial statistics* (TBSS). Third, the original SDM method was not able to benefit from the richer information contained in the (seldom available) statistical maps. Finally, the method was only able to analyze

one neuroimaging modality (e.g. grey matter volume) at a time. These limitations of the original SDM method are addressed in the following chapters.

2.4 REFERENCES

Alexander, G. E., M. D. Crutcher, et al. (1990). "Basal ganglia-thalamocortical circuits: parallel substrates for motor, oculomotor, "prefrontal" and "limbic" functions." Prog Brain Res **85**: 119-146.

An, S. K., D. Mataix-Cols, et al. (2009). "To discard or not to discard: the neural basis of hoarding symptoms in obsessive-compulsive disorder." Mol Psychiatry **14**(3): 318-331.

Ashburner, J. and K. J. Friston (2000). "Voxel-based morphometry-the methods." Neuroimage **11**(6 Pt 1): 805-821.

Ashburner, J. and K. J. Friston (2001). "Why voxel-based morphometry should be used." Neuroimage **14**(6): 1238-1243.

Aylward, E. H., G. J. Harris, et al. (1996). "Normal caudate nucleus in obsessive-compulsive disorder assessed by quantitative neuroimaging." Arch Gen Psychiatry **53**(7): 577-584.

Ballantine, H. T., Jr., A. J. Bouckoms, et al. (1987). "Treatment of psychiatric illness by stereotactic cingulotomy." Biol Psychiatry **22**(7): 807-819.

Baxter, L. R., Jr., S. Saxena, et al. (1996). "Brain Mediation of Obsessive-Compulsive Disorder Symptoms: Evidence From Functional Brain Imaging Studies in the Human and Nonhuman Primate." Semin Clin Neuropsychiatry **1**(1): 32-47.

Breiter, H. C., S. L. Rauch, et al. (1996). "Functional magnetic resonance imaging of symptom provocation in obsessive-compulsive disorder." Arch Gen Psychiatry **53**(7): 595-606.

Brett, M. (1999). "The MNI Brain and The Talairach Atlas, Cambridge Imagers. http://www.mrc-cbu.cam.ac.uk/Imaging/mnispace.html."

Cardoner, N., C. Soriano-Mas, et al. (2007). "Brain structural correlates of depressive comorbidity in obsessive-compulsive disorder." Neuroimage **38**(3): 413-421.

Carmona, S., N. Bassas, et al. (2007). "Pediatric OCD structural brain deficits in conflict monitoring circuits: a voxel-based morphometry study." Neurosci Lett **421**(3): 218-223.

Cecconi, J. P., A. C. Lopes, et al. (2008). "Gamma ventral capsulotomy for treatment of resistant obsessive-compulsive disorder: A structural MRI pilot prospective study." Neurosci.Lett. **447**(2-3): 138-142.

Chamberlain, S. R., A. D. Blackwell, et al. (2005). "The neuropsychology of obsessive compulsive disorder: the importance of failures in cognitive

and behavioural inhibition as candidate endophenotypic markers." Neurosci Biobehav Rev **29**(3): 399-419.

Christian, C. J., T. Lencz, et al. (2008). "Gray matter structural alterations in obsessive-compulsive disorder: relationship to neuropsychological functions." Psychiatry Res. **164**(2): 123-131.

Dougherty, D. D., L. Baer, et al. (2002). "Prospective long-term follow-up of 44 patients who received cingulotomy for treatment-refractory obsessive-compulsive disorder." Am J Psychiatry **159**(2): 269-275.

Fitzgerald, K. D., R. C. Welsh, et al. (2005). "Error-related hyperactivity of the anterior cingulate cortex in obsessive-compulsive disorder." Biol Psychiatry **57**(3): 287-294.

Genovese, C. R., N. A. Lazar, et al. (2002). "Thresholding of statistical maps in functional neuroimaging using the false discovery rate." Neuroimage **15**(4): 870-878.

Gilbert, A. R., M. S. Keshavan, et al. (2008). "Gray matter differences between pediatric obsessive-compulsive disorder patients and high-risk siblings: A preliminary voxel-based morphometry study." Neurosci Lett **435**(1): 45-50.

Gilbert, A. R., D. Mataix-Cols, et al. (2008). "Brain structure and symptom dimension relationships in obsessive-compulsive disorder: A voxel-based morphometry study." J Affect Disord **109**(1-2): 117-126.

Gilbert, A. R., G. J. Moore, et al. (2000). "Decrease in thalamic volumes of pediatric patients with obsessive-compulsive disorder who are taking paroxetine." Arch Gen Psychiatry **57**(5): 449-456.

Greenberg, B. D., L. A. Gabriels, et al. (2010). "Deep brain stimulation of the ventral internal capsule/ventral striatum for obsessive-compulsive disorder: worldwide experience." Mol Psychiatry **15**(1): 64-79.

Greenspan, J. D., R. C. Coghill, et al. (2008). "Quantitative somatic sensory testing and functional imaging of the response to painful stimuli before and after cingulotomy for obsessive-compulsive disorder (OCD)." Eur J Pain **12**(8): 990-999.

Kim, C. H., J. W. Chang, et al. (2003). "Anterior cingulotomy for refractory obsessive-compulsive disorder." Acta Psychiatr Scand **107**(4): 283-290.

Kim, J. J., M. C. Lee, et al. (2001). "Grey matter abnormalities in obsessive-compulsive disorder: statistical parametric mapping of segmented magnetic resonance images." Br J Psychiatry **179**: 330-334.

Kim, M. C., T. K. Lee, et al. (2002). "Review of long-term results of stereotactic psychosurgery." Neurol Med Chir (Tokyo) **42**(9): 365-371.

Kunishio, K. and S. N. Haber (1994). "Primate cingulostriatal projection: limbic striatal versus sensorimotor striatal input." J Comp Neurol **350**(3): 337-356.

Lancaster, J. L., D. Tordesillas-Gutierrez, et al. (2007). "Bias between MNI and Talairach coordinates analyzed using the ICBM-152 brain template." Hum Brain Mapp **28**(11): 1194-1205.

Lancaster, J. L., M. G. Woldorff, et al. (2000). "Automated Talairach atlas labels for functional brain mapping." Hum Brain Mapp **10**(3): 120-131.

Liu, K., H. Zhang, et al. (2008). "Stereotactic treatment of refractory obsessive compulsive disorder by bilateral capsulotomy with 3 years follow-up." J Clin Neurosci **15**(6): 622-629.

Maltby, N., D. F. Tolin, et al. (2005). "Dysfunctional action monitoring hyperactivates frontal-striatal circuits in obsessive-compulsive disorder: an event-related fMRI study." Neuroimage **24**(2): 495-503.

Mataix-Cols, D., A. Pertusa, et al. (2007). "Issues for DSM-V: how should obsessive-compulsive and related disorders be classified?" Am J Psychiatry **164**(9): 1313-1314.

Mataix-Cols, D., M. C. Rosario-Campos, et al. (2005). "A multidimensional model of obsessive-compulsive disorder." Am J Psychiatry **162**(2): 228-238.

Mataix-Cols, D. and O. A. van den Heuvel (2006). "Common and distinct neural correlates of obsessive-compulsive and related disorders." Psychiatr Clin North Am **29**(2): 391-410, viii.

Mataix-Cols, D., S. Wooderson, et al. (2004). "Distinct neural correlates of washing, checking, and hoarding symptom dimensions in obsessive-compulsive disorder." Arch Gen Psychiatry **61**(6): 564-576.

Mechelli, A., C. J. Price, et al. (2005). "Voxel-based morphometry of the human brain: methods and applications." Curr Med Imag Rev **1**(2): 105-113.

Menzies, L., S. Achard, et al. (2007). "Neurocognitive endophenotypes of obsessive-compulsive disorder." Brain **130**(Pt 12): 3223-3236.

Menzies, L., S. R. Chamberlain, et al. (2008). "Integrating evidence from neuroimaging and neuropsychological studies of obsessive-compulsive disorder: the orbitofronto-striatal model revisited." Neurosci Biobehav Rev **32**(3): 525-549.

Menzies, L., G. B. Williams, et al. (2008). "White matter abnormalities in patients with obsessive-compulsive disorder and their first-degree relatives." Am J Psychiatry **165**(10): 1308-1315.

Nuttin, B. J., L. A. Gabriels, et al. (2003). "Long-term electrical capsular stimulation in patients with obsessive-compulsive disorder." Neurosurgery **52**(6): 1263-1272.

Perani, D., C. Colombo, et al. (1995). "[18F]FDG PET study in obsessive-compulsive disorder. A clinical/metabolic correlation study after treatment." Br J Psychiatry **166**(2): 244-250.

Pujol, J., C. Soriano-Mas, et al. (2004). "Mapping structural brain alterations in obsessive-compulsive disorder." Arch Gen Psychiatry **61**(7): 720-730.

Rapoport, J. L. and S. P. Wise (1988). "Obsessive-compulsive disorder: evidence for basal ganglia dysfunction." Psychopharmacol Bull **24**(3): 380-384.

Rauch, S. L., D. D. Dougherty, et al. (2006). "A functional neuroimaging investigation of deep brain stimulation in patients with obsessive-compulsive disorder." J Neurosurg **104**(4): 558-565.

Rauch, S. L., M. A. Jenike, et al. (1994). "Regional cerebral blood flow measured during symptom provocation in obsessive-compulsive disorder using oxygen 15-labeled carbon dioxide and positron emission tomography." Arch Gen Psychiatry **51**(1): 62-70.

Rauch, S. L., H. Kim, et al. (2000). "Volume reduction in the caudate nucleus following stereotactic placement of lesions in the anterior cingulate cortex in humans: a morphometric magnetic resonance imaging study." J Neurosurg **93**(6): 1019-1025.

Riffkin, J., M. Yucel, et al. (2005). "A manual and automated MRI study of anterior cingulate and orbito-frontal cortices, and caudate nucleus in obsessive-compulsive disorder: comparison with healthy controls and patients with schizophrenia." Psychiatry Res **138**(2): 99-113.

Robinson, D., H. Wu, et al. (1995). "Reduced caudate nucleus volume in obsessive-compulsive disorder." Arch Gen Psychiatry **52**(5): 393-398.

Rosenberg, D. R., F. P. MacMaster, et al. (2000). "Decrease in caudate glutamatergic concentrations in pediatric obsessive-compulsive disorder patients taking paroxetine." J Am Acad Child Adolesc Psychiatry **39**(9): 1096-1103.

Salimi-Khorshidi, G., S. M. Smith, et al. (2009). "Meta-analysis of neuroimaging data: A comparison of image-based and coordinate-based Pooling of studies." Neuroimage **45**(3): 810-823.

Saxena, S., A. L. Brody, et al. (2004). "Cerebral glucose metabolism in obsessive-compulsive hoarding." Am J Psychiatry **161**(6): 1038-1048.

Saxena, S., A. L. Brody, et al. (1998). "Neuroimaging and frontal-subcortical circuitry in obsessive-compulsive disorder." Br J Psychiatry Suppl(35): 26-37.

Scarone, S., C. Colombo, et al. (1992). "Increased right caudate nucleus size in obsessive-compulsive disorder: detection with magnetic resonance imaging." Psychiatry Res **45**(2): 115-121.

Soriano-Mas, C., J. Pujol, et al. (2007). "Identifying patients with obsessive-compulsive disorder using whole-brain anatomy." Neuroimage **35**(3): 1028-1037.

Spangler, W. J., G. R. Cosgrove, et al. (1996). "Magnetic resonance image-guided stereotactic cingulotomy for intractable psychiatric disease." Neurosurgery **38**(6): 1071-1076.

Stroup, D. F., J. A. Berlin, et al. (2000). "Meta-analysis of observational studies in epidemiology: a proposal for reporting. Meta-analysis Of Observational Studies in Epidemiology (MOOSE) group." JAMA **283**(15): 2008-2012.

Swedo, S. E., M. B. Schapiro, et al. (1989). "Cerebral glucose metabolism in childhood-onset obsessive-compulsive disorder." Arch Gen Psychiatry **46**(6): 518-523.

Szeszko, P. R., C. Christian, et al. (2008). "Gray Matter Structural Alterations in Psychotropic Drug-Naive Pediatric Obsessive-Compulsive Disorder: An Optimized Voxel-Based Morphometry Study." Am J Psychiatry **165**(10): 1299-1307.

Turkeltaub, P. E., G. F. Eden, et al. (2002). "Meta-analysis of the functional neuroanatomy of single-word reading: method and validation." Neuroimage **16**(3 Pt 1): 765-780.

Ursu, S., V. A. Stenger, et al. (2003). "Overactive action monitoring in obsessive-compulsive disorder: evidence from functional magnetic resonance imaging." Psychol Sci **14**(4): 347-353.

Valente, A. A., Jr., E. C. Miguel, et al. (2005). "Regional gray matter abnormalities in obsessive-compulsive disorder: a voxel-based morphometry study." Biol Psychiatry **58**(6): 479-487.

van den Heuvel, O. A., P. L. Remijnse, et al. (2009). "The major symptom dimensions of obsessive-compulsive disorder are mediated by partially distinct neural systems." Brain **132**(Pt 4): 853-868.

Wager, T. D., M. Lindquist, et al. (2007). "Meta-analysis of functional neuroimaging data: current and future directions." Soc Cogn Affect Neurosci **2**(2): 150-158.

Yoo, S. Y., M. S. Roh, et al. (2008). "Voxel-based morphometry study of gray matter abnormalities in obsessive-compulsive disorder." J Korean Med Sci **23**(1): 24-30.

Yucel, M., B. J. Harrison, et al. (2007). "Functional and biochemical alterations of the medial frontal cortex in obsessive-compulsive disorder." Arch Gen Psychiatry **64**(8): 946-955.

CHAPTER 3

Implementation of the general linear model

3.1 THEORY

Chapter 2 presented the *signed differential mapping* (SDM) method for voxelwise meta-analyzing neuroimaging studies, and introduced the use of meta-regression by which the effects of a modulator (such as the mean symptom severity of the patients) could be studied (Radua and Mataix-Cols 2009). However, the original version of the method did not include the possibility of fitting more complex models such as multiple meta-regressions, meta-analytic comparisons of several groups of patients or the addition of covariates. This chapter introduces the general linear model to the SDM method, thus allowing multiple meta-regressions, comparisons of several groups of patients as well as the inclusion of covariates.

3.1.1. The general linear model

The *general linear model* (GLM) is a generalization of several statistical tests aimed to assess differences between groups (e.g. equal-variance Student's t-test and ANOVA) or linear relationships (e.g. simple and multiple linear regressions). Interestingly, the GLM allows combination of several group classifications and continuous variables in the same model.

Briefly, the GLM may be understood as a multiple regression in which categorical groups are coded as binary variables. For example, a comparison between two groups may be equivalently assessed by an equal-variance Student's t-test or by a simple regression in which the value of the regressor is 0 for individuals in one group and 1 for individuals in the other group, so that the regressor assesses the differences between both groups.

Multiple regressions, and thus GLM, may be written as:

$$\begin{pmatrix} y_1 = x_{11} \cdot \beta_1 + \ldots + x_{1m} \cdot \beta_m + \varepsilon_1 \\ \vdots \\ y_n = x_{n1} \cdot \beta_1 + \ldots + x_{nm} \cdot \beta_m + \varepsilon_n \end{pmatrix}$$

which may be rewritten in matrix form as:

$$Y = X \cdot \beta + U$$

where

$$Y = \begin{pmatrix} y_1 \\ \vdots \\ y_n \end{pmatrix},\ X = \begin{pmatrix} x_{11} & \cdots & x_{1m} \\ \vdots & & \vdots \\ x_{n1} & \cdots & x_{nm} \end{pmatrix},\ \beta = \begin{pmatrix} \beta_1 \\ \vdots \\ \beta_m \end{pmatrix},\ U = \begin{pmatrix} \varepsilon_1 \\ \vdots \\ \varepsilon_n \end{pmatrix}$$

A common approach to solve this system consists in discarding *U* and finding the value of *β*:

$$X \cdot \beta = Y$$
$$X^T \cdot X \cdot \beta = X^T \cdot Y$$
$$\beta = \left(X^T \cdot X\right)^{-1} \cdot X^T \cdot Y$$

Once the values of *β* have been estimated, a series of contrasts may be used to statistically assess the hypotheses of interest. For example, in the abovementioned comparison between two groups, we would be interested in whether the difference between the groups, β_1, is different than zero, so that the contrast to test would be:

$$\left(\beta_1 = 0\right)$$

which may be rewritten in matrix form as:

$$H \cdot \beta = O$$

where

$$H = \begin{pmatrix} 0 & 1 \end{pmatrix},\ \beta = \begin{pmatrix} \beta_0 \\ \beta_1 \end{pmatrix},\ O = \begin{pmatrix} 0 \\ 0 \end{pmatrix}$$

Creating such a contrast may seem unnecessary for this simple comparison, as we could just assess whether β_1 is different than 0. However, contrasts allow the assessment of more complex hypotheses. If we aimed to assess whether there are differences between three groups, for instance, we could code the difference between the second and the first groups with β_1, and the difference between the third and the first groups with β_2. Then, the null hypotheses would be:

$$\begin{pmatrix} \beta_1 = 0 \\ \beta_2 = 0 \end{pmatrix}$$

which may be rewritten in matrix form as:

$$H \cdot \beta = O$$

where

$$H = \begin{pmatrix} 0 & 1 & 0 \\ 0 & 0 & 1 \end{pmatrix},\ \beta = \begin{pmatrix} \beta_0 \\ \beta_1 \\ \beta_2 \end{pmatrix},\ O = \begin{pmatrix} 0 \\ 0 \\ 0 \end{pmatrix}$$

Relevantly, this contrast allows the assessment of both hypotheses at once, i.e. equivalent to a classic one-way ANOVA. Indeed, the assessment of the contrast is also conducted with an ANOVA and its F statistic.

3.1.2. Implementation in SDM meta-analyses

To implement GLM in the SDM algorithms presented in Chapter 2, formulas above had to be modified in order that each study is weighted by the square root of its sample size.

This was achieved by including a weighting diagonal matrix *W*:

$$X \cdot \beta = Y$$
$$X^T \cdot W \cdot X \cdot \beta = X^T \cdot W \cdot Y$$
$$\beta = \left(X^T \cdot W \cdot X\right)^{-1} \cdot X^T \cdot W \cdot Y$$

This formula can be rewritten after substitution of *Y* by the SDM values of the studies in the i[th] voxel, and *β* by $SDM_{i\beta}$, as:

$$SDM_{i\beta} = \left(X^T \cdot W \cdot X\right)^{-1} \cdot X^T \cdot W \cdot SDM_i$$

or simply:

$$SDM_{i\beta} = A \cdot SDM_i$$

where

$$A = \left(X^T \cdot W \cdot X\right)^{-1} \cdot X^T \cdot W$$

Contrast assessment had to be modified as well, so that multiple hypotheses are statistically assessed with the meta-analytic Q statistic (Cochran 1954) rather than with the F statistic. The formula of the Q statistic for the first two coefficients (1:2) is:

$$Q = SDM^{T}_{i\beta,1:2} \cdot B^{-1}_{1:2,1:2} \cdot SDM_{i\beta,1:2}$$

where

$$B = \left(X^{T} \cdot W \cdot X\right)^{-1}$$

This Q statistic should not be confounded with the *heterogeneity* Q statistic presented in the next chapter.

3.1.3 Considerations on the statistical significance

The statistical significance of complex models should be taken with caution. On the one hand there is increased risk of false positives in case of multiple contrasts. Bonferroni or other approaches could be useful in these cases. On

the other hand, the statistical significance of some contrasts may be overshadowed by the abnormalities present in the main meta-analyses. This issue is developed further below.

If a region is reported as abnormal in several studies, SDM values in a voxel of the region will probably range from 0 (in studies no reporting abnormalities) to relatively high values (in studies reporting an abnormality), thus allowing a potentially correct estimation of the contrasts of interest. Conversely, if a region is not reported abnormal in any study, SDM values will be constant (i.e. null) and thus coefficients other than the intercept will be estimated to be null. In other words, the power to detect complex effects is higher in those regions that show abnormalities than in those regions that do not.

Unfortunately, false negative rates in regions with no reported abnormalities cannot be reduced by using more liberal thresholds, because contrasts will be estimated to be null independently of the threshold. However, false positive rates in regions with reported abnormalities may be minimized by using more conservative thresholds. Thus, it is strongly recommended to use conservative thresholds in contrasts whose statistical significance may be potentially inflated such as meta-regressions.

3.2 EXAMPLE: APPLICATION OF THE METHOD

To illustrate the practical uses of the implementation of the general linear model, this section describes a meta-analytical comparison of voxel-based morphometry studies in obsessive-compulsive disorder (OCD) vs. other anxiety disorders.

This study was published in the *Archives of General Psychiatry* under the title '*Meta-analytical comparison of voxel-based morphometry studies in OCD vs. other anxiety disorders*' (Joaquim Radua, Odile A van den Heuvel, Simon A Surguladze and David Mataix-Cols 2010; 67:701-711). The definitive publisher-authenticated version is available online at http://archpsyc.jamanetwork.com/article.aspx?articleid=211201

3.2.1 Introduction

Obsessive-compulsive disorder (OCD) is a common and disabling form of mental illness characterized by frequent obsessions and/or compulsions that are associated with high levels of distress and interference. Obsessive-compulsive disorder is currently classified as an anxiety disorder in the *DSM-IV-TR* (APA 2000). In the *International Statistical Classification of Diseases, 10th Revision* (WHO 1992), OCD is not listed as an anxiety disorder but remains classified under the broad umbrella of "neurotic, stress-related, and somatoform

disorders," thus recognizing the historical inter-relationship between OCD and anxiety and their association with psychological distress.

Consistent with this classification, OCD shares many features with other anxiety disorders (OADs), such as excessive fear of disorder-specific situations, dysfunctional over-estimation of threat, avoidance/escape and safety-seeking behaviours, and increased physiological arousal (Storch, Abramowitz et al. 2008). Family studies show that OADs (particularly generalized anxiety disorder and agoraphobia), are more common in relatives of OCD-affected probands than in relatives of control probands, even after controlling for relative OCD diagnosis and proband diagnosis of the same anxiety disorder (Black, Noyes et al. 1992; Nestadt, Samuels et al. 2001; Bolton, Rijsdijk et al. 2007). A recent twin study showed that OCD shares a substantial proportion (55%) of its genetic liability with OADs but also has appreciable disorder-specific genetic and shared environmental influences (Tambs, Czajkowsky et al. 2009). Furthermore, OCD and OADs often respond to broadly similar pharmacological (selective serotonin reuptake inhibitors) and psychological (exposure-based) interventions. However, the status of OCD as an anxiety disorder has also been challenged in different ways over the years. Some suggested that OCD may be closer to the affective (Insel 1982) or even psychotic (Enright and Beech 1990) spectrum of disorders. More recently, a reclassification of OCD has been proposed whereby OCD should be removed from the anxiety disorders category on the basis that OCD is uniquely characterized by the presence of repetitive behaviours and the inability to resist urges and impulses (Hollander, Braun et al. 2008). According to this view, obsessions and compulsions are the core

features of OCD and anxiety, simply an epiphenomenon. Furthermore, it is suggested that a new grouping is created that includes OCD as well as other disorders that are thought to share phenomenological and other features with OCD and that are currently classified elsewhere in the DSM (Hollander, Braun et al. 2008). Remarkably, a recent survey among worldwide OCD experts revealed a clear lack of consensus regarding whether OCD should remain or be removed from the anxiety disorders category in the DSM-V (Mataix-Cols, Pertusa et al. 2007).

The research agenda for the DSM-V emphasizes the importance of applying the findings from basic and clinical neurosciences to guide psychiatric classification (APA, Kupfer et al. 2002). Neuroimaging tools have the potential to assist in such endeavours but, surprisingly, direct comparisons of brain function and structure between OCD and OADs are extremely rare (Rauch, Savage et al. 1997; van den Heuvel, Veltman et al. 2005). This paucity of data is partially due to different traditions in OCD and OADs research and the use of different experimental paradigms making comparisons difficult and precluding the establishment of a solid neuroscientific basis for classification (Mataix-Cols and van den Heuvel 2006). Indeed, while neuroimaging research in OCD has been long dominated by a predominant focus on the ventral prefrontal-striatal circuits, neuroimaging work in OADs has primarily focused on the amygdala-hippocampus complex and related limbic regions (Mataix-Cols and van den Heuvel 2006).

Structural magnetic resonance imaging studies are potentially more amenable to comparisons across the anxiety disorders because they are

paradigm-free but are not without their problems. Many morphometric studies in OCD and OADs have used manual or semi-automated methods to measure the volumes of brain regions defined a priori as being “abnormal”, therefore preventing the exploration of other brain regions potentially implicated in these disorders. The recent advent of fully-automated, whole-brain, voxel-based morphometry (VBM) methods (Ashburner and Friston 2000; Ashburner and Friston 2001; Mechelli, Price et al. 2005), which overcome some of the limitations of the region of interest approach, provide a powerful and unbiased tool to study the neural substrates of psychiatric disorders. Unfortunately, recent applications of these novel methods are often limited by relatively small sample sizes, resulting in insufficient statistical power and increased risk of false-positive results. Recently developed voxel-based meta-analytical methods have the potential to quantify the reproducibility of neuroimaging findings and to generate insights difficult to observe in isolated studies (Costafreda, David et al. 2009).

In this study, an exhaustive search of all published and unpublished VBM studies in all anxiety disorders was conducted, and the general SDM algorithms presented in Chapter 2 (Radua and Mataix-Cols 2009) plus the methods described at the beginning of the chapter were applied to examine the extent to which OCD shares neural substrates with OADs. The null hypothesis assumed that no differences in regional grey matter volumes would be found between OCD and OADs. To facilitate replication and further analyses by other colleagues, a readily accessible online database, which contains all the data

and methodological details from every study included in this meta-analysis, was also developed.

3.2.2 Methods

3.2.2.1 Inclusion of studies

Exhaustive literature searches of relevant articles published between 2001 (the date of the first VBM study in any anxiety disorder) and 2009 were conducted using the PubMed, ScienceDirect and Scopus databases. The search key words were “anxiety disorder,” “obsessive-compulsive disorder,” “panic disorder,” “agoraphobia,” “phobia,” and “stress disorder,” plus “morphometry,” “voxel-based.” or “voxelwise.” The key word “phobia” was intended to retrieve both specific and social phobias, and the key word “stress disorder” was intended to retrieve both acute stress disorder and posttraumatic stress disorder (PTSD). In addition, manual searches of the reference sections of the obtained articles were also conducted. Studies containing duplicated datasets, i.e. analyzed the same data in different articles and studies with fewer than 9 patients were excluded. Next, the corresponding authors were contacted by e-mail requesting any detail not included in the original manuscripts. MOOSE guidelines for meta-analyses of observational studies (Stroup, Berlin et al. 2000) were followed in the study.

3.2.2.2 Comparison of global grey matter volumes

Meta-analytical differences in global grey matter volumes were calculated using random-effects models with the MiMa function (Viechtbauer 2006) in R (R Development Core Team 2008).

3.2.2.3 Comparison of regional grey matter volumes

Regional differences in grey matter volume between patients and controls were analyzed using the general SDM algorithms presented in Chapter 2 (Radua and Mataix-Cols 2009) plus the methods described at the beginning of this chapter. An omnibus test (Q statistic (Cochran 1954)) was first employed to determine if there were differences in grey matter across the different anxiety disorders. Specifically, the Q statistic of the "anxiety disorder" factor was calculated in each voxel as it is usually calculated in standard meta-analyses, with the only difference that its statistical significance was determined by means of a randomization test (Radua and Mataix-Cols 2009). Age, percentage of male patients, age at onset, percentage of patients receiving medication and percentage of patients with comorbid major depressive disorder were considered potential confounders and included as covariates if they showed relevant differences across the different anxiety disorders (Cohen $f \geq 0.27$ for continuous variables; Cramer $\varphi \geq 0.21$ for binary variables). Missing values in these variables were obtained by imputation of the mean of the corresponding disorder. Variables with 20% or more missing values were discarded. Age of patients was included in its linear and quadratic forms (age + age squared, the

latter obtained from age sample mean and variance), as the developmental trajectories of some regions such as the medial prefrontal cortex are not linear (Shaw, Lerch et al. 2006). Brain regions with significant main effects of anxiety disorder were used to classify the disorders into 2 (or more) grey-matter-based groups of disorders.

Next, standard SDM meta-analyses (Radua and Mataix-Cols 2009) were conducted separately in each group of disorders to describe the differences in grey matter between patients and healthy controls. These were complemented with additional analyses to assess the robustness of the findings (Radua and Mataix-Cols 2009). These included descriptive analyses of quartiles to find the actual proportion of studies reporting results in a particular brain region (regardless of p-values) and jack-knife sensitivity analyses to assess the replicability of the results. Finally, whole-brain differences in grey matter volume between groups of disorders were formally tested by calculating the difference between both groups of disorders in each voxel and determining its statistical significance using a randomization test (Radua and Mataix-Cols 2009).

All analyses were conducted twice: first including all samples and subsequently including adult samples only.

Figure 3.1 Inclusion of studies.

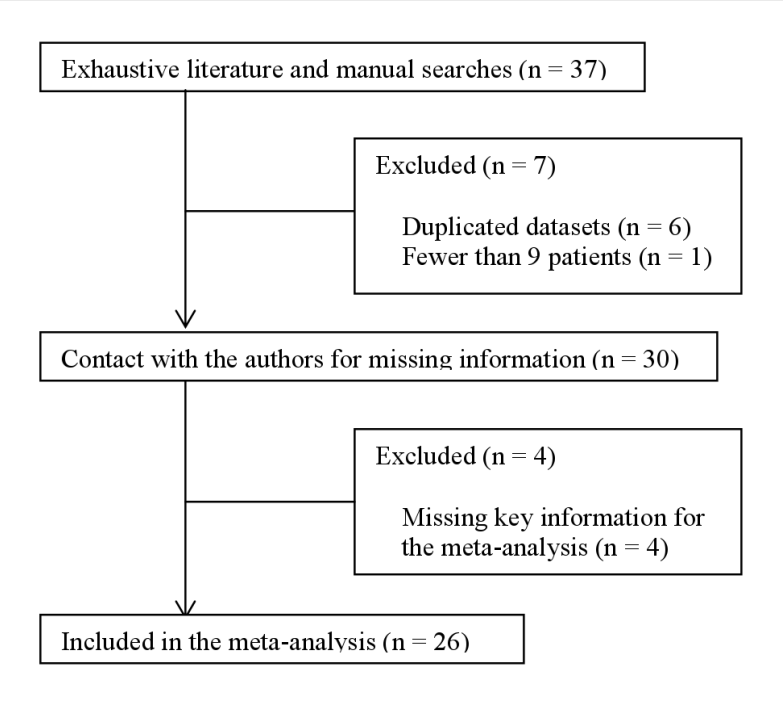

3.2.3 Results

3.2.3.1 Included studies and sample characteristics

As shown in **Figure 3.1**, the search retrieved a total of 37 studies (17 OCD; 8 panic disorder [PD]; 11 PTSD; 1 various anxiety disorders). Seven studies were discarded because they contained duplicated datasets (Cardoner, Soriano-Mas et al. 2007; Li, Chen et al. 2007; Soriano-Mas, Pujol et al. 2007; Asami, Hayano et al. 2008; Uchida, Del-Ben et al. 2008; Chen, Li et al. 2009) or fewer than 9 patients (Cecconi, Lopes et al. 2008).

After contacting the authors no methodological ambiguities remained regarding the design or analysis of 26 studies (14 OCD; 5 PD; 6 PTSD; 1 various anxiety disorders), while 4 had to be excluded because of missing key information for our meta-analysis (i.e. peak coordinates from whole-brain analyses) (Emdad, Bonekamp et al. 2006; Jatzko, Rothenhofer et al. 2006; Protopopescu, Pan et al. 2006; Bryant, Felmingham et al. 2008). Therefore, 26 high-quality studies could be included in this meta-analysis, of which 25 were published or accepted for publication and 1 was a previously unpublished sub-analysis within a published article (Soriano-Mas, Pujol et al. 2007) (new sample). Twelve of the 14 OCD studies were included in our previous meta-analysis conducted in December 2008 (Radua and Mataix-Cols 2009).

Because the samples from 2 studies (Asami, Yamasue et al. 2009; Hayano, Nakamura et al. 2009) partially overlapped, the meta-analysis was conducted twice, i.e. once with each study. Since the results were identical, only the results including the first of these studies are reported (Asami, Yamasue et al. 2009).

Combined, the studies included 639 patients with anxiety disorders (430 with OCD, 106 with PD, 86 with PTSD, and 17 patients from a study on various anxiety disorders) and 737 healthy controls. The demographic and clinical characteristics of the participants in each study are shown in **Table 3.1**. Further details and methodological aspects of each of the included studies can be found at http://www.sdmproject.com/database .

Table 3.1 Demographic and clinical characteristics of the 26 voxel-based morphometry studies included in the meta-analysis.

	Patients					Controls		
	Sample size	Age, y, Mean (SD)	Males, %	Antidepressant Treatment, %	Comorbid MDD, %	Sample size	Age, y, Mean (SD)	Males, %
OCD studies								
Carmona *et al.*	18	12.9 (2.8)	72	56	0	18	13.0 (3.0)	72
Christian *et al.*	21	38.0 (9.6)	71	81	33	21	38.9 (9.8)	71
Gilbert *et al.*	25	37.5 (10.7)	52	80	36	20	29.8 (7.9)	45
Gilbert *et al*	10	12.9 (2.7)	60	0	0	10	13.4 (2.6)	60
Kim *et al.*	25	27.4 (7.0)	68	0	16	25	27.0 (6.2)	68
Koprivova *et al.*	14	28.6 (6.1)	36	71	0	15	28.7 (6.5)	40
Lazaro *et al.*	15	13.7 (2.5)	53	0	0	15	14.3 (2.5)	53
Pujol *et al.*	72	29.8 (10.5)	56	75	36	72	30.1 (10.2)	56
Riffkin *et al.*	18	36.1 (13.0)	44	17	N/A	18	34.5 (11.8)	44
Soriano-Mas *et al.*	30	31.9 (9.3)	70	87	13	30	31.8 (10.2)	53
Szeszko *et al.*	37	13.0 (2.7)	38	0	0	26	13.0 (2.6)	35
Valente *et al.*	19	32.7 (8.8)	53	58	47	15	32.3 (11.8)	47
van den Heuvel *et al.*	55	33.7 (9.2)	29	0	18	50	31.4 (7.6)	40
Yoo *et al.*	71	26.6 (7.5)	66	83	6	71	26.7 (6.1)	66
Subtotal	430	27.9 (11.5)	54	49	18[a]	406	27.4 (10.5)	54
PD studies								
Asami *et al.*	24	37.0 (10.2)	38	80	13	24	37.0 (9.5)	38
Hayano *et al.*	27	38.2 (9.9)	37	89	11	30	35.3(10.5)	30
Massana *et al.*	18	36.8 (11.3)	39	N/A	0	18	36.7 (8.8)	44
Uchida *et al.*	19	37.1 (9.8)	16	74	63	20	36.5 (9.9)	20
Yoo *et al.*	18	33.3 (7.1)	50	N/A	0	18	32.0 (5.8)	61
Subtotal[b]	79	36.1 (9.7)	35	77[a]	19	80	35.7 (8.8)	40
PTSD studies								
Carrion *et al.*	19	11.5 (3.7)	58	26	11	22	11.1 (2.6)	55
Chen *et al.*	12	34.6 (4.9)	33	0	0	12	33.2 (5.3)	33
Corbo *et al.*	14	33.4 (12.1)	43	0	50	14	33.3 (12.3)	43
Hakamata *et al.*	14	45.6 (6.2)	0	0	50	100	47.1 (5.7)	0
Kasai *et al.*	18	52.8 (3.4)	100	N/A	56	23	51.8 (2.3)	100
Yamasue *et al.*	9	44.6 (16.0)	56	0	11	16	44.4 (14.0)	63
Subtotal	86	35.9 (16.7)	51	7[a]	31	187	41.3 (14.0)	29
Various anxiety disorders								
Milham *et al.*	17	12.9 (2.3)	47	0	24	34	12.4 (2.2)	47

N/A: not available; MDD: major depressive disorder; OCD: obsessive-compulsive disorder; PD: panic disorder; PTSD: posttraumatic stress disorder. SD: standard deviation.
[a]Result obtained after imputation of missing values using the mean of the corresponding disorder.
[b]Result obtained after excluding the study by Hayano *et al.*

No relevant differences between patients and controls were found in terms of age and sex, as the original studies were already well matched in this respect (**Table 3.1**). Because the age of the patients, as well as the percentage of patients receiving antidepressant medication, moderately varied across the different anxiety disorders (Cohen f = 0.30 and Cramer φ = 0.27, respectively), these potential confounds were controlled by including age, age squared, and percentage of patients receiving antidepressant medication as covariates in the omnibus test. Other reported medications were infrequent: anxiolytics (4.7%),

amphetamines (0.5%), antipsychotics (n=1), guanfacine hydrochlorid (n=1), lithium (n=1), and thyroxine (n=1).

The percentages of male and depressed patients were rather similar in the different disorders (Cramer φ = 0.09 and 0.11, respectively) and thus not included as covariates. Mean age at onset could not be considered because of a large proportion (44%) of missing values.

Regarding comorbidity, 3.5% patients from OCD studies and 5.6% patients from PTSD studies had comorbid PD. One patient from a PTSD study had comorbid OCD, and 1 patient from an OCD study had comorbid PTSD. With the exception of major depressive episode (**Table 3.1**), other individual comorbid disorders were relatively infrequent: generalized anxiety disorder, 6.3%; social phobia, 4.9%; and specific phobias, 1.9%.

3.2.3.2 Global differences in grey matter volume

Global grey matter volumes were obtained from 13 studies (9 OCD; 2 PD; 2 PTSD) (Kim, Lee et al. 2001; Pujol, Soriano-Mas et al. 2004; Valente, Miguel et al. 2005; Carmona, Bassas et al. 2007; Hakamata, Matsuoka et al. 2007; Szeszko, Christian et al. 2008; Uchida, Del-Ben et al. 2008; Yoo, Roh et al. 2008; Asami, Yamasue et al. 2009; Carrion, Weems et al. 2009; Koprivova , Hor cek et al. 2009; Lazaro, Bargallo et al. 2009; van den Heuvel, Remijnse et al. 2009). Comparisons across disorders and analyses in individual disorders other than OCD were not possible, as there were too few PD and PTSD studies

Table 3.2 Regions with significant differences in grey matter volumes across anxiety disorders (omnibus test)[a]

	Talairach Coordinates, x, y, z	*P* value[b]	Number of voxels[c]	OCD vs. controls	PD vs. controls	PTSD vs. controls
Left lenticular nucleus (mainly anterior putamen)	-24, 6, 0	< 0.001	286	+0.210	-0.199	-0.215
Right caudate head (extending to lenticular nucleus)	14, 16, 0	< 0.001	287	+0.143	-0.368	-0.009

Abbreviations: OCD, obsessive-compulsive disorder; PD, panic disorder; PTSD, posttraumatic stress disorder; SDM, signed differential mapping.
[a]Values in the OCD, PD and PTSD columns represent the difference in grey matter volume (SDM value) in patients vs. controls. Positive values represent increases and negative values represent decreases.
[b]*P* values were obtained from a randomization test (Radua and Mataix-Cols 2009).
[c]1 voxel = 8mm^3.

for analysis. No statistically significant differences in global grey matter volume were found between patients with OCD (n=326) and healthy controls (n=307) (unbiased Hedges (Hedges and Olkin 1985) *d* = -0.19; z = -1.51; P = 0.13). The same results emerged when the 3 paediatric OCD studies were excluded from the analysis (unbiased Hedges *d* = -0.15; z = -1.61; P = 0.11).

3.2.3.3 Regional differences in grey matter volume across anxiety disorders

Data for this analysis were obtained from 24 studies (14 OCD; 4 PD; 6 PTSD) including 595 patients (430 OCD; 79 PD; 86 PTSD) and 673 healthy controls. There was a main effect of anxiety disorder factor on grey matter volume in the left lenticular nucleus (mainly the anterior putamen) and right caudate extending to the lenticular nucleus (mainly the anterior putamen) (**Table 3.2**). When age was introduced as a linear covariate, the results remained unchanged but additional differences were also observed in a small bilateral region in the

Figure 3.2 Common and distinct neural correlates in obsessive-compulsive disorder (OCD) and other anxiety disorders (OADs).

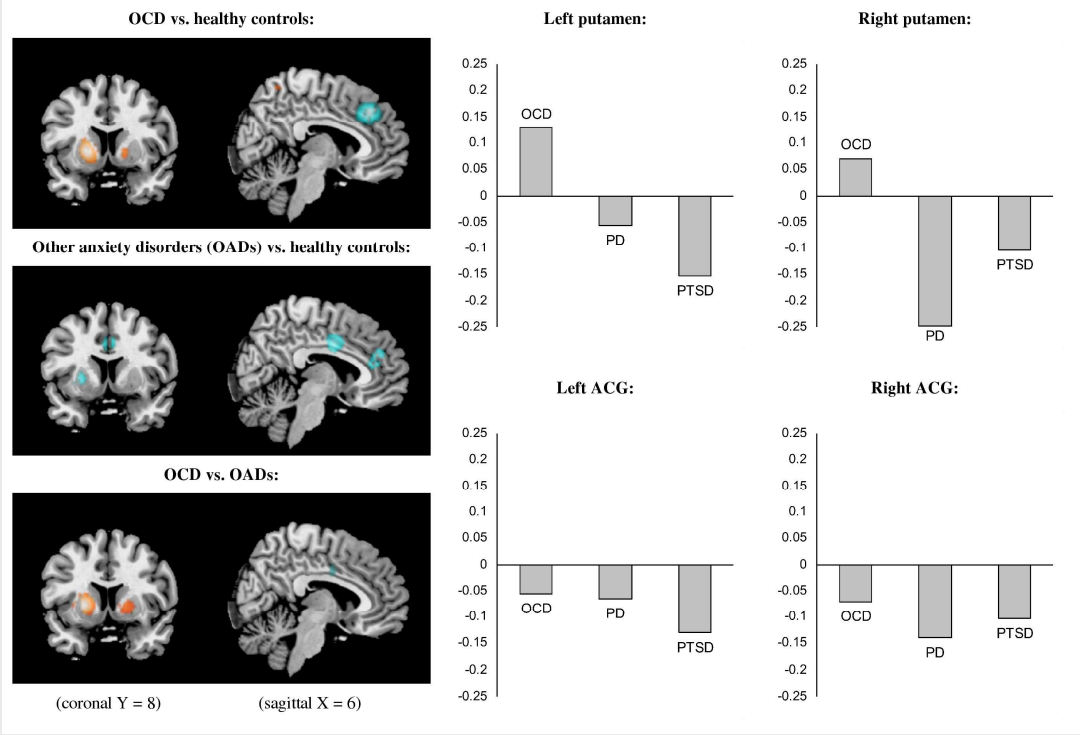

A, The coronal slices show significant differences across the different anxiety disorders in the bilateral lenticular nuclei (mainly the anterior putamen), with increased grey matter volume (orange) in OCD (first row) and decreased volume (cyan) in OADs (second row). The formal comparison between OCD and OADs confirmed these differences (third row). The sagittal slices show similarly decreased grey matter volumes in the dorsomedial frontal gyrus/anterior cingulate gyrus (ACG) region in the different anxiety disorders. Statistical threshold was set at $P \leq 0.001$ and significant clusters have been overlaid on an MRIcron template (http://www.mricro.com/mricron) for display purposes only. B, The bar graphs show the signed differential mapping (SDM) values of grey matter volume (as compared with healthy controls) in the putamen (first row) and ACG (second row) in each disorder derived from the omnibus test. PD indicates panic disorder; PTSD, posttraumatic stress disorder.

ventro-medial frontal gyri Brodmann area 11/32 (Talairach coordinates [x,y,z] 4,32,-12; P < 0.001; 46 voxels). When quadratic age (i.e. age + age squared) or the percentage of patients receiving antidepressant medication were introduced in the model, the results remained unchanged, i.e. only the left lenticular and right caudate (extending to lenticular) nuclei were significantly different across anxiety disorders. Finally, when 6 paediatric studies were excluded, the results also remained unchanged.

These omnibus tests were followed by inspection of grey matter volumes in the basal ganglia in OCD, PD and PTSD. As shown in **Table 3.2** and **Figure 3.2**, patients with OCD showed increased grey matter in the bilateral lenticular/caudate nuclei compared with controls, while both PD and PTSD showed decreased grey matter volume in these regions compared with controls.

3.2.3.4 Regional differences in grey matter volume: OCD vs. healthy controls

Data for this analysis were obtained from all 14 studies on OCD representing 430 patients and 406 healthy controls. Consistent with the meta-analysis presented in Chapter 1, which included 12 of the 14 OCD studies available at that time (Radua and Mataix-Cols 2009), patients with OCD showed robust increased regional grey matter volumes in the bilateral lenticular / caudate nuclei and right superior parietal lobule. Decreased grey matter volumes were found in the bilateral dorso-medial frontal gyrus (dMFG) / anterior cingulate gyrus (ACG) (**Table 3.3** and **Figure 3.2**). Results were similar after exclusion of 4 paediatric OCD studies, with increased grey matter volumes in the left lentiform / caudate nucleus and decreased grey matter volumes in the bilateral dMFG/ACG.

Table 3.3 Regions with significant differences in grey matter volume between patients with OCD and healthy controls.

	Maximum			Cluster[a]	
	Talairach Coordinates x, y, z	SDM value	*P* value	Number of voxels[b]	Breakdown (number of voxels)
Clusters of increased grey matter					
Left lenticular / caudate nuclei (mainly anterior putamen)	-18, 8, 0	+0.226	< 0.001	517	Left putamen (390) Left pallidum (64) Left caudate nucleus (44)
Right superior parietal lobule	14, -58, 60	+0.182	< 0.001	66	Right BA 7 (66)
Right lenticular /caudate nuclei (mainly anterior putamen)	18, 10, -2	+0.173	< 0.001	99	Right putamen (74) Right caudate (16)
Clusters of decreased grey matter					
Bilateral dMFG/ACG	2, 30, 38	-0.257	< 0.001	426	Bilateral BA 8 (170) Bilateral BA 32 (140) Bilateral BA 6 (70) Bilateral BA 9 (46)

Abbreviations; ACG, anterior cingulate gyrus; BA, Brodmann area; dMFG, dorso-medial frontal gyrus; OCD, obsessive-compulsive disorder; SDM, signed differential mapping.
[a]Regions smaller than 10 voxels are not shown. 1 voxel = 8mm^3.
[b]*P* values were obtained from a randomization test (Radua and Mataix-Cols 2009).

The results remained largely unchanged in the analysis of quartiles with the exception of the superior parietal lobule, which was no longer significant. Whole-brain jack-knife sensitivity analysis showed that the grey matter increase in the left lenticular nucleus was highly replicable, as this finding was preserved in all combinations of studies. Grey matter decrease in the dMFG/ACG emerged in all but one combination of studies, whereas grey matter increases in the right lenticular nucleus and superior parietal lobule emerged in all but 2 combinations of studies.

3.2.3.5 Regional differences in grey matter volume: OADs vs. healthy controls

Because the omnibus test revealed similar neural substrates in PD and PTSD, these disorders were collapsed together to form a new group called OADs and

Table 3.4 Regions with significant differences in grey matter volume between patients with OADs and healthy controls.

	Maximum			Cluster[a]	
	Talairach Coordinates x, y, z	SDM value	*P* value[b]	Number of voxels	Breakdown (number of voxels)
Clusters of increased grey matter					
(none)					
Clusters of decreased grey matter					
Bilateral dMFG/ACG	-2, 36, 20	-0.266	< 0.001	231	Bilateral BA 32 (116) Bilateral BA 9 (80) Bilateral BA 24 (35)
Bilateral posterior part of the ACG	4, 0, 34	-0.251	< 0.001	205	Bilateral BA 24 (205)
Left lenticular nucleus (mainly anterior putamen)	-26, 4, 0	-0.238	< 0.001	65	Left putamen (62)

Abbreviations: ACG, anterior cingulate gyrus; BA, Brodmann area; dMFG, dorso-medial frontal gyrus; OADs, other anxiety disorders; SDM, signed differential mapping.
[a]Regions smaller than 10 voxels are not shown. 1 voxel = $8mm^3$.
[b]*P* values were obtained from a randomization test (Radua and Mataix-Cols 2009).

used in all subsequent analyses. This group also included the study by Milham et al. (Milham, Nugent et al. 2005) on various paediatric anxiety disorders, making a total of 11 studies representing 199 patients and 301 healthy controls. As shown in **Table 3.4** and **Figure 3.2**, individuals with OADs had significant grey matter volume decreases in the bilateral dMFG/ACG, bilateral posterior part of the ACG and left lenticular nucleus (mainly the rostral putamen). No increases of grey matter volume were detected. The results did not change when the study by Milham et al. (Milham, Nugent et al. 2005) or the 2 paediatric studies were excluded, but additional decreases of grey matter volume were also observed in the right insula extending to the lentiform nucleus (Talairach coordinates [x,y,z] 40,-8,2; SDM = -0.256; P = 0.001; 24 voxels) and the left middle temporal gyrus, Brodmann area 21/22 (Talairach coordinates [x,y,z] -52,-42,6; SDM = -0.254; P = 0.001; 17 voxels).

Table 3.5 Regions with significant differences in grey matter volume between patients with OCD and patients with OADs.

	Maximum			Cluster[a]	
	Talairach Coordinates x, y, z	SDM value	*P* value[b]	Number of voxels	Breakdown (number of voxels)
OCD > OADs					
Left lenticular nucleus (mainly anterior putamen)	-24, 6, 0	0.436	Undectable	651	Left putamen (472) Left pallidum (109) Left claustrum (43) Left caudate nucleus (15)
Right lenticular nucleus (mainly anterior putamen)	18, 10, -2	0.315	< 0.001	392	Right putamen (213) Right caudate nucleus (103) Right pallidum (74)
OADs > OCD					
Right dMFG/ACG	6, 24, 38	0.195	< 0.001	43	Right BA 8 (22) Right BA 32 (19)

Abbreviations: ACG, anterior cingulate gyrus; BA, Brodmann area; dMFG, dorso-medial frontal gyrus; OADs, other anxiety disorders; OCD, obsessive-compulsive disorder; SDM, signed differential mapping.
[a]Regions smaller than 10 voxels are not shown. 1 voxel = $8mm^3$.
[b]*P* values were obtained from a randomization test (Radua and Mataix-Cols 2009).

In the quartiles / median analysis, decreases of grey matter were detected in the bilateral dMFG/ACG and bilateral lenticular/caudate nuclei, meaning that most of the studies had found some degree of decreased grey matter in or near these regions. No increases of grey matter were detected in the quartiles analyses. Finally, whole-brain jack-knife sensitivity analysis showed that the grey matter decrease in the bilateral dMFG/ACG was rather replicable, as these findings were preserved in 9 of the 11 combinations of studies. Grey matter decreases in the bilateral posterior part of the ACG and left lenticular nucleus emerged in all but 3 combinations of studies.

3.2.3.6 Regional differences in grey matter volume: OCD vs. OADs

The formal comparison between OCD and OADs largely confirmed the earlier-mentioned findings (**Table 3.5** and **Figure 3.2**). Patients with OCD had significantly greater grey matter volumes than patients with OADs in the bilateral lenticular/caudate nuclei and lower grey matter volumes in a small region in the right dMFG/ACG. The age, percentage of male patients, percentage of patients receiving an antidepressant medication and percentage of depressed patients were comparable between OCD and OADs (Cohen f = 0.22 and Cramer φ = 0.07, 0.08, and 0.08, respectively) and thus not included as covariates. The results remained largely unchanged after exclusion of 6 paediatric studies, with the exception that patients with OCD had significantly greater grey matter volumes in another small region in the bilateral dMFG/ACG, Brodmann area 24 (Talairach [x,y,z] -2,-4,34; SDM = -0.308; P < 0.001; 53 voxels).

3.2.4 Discussion

While OCD is currently classified as an anxiety disorder in the DSM-IV-TR, there is a substantial disagreement in the field as to whether this should be retained in the DSM-V or whether OCD should be removed from the broad umbrella of anxiety disorders and placed elsewhere (Mataix-Cols, Pertusa et al. 2007; Hollander, Braun et al. 2008; Storch, Abramowitz et al. 2008). The neurosciences have the potential to assist classification efforts by mapping the

common and distinct neural substrates of mental disorders. Several major conclusions can be drawn from the present meta-analysis of VBM studies.

3.2.4.1 Shared neural substrates in OCD and OADs

Patients with OCD and OADs showed decreased bilateral regional grey matter volumes in the dMFG/ACG compared with healthy controls. These findings were very robust as they consistently emerged using multiple statistical approaches and various sensitivity and subgroup analyses. A plethora of evidence from animal, lesion, and neuroimaging studies indicates that the dMFG/ACG is implicated in the mediation or modulation of both normal and pathological anxiety. For example, in humans, direct stimulation of the ACG evokes anxiety (Laitinen 1979). The thickness and degree of activation of the dorsal ACG are positively correlated with skin conductance responses during fear conditioning in healthy individuals (Milad, Quirk et al. 2007). Activation of this region is consistently seen during the processing of threat-related as well as other emotion-relevant stimuli (Bush, Luu et al. 2000; Phan, Wager et al. 2002), and seems important for the cognitive regulation of emotions (Phillips, Drevets et al. 2003; Phillips, Drevets et al. 2003; Ochsner and Gross 2005). The dorsal ACG also plays a key role in error monitoring, a process that may be common to most anxiety disorders, including OCD (Ursu, Stenger et al. 2003; Paulus, Feinstein et al. 2004; Maltby, Tolin et al. 2005). Activation in different ACG regions and the medial prefrontal cortex is associated with anticipatory anxiety both in healthy individuals (Chua, Krams et al. 1999; Straube, Schmidt et al.

2009) and patients with anxiety disorders (Straube, Mentzel et al. 2007). Functional neuroimaging studies of anxiety disorders, including OCD, have consistently found hyper-activation in the dMFG/ACG region using various symptom provocation procedures (Swedo, Schapiro et al. 1989; Rauch, Jenike et al. 1994; Perani, Colombo et al. 1995; Rauch, Savage et al. 1995; Breiter, Rauch et al. 1996; Rauch, Savage et al. 1997; Osuch, Ketter et al. 2000; Pissiota, Frans et al. 2003; Mataix-Cols, Wooderson et al. 2004). This hyperactivity is at least partially reversible with cognitive-behaviour therapy (Straube, Glauer et al. 2006; Saxena, Gorbis et al. 2009). Finally, the dorsal ACG region implicated in this meta-analysis corresponds to the target of anterior cingulotomy, an ablative surgical treatment that alleviates severe obsessive-compulsive symptoms, anxiety and depression (Jenike 1998). Taken together, these multiple lines of evidence suggest that this brain region is commonly implicated in all anxiety disorders including OCD.

3.2.4.2 Differences between OCD and OADs

Compared with healthy controls, individuals with OCD had increased bilateral regional grey matter volumes in the lenticular nuclei (mainly the ventral anterior putamen) extending to the caudate nuclei. Conversely, patients with OADs had decreased grey matter volumes (vs. healthy controls) in the left lenticular nucleus (mainly the ventral anterior putamen). The study of the differences in grey matter volume across the different anxiety disorders confirmed these findings: patients with OCD had increased bilateral grey matter volumes in the

lenticular nuclei, extending to the caudate on the right side, in comparison with OADs. These findings appeared to be robust as demonstrated by our descriptive analyses of medians and quartiles. The findings also remained largely unchanged when each study was removed from the analyses "only one at a time" (jack-knife sensitivity analysis) and when controlling for potential confounds such as age or antidepressant medication use.

The basal ganglia have long been hypothesized to play a key role in the mediation of obsessive-compulsive symptoms (Rapoport and Wise 1988). Indirect evidence is available from focal lesion studies, disorders of known basal ganglia pathology, and, more recently, neuroimaging studies (Rauch, Jenike et al. 1994; Baxter, Saxena et al. 1996; Saxena, Brody et al. 1998; Mataix-Cols and van den Heuvel 2006). Conversely, the role of the basal ganglia in OADs has been largely neglected so far. This may be due to different research traditions in OCD vs. OADs (Mataix-Cols and van den Heuvel 2006). The results of this meta-analysis suggest that the basal ganglia are implicated in OADs too, though the direction of the results is opposite to that in OCD. The functional significance of these findings is unclear but it may be a reflection of unique features of OCD vs. OADs. One obvious possibility is that increased basal ganglia volumes reflect the repetitive nature of compulsions, which are pathognomonic in OCD. Chapter 2 included a meta-regression analysis showing a significant positive correlation between the volume of the basal ganglia and the severity of OCD symptoms (scores on the Yale-Brown Obsessive-Compulsive Scale) (Radua and Mataix-Cols 2009). Conversely, Yoo

et al. (2005) reported a significant negative correlation between the duration and severity of panic disorder symptoms and bilateral putamen volume.

The identified region is anatomically very close to the usual targets of psychosurgical interventions for severe anxiety and depression, such as capsulotomy (Ruck, Andr,ewitch et al. 2003; Ruck, Svanborg et al. 2005) and deep brain stimulation (Nuttin, Cosyns et al. 1999; Greenberg, Gabriels et al. 2008). Our findings of increased grey matter volume in OCD and decreased grey matter volume in OADs suggest that these ablative procedures may be effective through the disruption of different pathological mechanisms. Indeed, these are relatively crude interventions that may result in anxiety reduction by restoring the balance of activity in the basal ganglia regardless of the exact nature of the dysfunction.

This meta-analysis did not reveal consistent changes in limbic regions, such as the amygdala and hippocampus, in OADs. These changes would be expected from the existing PTSD (Kitayama, Vaccarino et al. 2005; Smith 2005; Karl, Schaefer et al. 2006) and PD (Massana, Serra-Grabulosa et al. 2003) literature. This may be related to limitations inherent to the VBM method. Indeed, standard VBM may not be as sensitive as manual segmentation methods or newer automated algorithms to detect volume changes in these regions (Bergouignan, Chupin et al. 2009). It is also possible that the high smoothing commonly used in VBM studies contributes to the poor sensitivity for volumetric changes in the small limbic structures (Uchida, Del-Ben et al. 2008).

3.2.4.3 Strengths and limitations

The main strengths of this study are the unbiased inclusion of published as well as unpublished studies, even if their results were negative (i.e. when no significant differences between patients and controls were found), and the use of the novel voxel-wise meta-analytic method presented in Chapter 2 (Radua and Mataix-Cols 2009). This method has been further developed by the introduction of a new statistical approach for voxel-based meta-analysis, i.e. the GLM which allowed testing differences across different disorders with the Q statistic (Cochran 1954). The latter is an important new feature that effectively allows finding those brain regions in which significant differences exist across several disorders. Given the complexity of the classification of psychiatric disorders, this method should be useful to researchers planning to undertake meta-analytical comparisons between disorders – i.e. beyond simple binary comparisons. To facilitate replication and further analyses by other colleagues, an online database, which contains all the data and methodological details from every study included in this meta-analysis and that is readily accessible at http://www.sdmproject.com/database , was also developed.

There are several limitations of this study, some of which are inherent to all meta-analytical approaches. First, despite our attempts to contact worldwide OCD and anxiety experts and include as many unpublished VBM studies as possible, even if their results were negative, the possibility of publication bias cannot be entirely ruled out. Second, voxel-based meta-analyses are based on summarized (i.e. coordinates from published studies) rather than raw data and this may result in less accurate results (Salimi-Khorshidi, Smith et al. 2009).

However, obtaining the raw images from the original studies is logistically difficult. Third, while our method provides excellent control for false positive results, it is more difficult to completely avoid false negative results. As mentioned earlier, VBM may lack sufficient sensitivity to detect differences in small limbic structures of relevance to anxiety disorders such as the hippocampus and the amygdala (Uchida, Del-Ben et al. 2008; Bergouignan, Chupin et al. 2009). Fourth, almost no data from some OADs, such as generalized anxiety disorder or specific phobias, are available (Milham, Nugent et al. 2005). We encourage other researchers to publish their VBM results in these disorders, even if these results do not conform to a-priori hypotheses. Finally, separate analyses of paediatric studies could not be performed because of the insufficient number of studies. The latter is important given the likely developmental effects on the neural systems underlying anxiety disorders (Gilbert, Akkal et al. 2009). When age was included as covariate in the omnibus test, potential differences across the anxiety disorders in the ventromedial frontal gyri were also shown, though these findings should be interpreted with caution given that most of the studies included adult samples with a limited mean age range (27-38 years).

3.2.4.4 Conclusions

To conclude, the results of this meta-analysis suggest common as well as distinct neural substrates in OCD and OADs. Both types of disorders are characterized by volumetric grey matter reductions in the dMFG/ACG, a finding

that is entirely consistent with numerous sources of evidence linking this brain structure with both normal and pathological anxiety. While the basal ganglia seem implicated both in OCD and OADs, the direction of the findings is diametrically opposite: OCD is characterized by increased grey matter volume in the basal ganglia whereas OADs is characterized by decreased grey matter volume in the basal ganglia, perhaps suggesting a common neural substrate but distinct neural mechanisms. In this regard, OCD and OADs may be conceptualized as opposite ends of a neurobiological spectrum. The functional significance of this finding is unclear but since the volume of the basal ganglia correlates with the severity of OCD (Radua and Mataix-Cols 2009), it may reflect the unique repetitive nature of compulsions, which are pathognomonic to OCD.

The results have implications for the current debate surrounding the classification of OCD in DSM-V. Since there are neurobiological similarities as well as differences between OCD and OADs, our results support maintaining the current classification of OCD as an anxiety disorder while acknowledging its uniqueness. This conclusion is consistent with the current recommendations by the DSM-V Anxiety, Obsessive-Compulsive Spectrum, Post-Traumatic, and Dissociative Disorders Work Group (Phillips, Stein et al. 2009; Stein, Fineberg et al. 2009). Specifically, one proposal is to change the name of the anxiety disorders grouping to reflect the inclusion of both anxiety and obsessive-compulsive disorders as partially independent but closely related entities (e.g. “anxiety and obsessive-compulsive disorders”) (Phillips, Stein et al. 2009). Another, not incompatible, proposal is to also broaden this category to include

other OCD and anxiety-related disorders, such as body dysmorphic disorder, hypochondriasis or hoarding disorder (e.g. “anxiety and obsessive-compulsive spectrum disorders”) (Mataix-Cols, Frost et al. 2009; Phillips, Stein et al. 2009). A similar approach is already adopted by *International Statistical Classification of Diseases, 10th Revision* (WHO 1992), and would have the obvious advantage of bringing the *DSM* and *International Statistical Classification of Diseases* systems closer together.

3.2.5 Acknowledgements

We thank all the authors of the included studies and specially Takeshi Asami, MD, PhD, Cristina M. Del-Ben, MD, PhD, Geraldo F. Busatto, MD, PhD, Victor G. Carrion, MD, Vincent Corbo, PhD, Yuko Hakamata, PhD, Fumi Hayano, PhD, Jana Koprivova, MA, Jun Soo Kwon, MD, PhD, Carles Soriano-Mas, PhD, Philip R. Szeszko, PhD, and Hidenori Yamasue, MD, PhD, for kindly sharing their unpublished data for inclusion in this meta-analysis.

3.3 OVERALL DISCUSSION

The previous chapter introduced an improved yet basic approach to conduct voxelwise meta-analyses of neuroimaging data. However, this approach did not allow addressing questions typically encountered by applied researchers in the neurosciences, such as meta-analytical comparisons between several groups, multiple meta-regressions or the inclusion of covariates.

In this chapter, the statistical part of SDM has been rebuilt based on the *general linear model* (GLM) and the meta-analytic Q statistic (Cochran 1954), thus permitting the test of more sophisticated hypotheses than simple summaries of studies and simple meta-regressions. These methods have been illustrated in a study that meta-analytically compared grey matter volumes between various anxiety disorders. Other applications of the method include the meta-analytical comparison of various subtypes of Autism Spectrum Disorder (Via, Radua et al. 2011) and the use of multiple meta-regression methods to examine the relative impact of age and stimulant medication on grey matter volumes in Attention Deficit Hyperactivity Disorder (Nakao, Radua et al. 2011).

Despite its increased sophistication, the GLM is not entirely free from limitations. First, as it name indicates, GLM only models linear relationships. Some non-linear relationships may be modelled using mathematical transformations, as exemplified in the meta-analysis presented in this chapter where age was included in its quadratic form (age + age squared). However, other non-linear relationships, as well as non-linear combinations of variables,

cannot be modelled. Second, GLM is a fixed-effects model and therefore, it can only partially account for heterogeneity. This particular limitation of the GLM is addressed in the following chapter.

3.4 REFERENCES

APA (2000). Diagnostic and Statistical Manual of Mental Disorders: DSM-IV-TR. Washington DC, American Psychiatric Association.

APA, D. J. Kupfer, et al. (2002). A Research Agenda for DSM-V. Washington, DC, American Psychiatric Association.

Asami, T., F. Hayano, et al. (2008). "Anterior cingulate cortex volume reduction in patients with panic disorder." Psychiatry Clin Neurosci **62**(3): 322-330.

Asami, T., H. Yamasue, et al. (2009). "Sexually dimorphic gray matter volume reduction in patients with panic disorder." Psychiatry Research: Neuroimaging **173**(2): 128-134.

Ashburner, J. and K. J. Friston (2000). "Voxel-based morphometry-the methods." Neuroimage **11**(6 Pt 1): 805-821.

Ashburner, J. and K. J. Friston (2001). "Why voxel-based morphometry should be used." Neuroimage **14**(6): 1238-1243.

Baxter, L. R., Jr., S. Saxena, et al. (1996). "Brain Mediation of Obsessive-Compulsive Disorder Symptoms: Evidence From Functional Brain

Imaging Studies in the Human and Nonhuman Primate." Semin Clin Neuropsychiatry **1**(1): 32-47.

Bergouignan, L., M. Chupin, et al. (2009). "Can voxel based morphometry, manual segmentation and automated segmentation equally detect hippocampal volume differences in acute depression?" Neuroimage **45**(1): 29-37.

Black, D. W., R. Noyes, et al. (1992). "A Family Study of Obsessive-Compulsive Disorder." Arch Gen Psychiatry **49** (5): 362-368.

Bolton, D., F. Rijsdijk, et al. (2007). "Obsessive-compulsive disorder, tics and anxiety in 6-year-old twins." Psychol Med **37** (1): 39-48.

Breiter, H. C., S. L. Rauch, et al. (1996). "Functional magnetic resonance imaging of symptom provocation in obsessive-compulsive disorder." Arch Gen Psychiatry **53**(7): 595-606.

Bryant, R. A., K. Felmingham, et al. (2008). "Rostral anterior cingulate volume predicts treatment response to cognitive-behavioural therapy for posttraumatic stress disorder." Rev Psychiatr Neurosci **33**(2): 142-146.

Bush, G., P. Luu, et al. (2000). "Cognitive and emotional influences in anterior cingulate cortex." Trends Cogn Sci **4**(6): 215-222.

Cardoner, N., C. Soriano-Mas, et al. (2007). "Brain structural correlates of depressive comorbidity in obsessive-compulsive disorder." Neuroimage **38**(3): 413-421.

Carmona, S., N. Bassas, et al. (2007). "Pediatric OCD structural brain deficits in conflict monitoring circuits: a voxel-based morphometry study." Neurosci Lett **421**(3): 218-223.

Carrion, V. G., C. F. Weems, et al. (2009). "Converging evidence for abnormalities of the prefrontal cortex and evaluation of midsagittal structures in pediatric posttraumatic stress disorder: an MRI study." Psychiatry Res **172**(3): 226-234.

Cecconi, J. P., A. C. Lopes, et al. (2008). "Gamma ventral capsulotomy for treatment of resistant obsessive-compulsive disorder: A structural MRI pilot prospective study." Neurosci.Lett. **447**(2-3): 138-142.

Chen, S., L. Li, et al. (2009). "Insular cortex involvement in declarative memory deficits in patients with post-traumatic stress disorder." BMC Psychiatry **9**: 39.

Chua, P., M. Krams, et al. (1999). "A functional anatomy of anticipatory anxiety." Neuroimage **9**(6 Pt 1): 563-571.

Cochran, W. G. (1954). "The combination of estimates from different experiments." Biometrics **10**(1): 101-129.

Costafreda, S. G., A. S. David, et al. (2009). "A parametric approach to voxel-based meta-analysis." Neuroimage **46**(1): 115-122.

Emdad, R., D. Bonekamp, et al. (2006). "Morphometric and psychometric comparisons between non-substance-abusing patients with posttraumatic stress disorder and normal controls." Psychother Psychosom **75**(2): 122-132.

Enright, S. J. and A. R. Beech (1990). "Obsessional states: anxiety disorders or schizotypes? An information processing and personality assessment." Psychol Med **20**(3): 621-627.

Gilbert, A. R., D. Akkal, et al. (2009). "Neural correlates of symptom dimensions in pediatric obsessive-compulsive disorder: a functional magnetic resonance imaging study." J Am Acad Child Adolesc Psychiatry **48**(9): 936-944.

Greenberg, B. D., L. A. Gabriels, et al. (2008). "Deep brain stimulation of the ventral internal capsule/ventral striatum for obsessive-compulsive disorder: worldwide experience." Mol Psychiatry **15**(1): 64-79.

Hakamata, Y., Y. Matsuoka, et al. (2007). "Structure of orbitofrontal cortex and its longitudinal course in cancer-related post-traumatic stress disorder." Neuroscience Research **59**(4): 383-389.

Hayano, F., M. Nakamura, et al. (2009). "Smaller amygdala is associated with anxiety in patients with panic disorder." Psychiatry Clin Neurosci **63**(3): 266-276.

Hedges, L. V. and I. Olkin (1985). Statistical Methods for Meta-Analysis. Orlando, Academic Press.

Hollander, E., A. Braun, et al. (2008). "Should OCD leave the anxiety disorders in DSM-V? The case for obsessive compulsive-related disorders." Depress Anxiety **25**(4): 317-329.

Insel, T. R. (1982). "Obsessive compulsive disorder-five clinical questions and a suggested approach." Compr Psychiatry **23**(3): 241-251.

Jatzko, A., S. Rothenhofer, et al. (2006). "Hippocampal volume in chronic posttraumatic stress disorder (PTSD): MRI study using two different evaluation methods." J Affect Disord **94**(1-3): 121-126.

Jenike, M. A. (1998). "Neurosurgical treatment of obsessive-compulsive disorder." Br J Psychiatry **Suppl**(35): 79-90.

Karl, A., M. Schaefer, et al. (2006). "A meta-analysis of structural brain abnormalities in PTSD." Neurosci Biobehav Rev **30**(7): 1004-1031.

Kim, J. J., M. C. Lee, et al. (2001). "Grey matter abnormalities in obsessive-compulsive disorder: statistical parametric mapping of segmented magnetic resonance images." Br J Psychiatry **179**: 330-334.

Kitayama, N., V. Vaccarino, et al. (2005). "Magnetic resonance imaging (MRI) measurement of hippocampal volume in posttraumatic stress disorder: a meta-analysis." J Affect Disord **88**(1): 79-86.

Koprivova , J., J. Hor cek, et al. (2009). "Medial frontal and dorsal cortical morphometric abnormalities are related to obsessive-compulsive disorder." Neurosci Lett **464**(1): 62-66.

Laitinen, L. V. (1979). "Emotional responses to subcortical electrical stimulation in psychiatric patients." Clin Neurol Neurosurg **81**(3): 148-157.

Lazaro, L., N. Bargallo, et al. (2009). "Brain changes in children and adolescents with obsessive-compulsive disorder before and after treatment: A voxel-based morphometric MRI study." Psychiatry Res **172**(2): 140-146.

Li, L., S. Chen, et al. (2007). "Magnetic resonance imaging and magnetic resonance spectroscopy study of deficits in hippocampal structure in fire victims with recent-onset posttraumatic stress disorder." Can J Psychiatry **51**(7): 431-437.

Maltby, N., D. F. Tolin, et al. (2005). "Dysfunctional action monitoring hyperactivates frontal-striatal circuits in obsessive-compulsive disorder: an event-related fMRI study." Neuroimage **24**(2): 495-503.

Massana, G., J. M. Serra-Grabulosa, et al. (2003). "Amygdalar atrophy in panic disorder patients detected by volumetric magnetic resonance imaging." Neuroimage **19**(1): 80-90.

Mataix-Cols, D., R. O. Frost, et al. (2009). "Hoarding Disorder: A new diagnosis for DSM-V?" Depress Anxiety **27**(6): 556-572.

Mataix-Cols, D., A. Pertusa, et al. (2007). "Issues for DSM-V: how should obsessive-compulsive and related disorders be classified?" Am J Psychiatry **164**(9): 1313-1314.

Mataix-Cols, D. and O. A. van den Heuvel (2006). "Common and distinct neural correlates of obsessive-compulsive and related disorders." Psychiatr Clin North Am **29**(2): 391-410, viii.

Mataix-Cols, D., S. Wooderson, et al. (2004). "Distinct neural correlates of washing, checking, and hoarding symptom dimensions in obsessive-compulsive disorder." Arch Gen Psychiatry **61**(6): 564-576.

Mechelli, A., C. J. Price, et al. (2005). "Voxel-based morphometry of the human brain: methods and applications." Curr Med Imag Rev **1**(2): 105-113.

Milad, M. R., G. J. Quirk, et al. (2007). "A role for the human dorsal anterior cingulate cortex in fear expression." Biol Psychiatry **62**(10): 1191-1194.

Milham, M. P., A. C. Nugent, et al. (2005). "Selective reduction in amygdala volume in pediatric anxiety disorders: a voxel-based morphometry investigation." Biol Psychiatry **57**(9): 961-966.

Nakao, T., J. Radua, et al. (2011). "Gray matter volume abnormalities in ADHD: voxel-based meta-analysis exploring the effects of age and stimulant medication." Am J Psychiatry **168**(11): 1154-63.

Nestadt, G., J. Samuels, et al. (2001). "The relationship between obsessive-compulsive disorder and anxiety and affective disorders: results from the Johns Hopkins OCD Family Study." Psychol Med **31** (3): 481-487.

Nuttin, B., P. Cosyns, et al. (1999). "Electrical stimulation in anterior limbs of internal capsules in patients with obsessive-compulsive disorder." Lancet **354**(9189): 1526.

Ochsner, K. N. and J. J. Gross (2005). "The cognitive control of emotion." Trends Cogn Sci **9**(5): 242-249.

Osuch, E. A., T. A. Ketter, et al. (2000). "Regional cerebral metabolism associated with anxiety symptoms in affective disorder patients." Biol Psychiatry **48**(10): 1020-1023.

Paulus, M. P., J. S. Feinstein, et al. (2004). "Anterior cingulate activation in high trait anxious subjects is related to altered error processing during decision making." Biol Psychiatry **55**(12): 1179-1187.

Perani, D., C. Colombo, et al. (1995). "[18F]FDG PET study in obsessive-compulsive disorder. A clinical/metabolic correlation study after treatment." Br J Psychiatry **166**(2): 244-250.

Phan, K. L., T. Wager, et al. (2002). "Functional neuroanatomy of emotion: a meta-analysis of emotion activation studies in PET and fMRI." Neuroimage **16**(2): 331-348.

Phillips, K. A., D. J. Stein, et al. (2009). "Should an obsessive-compulsive spectrum grouping of disorders be included in DSM-V?" Depress Anxiety **27**(6): 528-555.

Phillips, M. L., W. C. Drevets, et al. (2003). "Neurobiology of emotion perception I: The neural basis of normal emotion perception." Biol Psychiatry **54**(5): 504-514.

Phillips, M. L., W. C. Drevets, et al. (2003). "Neurobiology of emotion perception II: Implications for major psychiatric disorders." Biol Psychiatry **54**(5): 515-528.

Pissiota, A., O. Frans, et al. (2003). "Amygdala and anterior cingulate cortex activation during affective startle modulation: a PET study of fear." Eur J Neurosci **18**(5): 1325-1331.

Protopopescu, X., H. Pan, et al. (2006). "Increased brainstem volume in panic disorder: a voxel-based morphometric study." Brain Imaging **17**(4): 361-363.

Pujol, J., C. Soriano-Mas, et al. (2004). "Mapping structural brain alterations in obsessive-compulsive disorder." Arch Gen Psychiatry **61**(7): 720-730.

R Development Core Team (2008). R: A language and environment for statistical computing. Vienna, Austria, R Foundation for Statistical Computing.

Radua, J. and D. Mataix-Cols (2009). "Voxel-wise meta-analysis of grey matter changes in obsessive-compulsive disorder." Br J Psychiatry **195**(5): 393-402.

Rapoport, J. L. and S. P. Wise (1988). "Obsessive-compulsive disorder: evidence for basal ganglia dysfunction." Psychopharmacol Bull **24**(3): 380-384.

Rauch, S. L., M. A. Jenike, et al. (1994). "Regional cerebral blood flow measured during symptom provocation in obsessive-compulsive disorder

using oxygen 15-labeled carbon dioxide and positron emission tomography." Arch Gen Psychiatry **51**(1): 62-70.

Rauch, S. L., C. R. Savage, et al. (1997). "The functional neuroanatomy of anxiety: a study of three disorders using positron emission tomography and symptom provocation." Biol Psychiatry **42**(6): 446-452.

Rauch, S. L., C. R. Savage, et al. (1995). "A positron emission tomographic study of simple phobic symptom provocation." Arch Gen Psychiatry **52**(1): 20-28.

Ruck, C., S. Andr,ewitch, et al. (2003). "Capsulotomy for refractory anxiety disorders: long-term follow-up of 26 patients." Am J Psychiatry **160**(3): 513-521.

Ruck, C., P. Svanborg, et al. (2005). "Lesion topography in capsulotomy for refractory anxiety--is the right side the right side?" Stereotact Funct Neurosurg **83**(4): 172-179.

Salimi-Khorshidi, G., S. M. Smith, et al. (2009). "Meta-analysis of neuroimaging data: A comparison of image-based and coordinate-based Pooling of studies." Neuroimage **45**(3): 810-823.

Saxena, S., A. L. Brody, et al. (1998). "Neuroimaging and frontal-subcortical circuitry in obsessive-compulsive disorder." Br J Psychiatry Suppl(35): 26-37.

Saxena, S., E. Gorbis, et al. (2009). "Rapid effects of brief intensive cognitive-behavioral therapy on brain glucose metabolism in obsessive-compulsive disorder." Mol Psychiatry **14**(2): 197-205.

Shaw, P., J. Lerch, et al. (2006). "Longitudinal mapping of cortical thickness and clinical outcome in children and adolescents with attention-deficit/hyperactivity disorder." Arch Gen Psychiatry **63**(5): 540-549.

Smith, M. E. (2005). "Bilateral hippocampal volume reduction in adults with post-traumatic stress disorder: a meta-analysis of structural MRI studies." Hippocampus **15**(6): 798-807.

Soriano-Mas, C., J. Pujol, et al. (2007). "Identifying patients with obsessive-compulsive disorder using whole-brain anatomy." Neuroimage **35**(3): 1028-1037.

Stein, D. J., N. A. Fineberg, et al. (2009). "Should OCD be Classified as an Anxiety Disorder in DSM-V?" Depress Anxiety **27**(6): 495-506.

Storch, E. A., J. Abramowitz, et al. (2008). "Where does obsessive-compulsive disorder belong in DSM-V?" Depress Anxiety **25**(4): 336-347.

Straube, T., M. Glauer, et al. (2006). "Effects of cognitive-behavioral therapy on brain activation in specific phobia." Neuroimage **29**(1): 125-135.

Straube, T., H. J. Mentzel, et al. (2007). "Waiting for spiders: brain activation during anticipatory anxiety in spider phobics." Neuroimage **37**(4): 1427-1436.

Straube, T., S. Schmidt, et al. (2009). "Dynamic activation of the anterior cingulate cortex during anticipatory anxiety." Neuroimage **44**(3): 975-981.

Stroup, D. F., J. A. Berlin, et al. (2000). "Meta-analysis of observational studies in epidemiology: a proposal for reporting. Meta-analysis Of Observational Studies in Epidemiology (MOOSE) group." JAMA **283**(15): 2008-2012.

Swedo, S. E., M. B. Schapiro, et al. (1989). "Cerebral glucose metabolism in childhood-onset obsessive-compulsive disorder." Arch Gen Psychiatry **46**(6): 518-523.

Szeszko, P. R., C. Christian, et al. (2008). "Gray Matter Structural Alterations in Psychotropic Drug-Naive Pediatric Obsessive-Compulsive Disorder: An Optimized Voxel-Based Morphometry Study." Am J Psychiatry **165**(10): 1299-1307.

Tambs, K., N. Czajkowsky, et al. (2009). "Structure of genetic and environmental risk factors for dimensional representations of DSM-IV anxiety disorders." Br J Psychiatry **195**(4): 301-307.

Uchida, R. R., C. M. Del-Ben, et al. (2008). "Correlation between voxel based morphometry and manual volumetry in magnetic resonance images of the human brain." An Acad Bras Cienc **80**(1): 149-156.

Uchida, R. R., C. M. Del-Ben, et al. (2008). "Regional gray matter abnormalities in panic disorder: A voxel-based morphometry study." Psychiatry Research: Neuroimaging **163**(1): 21-29.

Ursu, S., V. A. Stenger, et al. (2003). "Overactive action monitoring in obsessive-compulsive disorder: evidence from functional magnetic resonance imaging." Psychol Sci **14**(4): 347-353.

Valente, A. A., Jr., E. C. Miguel, et al. (2005). "Regional gray matter abnormalities in obsessive-compulsive disorder: a voxel-based morphometry study." Biol Psychiatry **58**(6): 479-487.

van den Heuvel, O. A., P. L. Remijnse, et al. (2009). "The major symptom dimensions of obsessive-compulsive disorder are mediated by partially distinct neural systems." Brain **132**(Pt 4): 853-868.

van den Heuvel, O. A., D. J. Veltman, et al. (2005). "Disorder-specific neuroanatomical correlates of attentional bias in obsessive-compulsive disorder, panic disorder, and hypochondriasis." Arch Gen Psychiatry **62**(8): 922-933.

Via, E., J. Radua, et al. (2011). "Meta-analysis of gray matter abnormalities in autism spectrum disorder: should Asperger disorder be subsumed under a broader umbrella of autistic spectrum disorder?" Arch Gen Psychiatry **68**(4): 409-18.

Viechtbauer, W. (2006). MiMa: An S-Plus/R function to fit meta-analytic mixed-, random-, and fixed-effects models [Computer software and manual].

WHO (1992). International Statistical Classification of Diseases and Related Health Problems (ICD-10). Geneva, World Health Organization.

Yoo, H. K., M. J. Kim, et al. (2005). "Putaminal gray matter volume decrease in panic disorder: an optimized voxel-based morphometry study." Eur J Neurosci **22**(8): 2089-2094.

Yoo, S. Y., M. S. Roh, et al. (2008). "Voxel-based morphometry study of gray matter abnormalities in obsessive-compulsive disorder." J Korean Med Sci **23**(1): 24-30.

CHAPTER 4

Incorporation of effect sizes and statistical parametric maps

4.1 INTRODUCTION

This study was published in *European Psychiatry* under the title '*A new meta-analytic method for neuroimaging studies that combines reported peak coordinates and statistical parametric maps*' (Joaquim Radua, David Mataix-Cols, Mary L. Phillips, Wissam El-Hage, Dina M. Kronhaus, Narcís Cardoner and Simon Surguladze 2011; 27:605:611). The definitive publisher-authenticated version is available online at http://www.elsevier.com/journals/european-psychiatry/0924-9338

As discussed in the introductory chapter, image-based meta-analyses *exclusively* employ statistical parametric maps in a similar way to that of standard meta-analyses (Lazar, Luna et al. 2002) do. In this context, a 'statistical parametric map' refers to the brain image resulting from a group-level

analysis, or from the comparison between two groups. These methods benefit from the inclusion of full information from a given study (e.g. mean and variance in each voxel) and the use of well-established statistics based on within- and between-study variances – the latter known as 'heterogeneity'. They are seriously limited, however, by the rare availability of the statistical parametric maps, thus making this kind of meta-analysis highly impractical and unfeasible.

On the other hand, peak-probability methods such as *activation likelihood estimate* (ALE) or *multilevel kernel density analysis* (MKDA), as well as the *signed differential mapping* (SDM) method presented in Chapter 2, are *exclusively* based on the regional likelihood or frequency of reported peaks locations of significant activation clusters (Turkeltaub, Eden et al. 2002; Wager, Lindquist et al. 2007; Radua and Mataix-Cols 2009). In contrast to the image-based methods, peak-probability methods allow investigators to conduct exhaustive meta-analyses of neuroimaging studies. While both peak-probability and SDM have enabled investigators to conduct exhaustive meta-analyses of neuroimaging studies and generate new insights, they are limited by the inclusion of relatively little information from each study, i.e. these methods all rely exclusively on reported peak coordinates, neglecting other important sources of information such as variance data.

This chapter describes the development and validation of a new version of SDM, called *effect-size signed differential mapping* (ES-SDM). ES-SDM enables investigators to combine *both* peak coordinates and statistical parametric maps in the same meta-analysis and uses standard effect size and variance-based meta-analytic calculations (Cooper and Hedges 1994). The

validity of the method is assessed by comparing the results of a simulated meta-analysis of studies of the brain response to fearful faces with the results of a pooled analysis of the original individual data (i.e. the “gold standard” (Stewart and Parmar 1993; Lambert, Sutton et al. 2002; Higgins and Green 2009)).

4.2 METHODS

The new version of SDM (ES-SDM) presented here includes a set of modifications regarding the pre-processing (use of effect size and variance, improved weighting of voxels close to a peak) and meta-analysis (use of random-effects models with explicit study of the heterogeneity), which allow the combination of peak coordinates and statistical parametric maps and the use of well-established standard statistics. For the sake of consistency, the new method is comprehensively presented in the following sections, including both the established features of the original SDM method presented in Chapter 2 (Radua and Mataix-Cols 2009) and the new features introduced in this chapter.

Before describing the algorithm details, it is worth highlighting that, rather than assigning voxels a conventional value (e.g. '0' or '1'), ES-SDM assigns each voxel a measure of effect-size, namely the standardized mean (for one-sample designs) and the standardized mean difference (for two-sample designs), known as Hedge's δ and referred to as Hedge's *d* (or *g*) at the sample level (Hedges 1981):

$$\delta = \frac{\mu}{\sigma} \qquad \delta = \frac{\mu_1 - \mu_2}{\sigma}$$

where μ is the one-sample mean, μ_1 is the population mean of group 1 (e.g. patients), μ_2 is the population mean of group 2 (e.g. healthy volunteers), and σ is the standard deviation.

The next three sections describe formulas for the distribution of the *t* statistic, the estimation of *δ* from the *t* statistic, and the estimation of the variance of *d*. The implementation of these formulas into the SDM algorithms is described in the section 4.2.4.

4.2.1 Distribution of the *t* statistic

It must be noted that neuroimaging pre-processing algorithms apply a Gaussian smoothing on the individual brain images, so that voxel values approximately follow a normal distribution $N(\mu,\sigma^2)$. As the sample mean $\overline{X}$ is an affine transformation of these values, it also follows a normal distribution:

$$\overline{X} \sim N\left(A \cdot \mu, A \cdot \Sigma \cdot A^T\right) = N\left(\mu, \frac{\sigma^2}{n}\right)$$

where the affine transformation A, the column of means μ and the variance-covariance matrix Σ are:

$$A = \left[\frac{1}{n} \quad \ldots \quad \frac{1}{n}\right]$$

$$\mu = \begin{bmatrix} \mu \\ ... \\ \mu \end{bmatrix}$$

$$\Sigma = \begin{bmatrix} \sigma^2 & 0 & 0 & ... & 0 \\ 0 & \sigma^2 & 0 & ... & 0 \\ 0 & 0 & \sigma^2 & & ... \\ ... & ... & & ... & 0 \\ 0 & 0 & ... & 0 & \sigma^2 \end{bmatrix}$$

Fisher's theorem states that the sample variance S^2 divided by the population variance σ^2 follows a χ^2_{n-1} distribution divided by n-1, and that this term is independent from the sample mean. It can be then derived that the one-sample *t* statistic follows a non-central $T_{n-1,ncp}$ distribution:

$$t = \frac{\overline{X}}{S \cdot \sqrt{\frac{1}{n}}} = \frac{\frac{\overline{X} - \mu}{\sigma \cdot \sqrt{\frac{1}{n}}} + \frac{\mu}{\sigma \cdot \sqrt{\frac{1}{n}}}}{\sqrt{\frac{S^2}{\sigma^2}}} \sim \frac{Z + ncp}{\sqrt{\frac{\chi^2_{n-1}}{n-1}}} = ncT_{n-1,ncp}$$

where the non-centrality parameter *ncp* is:

$$ncp = \frac{\mu}{\sigma \cdot \sqrt{\frac{1}{n}}} \quad (1)$$

In paired two-sample designs (e.g. studies investigating the brain response to fearful vs. neutral faces in healthy volunteers), the voxel value difference X_d in each individual is also an affine transformation of the values in each condition (e.g. fearful minus neutral), thus also following a normal distribution:

$$X_d \sim N\left(A \cdot \mu, A \cdot \Sigma \cdot A^T\right) = N\left(\mu_1 - \mu_0, \sigma_0^2 + \sigma_1^2 - 2 \cdot \sigma_{0,1}\right) = N\left(\mu_d, \sigma_d^2\right)$$

where the affine transformation A, the column of means μ and the variance-covariance matrix Σ are:

$$A = \begin{bmatrix} -1 & 1 \end{bmatrix}$$

$$\mu = \begin{bmatrix} \mu_0 \\ \mu_1 \end{bmatrix}$$

$$\Sigma = \begin{bmatrix} \sigma_0^2 & \sigma_{0,1} \\ \sigma_{0,1} & \sigma_1^2 \end{bmatrix}$$

Therefore paired two-sample designs might be treated as one-sample designs, replacing individual voxel values by individual voxel differences.

Finally, in a comparison between two homocedastic groups a voxel value follows either a $N(\mu_1,\sigma^2)$ (in the first sample, e.g. patients) or a $N(\mu_2,\sigma^2)$ (in the second sample, e.g. healthy volunteers). The difference between both groups sample means $\overline{X}_1 - \overline{X}_2$ is once more an affine transformation of these individual values, so that it also follows a normal distribution:

$$\overline{X}_1 - \overline{X}_2 \sim N\left(A \cdot \mu, A \cdot \Sigma \cdot A^T\right) = N\left(\mu_1 - \mu_2, \sigma^2 \cdot \left(\frac{1}{n_1} + \frac{1}{n_2}\right)\right)$$

where the affine transformation *A*, the column of means μ and the variance-covariance matrix Σ are:

$$A = \left[\frac{1}{n_1} \quad \ldots \quad \frac{1}{n_1} \quad \frac{1}{n_2} \quad \ldots \quad \frac{1}{n_2}\right]$$

$$\mu = \begin{bmatrix} \mu_1 \\ \ldots \\ \mu_1 \\ \mu_2 \\ \ldots \\ \mu_2 \end{bmatrix}$$

$$\Sigma = \begin{bmatrix} \sigma^2 & 0 & 0 & ... & 0 \\ 0 & \sigma^2 & 0 & ... & 0 \\ 0 & 0 & \sigma^2 & & ... \\ ... & ... & & ... & 0 \\ 0 & 0 & ... & 0 & \sigma^2 \end{bmatrix}$$

Again, Fisher's theorem can be used to derive that the two-sample *t* statistic follows a non-central $T_{n-2,ncp}$ distribution:

$$t = \frac{\overline{X}_1 - \overline{X}_2}{S \cdot \sqrt{\frac{1}{n_1} + \frac{1}{n_2}}} = \frac{\frac{\left(\overline{X}_1 - \overline{X}_2\right) - \left(\mu_1 - \mu_2\right)}{\sigma \cdot \sqrt{\frac{1}{n_1} + \frac{1}{n_2}}} + \frac{\mu_1 - \mu_2}{\sigma \cdot \sqrt{\frac{1}{n_1} + \frac{1}{n_2}}}}{\sqrt{\frac{S^2}{\sigma^2}}} \sim \frac{Z + ncp}{\sqrt{\frac{\chi^2_{n-2}}{n-2}}} = ncT_{n-2,ncp}$$

where the non-centrality parameter *ncp* is:

$$ncp = \frac{\mu_1 - \mu_2}{\sigma \cdot \sqrt{\frac{1}{n_1} + \frac{1}{n_2}}} \quad (2)$$

If the sample sizes are equal, the unequal-variances two-sample *t* statistic coincides with the equal-variances two-sample *t* statistic, and thus the former can be treated as the latter:

$$t = \frac{\overline{X}_1 - \overline{X}_2}{\sqrt{\frac{S_1^2}{n_1} + \frac{S_2^2}{n_1}}} = \frac{\overline{X}_1 - \overline{X}_2}{\sqrt{\frac{S_1^2 + S_2^2}{n_1}}} = \frac{\overline{X}_1 - \overline{X}_2}{\sqrt{\frac{(n_1 - 1) \cdot S_1^2 + (n_1 - 1) \cdot S_2^2}{\frac{2n_1 - 2}{n_1}}}} = \frac{\overline{X}_1 - \overline{X}_2}{\sqrt{\frac{S^2}{\frac{n_1}{2}}}} = \frac{\overline{X}_1 - \overline{X}_2}{S\sqrt{\frac{1}{n_1} + \frac{1}{n_1}}}$$

Unequal-size unequal-variances unpaired two-sample *t* statistics are not considered here, but the general formula may be used as a good approximation when the differences in sample size or variance are small.

4.2.2 Estimation of δ from the *t* statistic

An estimator of the standardized mean *δ* (Hedges 1981) as a function of the one-sample *t* statistic could be:

$$d^* = \frac{\overline{X}}{S} = \sqrt{\frac{1}{n}} \cdot \frac{\overline{X}}{S \cdot \sqrt{\frac{1}{n}}} = \sqrt{\frac{1}{n}} \cdot t$$

However, d^* is a biased estimator of δ (Hedges and Olkin 1985), as its expected value is:

$$E(d^*) = E\left(\sqrt{\frac{1}{n}} \cdot t\right) = \sqrt{\frac{1}{n}} \cdot E(t)$$

which developing the expected value of a non-central $T_{n-1,ncp}$ distribution is:

$$= \sqrt{\frac{1}{n}} \cdot \frac{\Gamma\left(\frac{n-2}{2}\right)}{\Gamma\left(\frac{n-1}{2}\right)} \cdot \sqrt{\frac{n-1}{2}} \cdot ncp$$

where Γ is the gamma function, and replacing *ncp* by (1) is:

$$= \sqrt{\frac{1}{n}} \cdot \frac{\Gamma\left(\frac{n-2}{2}\right)}{\Gamma\left(\frac{n-1}{2}\right)} \cdot \sqrt{\frac{n-1}{2}} \cdot \frac{\mu}{\sigma \cdot \sqrt{\frac{1}{n}}} = \frac{\Gamma\left(\frac{n-2}{2}\right)}{\Gamma\left(\frac{n-1}{2}\right)} \cdot \sqrt{\frac{n-1}{2}} \cdot \delta$$

Figure 4.1 Expected value of d (one-sample studies).

```
randomizations = 5000
ev_of_biased_d = function(delta, n) {
        pop_sd = runif(1, 1, 10) # Set a random standard deviation
        pop_mean_x = delta * pop_sd # Set the mean according to delta
        x = matrix(rnorm(randomizations * n, pop_mean_x, pop_sd), nrow=n) # Generate random
normally distributed voxel values
        mean_x = apply(x, 2, mean) # Calculate t values
        sd_x = apply(x, 2, sd)
        t = mean_x / (sd_x * sqrt(1 / n))
        d = sqrt(1 / n) * t # Convert t values into d* values
        mean(d) # Return the expected value of d*
}
ev_of_unbiased_d = function(delta, n) {
        pop_sd = runif(1, 1, 10) # Set a random standard deviation
        pop_mean_x = delta * pop_sd # Set the mean according to delta
        x = matrix(rnorm(randomizations * n, pop_mean_x, pop_sd), nrow=n) # Generate random
normally distributed voxel values
        mean_x = apply(x, 2, mean) # Calculate t values
        sd_x = apply(x, 2, sd)
        t = mean_x / (sd_x * sqrt(1 / n))
        d = gamma((n - 1) / 2) / gamma((n - 2) / 2) * sqrt(2 / (n - 1)) * sqrt(1 / n) * t #
Convert t values into d values
        mean(d) # Return the expected value of d
}
ev_of_d = function(delta, n) {
        cat("Expected value of d:\n")
        cat("- Population delta =", round(delta, 2), "\n") # Print the parameters
        cat("- Size of the sample =", n, "\n")
        cat("- Expected value of biased d = ") # Print the expected values of d
        cat(round(ev_of_biased_d(delta, n), 2), "\n")
        cat("- Expected value of unbiased d = ")
        cat(round(ev_of_unbiased_d(delta, n), 2), "\n")
}
# Usage: ev_of_d(delta, n), e.g.:
ev_of_d(0, 10)
ev_of_d(pi / 2, 10)
ev_of_d(pi / 2, 25)
```

An *unbiased* estimator *d* from *t* can be thus obtained as:

$$d = \frac{\Gamma\left(\frac{n-1}{2}\right)}{\Gamma\left(\frac{n-2}{2}\right)} \cdot \sqrt{\frac{2}{n-1}} \cdot d^{*} = \frac{\Gamma\left(\frac{n-1}{2}\right)}{\Gamma\left(\frac{n-2}{2}\right)} \cdot \sqrt{\frac{2}{n-1}} \cdot \sqrt{\frac{1}{n}} \cdot t \tag{3}$$

The validity of this formula and the magnitude of the bias can be readily checked with the script in R shown in **Figure 4.1**.

As regard to the standardized mean difference δ (Hedges 1981) , an estimator as a function of the two-sample *t* statistic could be:

$$d^* = \frac{\overline{X}_1 - \overline{X}_2}{S} = \sqrt{\frac{1}{n_1} + \frac{1}{n_2}} \cdot \frac{\overline{X}_1 - \overline{X}_2}{S \cdot \sqrt{\frac{1}{n_1} + \frac{1}{n_2}}} = \sqrt{\frac{1}{n_1} + \frac{1}{n_2}} \cdot t$$

though d^* is again biased (Hedges and Olkin 1985), as its expected value is:

$$E\left(d^*\right) = E\left(\sqrt{\frac{1}{n_1} + \frac{1}{n_2}} \cdot t\right) = \sqrt{\frac{1}{n_1} + \frac{1}{n_2}} \cdot E\left(t\right)$$

which developing the expected value of a non-central $T_{n-2,ncp}$ distribution is:

$$= \sqrt{\frac{1}{n_1} + \frac{1}{n_2}} \cdot \frac{\Gamma\left(\frac{n-3}{2}\right)}{\Gamma\left(\frac{n-2}{2}\right)} \cdot \sqrt{\frac{n-2}{2}} \cdot ncp$$

Figure 4.2 Expected value of d (unpaired two-sample studies).

```
randomizations = 5000
ev_of_biased_d = function(delta, n1, n2) {
        n = n1 + n2
        pop_sd = runif(1, 1, 10) # Define a random population standard deviation
        pop_mean_x2 = runif(1, -10, 10) # Define a random mean for the second population
        pop_mean_x1 = delta * pop_sd + pop_mean_x2 # Define the mean of the first population
according to the delta
        x1 = matrix(rnorm(randomizations * n1, pop_mean_x1, pop_sd), nrow=n1) # Generate random
normally distributed voxel values
        x2 = matrix(rnorm(randomizations * n2, pop_mean_x2, pop_sd), nrow=n2)
        mean_x1 = apply(x1, 2, mean) # Calculate the t values
        mean_x2 = apply(x2, 2, mean)
        var_x1 = apply(x1, 2, var)
        var_x2 = apply(x2, 2, var)
        s = sqrt((var_x1 * (n1 - 1) + var_x2 * (n2 - 1)) / (n - 2))
        t = (mean_x1 - mean_x2) / (s * sqrt(1 / n1 + 1 / n2))
        d = sqrt(1 / n1 + 1 / n2)*t # Convert t values into d* values
        mean(d) # Return the expected value of d*
}
ev_of_unbiased_d = function(delta, n1, n2) {
        n = n1 + n2
        pop_sd = runif(1, 1, 10) # Define a random population standard deviation
        pop_mean_x2 = runif(1, -10, 10) # Define a random mean for the second population
        pop_mean_x1 = delta * pop_sd + pop_mean_x2 # Define the mean of the first population
according to the delta
        x1 = matrix(rnorm(randomizations * n1, pop_mean_x1, pop_sd), nrow=n1) # Generate random
normally distributed voxel values
        x2 = matrix(rnorm(randomizations * n2, pop_mean_x2, pop_sd), nrow=n2)
        mean_x1 = apply(x1, 2, mean) # Calculate the t values
        mean_x2 = apply(x2, 2, mean)
        var_x1 = apply(x1, 2, var)
        var_x2 = apply(x2, 2, var)
        s = sqrt((var_x1 * (n1 - 1) + var_x2 * (n2 - 1)) / (n - 2))
        t = (mean_x1 - mean_x2) / (s * sqrt(1 / n1 + 1 / n2))
        d = gamma((n - 2) / 2) / gamma((n - 3) / 2) * sqrt(2 / (n - 2)) * sqrt(1 / n1 + 1 / n2)
* t # Convert t values into d values
        mean(d) # Return the expected value of d
}
est_of_d = function(delta, n1, n2) {
        cat("Expected value of d:\n")
        cat("- Population delta =", round(delta, 2), "\n") # Print the parameters
        cat("- Size of the sample from the first population =", n1, "\n")
        cat("- Size of the sample from the second population =", n2, "\n");
        cat("- Expected value of biased d = ") # Print the expected values of d
        cat(round(ev_of_biased_d(delta, n1, n2), 2), "\n")
        cat("- Expected value of unbiased d = ")
        cat(round(ev_of_unbiased_d(delta, n1, n2), 2), "\n")
}
# Usage: est_of_d(delta, n1, n2), e.g.:
est_of_d(0, 10, 10)
est_of_d(pi / 2, 10, 10)
est_of_d(pi / 2, 25, 25)
```

and replacing *ncp* by (2) is:

$$= \sqrt{\frac{1}{n_1}+\frac{1}{n_2}} \cdot \frac{\Gamma\left(\frac{n-3}{2}\right)}{\Gamma\left(\frac{n-2}{2}\right)} \cdot \sqrt{\frac{n-2}{2}} \cdot \frac{\mu_1-\mu_2}{\sigma \cdot \sqrt{\frac{1}{n_1}+\frac{1}{n_2}}} = \frac{\Gamma\left(\frac{n-3}{2}\right)}{\Gamma\left(\frac{n-2}{2}\right)} \cdot \sqrt{\frac{n-2}{2}} \cdot \delta$$

An *unbiased* estimator *d* from *t* can be thus obtained as:

$$d = \frac{\Gamma\left(\frac{n-2}{2}\right)}{\Gamma\left(\frac{n-3}{2}\right)} \cdot \sqrt{\frac{2}{n-2}} \cdot d^{*} = \frac{\Gamma\left(\frac{n-2}{2}\right)}{\Gamma\left(\frac{n-3}{2}\right)} \cdot \sqrt{\frac{2}{n-2}} \cdot \sqrt{\frac{1}{n_1} + \frac{1}{n_2}} \cdot t \tag{4}$$

The validity of this formula and the magnitude of the bias can be readily checked with the script in R shown in **Figure 4.2**.

4.2.3 Estimation of the variance of *d*

The variance of *d* in on-sample studies can be obtained replacing *d* by (3) as follows:

$$Var(d) = Var\left(\frac{\Gamma\left(\frac{n-1}{2}\right)}{\Gamma\left(\frac{n-2}{2}\right)} \cdot \sqrt{\frac{2}{n-1}} \cdot \sqrt{\frac{1}{n}} \cdot t \right) = \left(\frac{\Gamma\left(\frac{n-1}{2}\right)}{\Gamma\left(\frac{n-2}{2}\right)} \right)^{2} \cdot \frac{2}{n-1} \cdot \frac{1}{n} \cdot Var(t)$$

which developing the variance of a non-central T distribution is:

$$= \left(\frac{\Gamma\left(\frac{n-1}{2}\right)}{\Gamma\left(\frac{n-2}{2}\right)} \right)^2 \cdot \frac{2}{n-1} \cdot \frac{1}{n} \cdot \left(\frac{(n-1)\cdot\left(1+ncp^2\right)}{n-3} - \frac{ncp^2\cdot(n-1)}{2} \cdot \left(\frac{\Gamma\left(\frac{n-2}{2}\right)}{\Gamma\left(\frac{n-1}{2}\right)} \right)^2 \right)$$

$$= \left(\frac{\Gamma\left(\frac{n-1}{2}\right)}{\Gamma\left(\frac{n-2}{2}\right)} \right)^2 \cdot \frac{2}{n-3} \cdot \left(\frac{1}{n} + \frac{1}{n} \cdot ncp^2 \right) - \frac{1}{n} \cdot ncp^2$$

and replacing *ncp* by (1) is:

$$= \left(\frac{\Gamma\left(\frac{n-1}{2}\right)}{\Gamma\left(\frac{n-2}{2}\right)} \right)^2 \cdot \frac{2}{n-3} \cdot \left(\frac{1}{n} + \frac{1}{n} \cdot \left(\frac{\mu}{\sigma \cdot \sqrt{\frac{1}{n}}} \right)^2 \right) - \frac{1}{n} \cdot \left(\frac{\mu}{\sigma \cdot \sqrt{\frac{1}{n}}} \right)^2$$

$$= \left(\frac{\Gamma\left(\frac{n-1}{2}\right)}{\Gamma\left(\frac{n-2}{2}\right)} \right)^2 \cdot \frac{2}{n-3} \cdot \left(\frac{1}{n} + \delta^2 \right) - \delta^2$$

An estimator of the variance could be then obtained by substituting δ by d, but this estimator would be biased because the expected value of d^2 is $\delta^2 + Var(d)$:

$$E\left(\hat{V}ar(d)^*\right) = \left(\frac{\Gamma\left(\frac{n-1}{2}\right)}{\Gamma\left(\frac{n-2}{2}\right)}\right)^2 \cdot \frac{2}{n-3} \cdot \left(\frac{1}{n} + \delta^2 + Var(d)\right) - \delta^2 - Var(d)$$

$$= \left(\frac{\Gamma\left(\frac{n-1}{2}\right)}{\Gamma\left(\frac{n-2}{2}\right)}\right)^2 \cdot \frac{2}{n-3} \cdot Var(d)$$

An *unbiased* estimator of the variance of d from d can be thus obtained as:

$$\hat{V}ar(d) = \frac{1}{n} + d^2 - \left(\frac{\Gamma\left(\frac{n-2}{2}\right)}{\Gamma\left(\frac{n-1}{2}\right)}\right)^2 \cdot \frac{n-3}{2} \cdot d^2$$

The validity of this formula and the magnitude of the bias can be readily checked with the script in R shown in **Figure 4.3**.

Figure 4.3 Calculation of the variance of d (one-sample studies).

```
randomizations = 5000
var_of_d_using_formula = function(delta, n) {
        (gamma((n - 1) / 2) / gamma((n - 2) / 2))^2 * 2 / (n - 3) * (1 / n + delta^2) - delta^2
# Return the result of the formula
}
var_of_d_using_simulations = function(delta, n) {
        pop_sd = runif(1, 1, 10) # Define a random population standard deviation
        pop_mean = delta * pop_sd # Define the mean according to the delta
        x = matrix(rnorm(randomizations * n, pop_mean, pop_sd), nrow=n) # Generate random
normally distributed voxel values
        mean_x = apply(x, 2, mean) # Calculate t values
        sd_x = apply(x, 2, sd)
        t = mean_x / (sd_x * sqrt(1 / n))
        d = gamma((n - 1) / 2) / gamma((n - 2) / 2) * sqrt(2 / (n - 1)) * sqrt(1 / n) * t #
Convert t values into d values
        var(d) # Return the empirical variance of d
}
ev_of_biased_var_of_d = function(delta, n) {
        pop_sd = runif(1, 1, 10) # Define a random population standard deviation
        pop_mean = delta * pop_sd # Define the mean according to the delta
        x = matrix(rnorm(randomizations * n, pop_mean, pop_sd), nrow=n) # Generate random
normally distributed voxel values
        mean_x = apply(x, 2, mean) # Calculate t values
        sd_x = apply(x, 2, sd)
        t = mean_x / (sd_x * sqrt(1 / n))
        d = gamma((n - 1) / 2) / gamma((n - 2) / 2) * sqrt(2 / (n - 1)) * sqrt(1 / n) * t #
Convert t values into d values
        var_d = (gamma((n - 1) / 2) / gamma((n - 2) / 2))^2 * 2 / (n - 3) * (1 / n + d^2) - d^2
# Estimate the variance* of d
        mean(var_d) # Return the expected value of the estimate of the variance* of d
}
ev_of_unbiased_var_of_d = function(delta, n) {
        pop_sd = runif(1, 1, 10) # Define a random population standard deviation
        pop_mean = delta * pop_sd # Define the mean according to the delta
        x = matrix(rnorm(randomizations * n, pop_mean, pop_sd), nrow=n) # Generate random
normally distributed voxel values
        mean_x = apply(x, 2, mean) # Calculate t values
        sd_x = apply(x, 2, sd)
        t = mean_x / (sd_x * sqrt(1 / n))
        d = gamma((n - 1) / 2) / gamma((n - 2) / 2) * sqrt(2 / (n - 1)) * sqrt(1 / n) * t #
Convert t values into d values
        var_d = 1 / n + d^2 - (gamma((n - 2) / 2) / gamma((n - 1) / 2))^2 * (n - 3) / 2 * d^2 #
Estimate the variance of d
        mean(var_d) # Return the expected value of the estimate of the variance of d
}
var_of_d = function(delta, n) {
        cat("Variance of d:\n")
        cat("- Population delta =", round(delta, 2), "\n") # Print the parameters
        cat("- Size of the sample =", n, "\n")
        cat("- Variance of d knowing delta (using formula) = ") # Print the variance calculated
with the formula
        cat(round(var_of_d_using_formula(delta, n), 2), "\n")
        cat("- Variance of d (using simulations) = ") # Print the variance obtained with the
simulations
        cat(round(var_of_d_using_simulations(delta, n), 2), "\n")
        cat("- Expected value of the biased estimate of the variance of d = ") # Print the
expected values of the estimates of the variance of d
        cat(round(ev_of_biased_var_of_d(delta, n), 2), "\n")
        cat("- Expected value of the unbiased estimate of the variance of d = ")
        cat(round(ev_of_unbiased_var_of_d(delta, n), 2), "\n")
}
# Usage: var_of_d(delta, n), e.g.:
var_of_d(0, 10)
var_of_d(pi / 2, 10)
var_of_d(pi / 2, 25)
```

Finally, the variance of *d* in two-sample studies can be obtained replacing *d* by (4) as follows:

$$Var(d) = Var\left(\frac{\Gamma\left(\frac{n-2}{2}\right)}{\Gamma\left(\frac{n-3}{2}\right)} \cdot \sqrt{\frac{2}{n-2}} \cdot \sqrt{\frac{1}{n_1}+\frac{1}{n_2}} \cdot t \right) = \left(\frac{\Gamma\left(\frac{n-2}{2}\right)}{\Gamma\left(\frac{n-3}{2}\right)} \right)^2 \cdot \frac{2}{n-2} \cdot \left(\frac{1}{n_1}+\frac{1}{n_2} \right) \cdot Var(t)$$

which developing the variance of a non-central T distribution is:

$$= \left(\frac{\Gamma\left(\frac{n-2}{2}\right)}{\Gamma\left(\frac{n-3}{2}\right)} \right)^2 \cdot \frac{2}{n-2} \cdot \left(\frac{1}{n_1}+\frac{1}{n_2} \right) \cdot \left(\frac{(n-2)\cdot\left(1+ncp^2\right)}{n-4} - \frac{ncp^2\cdot(n-2)}{2} \cdot \left(\frac{\Gamma\left(\frac{n-3}{2}\right)}{\Gamma\left(\frac{n-2}{2}\right)} \right)^2 \right)$$

$$= \left(\frac{\Gamma\left(\frac{n-2}{2}\right)}{\Gamma\left(\frac{n-3}{2}\right)} \right)^2 \cdot \frac{2}{n-4} \cdot \left(\frac{1}{n_1}+\frac{1}{n_2}+\left(\frac{1}{n_1}+\frac{1}{n_2} \right) \cdot ncp^2 \right) - \left(\frac{1}{n_1}+\frac{1}{n_2} \right) \cdot ncp^2$$

and replacing *ncp* by (2) is:

$$= \left(\frac{\Gamma\left(\frac{n-2}{2}\right)}{\Gamma\left(\frac{n-3}{2}\right)} \right)^2 \cdot \frac{2}{n-4} \cdot \left(\frac{1}{n_1} + \frac{1}{n_2} + \left(\frac{1}{n_1} + \frac{1}{n_2} \right) \cdot \left(\frac{\mu_1 - \mu_2}{\sigma \cdot \sqrt{\frac{1}{n_1} + \frac{1}{n_2}}} \right)^2 \right)$$

$$- \left(\frac{1}{n_1} + \frac{1}{n_2} \right) \cdot \left(\frac{\mu_1 - \mu_2}{\sigma \cdot \sqrt{\frac{1}{n_1} + \frac{1}{n_2}}} \right)^2$$

$$= \left(\frac{\Gamma\left(\frac{n-2}{2}\right)}{\Gamma\left(\frac{n-3}{2}\right)} \right)^2 \cdot \frac{2}{n-4} \cdot \left(\frac{1}{n_1} + \frac{1}{n_2} + \delta^2 \right) - \delta^2$$

An estimator of the variance could be then obtained by substituting δ by d, but this estimator would be again biased because the expected value of d^2 is δ^2 + $Var(d)$:

$$E\left(\hat{V}ar(d)^*\right) = \left(\frac{\Gamma\left(\frac{n-2}{2}\right)}{\Gamma\left(\frac{n-3}{2}\right)} \right)^2 \cdot \frac{2}{n-4} \cdot \left(\frac{1}{n_1} + \frac{1}{n_2} + \delta^2 + Var(d) \right) - \delta^2 - Var(d)$$

$$= \left(\frac{\Gamma\left(\frac{n-2}{2}\right)}{\Gamma\left(\frac{n-3}{2}\right)} \right)^2 \cdot \frac{2}{n-4} \cdot Var(d)$$

An *unbiased* estimator of the variance of *d* from *d* can be thus obtained as:

$$\hat{Var}(d) = \frac{1}{n_1} + \frac{1}{n_2} + d^2 - \left(\frac{\Gamma\left(\frac{n-3}{2}\right)}{\Gamma\left(\frac{n-2}{2}\right)} \right)^2 \cdot \frac{n-4}{2} \cdot d^2$$

The validity of this formula and the magnitude of the bias can be readily checked with the script in R shown in **Figure 4.4**.

Figure 4.4 Calculation of the variance of d (unpaired two-sample studies).

```
randomizations = 5000
var_of_d_using_formula = function(delta, n1, n2) {
          n = n1 + n2
          (gamma((n - 2) / 2) / gamma((n - 3) / 2))^2 * 2 / (n - 4) * (1 / n1 + 1 / n2 + delta^2) - delta^2 # Return the
result of the formula
}
var_of_d_using_simulations = function(delta, n1, n2) {
          n = n1 + n2
          pop_sd = runif(1, 1, 10) # Define a random population standard deviation
          pop_mean_x2 = runif(1, -10, 10) # Define a random mean for the second population
          pop_mean_x1 = delta * pop_sd + pop_mean_x2 # Define the mean of the first population according to the delta
          x1 = matrix(rnorm(randomizations * n1, pop_mean_x1, pop_sd), nrow=n1) # Generate random normally distributed
voxel values
          x2 = matrix(rnorm(randomizations * n2, pop_mean_x2, pop_sd), nrow=n2)
          mean_x1 = apply(x1, 2, mean) # Calculate the t values
          mean_x2 = apply(x2, 2, mean)
          var_x1 = apply(x1, 2, var)
          var_x2 = apply(x2, 2, var)
          s = sqrt((var_x1 * (n1 - 1) + var_x2 * (n2 - 1)) / (n - 2))
          t = (mean_x1 - mean_x2) / (s * sqrt(1 / n1 + 1 / n2))
          d = gamma((n - 2) / 2) / gamma((n - 3) / 2) * sqrt(2 / (n - 2)) * sqrt(1 / n1 + 1 / n2) * t # Convert t values
into d values
          var(d) # Return the empirical variance of d
}
ev_of_biased_var_of_d = function(delta, n1, n2) {
          n = n1 + n2
          pop_sd = runif(1, 1, 10) # Define a random population standard deviation
          pop_mean_x2 = runif(1, -10, 10) # Define a random mean for the second population
          pop_mean_x1 = delta * pop_sd + pop_mean_x2 # Define the mean of the first population according to the delta
          x1 = matrix(rnorm(randomizations * n1, pop_mean_x1, pop_sd), nrow=n1) # Generate random normally distributed
voxel values
          x2 = matrix(rnorm(randomizations * n2, pop_mean_x2, pop_sd), nrow=n2)
          mean_x1 = apply(x1, 2, mean) # Calculate the t values
          mean_x2 = apply(x2, 2, mean)
          var_x1 = apply(x1, 2, var)
          var_x2 = apply(x2, 2, var)
          s = sqrt((var_x1 * (n1 - 1) + var_x2 * (n2 - 1)) / (n - 2))
          t = (mean_x1 - mean_x2) / (s * sqrt(1 / n1 + 1 / n2))
          d = gamma((n - 2) / 2) / gamma((n - 3) / 2) * sqrt(2 / (n - 2)) * sqrt(1 / n1 + 1 / n2) * t # Convert t values
into d values
          var_d = (gamma((n - 2) / 2) / gamma((n - 3) / 2))^2 * 2 / (n - 4) * (1 / n1 + 1 / n2 + d^2) - d^2 # Estimate
the variance* of d
          mean(var_d) # Return the expected value of the estimate of the variance* of d
}
ev_of_unbiased_var_of_d = function(delta, n1, n2) {
          n = n1 + n2
          pop_sd = runif(1, 1, 10) # Define a random population standard deviation
          pop_mean_x2 = runif(1, -10, 10) # Define a random mean for the second population
          pop_mean_x1 = delta * pop_sd + pop_mean_x2 # Define the mean of the first population according to the delta
          x1 = matrix(rnorm(randomizations * n1, pop_mean_x1, pop_sd), nrow=n1) # Generate random normally distributed
voxel values
          x2 = matrix(rnorm(randomizations * n2, pop_mean_x2, pop_sd), nrow=n2)
          mean_x1 = apply(x1, 2, mean) # Calculate the t values
          mean_x2 = apply(x2, 2, mean)
          var_x1 = apply(x1, 2, var)
          var_x2 = apply(x2, 2, var)
          s = sqrt((var_x1 * (n1 - 1) + var_x2 * (n2 - 1)) / (n - 2))
          t = (mean_x1 - mean_x2) / (s * sqrt(1 / n1 + 1 / n2))
          d = gamma((n - 2) / 2) / gamma((n - 3) / 2) * sqrt(2 / (n - 2)) * sqrt(1 / n1 + 1 / n2) * t # Convert t values
into d values
          var_d = 1 / n1 + 1 / n2 + d^2 - (gamma((n - 3) / 2) / gamma((n - 2) / 2))^2 * (n - 4) / 2 * d^2 # Estimate the
variance of d
          mean(var_d) # Return the expected value of the estimate of the variance of d
}
var_of_d = function(delta, n1, n2) {
          cat("Variance of d:\n")
          cat("- Population delta =", round(delta, 2), "\n") # Print the parameters
          cat("- Size of the samples from the first population =", n1, "\n")
          cat("- Size of the samples from the second population =", n2, "\n");
          cat("- Variance of d knowing delta (using formula) = ") # Print the variance calculated with the formula
          cat(round(var_of_d_using_formula(delta, n1, n2), 2), "\n")
          cat("- Variance of d (using simulations) = ") # Print the variance obtained with the simulations
          cat(round(var_of_d_using_simulations(delta, n1, n2), 2), "\n")
          cat("- Expected value of the biased estimate of the variance of d = ") # Print the expected values of the
estimates of the variance of d
          cat(round(ev_of_biased_var_of_d(delta, n1, n2), 2), "\n")
          cat("- Expected value of the unbiased estimate of the variance of d = ")
          cat(round(ev_of_unbiased_var_of_d(delta, n1, n2), 2),"\n")
}
# Usage: var_of_d(delta, n1, n2), e.g.:
var_of_d(0, 10, 10)
var_of_d(pi / 2, 10, 10)
var_of_d(pi / 2, 25, 25)
```

4.2.4 Pre-processing

Pre-processing of studies in ES-SDM consists of creating, for each study, a map of *d* values (Hedges and Olkin 1985) and a map of their variances. These maps are later combined to obtain the meta-analytic maps.

If a *t* map is available, the conversion to unbiased effect size and variance maps is straightforward using the formulas described in sections 4.2.2 and 4.2.3. These conversions were included in the SDM software library (available at http://www.sdmproject.com/) after NIfTI affine transformation and Talairach conversion using trilinear interpolation. Maps of statistics other than *t* values, such as *z* maps or probabilistic non-parametric maps, might also be included as long as they can be converted to *t* maps. Usual conversions have been already included in the SDM software to simplify the procedure.

When a statistical parametric map is not available, the effect size can only be exactly calculated in those voxels containing a peak (applying the same conversions than in maps), while it must be estimated for the rest of the voxels. As in the original SDM method presented in Chapter 2 (Radua and Mataix-Cols 2009), this estimation is conducted by assigning an effect size to each voxel depending on its distance to close peaks (≤20mm) by means of an un-normalized Gaussian kernel *K*:

$$K(D) = \exp\left(-\frac{4 \cdot \log(2)}{FWHM^2} \cdot D^2\right)$$

where *FWHM* is the full width at half maximum, and *D* is the distance between the voxel and the peak (*D* = 0 in the voxel containing the peak). Setting *FWHM* to 20mm, slightly narrower than in previous versions of SDM, is recommended because this setting was found to optimally balance sensitivity and specificity in ES-SDM (see section 4.3), and might account for several spatial errors such as coregistration mismatch or cluster size (the larger the cluster, the more error between the peak and the centre of the cluster) (Gartus, Geissler et al. 2007; Radua and Mataix-Cols 2010). It must be noted that although the kernel has a different aim in SDM (i.e. recreating the cluster of signed differences) than in peak-probability methods (i.e. establishing the probability of a peak), similar FWHM have been indeed recommended for ALE and MKDA (Salimi-Khorshidi, Smith et al. 2009; Radua and Mataix-Cols 2010). In ES-SDM, the kernel is multiplied by the effect size of the peak, and when a voxel can be assigned values from more than one coordinate in the same study, these values are averaged weighting by the square of the distance to each close peak. As shown in **Figure 4.5**, this weighted averaging results in more plausible estimations than in previous methods.

Finally, if the *t* values of the peak coordinates are unknown, a threshold-based imputation of the effect size might be conducted. This consists of estimating the mean effect-size of peaks from studies reporting *t* values, separately for each type of threshold (e.g. “corrected P = 0.05” and “uncorrected P = 0.001”). We recommend basing these estimations on careful meta-analyses, ensuring that enough studies are present in each threshold-type group and checking for plausible results and heterogeneity. For simplicity,

Figure 4.5 Peak-coordinates mapping in some voxel-based meta-analytic methods.

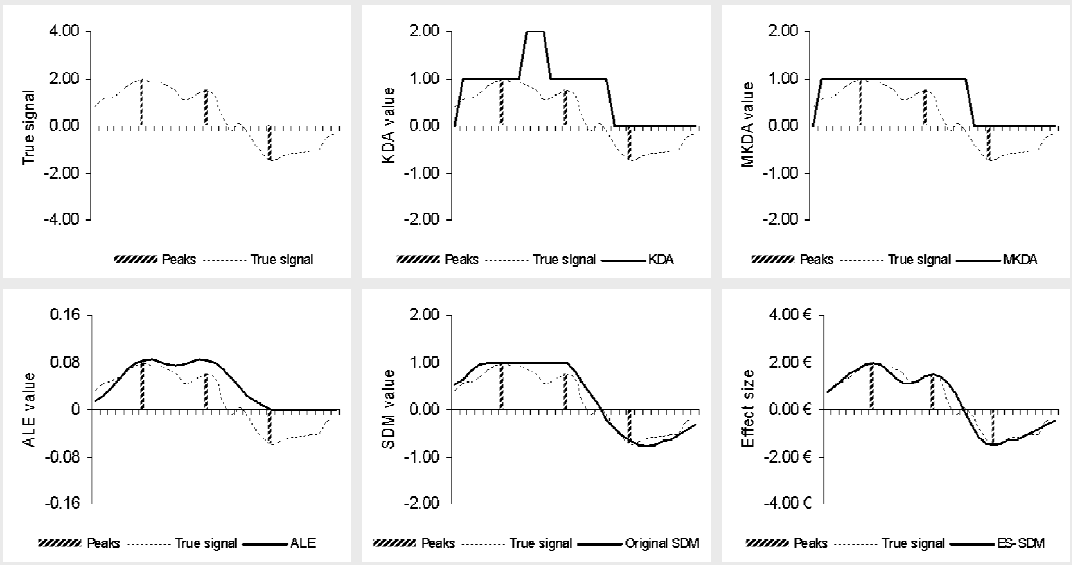

True signal refers to the values obtained in the original study within a straight line of grey matter, e.g. difference in grey matter volume between patients and controls in a straight line of voxels from parietal cortex. True signal and peak heights have been scaled in each plot for graphical purposes.
ALE: activation likelihood estimator. ES-SDM: effect size SDM. KDA: kernel density analysis. MKDA: multilevel KDA. SDM: signed differential mapping.

calculations are now automatically conducted within the ES-SDM software. In case that no studies can be used to estimate the mean effect-size of peaks, $d = 2\pi /5 = 1.26$ (one-sample) and $d = 2\pi /4 = 1.57$ (two-sample) might represent plausible conventional effect size values for positive peaks with unknown *t* value, as they can be checked to ensure uncorrected $p < 0.001$. Similarly, $d = -2\pi /5$ (one-sample) and $d = -2\pi /4$ (two-sample) might represent plausible conventional effect size values for negative peaks. In this last case ES-SDM behaves like previous SDM versions.

4.2.5 Meta-analytical models

A meta-analysis consists of combining the data from each study, e.g. calculating the mean of all the studies or fitting a general linear model. ES-SDM implements random-effects models in which each study is weighted by the inverse of the sum of its variance plus the between-study variance as obtained by the DerSimonian–Laird estimator (DerSimonian and Laird 1986), which is statistically comparable to the restricted maximum likelihood while much less computer-demanding (Viechtbauer 2005). Specifically, the heterogeneity Q statistic and the DerSimonian–Laird estimator are calculated with the following formulas:

$$W_{fixed} = \left(\frac{1}{Var(d_i)}\right) \times I_N \;,\; W_{random} = \left(\frac{1}{Var(d_i) + Var_{between}}\right) \times I_N$$

$$B = \left(X^T \times W \times X\right)^{-1} \;,\; \beta = B \times X^T \times W \times (d_i)$$

$$Q_H = (d_i)^T \times W_{fixed} \times (d_i) - \left(X \times \beta_{fixed}\right)^T \times W_{fixed} \times \left(X \times \beta_{fixed}\right)$$

$$Var_{between} = \frac{Q_H - (N - p)}{tr\left(W_{fixed}\right) - tr\left(X^T \times W_{fixed} \times W_{fixed} \times X \times B_{fixed}\right)} \geq 0$$

where *W* are the weight matrixes, $Var(d_i)$ is the vector of study effect-size variances, *I* is the identity matrix, $Var_{between}$ is the between-studies variance, *B* are the linear model B matrixes, X is the regressors matrix, *β* are the coefficient vectors, Q_H is the heterogeneity statistic, *N* is the number of studies, *p* is the

number of regressors (including the intercept or mean) and *tr* is the trace of the matrix.

With this approach: a) studies with larger sample size or lower variability contribute more; b) effects are assumed to randomly vary between samples; and c) heterogeneity Q statistic maps can be used to explore those brain regions with higher heterogeneity. This heterogeneity Q statistic is commonly assessed in terms of a χ^2 distribution, but for software and user conveniences its values are automatically converted to standard *z* values in ES-SDM. Please note that the heterogeneity Q statistic is not the same than the Q statistics presented in Chapter 3, which summarize the differences between more than two groups (or the effect of more than one regressor) (Radua, van den Heuvel et al. 2010).

4.2.6 Assessment of the statistical significance

Despite the fact that meta-analytic estimates are *z* values, assessment of their statistical significance is not straightforward. The systematic use of null effect sizes when pre-processing voxels far from any peak coordinate bias *z* values towards 0, making the standard test based on the normal distribution too conservative. Moreover, previous randomization tests based on randomizing the location of the peaks (Radua and Mataix-Cols 2009) are not applicable here because of the potential use of statistical parametric maps.

Table 4.1 ES-SDM thresholds (z values) obtained in the validation work.

Number of permutations	Only peaks (with *t* value)	20% statistical parametric maps	100% statistical parametric maps	Only peaks *without t* value
1	1.202	1.239	2.180	1.018
2	1.204	1.244	2.167	1.016
3	1.203	1.249	2.166	1.022
4	1.200	1.250	2.171	1.025
5	1.200	1.250	2.167	1.029
6	1.201	1.254	2.168	1.030
7	1.206	1.254	2.168	1.030
8	1.206	1.258	2.164	1.030
9	1.206	1.255	2.165	1.030
10	1.207	1.254	2.164	1.030
11	1.207	1.252	2.164	1.032
12	1.207	1.252	2.164	1.032
13	1.207	1.253	2.166	1.032
14	1.206	1.252	2.165	1.031
15	1.206	1.252	2.168	1.030
16	1.207	1.250	2.168	1.029
17	1.206	1.250	2.167	1.028
18	1.207	1.251	2.169	1.029
19	1.207	1.250	2.170	1.030
20	1.207	1.250	2.173	1.030

To solve this issue, the randomization test was modified so that instead of randomizing the location of the peaks, it randomizes the location of the voxels within the standard SDM grey matter template. Thus, the null hypothesis assumes that effect-sizes (rather than only peaks) are randomly distributed throughout the brain. In practice, this approach is similar to that adopted by newer versions of ALE, i.e. picking a random voxel from study 1, then picking a random voxel from study 2, then picking a random voxel from study 3, etc. until one voxel is selected from each study (Eickhoff, Laird et al. 2009). Interestingly, this test empirically showed to be much more reliable than the previous one, returning a high statistical stability with just 20 permutations (each of them retrieving 77,850 voxel values for the null distribution). **Table 4.1** shows the fast convergence of the statistical thresholds in the data used to validate the method.

Corrected p-values in neuroimaging are known to be critically affected by methodological factors such as the use of one or other correction method (e.g. FDR, family wise error (FWE), cluster-based, etc.), or the selection of one or another template (with more or less voxels, or with one shape or another). It is not uncommon in original neuroimaging studies, for example, that a FWE-corrected p-value is about 0.9 and the corresponding FDR-corrected p-value is about 0.01 (see for example (Bonilha, Rorden et al. 2004)). Thus, it is not recommended that meta-analytic researchers solely rely on (uncorrected or corrected) p-values, but it is strongly suggested that they use the combination of two thresholds and complement the analysis with several tests to assess the robustness and heterogeneity of the findings (Radua and Mataix-Cols 2009). Based on the empirical validation detailed in section 4.3, a main threshold of uncorrected P = 0.005 is proposed, as this was found to optimally balance sensitivity and specificity and to be an approximate equivalent to corrected p-value = 0.05 (indeed 0.025) in ES-SDM. Of course, this equivalence is only approximate, so that some thresholding error is expected when using this approach, and researchers might prefer to use other thresholds. To reduce the possibility of false positive results, an additional *z*-based threshold (e.g. $z > 1$) is suggested. It must be noted that $z > 1$ would be associated to a clearly non-significant p-value under the standard normal distribution, but this is not the case under the empirical distributions found by the permutation tests, as the use of null effect sizes when pre-processing voxels far from any peak coordinate makes $z > 1$ much more unlikely (i.e. associated to a much lower p-value). Importantly, the inclusion of studies with no findings would cause a decrease of

all *z* values which would cause a number of voxels cease to be detected as "significant".

4.2.7 Complementary analyses

As in previous SDM versions, complementary analyses such as jack-knife, subgroups, meta-regression and covariate analyses (Radua and Mataix-Cols 2009; Radua, van den Heuvel et al. 2010) are strongly recommended to assess the robustness and heterogeneity of the results. Briefly, jack-knife sensitivity analyses consists of repeating the analysis discarding (only) one study each time, and is used to assess the reproducibility of the results. Meta-regression and covariate analyses are used to look for potential confounding variables and moderators.

Of special interest is the now available combination of heterogeneity Q maps and meta-regression in order to correctly explore the meta-analytic heterogeneity. Similarly to the main outcome maps, it must be highlighted that heterogeneity Q maps only show which brain regions present significant between-study heterogeneity *as compared to the global set of voxels*, even if they are only marginally heterogeneous. It is also important to note that regions with differences between patients and controls may be falsely detected as heterogeneous because of the discrepancy between the real effect sizes from studies reporting peaks and the null effect sizes from studies not reporting peaks.

4.2.8 Validation of ES-SDM

Assessment of the validity of the method required the comparison of the results of an ES-SDM meta-analysis with the results of a reference analysis. In a study of peak-probability methods, Salimi-Khorshidi *et al.* used an image-based meta-analysis as the reference analysis (Salimi-Khorshidi, Smith et al. 2009). However, this possibility was discarded because one of the aims of this study was, precisely, to assess the validity of image-based ES-SDM meta-analyses. As an alternative, a pooled analysis of the original individual data was employed, as this analysis can be considered the "gold standard" (Stewart and Parmar 1993; Lambert, Sutton et al. 2002; Higgins and Green 2009).

First, data of 91 healthy participants in functional magnetic resonance imaging (fMRI) experiments of fearful face processing were allocated to 10 subgroups and standard fMRI analyses were conducted in each subgroup. Second, the data pertaining to these 10 subgroups were meta-analyzed with ES-SDM software - emulating thus the standard meta-analytical procedure of 10 studies. Finally, the results of this simulated "meta-analysis" were compared with the results of the pooled analysis of all these participants' data taken together (i.e. the "true map").

Ninety-one right-handed white Caucasian healthy individuals (46 males; age = 32.5±9, range 19-56 years), with no personal or family history of psychiatric disorder participated in this study. Exclusion criteria were current or past substance abuse, head injury, mental retardation, or any pre-existing psychiatric or neurological diagnosis. The study was approved by the Ethics

Committee of the Institute of Psychiatry, King's College London. Participants were given full details about the experimental protocol and gave their written informed consent before the beginning of the experiments.

The fMRI stimuli were blocks of dynamic emotional facial expressions of fear, consisting of short (1 sec) black and white movie clips based on the NimStim set of facial pictures (http://www.macbrain.org/), alternated with blocks of dynamic geometric figures (ovals). The participants were requested to press a button with their index finger as soon as they saw a colour filter at the end of each black and white movie clip. This instruction was aimed to ensure that participants were attending to the stimuli and to favour an implicit emotional processing.

All imaging acquisition was performed on a General Electric Signa 3 Tesla scanner (Milwaukee, WI, USA) at the Centre for Neuroimaging Research of the Institute of Psychiatry (London, UK). Reliable image quality was obtained by using a semi-automated quality control procedure. A quadrature birdcage headcoil was used for radiofrequency transmission and reception. For blood oxygen level-dependent (BOLD) functional imaging, 189 T2*-weighted whole-brain volumes were acquired during the task. For high-resolution gradient-echo structural imaging, a whole brain volume was acquired in the intercommissural plane consisting of 38 slices: TR = 2000 ms, TE = 25 ms, flip angle = 80°, slice thickness = 2.4 mm, interslice gap = 1.0 mm, image acquisition matrix = 64^2, in-plane spatial resolution = 3.75 × 3.75 mm^2. The EPI data set provided complete brain coverage.

Functional images were first motion-corrected by registering them to their mean with SPM5 (Wellcome Department of Cognitive Neurology, London, UK). The structural image was then coregistered to the mean functional image and segmented into grey matter, white matter and cerebro-spinal fluid. The normalization parameters to the standard MNI space obtained in this segmentation were applied to the functional images, thus providing a grey matter-optimized normalization. Finally, the functional images were smoothed with an 8mm-FWHM Gaussian kernel and modelled by the different experimental conditions with a standard hemodynamic response function. At the end of the first-level analysis there was one contrast map per each individual, representing the BOLD response to the perception of dynamic fearful faces as compared to dynamic ovals.

Contrast images were included into a standard SPM second-level (i.e. group) analyses and thresholded with uncorrected $P < 0.001$ and cluster extent ≥ 10 voxels. Participants were allocated to 10 subgroups by scan date order, i.e. the first 9 participants scanned were allocated to the first subgroup, the next 9 participants to the second subgroup, and so on, with the last subgroup composed of 10 rather than 9 participants. These subgroups should be understood as the samples included in a meta-analysis. We also conducted a group analysis including all 91 participants, i.e. a pooled analysis, which should be understood as the reference or “true” map.

Finally, the group data was subjected to the following meta-analytical procedures: ALE, original SDM, ES-SDM using only coordinates, ES-SDM using both coordinates and images, and ES-SDM using only images. Results

from these meta-analyses were compared with the results of the pooled analysis (after Talairach conversion by trilinear interpolation) by means of the following statistics (Salimi-Khorshidi, Smith et al. 2009): Dice similarity coefficient (a measure of overlap between the two images) (Dice 1945), sensitivity (i.e. the proportion of significant voxels in the pooled analysis detected as significant in the meta-analysis) and false positive rate (i.e. the proportion of non-significant voxels in the pooled analysis detected as significant in the meta-analysis). In order to test the adequacy of the statistical threshold (uncorrected $P \leq 0.005$) and FWHM (20mm), the above ES-SDM validation was repeated setting uncorrected $P \leq 0.001$, 0.005 or 0.010, and FWHM = 10mm, 15mm, 20mm, 25mm or 30mm.

4.3 RESULTS

As shown in **Figure 4.6 F** (pooled analysis), the perception of dynamic fearful faces was associated with activation of bilateral occipital visual areas and amygdala (see **Tables 4.2** to **4.12** for detailed results of the SPM analyses). The new ES-SDM method showed a good overlap with this analysis (47-74%), with an adequate sensitivity (52-100%) and control of false positives (1.5-3.5%) (**Figure 4.6 C-E**, **Table 4.13**). ALE showed a lower overlap (29%), and the original SDM-based maps lay somewhere in between those of ALE and ES-SDM (see **Table 4.13** for detailed results).

Both the overlap and sensitivity were substantially higher when the statistical parametric maps replaced the peak coordinates, with clear improvements already apparent when using statistical parametric maps from just few samples. For instance, the sensitivity increased from 55% to 73% when including the statistical parametric map of the first subgroup, and to 87% when also including the statistical parametric map of the second subgroup. The omission of *t* values neither relevantly decreased the overlap or sensitivity, nor increased the false positive rate of coordinate-based meta-analyses.

A more conservative threshold (P = 0.001) resulted in a large reduction of overlap and sensitivity. Conversely, a more liberal threshold (P = 0.010)

Figure 4.6 Validation of ES-SDM.

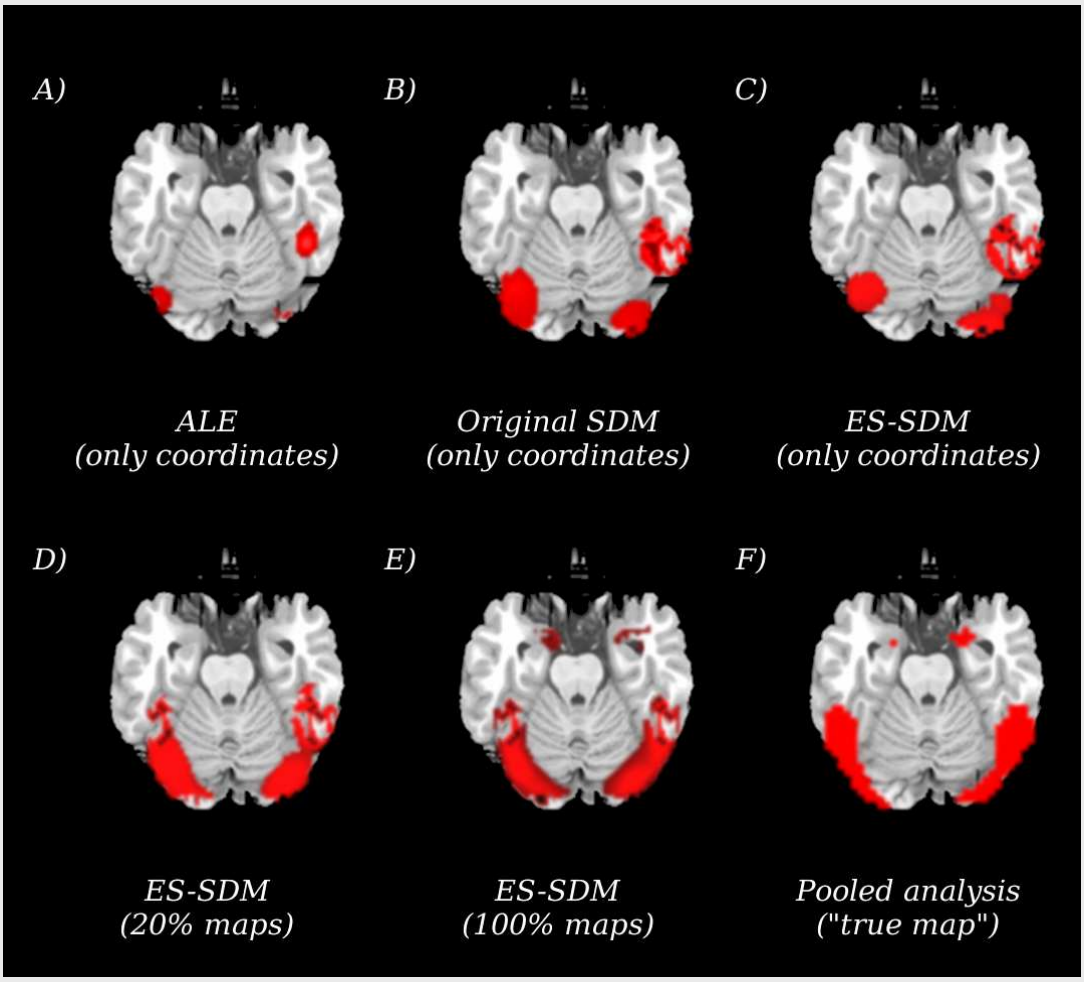

Significant activations to fearful faces (as compared to ovals) in the different meta-analytic methods and in the pooled analysis of individual original data are presented in red. Brain axial slices are in Talairach space (z = -19). Results from the ALE meta-analysis (A) showed a 29% overlap with the true map (F). Results from the original SDM meta-analysis (B) showed a 49% overlap with the true map (F). Results from the ES-SDM meta-analyses (C-E) showed 47-74% overlap with the true map (F).

ALE: activation likelihood estimator. ES-SDM: effect size SDM. SDM: signed differential mapping.

resulted in slightly higher sensitivity, higher false positive rate and similar overlap. Regarding the smoothing kernel (FWHM), the use of narrower kernels (FWHM = 10mm) resulted in a large reduction of overlap and sensitivity, while the use of wider kernels (FWHM = 30mm) resulted in an inferior overlap.

Table 4.2. Results from fMRI analysis in subgroup 1 (participants 1-9)

	MNI(x)	MNI(y)	MNI(z)	*T* value	*P* value
Right occipitotemporocerebellar region					
Right fusiform gyrus (BA 37)	48	-48	-20	8.31	< 0.001
Right fusiform gyrus (BA 37)	51	-68	-14	6.14	< 0.001
Right middle temporal gyrus (BA 39)	58	-58	10	5.91	< 0.001

Table 4.3. Results from fMRI analysis in subgroup 2 (participants 10-18)

	MNI(x)	MNI(y)	MNI(z)	*T* value	*P* value
Right occipitotemporocerebellar region					
Right inferior occipital gyrus (BA 17)	27	-99	-7	7.22	< 0.001

Table 4.4. Results from fMRI analysis in subgroup 3 (participants 19-27)

	MNI(x)	MNI(y)	MNI(z)	*T* value	*P* value
Right occipitotemporocerebellar region					
Right cerebellum (culmen)	44	-48	-24	9.28	< 0.001

Table 4.5. Results from fMRI analysis in subgroup 4 (participants 28-36)

	MNI(x)	MNI(y)	MNI(z)	*T* value	*P* value
(none)					

Table 4.6. Results from fMRI analysis in subgroup 5 (participants 37-45)

	MNI(x)	MNI(y)	MNI(z)	*T* value	*P* value
Left occipitotemporocerebellar region					
Left middle temporal gyrus (BA 39)	-51	-68	17	7.21	< 0.001

Threshold: uncorrected P < 0.001, cluster extent ≥ 10 voxels

Thresholds were very stable from the first permutations (**Table 4.1**). As expected for the systematic use of null effect sizes when pre-processing voxels far from any peak coordinate, thresholds were clearly lower as more coordinates rather than statistical parametric maps were included in the meta-analysis.

Table 4.7. Results from fMRI analysis in subgroup 6 (participants 46-54)

	MNI(x)	MNI(y)	MNI(z)	*T* value	*P* value
Left occipitotemporocerebellar region					
Left cerebellum (declive)	-37	-85	-14	7.03	< 0.001
Left cerebellum (declive)	-37	-78	-20	6.12	< 0.001
Left lingual gyrus (BA 17)	-17	-99	-10	5.92	< 0.001
Right occipitotemporocerebellar region					
Right fusiform gyrus (BA 37)	48	-44	-20	6.28	< 0.001

Table 4.8. Results from fMRI analysis in subgroup 7 (participants 55-63)

	MNI(x)	MNI(y)	MNI(z)	*T* value	*P* value
(none)					

Table 4.9. Results from fMRI analysis in subgroup 8 (participants 64-72)

	MNI(x)	MNI(y)	MNI(z)	*T* value	*P* value
Left occipitotemporocerebellar region					
Left inferior occipital gyrus (BA 18)	-37	-95	-10	9.13	< 0.001
Left cerebellum (culmen)	-44	-41	-34	7.86	< 0.001
Left cerebellum (declive)	-41	-75	-17	5.34	< 0.001
Right frontal region					
Right middle frontal gyrus (BA 11)	24	27	-20	7.06	< 0.001
Right inferior frontal gyrus (BA 47)	31	24	-24	5.56	< 0.001
Right occipitotemporocerebellar region					
Right lingual gyrus (BA 17)	17	-102	-10	6.98	< 0.001
Right fusiform gyrus (BA 18)	27	-95	-10	5.98	< 0.001
Right cerebellum (declive)	37	-88	-17	5.47	< 0.001
Right insular region					
Right insula (BA 13)	48	-20	0	6.53	< 0.001
Left frontal region					
Left inferior frontal gyrus (BA 47)	-41	24	-17	5.43	< 0.001
Left inferior frontal gyrus (BA 47)	-51	27	-10	4.86	0.001

Threshold: uncorrected P < 0.001, cluster extent ≥ 10 voxels

Table 4.10. Results from fMRI analysis in subgroup 9 (participants 73-81)

	MNI(x)	MNI(y)	MNI(z)	*T* value	*P* value
Right occipitotemporocerebellar region					
Right cerebellum (culmen)	48	-48	-27	6.31	< 0.001
Right fusiform gyrus (BA 36)	48	-37	-24	6.14	< 0.001

Table 4.11. Results from fMRI analysis in subgroup 10 (participants 82-91)

	MNI(x)	MNI(y)	MNI(z)	*T* value	*P* value
Left frontal region					
Left middle frontal gyrus (BA 6)	-37	-3	48	8.88	< 0.001
Left precentral gyrus (BA 6)	-48	3	44	8.46	< 0.001
Left precentral gyrus (BA 6)	-37	0	37	6.55	< 0.001
Right occipitotemporocerebellar region					
Right cerebellum (declive)	27	-85	-14	7.58	< 0.001
Right frontal region					
Right middle frontal gyrus (BA 6)	34	0	54	7.42	< 0.001
Left occipitotemporocerebellar region					
Left cerebellum (culmen)	-3	-34	-3	7.18	< 0.001
Left cerebellum (culmen)	-41	-44	-31	6.59	< 0.001
Left fusiform gyrus (BA 36)	-48	-41	-27	5.90	< 0.001
Left cerebellum (tuber)	-44	-65	-24	5.68	< 0.001

Table 4.12. Results from fMRI analysis in all subgroups ("pooled analysis")

	MNI(x)	MNI(y)	MNI(z)	*T* value	*P* value
Right occipitotemporocerebellar region					
Right cerebellum (culmen)	48	-51	-24	12.17	< 0.001
Right middle occipital gyrus (BA 18)	44	-82	-7	10.34	< 0.001
Right inferior occipital gyrus (BA 18)	27	-95	-7	9.18	< 0.001
Right cerebellum (declive)	7	-75	-7	3.62	< 0.001
Right middle temporal gyrus (BA 21)	54	-41	10	3.62	< 0.001
Left occipitotemporocerebellar region					
Left cerebellum (declive)	-41	-78	-14	9.24	< 0.001
Left cerebellum (culmen)	-44	-44	-24	8.94	< 0.001
Left cerebellum (declive)	-44	-68	-20	8.16	< 0.001
Left superior temporal gyrus (BA 22)	-58	-51	10	5.18	< 0.001
Left middle temporal gyrus (BA 19)	-41	-65	17	3.59	< 0.001
Right amygdala / parahippocampal region					
Right parahippocampal gyrus (BA 34)	17	0	-20	4.53	< 0.001
Right uncus (BA 34)	20	3	-27	3.81	< 0.001
Left amygdala / parahippocampal region					
Left parahippocampal gyrus (BA 34)	-17	0	-24	3.69	< 0.001

Threshold: uncorrected P < 0.001, cluster extent ≥ 10 voxels

Table 4.13 Validation of ES-SDM.

	Overlap [(a)]	Sensitivity	False positives rate
ES-SDM with default settings:			
Only peaks (with *t* value)	47.0 %	55.1 %	2.5 %
10% statistical parametric maps [(b)]	65.5 %	72.7 %	1.5 %
20% statistical parametric maps [(b)]	72.0 %	86.7 %	1.7 %
30% statistical parametric maps [(b)]	73.8 %	92.5 %	1.8 %
40% statistical parametric maps [(b)]	69.5 %	95.6 %	2.5 %
50% statistical parametric maps [(b)]	67.2 %	96.9 %	2.9 %
60% statistical parametric maps [(b)]	68.3 %	98.0 %	2.8 %
70% statistical parametric maps [(b)]	65.7 %	98.6 %	3.2 %
80% statistical parametric maps [(b)]	66.0 %	99.3 %	3.2 %
90% statistical parametric maps [(b)]	63.8 %	100 %	3.5 %
100% statistical parametric maps	64.0 %	100 %	3.5 %
Only peaks *without t* value	48.5 %	51.6 %	1.9 %
ES-SDM with other settings:			
P = 0.001 (only peaks with *t* value)	36.0 %	30.5 %	1.2 %
P = 0.005 (only peaks with *t* value)	47.0 %	55.1 %	2.5 %
P = 0.010 (only peaks with *t* value)	48.4 %	64.7 %	3.2 %
FWHM = 10mm (only peaks with *t* value)	40.7 %	31.9 %	0.8 %
FWHM = 15mm (only peaks with *t* value)	47.2 %	45.0 %	1.4 %
FWHM = 20mm (only peaks with *t* value)	47.0 %	55.1 %	2.5 %
FWHM = 25mm (only peaks with *t* value)	41.8 %	54.6 %	3.3 %
FWHM = 30mm (only peaks with *t* value)	38.8 %	55.7 %	4.1 %
Other methods:			
ALE (FWHM = 10mm, FDR = 0.05)	28.9 %	19.9 %	0.6 %
Original SDM (FWHM = 25mm, *P* = 0.001)	49.0 %	51.3 %	1.8 %

(a) Overlap is defined as the Dice similarity coefficient (Dice 1945).
(b) The statistical parametric map of the first subgroup was used for testing “10% statistical parametric maps”, the statistical parametric maps of the first 2 subgroups were used for testing “20% statistical parametric maps”, and so on.
ALE: activation likelihood estimator. ES-SDM: effect size signed differential mapping. FDR: false discovery rate. FWHM: full width at half maximum. SDM: signed differential mapping.

4.4 DISCUSSION

This chapter introduced a new version of the SDM meta-analytic method, ES-SDM. Its main innovations are the possibility of combining peak coordinates and statistical parametric maps in the same meta-analysis, as well as the use of well-established statistics accounting for within- and between-study variance. The software is freely available at http://www.sdmproject.com/ .

To validate the new version the results of a simulated meta-analysis of the data pertaining to 10 subgroups of participants were compared with the results of the pooled analysis of all 91 participants together. Results from the pooled analysis were fully consistent with previous literature on the neural networks involved in fearful faces perception (Fusar-Poli, Placentino et al. 2009; Radua, Phillips et al. 2010). ES-SDM showed a good overlap with the pooled analysis, indicating that this method was able to replicate, to a great extent, the results obtained when the original individual data were available. It also showed an adequate sensitivity and control of false positives.

As expected, overlap and sensitivity were substantially higher when peak coordinates were replaced by statistical parametric maps. Importantly, this effect was already observed when statistical parametric maps were used from only few samples, using peak coordinates for the rest of samples. The crucial implication is that a meta-analysis can be substantially improved by including statistical parametric maps, instead of coordinates, even from just one sample.

Overlap and sensitivity were similar when peak coordinates without *t* value, or with *t* value, were used. This lack of significant improvement when using *t* values might indicate that the use of effect sizes has limited influence on the results. A potential explanation for this might be that the effect sizes are indeed rather similar across the different peak-coordinates of a study, as all of them are above a statistical threshold.

The overlap and sensitivity of ES-SDM were higher than those of ALE, comparable to the original SDM when only coordinates were included and higher than both previous methods when statistical parametric maps were also included. It must be noted that the sensitivity values should not be directly extrapolated to publication-based meta-analyses. On the one hand, samples of such meta-analyses might be more heterogeneous, thus decreasing the sensitivity of any meta-analytic method. On the other hand, a publication-based meta-analysis typically includes more studies and with larger samples, a fact which substantially increases the sensitivity. In any case, ALE, original SDM and the different settings of ES-SDM meta-analyses were tested using the same 10 samples, and therefore their results are comparable.

4.4.1 Limitations

Some limitations of the new ES-SDM method must be highlighted. First, while threshold-based imputation procedures do not bias the results towards studies using one or another threshold type, they are associated to a variable degree of imprecision. However, it must be noted that this imprecision is lower than that in

previous coordinate-based methods, which assigned the same effect-size to all studies – the simplicity of some methods might conceal the artificially constant effect-sizes but not its effects, e.g. methods based on counting peaks are mathematically equivalent to methods setting an effect-size of "1" to all peaks. Furthermore, according to the validation data, the use of effect sizes, even if necessary for the most of the new features, only has limited influence on the results. Second, ES-SDM assumes effect sizes to come from homogenous *t* contrasts, while they might come from different covariate models or from different raw statistics. However, this is a limitation of all coordinate-based methods (all of them combine peaks from different origin), which could be controlled by SDM covariate analyses if relevant. And again, this limitation might have a subtle relevance as the effect sizes only have limited influence on the results. Finally, as in any other coordinate-based method, the inclusion of more or fewer secondary peaks will cause the recreated effect-size maps to be more or less precise.

4.4.2 Conclusions

To conclude, ES-SDM is a new version of the SDM meta-analytic method, based on well-established statistics accounting for within- and between-study variance, which allows combining both peak coordinates and statistical parametric maps in the same meta-analysis. The new version has been shown to be valid and superior to previous coordinate-based meta-analytical methods.

Default settings have been shown to optimize the sensitivity while protecting against the false positives.

4.5 ACKNOWLEDGEMENTS

Development of the MacBrain Face Stimulus Set was overseen by Nim Tottenham and supported by the John D. and Catherine T. MacArthur Foundation Research Network on Early Experience and Brain Development. Please contact Nim Tottenham at *tott0006@tc.umn.edu* for more information concerning the stimulus set.

4.6 REFERENCES

Bonilha, L., C. Rorden, et al. (2004). "Voxel-based morphometry reveals gray matter network atrophy in refractory medial temporal lobe epilepsy." Arch.Neurol. **61**(9): 1379-1384.

Cooper, H. and L. V. Hedges (1994). Handbook of research synthesis. New York, Russell Sage Foundation.

DerSimonian, R. and N. Laird (1986). "Meta-analysis in clinical trials." Control Clin Trials **7**(3): 177-188.

Dice, L. R. (1945). "Measures of the amount of ecologic association between species." Ecology **26**(3): 297-302.

Eickhoff, S. B., A. R. Laird, et al. (2009). "Coordinate-based activation likelihood estimation meta-analysis of neuroimaging data: a random-effects approach based on empirical estimates of spatial uncertainty." Hum Brain Mapp **30**(9): 2907-2926.

Fusar-Poli, P., A. Placentino, et al. (2009). "Functional atlas of emotional faces processing: a voxel-based meta-analysis of 105 functional magnetic resonance imaging studies." J Psychiatry Neurosci. **34**(6): 418-432.

Gartus, A., A. Geissler, et al. (2007). "Comparison of fMRI coregistration results between human experts and software solutions in patients and healthy subjects." Eur.Radiol. **17**(6): 1634-1643.

Hedges, L. V. (1981). "Distribution theory for Glass's estimator of effect size and related estimators." J Educ Stat **6**(2): 107-128.

Hedges, L. V. and I. Olkin (1985). Statistical Methods for Meta-Analysis. Orlando, Academic Press.

Higgins, J. P. T. and S. Green (2009). Cochrane Handbook for Systematic Reviews of Interventions. Version 5.0.2. http://www.cochrane-handbook.org/, The Cochrane Collaboration.

Lambert, P. C., A. J. Sutton, et al. (2002). "A comparison of summary patient-level covariates in meta-regression with individual patient data meta-analysis." J Clin Epidemiol. **55**(1): 86-94.

Lazar, N. A., B. Luna, et al. (2002). "Combining Brains: A Survey of Methods for Statistical Pooling of Information." Neuroimage **16**(2): 538-550.

Radua, J. and D. Mataix-Cols (2009). "Voxel-wise meta-analysis of grey matter changes in obsessive-compulsive disorder." Br J Psychiatry **195**(5): 393-402.

Radua, J. and D. Mataix-Cols (2010). "Heterogeneity of coordinate-based meta-analyses of neuroimaging data: an example from studies in OCD - Authors' reply." Br J Psychiatry **197**(1): 77.

Radua, J., M. L. Phillips, et al. (2010). "Neural response to specific components of fearful faces in healthy and schizophrenic adults." Neuroimage **49**(1): 939-946.

Radua, J., O. A. van den Heuvel, et al. (2010). "Meta-analytical comparison of voxel-based morphometry studies in obsessive-compulsive disorder vs other anxiety disorders." Arch Gen Psychiatry **67**(7): 701-711.

Salimi-Khorshidi, G., S. M. Smith, et al. (2009). "Meta-analysis of neuroimaging data: A comparison of image-based and coordinate-based Pooling of studies." Neuroimage **45**(3): 810-823.

Stewart, L. A. and M. K. Parmar (1993). "Meta-analysis of the literature or of individual patient data: is there a difference?" Lancet **341**(8842): 418-422.

Turkeltaub, P. E., G. F. Eden, et al. (2002). "Meta-analysis of the functional neuroanatomy of single-word reading: method and validation." Neuroimage **16**(3 Pt 1): 765-780.

Viechtbauer, W. (2005). "Bias and efficiency of meta-analytic variance estimators in the random-effects model." Journal of Educational and Behavioral Statistics **30**(3): 261-293.

Wager, T. D., M. Lindquist, et al. (2007). "Meta-analysis of functional neuroimaging data: current and future directions." Soc Cogn Affect Neurosci **2**(2): 150-158.

CHAPTER 5

Meta-analysis of studies investigating white matter volume or water diffusivity

5.1 THEORY

One of the limitations of *signed differential mapping* (SDM) (Radua and Mataix-Cols 2009), *effect size* SDM (ES-SDM) (Radua, Mataix-Cols et al. 2012) and other existing voxel-based meta-analytic algorithms such as *activation likelihood estimate* (ALE) (Turkeltaub, Eden et al. 2002) and *multilevel kernel density analysis* (MKDA) (Wager, Lindquist et al. 2007) was that they are limited to meta-analyses of grey matter studies. Relevant neuroimaging modalities such as regional white-matter volumes (white matter voxel-based morphometry, VBM) or the set of measures derived from analyses of water diffusitivity (e.g. fractional anisotropy, FA) (Beaulieu 2002) could not be assessed with these existing methods. This chapter presents the adaptation of SDM for its application to white matter measures.

5.1.1 Justification

To appreciate the importance of adapting SDM (and, by extension all voxel-based methods) for the meta-analysis of white-matter studies, it must be noted that the null hypothesis of the standard randomization test presented in Chapter 2 (Radua and Mataix-Cols 2009) is that peak coordinates are uniformly distributed throughout all the *grey* matter of the brain. The test consists of randomly relocating the original peak coordinates in all *grey* matter voxels as defined by a *grey* matter randomization template, and comparing the original values with the values obtained from these randomizations (Wager, Lindquist et al. 2007).

However, if the aim is to assess the statistical significance of *white* (rather than grey) matter volumes or fractional anisotropy values, a specific *white* matter randomization template is needed. Although some authors have employed grey matter or whole brain templates to meta-analyze white matter volumes or other measures (Di, Chan et al. 2009), this is clearly inadequate, because the corresponding null hypothesis would assume that *white* matter peak coordinates are uniformly distribute throughout all the *grey* matter of the brain. The effects of such practice are that white matter peaks show artificially concentrated in some regions of the brain (i.e. in the white matter) while not in other regions (i.e. in the grey matter), leading to increased false positive rates. The use of a *grey* matter randomization template to assess *white* matter parameters would be equivalent to the use of the body weight variance to assess the statistical significance of body height differences.

5.1.2 Creation of the white matter templates

The white matter mask was created with the standard parameters for grey matter masks (Wager, Lindquist et al. 2007), but including white instead of grey matter. Specifically, a map of white matter was created based on the Talairach Daemon (Lancaster, Woldorff et al. 2000), with a voxel size = 2 x 2 x 2m^3. In addition, a randomization map consisting of the mask of white matter plus an 8mm margin of grey matter was created.

These new templates were included in a new readily available version of SDM software (http://www.sdmproject.com/) to allow other researchers to conduct *statistically correct* voxel-based meta-analyses of white matter studies.

5.2 EXAMPLE: APPLICATION OF THE METHOD

To illustrate the practical uses of these new templates, this section describes a meta-analysis of white matter voxel-based morphometry studies in autism spectrum disorders (ASD).

This study was published in *Psychological Medicine* under the title '*Voxel-based meta-analysis of regional white-matter volume differences in autism spectrum disorder versus healthy controls*' (Joaquim Radua, Esther Via, Marco Catani and David Mataix-Cols 2011; 41:1539-1550). The definitive publisher-authenticated version is available online at http://journals.cambridge.org/action/displayAbstract?fileId=S0033291710002187 Copyright © Cambridge University Press 2010

5.2.1 Introduction

ASD, including autism and Asperger's syndrome, are characterized by impairments in social interaction, communication and imagination, as well as a rigid, repetitive pattern of behaviour (Wing 1996; APA 2000). The prevalence of ASD has been recently estimated to be approximately 9 per 1,000 children, and is more frequent in males (ADDMNS 2009). In adults, the prevalence of ASD might be similar (Brugha, McManus et al. 2009).

The precise aetiology of ASD is unknown but it is thought to have a strong genetic basis (Volkmar, Klin et al. 1998; Abrahams and Geschwind

2008). There is a large body of evidence highlighting the role of abnormal brain development in ASD (Schultz 2005). For example, structural neuroimaging studies have identified several brain systems implicated in the disorder, including the cerebellum, visual cortex, amygdala and hippocampus (Abell, Krams et al. 1999; McAlonan, Daly et al. 2002; Waiter, Williams et al. 2004; Brieber, Neufang et al. 2007; Craig, Zaman et al. 2007; Bonilha, Cendes et al. 2008; Ke, Hong et al. 2008; McAlonan, Suckling et al. 2008; Toal, Daly et al. 2009). Functional neuroimaging studies have reported reduced activations in the amygdala and related limbic regions including the cingulate cortex (Baron-Cohen, Ring et al. 1999; Pierce, Muller et al. 2001; Ashwin, Baron-Cohen et al. 2007), all of which are thought to be consistent with the deficits in social behavior that are characteristic of the disorder (Baron-Cohen, Ring et al. 2000).

A complementary and potentially more informative approach would be to identify systems-level or “supraregional” brain abnormalities in ASD, rather than within discrete brain regions. Cortical and subcortical regions that are altered in ASD are interconnected through a complex system of short and long-range tracts running within the white matter of each hemisphere. Regional white matter abnormalities in ASD have been investigated using different methods including a region of interest approach on structural magnetic resonance imaging (MRI) scans (e.g. T2-wieghted images) and more recent tract specific dissections of diffusion tensor imaging (DTI) datasets. These approaches are mainly hypothesis-driven and therefore have been usually limited to single structures such as the corpus callosum (Piven, Bailey et al. 1997; Hardan, Minshew et al. 2000), cerebellar tracts (Catani, Jones et al. 2008) and the

cingulum (Pugliese, Catani et al. 2009). This paucity of research might be partially due to the difficulties of manually delimitating some white matter regions, which is time consuming and requires extensive anatomical knowledge (Waiter, Williams et al. 2005).

The recent development of fully-automated, whole-brain, voxel-based morphometry (VBM) methods (Ashburner and Friston 2000; Ashburner and Friston 2001; Mechelli, Price et al. 2005), which overcome the difficulties in the manual delimitation of white matter regions, provides a powerful tool to study the potential changes in white matter volume in ASD. Unfortunately, recent applications of these novel methods to the study of white matter volumetric changes in ASD are often limited by relatively small sample sizes, resulting in insufficient statistical power. In this context, we considered it timely to perform a voxel-based quantitative meta-analysis of all published VBM studies in ASD reporting changes in white matter volume. This was conducted with the SDM methods described in the previous chapters (Radua and Mataix-Cols 2009; Radua, van den Heuvel et al. 2010), plus the white matter templates presented at the beginning of this chapter. In order to facilitate replication and further analyses by other colleagues, a readily accessible online database (http:/www.sdmproject.com/database), which contains all the data and methodological details from every study included in this meta-analysis, was also developed.

5.2.2 Methods

5.2.2.1 Criteria for inclusion and exclusion of studies

We conducted a comprehensive literature search of studies conducting VBM comparisons between patients with ASD and healthy controls published between 2002 –the date of the first white matter VBM study in ASD– and September 2010 using the PubMed, ScienceDirect, Web of Knowledge and Scopus databases. The search keywords were “Asperger” or “autism”, plus “morphometry”, “voxel-based” or “voxelwise”. In addition, the authors also conducted manual searches within several review papers and the reference sections of the obtained articles. Studies containing duplicated datasets, i.e. analyzed the same data in different manuscripts and studies with fewer than 10 patients were excluded. Next, the corresponding authors were contacted by email requesting any details not included in the original manuscripts. MOOSE guidelines for meta-analyses of observational studies (Stroup, Berlin et al. 2000) were followed in the study.

5.2.2.2 Comparison of global and regional white matter volumes

Meta-analytical differences in *global* white matter volumes were calculated using standard random-effects models with the “globals” procedure in SDM software (http://www.sdmproject.com/), which uses restricted maximum-likelihood estimation of the variance, a fitting method which has been

recommended over previous ones for its good balance between unbiasedness and efficiency (Viechtbauer 2005).

Regional differences in white matter volume between patients and controls were analyzed using the SDM methods described in the previous chapters (Radua and Mataix-Cols 2009; Radua, van den Heuvel et al. 2010), plus the white matter templates presented at the beginning of this chapter. The main analysis was complemented with additional analyses to assess the robustness of the findings (Radua and Mataix-Cols 2009), namely descriptive analyses of quartiles to find the actual proportion of studies reporting results in a particular brain region (regardless of p-values) and jack-knife sensitivity analyses to assess the reproducibility of the results. Reproducibility of the results was also assessed by separately analyzing paediatric and adult samples, though formal statistical tests could not be performed given the small number of studies in each group.

5.2.2.3 Localization of changes in white matter volume

A DTI derived atlas (Catani and Thiebaut de Schotten 2010) was used to optimally localize the changes in white matter volume detected in the meta-analysis. This atlas provides digital maps of long range white matter tracts normalized in a common space of reference. The maps are derived from virtual *in vivo* dissections (Catani, Howard et al. 2002; Catani and Thiebaut de 2008) of diffusion tensor datasets and provide information on the degree of anatomical variability within the normal population by quantifying the percentage of overlap

Figure 5.1 Inclusion of studies.

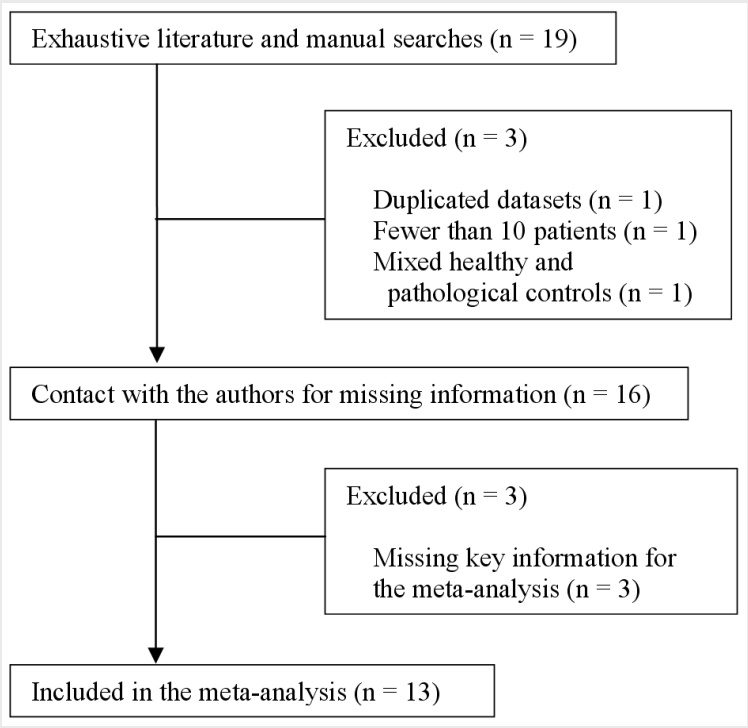

for each single voxel (e.g. 50%, 75% and >90%). The results from the VBM meta-analyses were therefore overlapped on the digital masks of each tract provided in the atlas to localize the regional differences.

5.2.3 Results

5.2.3.1 Included studies and sample characteristics

As shown in **Figure 5.1**, the search retrieved a total of 17 publications or abstracts comprising 19 studies (that is, independent comparisons between ASD and healthy control samples). Three publications were discarded because they contained duplicated datasets (McAlonan, Cheung et al. 2005), fewer than

10 patients (Yamasue, Ishijima et al. 2005) or a mixed control group that included healthy controls, children with reading disability and children with benign macrocephaly (Bigler, Abildskov et al. 2010). After contacting the authors no methodological ambiguities remained regarding the design or analysis of 11 publications comprising 13 independent comparisons, while 3 studies had to be excluded due to missing key information for our meta-analysis (i.e. peak coordinates from whole-brain analyses) (Schmitz, Daly et al. 2007; Hong, Ke et al. 2008; Langen, Schnack et al. 2009). Therefore, thirteen high-quality datasets could be included in this meta-analysis, of which 6 consisted of adult ASD samples and 7 of pediatric or adolescent samples. There was a partial sample overlap between two studies (McAlonan, Daly et al. 2002; Toal, Daly et al. 2009). For this reason the meta-analysis was first conducted with all studies and then repeated excluding the latter study. Finally, a potential overlap in the samples of two other studies could not be discarded (Ke, Hong et al. 2008; Ke, Tang et al. 2009), and for this reason the meta-analysis was also repeated excluding the latter.

Table 5.1 Demographic and clinical characteristics of the 13 voxel-based morphometry datasets included in the meta-analysis.

	Methodological aspects		Patients						Controls			
	Software name	Threshold	N	Age (SD)	Males	Full IQ (SD)	Autism	Asperger	N	Age (SD)	Males	Full IQ (SD)
Boddaert *et al.*	SPM99	$P < 0.05$ corrected	21	9.3 (2.2)	76%	42 (21)	100%	0%	12	10.8 (2.7)	58%	N/A
Bonilha *et al.*	SPM5	$P < 0.05$ corrected	12	12.4 (4.0)	100%	N/A	100%	0%	16	13.2 (5.0)	100%	N/A
Craig *et al.*	SPM2 + XBAMM	< 1 false-positive cluster	14	37.9 (11.4)	0%	103 (17)	29%	71%	19	35.0 (14.0)	0%	111 (14)
Ecker *et al.*	SPM5	$P < 0.001$ uncorrected	22	27.0 (7.0)	100%	104 (15)	N/A	N/A	22	28.0 (7.0)	100%	111 (10)
Hyde *et al.*	CIVET	$P < 0.05$ corrected	15	22.7 (6.4)	100%	100 (13)	100%	0%	15	19.2 (5.0)	100%	107 (12)
Ke *et al.*	SPM5	$P < 0.001$ uncorrected	17	8.9 (2.0)	82%	109 (19)	100%	0%	15	9.7 (1.7)	80%	110 (19)
Ke *et al.*	SPM5	$P < 0.001$ uncorrected	12	8.8 (2.3)	100%	101 (19)	100%	0%	10	9.4 (2.1)	100%	100 (18)
McAlonan *et al.* 2002	XBAMM	< 1 false-positive cluster	17	32.0 (10.0)	N/A	96 (15)	0%	100%	24	33.0 (7.0)	92%	114 (14)
McAlonan *et al.* 2009												
(Asperger sample)	XBAMM	< 1 false-positive cluster	18	11.2 (2.5)	83%	N/A	0%	100%	55	10.7 (2.7)	85%	N/A
(autism sample)	XBAMM	< 1 false-positive cluster	18	11.6 (3.0)	83%	N/A	100%	0%				
Toal *et al.*												
(Asperger sample)	SPM2 + XBAMM	< 1 false-positive cluster	39	32.0 (12.0)	90%	106 (15)	0%	100%	33	32.0 (9.0)	91%	105 (12)
(autism sample)	SPM2 + XBAMM	< 1 false-positive cluster	26	30.0 (8.0)	81%	84 (23)	100%	0%				
Waiter *et al.*	SPM2	$P < 0.05$ corrected	15	15.2 (2.2)	100%	100 (22)	N/A	N/A	16	15.5 (1.6)	100%	100 (18)
Total			246	21.4 (12.5)	84% [(a)]	94 [(a)] (25)	60% [(a)]	40% [(a)]	237	20.4 (11.9)	83%	108 [(a)] (14)

CIVET: an image processing environment. N/A: not available; IQ: intelligence quotient. SPM: statistical parametric mapping. XBAMM: brain activation and morphological mapping.
[(a)] Result obtained after imputation of missing values using the mean.

Combined, the studies included 246 patients with ASD (125 autism; 84 Asperger; 37 unknown) and 237 healthy controls. Patients comprised 133 adults (45 autism; 66 Asperger; 22 unknown) and 113 children/adolescents (80 autism; 18 Asperger; 15 unknown). As shown in **Table 5.1**, no relevant differences between patients and controls were found in terms of age and gender, as the original studies were already well matched in this respect. Full IQ was slightly lower in the ASD group, though this difference was largely due to a single study in which the patients had a rather low IQ (Boddaert, Chabane et al.

2004). Therefore, the meta-analysis was also repeated excluding this study in order to remove the potential confounding effects of IQ. Further details of each of the included studies, such as comorbid conditions, medication status or diagnostic criteria, can be found at http:/www.sdmproject.com/database .

5.2.3.2 Global differences in white matter volume

Global white matter volumes were available from 5 independent datasets within 4 publications (Waiter, Williams et al. 2005; Hyde, Samson et al. 2009; McAlonan, Cheung et al. 2009; Ecker, Rocha-Rego et al. 2010). No statistically significant differences in global white matter volume were found between ASD patients (n=87) and healthy controls (n=108) (unbiased Hedges (Hedges and Olkin 1985) d = -0.10, z = -0.70, P = 0.481). This was true for both pediatric/adolescent (d = -0.12, z = -0.67, P = 0.501) (Waiter, Williams et al. 2005; McAlonan, Cheung et al. 2009) and adult (d = -0.05, z = -0.18, P = 0.857) (Hyde, Samson et al. 2009; Ecker, Rocha-Rego et al. 2010) samples. No significant heterogeneity was found in any of the analyses (all studies: Q = 2.16, 4 df, P = 0.707; children/adolescents: Q = 0.77, 2 df, P = 0.680; adults: Q = 1.35, 1 df, P = 0.245).

5.2.3.3 Regional differences in white matter volume

Data for this analysis was obtained from all the studies included in the meta-analysis. As shown in **Table 5.2** and **Figure 5.2**, ASD patients showed a large

Table 5.2 Regional differences in white matter volume between individuals with autistic spectrum disorders and healthy controls.

	Maximum			Cluster		Jackknife sensitivity analysis
	Talairach coordinates	SDM value	Uncorrected *P*	Number of voxels	DTI atlas-derived main tracts	Combinations of studies detecting the difference
Increase of white matter volume (ASD > healthy)						
R centrum semiovale	34,-2,32	0.160	0.00001	1187	R arcuate fasciculus R extreme capsule	12 out of 13
L external/extreme capsule	-26,6,-4	0.159	0.00001	418	L uncinate fasciculus L inferior fronto-occipital fasciculus	12 out of 13
Decrease of white matter volume (ASD < healthy)						
R anterior cingulum	-4,24,20	-0.254	0.0006	15	R anterior cingulum / corpus callosum	9 out of 13

DTI: diffusion tensor imaging, L: left; R: right; SDM: signed differential mapping.

increase of white matter volume (1,187 voxels, maximum at [34,-2,32], SDM = 0.160) in the right centrum semiovale, comprising the arcuate fasciculus as well as a small part of extreme capsule. Patients also showed a moderately large increase of white matter volume (418 voxels, maximum at [-26,6,-4], SDM = 0.159) in the left external/extreme capsule, comprising the inferior fronto-occipital and the uncinate fasciculi. These increases of white matter volume were separately detected in both pediatric and adult samples (right increase maxima: [38,-4,40], SDM = 0.122 in children and [30,-6,22], SDM = 0.337 in adults; left increase maxima: [-28,4,-2], SDM = 0.159 in children and [-32,-14,-6], SDM = 0.215 in adults), although formal statistical tests could not be performed due to an insufficient number of studies.

Finally, a small decrease of white matter volume (15 voxels) in right anterior cingulum and the corpus callosum was also detected.

Figure 5.2 Main decreased white matter regions in individuals with autistic spectrum disorders compared with healthy controls.

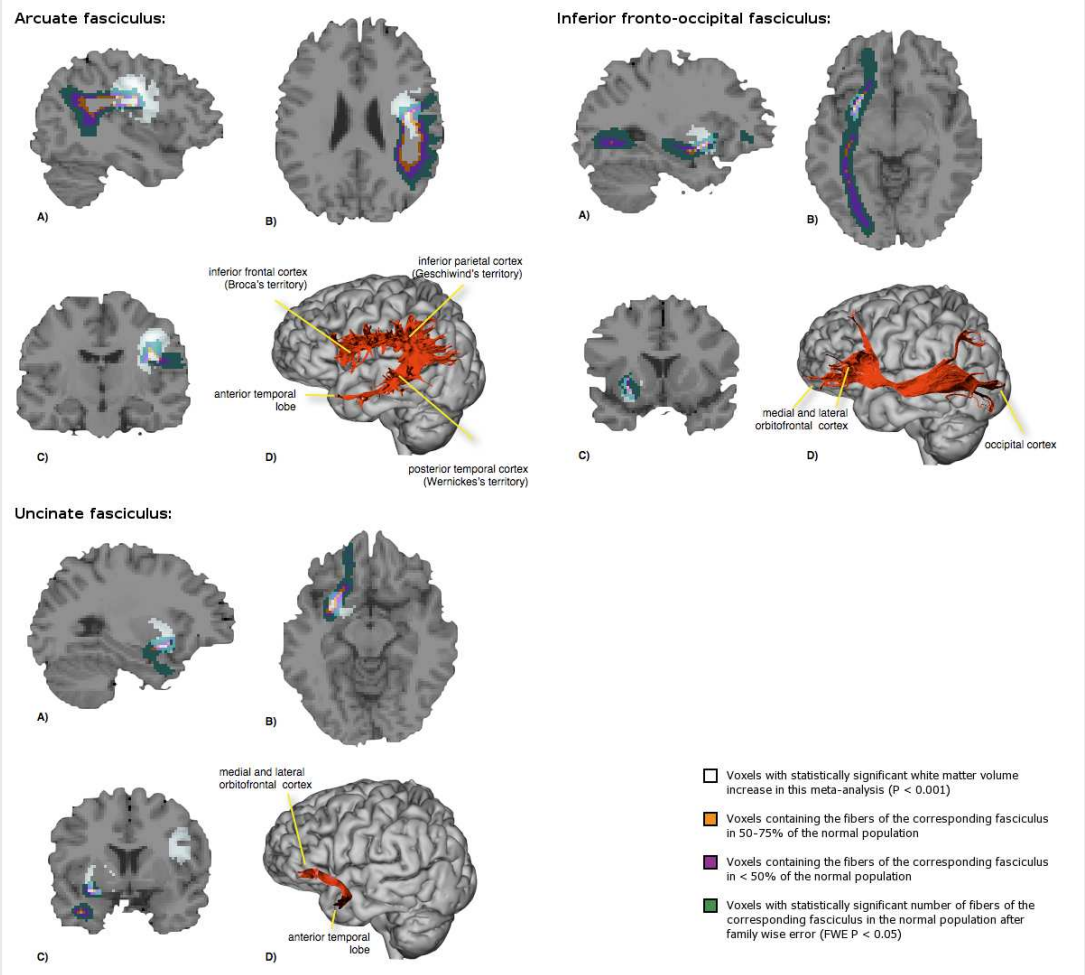

Localization of the white matter changes in the right arcuate fasciculus (top left), the left inferior fronto-occipital fasciculus (bottom left) and the left uncinate fasciculus (top right). A-C) Overlapping between the white matter maps of the meta-analysis (white area) and the digital maps of the corresponding fasciculus derived from an atlas of human brain connections (Catani and Thiebaut de Schotten 2010). The different colors indicate the percentage of overlap of the voxel containing the fibres of the fasciculus in the normal population. The green voxels represent voxels that are visited by a statistically significant number of fibres of the fasciculus in the normal population after family wise error (FWE) correction. D) Tractography reconstruction of the fasciculus, modified from Catani *et al.* (Catani, Howard et al. 2002).

The results remained largely unchanged in the analysis of quartiles, with the specified white matter increases detected in the third quartile map (i.e. at least 25% of the studies had found some increase in those regions) and the anterior cingulum/corpus callosum decrease in the median map. Whole-brain jack-knife sensitivity analysis showed that the results were highly replicable, as

white matter increases in right arcuate fasciculus and in left inferior fronto-occipital/uncinate fasciculi were preserved in all but one combinations of studies. Conversely, white matter decrease in anterior cingulum/corpus callosum failed to emerge in 4 combinations of studies. Finally, findings were nearly identical when the studies which had a potential sample overlap (Ke, Tang et al. 2009; Toal, Daly et al. 2009) or included patients with very low IQ (Boddaert, Chabane et al. 2004) were excluded from the analyses, with the exception of the white matter volume decrease in anterior cingulum/corpus callosum, which was no longer significant after the exclusion of Toal *et al.* (2009) and Ke *et al.* (2009).

5.2.4 Discussion

To our knowledge, this is the first meta-analysis of VBM studies of white matter volume in ASD. The study is timely given that a sufficient number of high-quality studies have only recently become available. The main findings were that individuals with ASD consistently display increases of white matter volume in right arcuate fasciculus and left inferior fronto-occipital and uncinate fasciculi. These results were obtained in both pediatric/adolescent and adult samples.

The arcuate fasciculus is a white matter bundle connecting perisylvian areas in the frontal, parietal and temporal lobes (**Figure 5.2 top left**). In the left hemisphere, it connects the classic brain language regions: Wernicke's territory in the superior temporal gyrus, Broca's territory in the inferior frontal gyrus, and the recently confirmed Geschwind's territory in the inferior parietal lobule

(Catani, Jones et al. 2005; Makris, Kennedy et al. 2005). In the right hemisphere, it participates to visuo-spatial processing and other aspects of language, including affective prosody and semantics (Heilman, Scholes et al. 1975; Ross and Monnot 2008). Lesions to the right arcuate fasciculus impair understanding and production of modulation of pitch, intonation contours, melody, cadence, loudness, tempo, stress, accent and pauses (Tucker, Watson et al. 1977; Bowers, Coslett et al. 1987). Prosody is used to transmit information above and beyond verbal-linguistic intent and to clarify the meaning of potentially ambiguous sentences by the judicious use of pauses and stresses (Ross 2010). Our findings of increased white matter in this region could represent the anatomical correlate of some of the verbal and non-verbal communication impairments observed in ASD (Koning and Magill-Evans 2001; Shriberg, Paul et al. 2001). Recent DTI studies in patients with ASD have found abnormal diffusivities in the arcuate fasciculus suggesting that changes in volume detected by VBM studies could be accompanied by microstructural abnormalities of the axonal membranes and/or myelin (Kumar, Sundaram et al. 2009; Fletcher, Whitaker et al. 2010; Knaus, Silver et al. 2010).

The uncinate fasciculus (**Figure 5.2 bottom left**) is a hook-shaped bundle that connects the inferior frontal gyrus and the inferior surfaces of the frontal lobe with the anterior portions of the temporal lobe including the cortical nuclei of the amygdala (Ebeling and von Cramon 1992; Hasan, Iftikhar et al. 2009). It has traditionally been considered to be part of the limbic system and is known for its involvement in human emotion processing, memory and language functions (Schmahmann, Pandya et al. 2007), all of which are impaired in ASD.

Our findings of increased white matter in these regions are thus consistent with a substantial body of evidence from both structural (Stanfield, McIntosh et al. 2008) and functional (Baron-Cohen, Ring et al. 1999; Monk, Weng et al. 2010) neuroimaging studies implicating the amygdala and related limbic structures in ASD. Also, several DTI studies in patients with ASD have found abnormalities in this fasciculus (Kumar, Sundaram et al. 2009; Pugliese, Catani et al. 2009). These abnormal limbic circuits may be related to some of the social and communication impairments typically found in people with ASD (Damasio and Maurer 1978; Courchesne and Pierce 2005; Wickelgren 2005). A recent DTI tractography study found abnormalities in the uncinate fasciculus of adults with psychopathy (Craig, Catani et al. 2009). These anatomical changes correlated with the severity of antisocial behavior, suggesting that uncinate abnormalities may underpin the neurobiological basis of social impairment irrespective of the etiology. Finally changes in these uncinate connections may also account for the much higher prevalence than would be expected in the general population, of emotional disorders, particularly anxiety and mood disorders in ASD (Ghaziuddin and Greden 1998; Ghaziuddin, Weidmer-Mikhail et al. 1998; Gadow, Devincent et al. 2005). Less is known about the inferior fronto-occipital fasciculus (**Figure 5.2 top right**), though it has been suggested that it may also be involved in language as its electrical stimulation induces semantic paraphasias (i.e., errors with regard to the meaning of the word target) (Duffau, Gatignol et al. 2005).

A small decrease of white matter in anterior cingulum / corpus callosum was also detected, though the jackknife sensitivity analysis suggested that this

may be a less robust finding. Nevertheless, this finding echoes some other studies reporting decreased volume of the anterior cingulum and corpus callosum using manual delimitation methods (Haznedar, Buchsbaum et al. 1997; Cody, Pelphrey et al. 2002; Stanfield, McIntosh et al. 2008), as well as DTI methods (Alexander, Lee et al. 2007; Kumar, Sundaram et al. 2009). The adjacent cingulate cortex has a well documented role in social cognition (Hadland, Rushworth et al. 2003; Shinozaki, Hanakawa et al. 2007) and has been found to be hypoactivated in patients with ASD while performing social tasks (Di Martino, Ross et al. 2009).

It is important to highlight that all but one of the studies included in this meta-analysis recruited patients who, on average, had normal IQ. The exclusion of the only study that recruited individuals with mental retardation (Boddaert, Chabane et al. 2004) from the meta-analysis did not modify the results. Therefore, it is fair to conclude that our results may only apply to individuals with 'high functioning' ASD. Whether patients with lower IQs will display a different set of volumetric changes remains to be investigated.

5.2.4.1 Strengths and limitations

A major strength of the study is the use of the new white matter-specific templates presented at the beginning of this chapter. These templates were needed to randomly relocate the white matter peak coordinates in a *white* matter template, as using a *grey* matter randomization template to assess differences in *white* matter volumes would be statistically incorrect. We hope

that the creation of a publicly available database with all the data and methodological details from every study included in this meta-analysis (http://www.sdmproject.com/database) will facilitate future reviews and meta-analyses as the body of evidence continues to grow.

There are also several limitations, some of which inherent to all meta-analytical approaches. First, voxel-based meta-analyses are based on summarized (i.e. coordinates from published studies) rather than raw data and this may result in less accurate results (Salimi-Khorshidi, Smith et al. 2009). However, obtaining the raw images from the original studies is logistically difficult. Second, the different studies included in this meta-analysis used different statistical thresholds. However, it must be noted that, while thresholds involving correction for multiple comparisons are usually preferred, the inclusion of studies with more liberal thresholds is still statistically correct. Indeed, SDM pre-processing uses the coordinates of the voxels with highest differences to approximately recreate the statistical parametric map, but does not make assumptions about whether these differences were significant or not. Third, while voxel-wise meta-analytical methods provide excellent control for false positive results, it is more difficult to completely avoid false negative results (Salimi-Khorshidi, Smith et al. 2009). Forth, there are some inherent limitations to the VBM method, such as reduced effectiveness to detect spatially complex and subtle group differences (Davatzikos 2004). Fifth, some of the included studies reported white matter density rather than volume. It must be noted that white matter density might be understood as a type of white matter volume which has not been corrected by the distorting effects of the normalization to the

stereotactic space; therefore, its inclusion in the meta-analysis is valid (it is also a “volume”) although it may add a source of noise. Sixth, there were too few studies to conduct separate sub-analyses in children/adolescents and adults with ASD, although descriptive analyses suggested that the results were similar in these two age groups. Because the mean age of the ‘pediatric’ subgroup was 11.0±3.3 years, one remaining question is whether younger patients with ASD may show a distinctive pattern of volumetric changes. Indeed, global brain volume increases in ASD have been mainly reported in childhood autism and thought to be related to an early acceleration in brain growth (Courchesne, Karns et al. 2001; Aylward, Minshew et al. 2002; Carper, Moses et al. 2002; Hazlett, Poe et al. 2005) but might not persist into adulthood (Aylward, Minshew et al. 2002). Finally, a formal comparison between the two main subtypes of ASD (i.e. autism and Asperger syndrome) was not possible due to insufficient number of studies. This might be important as some studies have suggested that there may be some differences in brain structure and function between these subtypes (Ghaziuddin, Leininger et al. 1995; Ghaziuddin and Mountain-Kimchi 2004; Kwon, Ow et al. 2004), although this evidence is still preliminary and the distinction remains a matter of debate (Howlin 2003; Klin, Pauls et al. 2005; Volkmar, State et al. 2009). Even less is known about the neural substrates of the miscellaneous pervasive developmental disorder not otherwise specified (PDD NOS) category, despite being by far the most prevalent (Volkmar, State et al. 2009).

5.2.4.2 Conclusions

Taken together, results from this meta-analysis suggest that patients with ASD display increases of white matter volume in specific white matter tracts, known to be important for language and social cognition. Whether the results apply to individuals with lower IQ or younger age and whether there are meaningful neurobiological differences between the subtypes of ASD remains to be investigated. Similarly, direct comparisons with other neuro-developmental disorders are needed in order to establish the specificity of the findings.

5.2.5 Acknowledgements

We thank the authors of the included studies for providing additional data and methodological details that were not reported in the original publications.

5.3 OVERALL DISCUSSION

Voxel-based meta-analytic software packages have been traditionally limited to the study of *grey matter*, comprising either brain functions in healthy people, or (structural or functional) grey matter abnormalities in patients with neuropsychiatric disorders. However, there is also a growing body of neuroimaging research aimed to investigate *white matter* abnormalities, for instance differences in regional white matter volume, or changes related to water diffusivity and axonal myelin integrity.

This chapter described the adaptation of SDM for its application to meta-analyze studies investigating white matter abnormalities. This consisted of the creation of specific templates for white matter, following the same standard parameters that were used to create the templates for grey matter studies in Chapter 2. As an example, these methods were applied to white matter voxel-based morphometry studies in autism spectrum disorders. Another example of the application of these methods is a meta-analysis of the white matter voxel-based morphometry studies in schizophrenia (Bora, Fornito et al. 2011).

The hope is that these new templates, already available in the SDM online library, will allow researchers to conduct voxel-based meta-analyses of a range of white matter studies. However, not all white matter studies can be included in a meta-analysis that uses the templates presented in this chapter. There is a set of published water diffusivity studies that do not investigate the entire white matter but only its main tracts (Smith, Jenkinson et al. 2006). The

inclusion of these studies would bias the results towards the main tracts. This issue is addressed in the next chapter.

5.4 REFERENCES

Abell, F., M. Krams, et al. (1999). "The neuroanatomy of autism: a voxel-based whole brain analysis of structural scans." Neuroreport **10**(8): 1647-1651.

Abrahams, B. S. and D. H. Geschwind (2008). "Advances in autism genetics: on the threshold of a new neurobiology." Nat.Rev.Genet. **9**(5): 341-355.

ADDMNS (2009). "Prevalence of autism spectrum disorders - Autism and Developmental Disabilities Monitoring Network, United States, 2006." MMWR Surveill Summ **58**(10): 1-20.

Alexander, A. L., J. E. Lee, et al. (2007). "Diffusion tensor imaging of the corpus callosum in Autism." Neuroimage. **34**(1): 61-73.

APA (2000). Diagnostic and Statistical Manual of Mental Disorders: DSM-IV-TR. Washington DC, American Psychiatric Association.

Ashburner, J. and K. J. Friston (2000). "Voxel-based morphometry-the methods." Neuroimage **11**(6 Pt 1): 805-821.

Ashburner, J. and K. J. Friston (2001). "Why voxel-based morphometry should be used." Neuroimage **14**(6): 1238-1243.

Ashwin, C., S. Baron-Cohen, et al. (2007). "Differential activation of the amygdala and the 'social brain' during fearful face-processing in Asperger Syndrome." Neuropsychologia **45**(1): 2-14.

Aylward, E. H., N. J. Minshew, et al. (2002). "Effects of age on brain volume and head circumference in autism." Neurology **59**(2): 175-183.

Baron-Cohen, S., H. A. Ring, et al. (2000). "The amygdala theory of autism." Neurosci.Biobehav.Rev. **24**(3): 355-364.

Baron-Cohen, S., H. A. Ring, et al. (1999). "Social intelligence in the normal and autistic brain: an fMRI study." Eur.J Neurosci. **11**(6): 1891-1898.

Beaulieu, C. (2002). "The basis of anisotropic water diffusion in the nervous system - a technical review." NMR Biomed **15**(7-8): 435-55.

Bigler, E. D., T. J. Abildskov, et al. (2010). "Volumetric and voxel-based morphometry findings in autism subjects with and without macrocephaly." Dev.Neuropsychol. **35**(3): 278-295.

Boddaert, N., N. Chabane, et al. (2004). "Superior temporal sulcus anatomical abnormalities in childhood autism: a voxel-based morphometry MRI study." Neuroimage **23**(1): 364-369.

Bonilha, L., F. Cendes, et al. (2008). "Gray and white matter imbalance--typical structural abnormality underlying classic autism?" Brain Dev **30**(6): 396-401.

Bora, E., A. Fornito, et al. (2011). "Neuroanatomical abnormalities in schizophrenia: a multimodal voxelwise meta-analysis and meta-regression analysis." Schizophr Res **127**(1-3): 46-57.

Bowers, D., H. B. Coslett, et al. (1987). "Comprehension of emotional prosody following unilateral hemispheric lesions: processing defect versus distraction defect." Neuropsychologia **25**(2): 317-328.

Brieber, S., S. Neufang, et al. (2007). "Structural brain abnormalities in adolescents with autism spectrum disorder and patients with attention deficit/hyperactivity disorder." J Child Psychol Psychiatry **48**(12): 1251-1258.

Brugha, T., S. McManus, et al. (2009). "Autism Spectrum Disorders in adults living in households throughout England. Report from the Adult Psychiatric Morbidity Survey 2007." from http://www.ic.nhs.uk/asdpsychiatricmorbidity07.

Carper, R. A., P. Moses, et al. (2002). "Cerebral lobes in autism: early hyperplasia and abnormal age effects." Neuroimage **16**(4): 1038-1051.

Catani, M., R. J. Howard, et al. (2002). "Virtual in vivo interactive dissection of white matter fasciculi in the human brain." Neuroimage **17**(1): 77-94.

Catani, M., D. K. Jones, et al. (2008). "Altered cerebellar feedback projections in Asperger syndrome." Neuroimage. **41**(4): 1184-1191.

Catani, M., D. K. Jones, et al. (2005). "Perisylvian language networks of the human brain." Ann.Neurol **57**(1): 8-16.

Catani, M. and M. Thiebaut de Schotten (2010). Atlas of human brain connections. Oxford, Oxford University Press.

Catani, M. and S. M. Thiebaut de (2008). "A diffusion tensor imaging tractography atlas for virtual in vivo dissections." Cortex **44**(8): 1105-1132.

Cody, H., K. Pelphrey, et al. (2002). "Structural and functional magnetic resonance imaging of autism." Int.J Dev.Neurosci. **20**(3-5): 421-438.

Courchesne, E., C. M. Karns, et al. (2001). "Unusual brain growth patterns in early life in patients with autistic disorder: an MRI study." Neurology **57**(2): 245-254.

Courchesne, E. and K. Pierce (2005). "Why the frontal cortex in autism might be talking only to itself: local over-connectivity but long-distance disconnection." Curr Opin Neurobiol. **15**(2): 225-230.

Craig, M. C., M. Catani, et al. (2009). "Altered connections on the road to psychopathy." Mol Psychiatry **14**(10): 946-953.

Craig, M. C., S. H. Zaman, et al. (2007). "Women with autistic-spectrum disorder: magnetic resonance imaging study of brain anatomy." Br J Psychiatry **191**: 224-228.

Damasio, A. R. and R. G. Maurer (1978). "A neurological model for childhood autism." Arch Neurol **35**(12): 777-786.

Davatzikos, C. (2004). "Why voxel-based morphometric analysis should be used with great caution when characterizing group differences." Neuroimage **23**(1): 17-20.

Di Martino, A., K. Ross, et al. (2009). "Functional brain correlates of social and nonsocial processes in autism spectrum disorders: an activation likelihood estimation meta-analysis." Biol Psychiatry **65**(1): 63-74.

Di, X., R. C. Chan, et al. (2009). "White matter reduction in patients with schizophrenia as revealed by voxel-based morphometry: an activation likelihood estimation meta-analysis." Prog Neuropsychopharmacol Biol Psychiatry **33**(8): 1390-4.

Duffau, H., P. Gatignol, et al. (2005). "New insights into the anatomo-functional connectivity of the semantic system: a study using cortico-subcortical electrostimulations." Brain **128**(Pt 4): 797-810.

Ebeling, U. and D. von Cramon (1992). "Topography of the uncinate fascicle and adjacent temporal fiber tracts." Acta Neurochir.(Wien.) **115**(3-4): 143-148.

Ecker, C., V. Rocha-Rego, et al. (2010). "Investigating the predictive value of whole-brain structural MR scans in autism: a pattern classification approach." Neuroimage **49**(1): 44-56.

Fletcher, P. T., R. T. Whitaker, et al. (2010). "Microstructural connectivity of the arcuate fasciculus in adolescents with high-functioning autism." Neuroimage **51**(3): 1117-25.

Gadow, K. D., C. J. Devincent, et al. (2005). "Comparison of DSM-IV symptoms in elementary school-age children with PDD versus clinic and community samples." Autism **9**(4): 392-415.

Ghaziuddin, M. and J. Greden (1998). "Depression in children with autism/pervasive developmental disorders: a case-control family history study." J.Autism Dev.Disord. **28**(2): 111-115.

Ghaziuddin, M., L. Leininger, et al. (1995). "Brief report: thought disorder in Asperger syndrome: comparison with high-functioning autism." J.Autism Dev.Disord. **25**(3): 311-317.

Ghaziuddin, M. and K. Mountain-Kimchi (2004). "Defining the intellectual profile of Asperger Syndrome: comparison with high-functioning autism." J.Autism Dev.Disord. **34**(3): 279-284.

Ghaziuddin, M., E. Weidmer-Mikhail, et al. (1998). "Comorbidity of Asperger syndrome: a preliminary report." J.Intellect.Disabil.Res. **42**(Pt 4): 279-283.

Hadland, K. A., M. F. Rushworth, et al. (2003). "The effect of cingulate lesions on social behaviour and emotion." Neuropsychologia **41**(8): 919-931.

Hardan, A. Y., N. J. Minshew, et al. (2000). "Corpus callosum size in autism." Neurology **55**(7): 1033-1036.

Hasan, K. M., A. Iftikhar, et al. (2009). "Development and aging of the healthy human brain uncinate fasciculus across the lifespan using diffusion tensor tractography." Brain Res **1276**(67): 76.

Hazlett, H. C., M. Poe, et al. (2005). "Magnetic resonance imaging and head circumference study of brain size in autism: birth through age 2 years." Arch Gen Psychiatry **62**(12): 1366-1376.

Haznedar, M. M., M. S. Buchsbaum, et al. (1997). "Anterior cingulate gyrus volume and glucose metabolism in autistic disorder." Am J Psychiatry **154**(8): 1047-1050.

Hedges, L. V. and I. Olkin (1985). Statistical Methods for Meta-Analysis. Orlando, Academic Press.

Heilman, K. M., R. Scholes, et al. (1975). "Auditory affective agnosia. Disturbed comprehension of affective speech." J Neurol Neurosurg Psychiatry **38**(1): 69-72.

Hong, S. S., X. Y. Ke, et al. (2008). "Corpus callosum morphometry in high functioning autism." Asia-Pacific Conference on Mind Brain and Education: 404-407.

Howlin, P. (2003). "Outcome in high-functioning adults with autism with and without early language delays: implications for the differentiation between autism and Asperger syndrome." J Autism Dev.Disord. **33**(1): 3-13.

Hyde, K. L., F. Samson, et al. (2009). "Neuroanatomical differences in brain areas implicated in perceptual and other core features of autism revealed by cortical thickness analysis and voxel-based morphometry." Hum Brain Mapp **31**(4): 556-566.

Ke, X., S. Hong, et al. (2008). "Voxel-based morphometry study on brain structure in children with high-functioning autism." Neuroreport **19**(9): 921-925.

Ke, X., T. Tang, et al. (2009). "White matter impairments in autism, evidence from voxel-based morphometry and diffusion tensor imaging." Brain Res **1265**: 171-177.

Klin, A., D. Pauls, et al. (2005). "Three diagnostic approaches to Asperger syndrome: implications for research." J Autism Dev.Disord. **35**(2): 221-234.

Knaus, T. A., A. M. Silver, et al. (2010). "Language laterality in autism spectrum disorder and typical controls: a functional, volumetric, and diffusion tensor MRI study." Brain Lang **112**(2): 113-120.

Koning, C. and J. Magill-Evans (2001). "Social and language skills in adolescent boys with Asperger syndrome." Autism **5**(1): 23-36.

Kumar, A., S. K. Sundaram, et al. (2009). "Alterations in Frontal Lobe Tracts and Corpus Callosum in Young Children with Autism Spectrum Disorder." Cereb.Cortex **20**(9): 2103-2113.

Kwon, H., A. W. Ow, et al. (2004). "Voxel-based morphometry elucidates structural neuroanatomy of high-functioning autism and Asperger syndrome." Dev.Med.Child Neurol. **46**(11): 760-764.

Lancaster, J. L., M. G. Woldorff, et al. (2000). "Automated Talairach atlas labels for functional brain mapping." Hum Brain Mapp **10**(3): 120-131.

Langen, M., H. G. Schnack, et al. (2009). "Changes in the developmental trajectories of striatum in autism." Biol.Psychiatry **66**(4): 327-333.

Makris, N., D. N. Kennedy, et al. (2005). "Segmentation of subcomponents within the superior longitudinal fascicle in humans: a quantitative, in vivo, DT-MRI study." Cereb Cortex **15**(6): 854-869.

McAlonan, G. M., C. Cheung, et al. (2009). "Differential effects on white-matter systems in high-functioning autism and Asperger's syndrome." Psychol Med **39**(11): 1885-1893.

McAlonan, G. M., V. Cheung, et al. (2005). "Mapping the brain in autism. A voxel-based MRI study of volumetric differences and intercorrelations in autism." Brain **128**(Pt 2): 268-276.

McAlonan, G. M., E. Daly, et al. (2002). "Brain anatomy and sensorimotor gating in Asperger's syndrome." Brain **125**(Pt 7): 1594-1606.

McAlonan, G. M., J. Suckling, et al. (2008). "Distinct patterns of grey matter abnormality in high-functioning autism and Asperger's syndrome." J Child Psychol Psychiatry **49**(12): 1287-1295.

Mechelli, A., C. J. Price, et al. (2005). "Voxel-based morphometry of the human brain: methods and applications." Curr Med Imag Rev **1**(2): 105-113.

Monk, C. S., S. J. Weng, et al. (2010). "Neural circuitry of emotional face processing in autism spectrum disorders." J Psychiatry Neurosci. **35**(2): 105-114.

Pierce, K., R. A. Muller, et al. (2001). "Face processing occurs outside the fusiform 'face area' in autism: evidence from functional MRI." Brain **124**(Pt 10): 2059-2073.

Piven, J., J. Bailey, et al. (1997). "An MRI study of the corpus callosum in autism." Am J Psychiatry **154**(8): 1051-1056.

Pugliese, L., M. Catani, et al. (2009). "The anatomy of extended limbic pathways in Asperger syndrome: a preliminary diffusion tensor imaging tractography study." Neuroimage **47**(2): 427-434.

Radua, J. and D. Mataix-Cols (2009). "Voxel-wise meta-analysis of grey matter changes in obsessive-compulsive disorder." Br J Psychiatry **195**(5): 393-402.

Radua, J., D. Mataix-Cols, et al. (2012). "A new meta-analytic method for neuroimaging studies that combines reported peak coordinates and statistical parametric maps." Eur Psychiatry **27**: 605-611.

Radua, J., O. A. van den Heuvel, et al. (2010). "Meta-analytical comparison of voxel-based morphometry studies in obsessive-compulsive disorder vs other anxiety disorders." Arch Gen Psychiatry **67**(7): 701-711.

Ross, E. D. (2010). "Cerebral Localization of Functions and the Neurology of Language: Fact versus Fiction or Is It Something Else?" Neuroscientist. **16**(3): 222-243.

Ross, E. D. and M. Monnot (2008). "Neurology of affective prosody and its functional-anatomic organization in right hemisphere." Brain Lang **104**(1): 51-74.

Salimi-Khorshidi, G., S. M. Smith, et al. (2009). "Meta-analysis of neuroimaging data: A comparison of image-based and coordinate-based Pooling of studies." Neuroimage **45**(3): 810-823.

Schmahmann, J. D., D. N. Pandya, et al. (2007). "Association fibre pathways of the brain: parallel observations from diffusion spectrum imaging and autoradiography." Brain **130**(Pt 3): 630-653.

Schmitz, N., E. Daly, et al. (2007). "Frontal anatomy and reaction time in Autism." Neurosci Lett **412**(1): 12-17.

Schultz, R. T. (2005). "Developmental deficits in social perception in autism: the role of the amygdala and fusiform face area." Int.J Dev.Neurosci. **23**(2-3): 125-141.

Shinozaki, J., T. Hanakawa, et al. (2007). "Heterospecific and conspecific social cognition in the anterior cingulate cortex." Neuroreport **18**(10): 993-997.

Shriberg, L. D., R. Paul, et al. (2001). "Speech and prosody characteristics of adolescents and adults with high-functioning autism and Asperger syndrome." J Speech Lang Hear.Res. **44**(5): 1097-1115.

Smith, S. M., M. Jenkinson, et al. (2006). "Tract-based spatial statistics: voxelwise analysis of multi-subject diffusion data." Neuroimage **31**(4): 1487-505.

Stanfield, A. C., A. M. McIntosh, et al. (2008). "Towards a neuroanatomy of autism: a systematic review and meta-analysis of structural magnetic resonance imaging studies." Eur.Psychiatry **23**(4): 289-299.

Stroup, D. F., J. A. Berlin, et al. (2000). "Meta-analysis of observational studies in epidemiology: a proposal for reporting. Meta-analysis Of Observational Studies in Epidemiology (MOOSE) group." JAMA **283**(15): 2008-2012.

Toal, F., E. M. Daly, et al. (2009). "Clinical and anatomical heterogeneity in autistic spectrum disorder: a structural MRI study." Psychol Med **40**(7): 1171-1181.

Tucker, D. M., R. T. Watson, et al. (1977). "Discrimination and evocation of affectively intoned speech in patients with right parietal disease." Neurology **27**(10): 947-950.

Turkeltaub, P. E., G. F. Eden, et al. (2002). "Meta-analysis of the functional neuroanatomy of single-word reading: method and validation." Neuroimage **16**(3 Pt 1): 765-780.

Viechtbauer, W. (2005). "Bias and efficiency of meta-analytic variance estimators in the random-effects model." Journal of Educational and Behavioral Statistics **30**(3): 261-293.

Volkmar, F. R., A. Klin, et al. (1998). "Nosological and genetic aspects of Asperger syndrome." J Autism Dev.Disord. **28**(5): 457-463.

Volkmar, F. R., M. State, et al. (2009). "Autism and autism spectrum disorders: diagnostic issues for the coming decade." J Child Psychol Psychiatry **50**(1-2): 108-115.

Wager, T. D., M. Lindquist, et al. (2007). "Meta-analysis of functional neuroimaging data: current and future directions." Soc Cogn Affect Neurosci **2**(2): 150-158.

Waiter, G. D., J. H. Williams, et al. (2004). "A voxel-based investigation of brain structure in male adolescents with autistic spectrum disorder." Neuroimage **22**(2): 619-625.

Waiter, G. D., J. H. Williams, et al. (2005). "Structural white matter deficits in high-functioning individuals with autistic spectrum disorder: a voxel-based investigation." Neuroimage **24**(2): 455-461.

Wickelgren, I. (2005). "Neurology. Autistic brains out of synch?" Science **308**(5730): 1856-1858.

Wing, L. (1996). "Autistic spectrum disorders." BMJ **312**(7027): 327-328.

Yamasue, H., M. Ishijima, et al. (2005). "Neuroanatomy in monozygotic twins with Asperger disorder discordant for comorbid depression." Neurology **65**(3): 491-492.

CHAPTER 6

Meta-analyses of studies using tract-based spatial statistics (TBSS)

6.1 THEORY

6.1.1 Tract-based spatial statistics (TBSS)

An interesting application of magnetic resonance imaging is the study of the integrity of the white matter tracts in patients with neuropsychiatric disorders. Briefly, this consists in assessing the degree of anisotropy in the diffusion of water molecules, as the membrane of the axons restricts the motion of the water molecules in directions other than those of the tract. The most common index of such anisotropy is fractional anisotropy (FA). In case of tract abnormalities (e.g. myelin loss or fibre incoherence), water freely diffuses in any direction, thus resulting in a decrease of the observed FA (Beaulieu 2002).

Comparisons of FA between patients and controls can be conducted as standard voxel-based analyses, but an increasingly common alternative consists on projecting the values of the voxels into one-dimensional tracts, and then conducting the comparisons on these tracts (i.e. *tract-based spatial*

Figure 6.1 Lack of complete spatial overlap between the skeletons of two studies of fractional anisotropy (FA) employing 'tract-based spatial statistics' (TBSS)

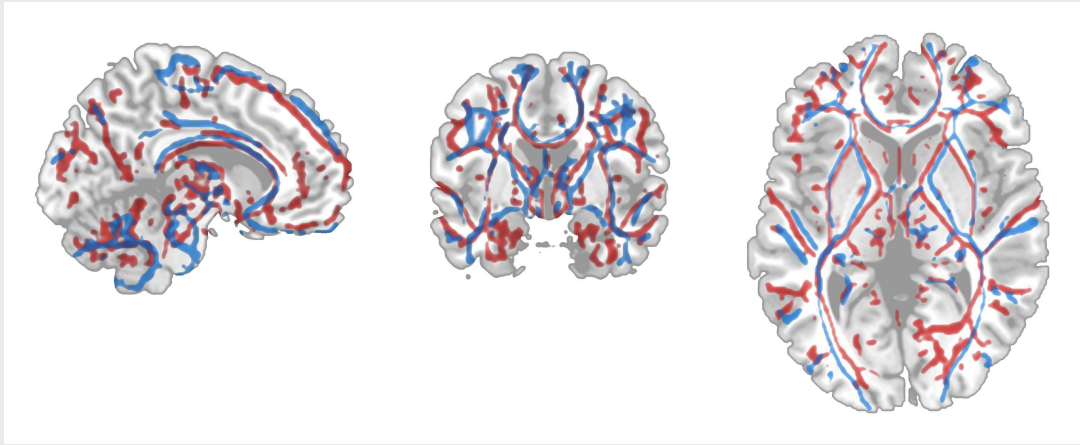

The skeleton of one study is shown in red and the skeleton of the other study in blue.

Note that raw pixel-based skeletons have been smoothed and thresholded for graphical purposes.

statistics, TBSS, http://www.fmrib.ox.ac.uk/fsl/tbss/) (Smith, Jenkinson et al. 2006). In other words, each tract is represented by a single line in which each point summarizes the maximum FA of the perpendicularly surrounding voxels.

Unfortunately, while voxel-based FA studies are meta-analyzable with the template presented in Chapter 5 (Radua, Via et al. 2011), meta-analyses of TBSS studies are less straightforward. Despite the fact that the skeletons of tracts are based on the same MNI template, they only cover the main white matter tracts of the brain and are spatially optimized for each study, and thus do not completely overlap across studies (**Figure 6.1**).

Taking advantage of the new capabilities of the *effect-size signed differential mapping* (ES-SDM) algorithms presented in Chapter 4 (Radua, Mataix-Cols et al. 2012), this chapter describes the adaptation of ES-SDM in order to allow meta-analyses of TBSS studies. This adaptation consisted of: a)

creating a new TBSS template for SDM; and b), developing a new indirect approach to pre-process the TBSS statistical maps.

6.1.2 Creation of the meta-analytic TBSS template

The process of creation of the new template was similar to those of the grey and white matter templates described in Chapters 2 and 5 (Radua and Mataix-Cols 2009; Radua, Via et al. 2011). Specifically, the process consisted of taking the MNI template FMRIB58 FA skeleton included in the FMRIB software library of neuroimaging tools (FSL; http://www.fmrib.ox.ac.uk/fsl/), converting it into Talairach space, and saving the coordinates in the SDM 2 x 2 x 2m^3 voxel-size format.

As explained in the following sections, meta-analyses of TBSS studies should be conducted with the ES-SDM approach described in Chapter 4 (Radua, Mataix-Cols et al. 2012), for what no randomization mask would be needed. Nevertheless, this was also created for the sake of completion.

6.1.3 New pre-processing algorithms for TBSS meta-analyses

Despite the fact that the TBSS skeletons of different studies are based on the same MNI skeleton, they are spatially optimized for each study, resulting in slight spatial differences which prevent a direct overlap of the FA maps. The "line" corresponding to the corpus callosum, for example, may be slightly superiorly placed in one study as compared to another. **Figure 6.1** shows an example of the lack of complete overlap from two TBSS studies.

Figure 6.2 Linux / FSL script used to retrieve the peaks.

```
# Retrieve the local positive peaks
cluster -i ${1} --mm -n 100000 --olmax=${1}_pos.txt -t 0.1

# Create a negative image to subsequently extract negative peaks
fslmaths ${1} -mul -1 ${1}_neg.nii.gz

# Retrieve the local negative peaks
cluster -i ${1}_neg --mm -n 100000 --olmax=${1}_neg.txt -t 0.1

# Remove the negative image
rm ${1}_neg.nii.gz
```

Note: the first argument (`${1}`) is the name of the t-statistical TBSS map.

In order to allow a correct overlap of the skeletons of the different studies, the tracts are “thickened” so that they occupy all the tract space defined in the new ES-SDM TBSS template. This is achieved with a two-step procedure: a) retrieval of a large number (e.g. 5,000) of low-thresholded local peaks from the original t-statistical maps; and b) incorporation of these peaks into the peak-based pre-processing procedure to reconstruct the effect-size maps. With this indirect approach, all recreated effect-size maps correctly overlap.

In the practical application described next, the Linux / FSL script shown in **Figure 6.2** was used to retrieve the peaks. The resulting text files contained a mass number of t-values and coordinates. A conventional spreadsheet, like Excel, was then used to combine the files, discard surplus information and set negative peak t-values as negative.

6.2 EXAMPLE: APPLICATION OF THE METHOD

To illustrate the use of the new ES-SDM TBSS template and pre-processing algorithm, this section describes a meta-analysis of TBSS studies investigating the development of white matter in adolescence.

This study was published in *Schizophrenia Bulletin* under the title '*White matter development in adolescence: Diffusion tensor imaging and meta-analytic results*' (Bart D. Peters, Philip R. Szeszko, Joaquim Radua, Toshikuza Ikuta, Patricia Gruner, Pamela Derosse, Jian-Ping Zhang, Antonio Giorgio, Deqiang Qiu, Susan F. Tapert, Jens Brauer, Miya R. Asato, P.L. Khong, Anthony C. James, Juan A. Gallego and Anil K. Malhotra 2012; 38:1308-1317). This is a pre-copy-editing, author-produced PDF of an article accepted for publication in Schizophrenia Bulletin following peer review. The definitive publisher-authenticated version is available online at http://schizophreniabulletin.oxfordjournals.org/content/38/6/1308.long

Note that this publication combines the findings of an analysis of original FA data with the results of an ES-SDM TBSS meta-analysis. The PhD candidate was mainly involved in the adaptation of ES-SDM for TBSS studies and performing the meta-analysis in close collaboration with the first author, Dr Peters. Interestingly, there was a convergence of the findings of the analysis of original data and the results of the meta-analysis.

6.2.1 Introduction

Schizophrenia is considered a neurodevelopmental disorder (Insel 2010), and abnormal trajectories of brain development in adolescence have been associated with the typical onset of psychosis in late adolescence (Shaw, Gogtay et al. 2010). Therefore, study of normal brain maturation across

adolescence may provide critical insights into the developmental processes involved in the disorder. Considering the strong evidence for brain white matter (WM) abnormalities in schizophrenia (Peters, Blaas et al. 2010; Walterfang, Velakoulis et al. 2011), study of normal adolescent WM development is highly relevant. In particular diffusion tensor imaging (DTI), an MRI measure sensitive to microstructural WM changes (Beaulieu 2002), has demonstrated WM abnormalities in first-episode and medication-naïve patients and patients at clinical high risk for psychosis, suggesting a primary role for WM abnormalities in the disease process (Peters, Blaas et al. 2010). Moreover, microstructural integrity of specific WM tracts is found to be associated with severity of positive symptoms, negative symptoms, or neurocognitive dysfunction in first-episode and recent-onset patients, and predictive of psychosis and functional outcome in individuals at high risk for psychosis (Peters, Blaas et al. 2010). For example, reduced integrity of the superior longitudinal fasciculus (SLF) correlated with poorer verbal working memory performance in recent-onset patients (Karlsgodt, van Erp et al. 2008). In adolescents at high risk for psychosis, microstructural integrity of the inferior longitudinal fasciculus (ILF) predicted social and role functioning at 15 month follow-up, and interestingly, failed to show the same age-related changes as observed in healthy controls (Karlsgodt, Niendam et al. 2009).

Early structural MRI studies have demonstrated global increases in WM volume across the lobes (Giedd, Blumenthal et al. 1999), and specific increases in WM density of the corticospinal tract (CST) and SLF from childhood into adolescence (Paus, Zijdenbos et al. 1999). DTI has demonstrated significant increases in fractional anisotropy (FA) from childhood into adolescence and

early adulthood (Ashtari, Cervellione et al. 2007; Snook, Plewes et al. 2007), suggestive of increasing myelination, fibre packing density, axon diameter or fibre coherence (Beaulieu 2002). Voxel-based analyses (VBA) identified FA increases in several WM areas, including the posterior limbs of the internal capsule (PLIC), left SLF, right cingulum, posterior corpus callosum (CC), and left prefrontal WM (Ashtari, Cervellione et al. 2007; Snook, Plewes et al. 2007).

While VBA has the advantages of unbiased, automated, whole brain analyses, limitations include partial volume effects and mis-registration errors. Tract-based spatial statistics (TBSS), a variant of VBA designed for DTI data (Smith, Jenkinson et al. 2006), minimizes these limitations. Several TBSS studies have confirmed increases in FA from childhood into adolescence and early adulthood (Giorgio, Watkins et al. 2008; Qiu, Tan et al. 2008; Asato, Terwilliger et al. 2010; Bava, Thayer et al. 2010; Brauer, Anwander et al. 2011). However, while specific tracts were identified in different studies, clear findings are not evident. One study found significant FA increases in the body of the CC and right superior corona radiata (sCR) (Giorgio, Watkins et al. 2008), while another study did not observe FA increases in the CC, but found increases in the right sCR, right PLIC, right SLF, and right anterior thalamic radiation (ATR) (Bava, Thayer et al. 2010). Other studies identified more widespread FA changes, which included the left SLF (Asato, Terwilliger et al. 2010; Brauer, Anwander et al. 2011), anterior limbs of the internal capsule (ALIC) (Qiu, Tan et al. 2008), bilateral ILF/inferior fronto-occipital fasciculus (IFOF) (Asato, Terwilliger et al. 2010), and right cingulum (Brauer, Anwander et al. 2011). These data suggest that FA increases are notable across adolescent

development, but variable results limit the specificity, and thus interpretation of these findings.

Therefore, the present study aimed to determine which WM tracts, as measured with TBSS, show the most consistent change across adolescence. For this purpose, a cohort of 8-21 year-old healthy subjects was assessed using DTI, and age-related FA changes were examined with TBSS. Next, the first meta-analysis of TBSS studies on healthy adolescent WM development was conducted to assess the results in the context of the larger sample sizes available with meta-analysis. As normal development is associated with changes in frontal lobe functioning (Galvan, Hare et al. 2006), we hypothesized that WM tracts connecting the frontal lobe with other cortical and subcortical regions would exhibit the most pronounced FA increases. In addition, this study evaluated the relationship between neurocognitive performance and the WM tracts that were identified in both the original sample and the meta-analysis, to provide data on the functional consequences of WM tract development. Finally, results are discussed in the context of DTI findings in schizophrenia, to examine the extent to which WM regions that actively develop during adolescence may also be implicated in the early stages of the disorder.

6.2.2 Methods for the analysis of original DTI-TBSS data

6.2.2.1 Participants

Seventy-eight healthy individuals (53% females) between the ages of 8 and 21 years (mean 15.3±3.7) were recruited through local advertisements and by word of mouth. Age distribution was as follows: 8-12 years, *n* = 16 (21%); 13-17

years, *n* = 33 (42%); 18-21 years, *n* = 29 (37%). Written informed consent was obtained from participants or if the participant was a minor, from a parent or guardian; all minors provided assent. Participants had no current or past history of a DSM-IV axis I psychiatric disorder as assessed by structured or semi-structured diagnostic interview. Other exclusion criteria included: (1) intellectual disability; (2) learning disability; (3) medications with known adverse cognitive effects; (4) MRI contraindications; (5) pregnancy; (6) significant medical illness that could affect brain structure. Mean full scale IQ was 106±12, as measured using the Wechsler Abbreviated Scale of Intelligence (WASI) for 60 subjects and estimated from the Wide Range Achievement Test (WRAT-3) for 12 subjects (data missing for 6 subjects). Handedness was determined using the Edinburgh Handedness Inventory, and median laterality quotient was 0.88 (range -1 to 1; data missing for 8 subjects). Subjects were administered a battery of neurocognitive tests designed to assess attention, executive functions, language ability, visuospatial processing, sensorimotor functions, memory and learning. This study was approved by the Institutional Review Board of the North Shore – Long Island Jewish Health System.

6.2.2.2 DTI Acquisition

MRI exams were conducted at North Shore University Hospital, Manhasset, NY, on a 3T GE scanner (GE Signa HDx; General Electric, Milwaukee, Wisconsin). DTI data were acquired using single shot echo planner imaging, and a double spin echo to decrease distortions due to eddy currents, with the following parameters: TR = 14000ms, TE = minimum, matrix = 128x128, FOV = 240mm,

slice thickness = 2.5mm, 51 continuous AC-PC aligned axial slices. A total of 36 DTI volumes were obtained for each subject that included 31 volumes with diffusion gradients applied along 31 non-collinear directions (b = 1000 s/mm^2) and 5 volumes without diffusion weighting.

6.2.2.3 DTI processing and analysis

All scans were reviewed by a radiologist to ensure that no gross abnormalities were evident. All images were visually inspected and four subjects were excluded due to significant motion artefacts. DTI data were processed and analyzed using the FMRIB Software Library (FSL) (http://www.fmrib.ox.ac.uk/fsl/). Head motion and eddy current induced distortions were corrected through affine registration of the diffusion-weighted images to the first B0 image. The gradient directions were corrected according to the rotation parameters. Next, non-brain tissue was removed using the Brain Extraction Tool. The DTIFIT tool was then used to fit a diffusion tensor model to the raw diffusion data at each voxel, fitting the model with weighted least squares.

Voxel-wise statistical analysis of the FA data was carried out using TBSS in FSL (Smith, Jenkinson et al. 2006). First, all subjects' FA data were aligned into a common space through nonlinear registration to a target image. Because of the age-range of our subjects, registration was done by aligning every FA image to every other one, to identify the "most representative" subject, and using this as the target image. The target image was then affine-aligned into MNI152 standard space, and every image was transformed into 1x1x1mm

MNI152 space by combining the obtained nonlinear and linear transformation parameters. Next, the mean FA image was created and thinned to create a mean FA skeleton which represents the centres of all tracts common to the group. The FA threshold for the mean FA skeleton was set at 0.2. Each subject's aligned FA data were then projected onto this skeleton and the resulting data were fed into voxel-wise cross-subject statistics. To test for local correlations between age and FA, permutation-based testing was done and inference on the statistic maps carried out using threshold-free cluster enhancement (Smith and Nichols 2009). The null distribution was built up over 5000 random permutations across the image. The clusters were then thresholded at a level of $P < 0.05$, which is fully corrected for multiple comparisons (i.e. family-wise error). Anatomical localization of significant WM clusters was determined with the probabilistic cortical, subcortical and WM tractography atlases provided in FSL, and an MRI atlas of human WM anatomy (Mori, Wakana et al. 2005).

6.2.3 Methods for the meta-analysis of DTI-TBSS studies

A literature search was performed in PubMed (National Library of Medicine; http://www.pubmed.com/) using the terms 'Diffusion Tensor Imaging' AND ('Adolescence OR Development*'). Articles that met inclusion criteria were cross-referenced to identify additional studies. Inclusion criteria were: (1) application of DTI to assess age-related WM changes in healthy subjects; (2) mean age of subjects between 12 and 18 years *or* inclusion of a child group (mean age < 12 years) and a young adult group (mean age > 18 years) for

group comparison; (3) analysis of DTI images with TBSS; (4) direct analyses of age-FA relationships, either through correlation or group comparison. Studies that conducted only age-FA correlations in WM areas that had first demonstrated a relationship between FA and a cognitive measure were not included. WM FA was the primary DTI measure of interest. Only TBSS results that were corrected for multiple comparisons or used a cluster-size threshold were included for meta-analysis.

Meta-analysis was conducted with the special algorithms detailed at the beginning of this chapter. T-statistic images were provided by the primary authors of three studies (Giorgio, Watkins et al. 2008; Qiu, Tan et al. 2008; Bava, Thayer et al. 2010), while for the other two studies we used the peak coordinates (Asato, Terwilliger et al. 2010; Brauer, Anwander et al. 2011). Based on the empirical validation of ES-SDM described in Chapter 4 (Radua, Mataix-Cols et al. 2012), an uncorrected $P = 0.005$ was used as the main threshold. To further reduce the possibility of false positive results, a peak-height threshold of $Z > 1$ and extent threshold of 10 voxels were also applied. Furthermore, to assess the robustness of findings, sensitivity analyses (repeating the meta-analysis leaving one study out each time) were conducted.

6.2.4 Methods for the common analyses

Tracts that showed significant age-associated increases in FA in both the original sample and the meta-analysis were then investigated in relationship to neurocognitive function in the sample. Appropriate neurocognitive tests were selected based on reports from the literature relating specific test performance

to implicated tracts. Tracts were segmented using probabilistic tractography in each subject's native space (Behrens, Woolrich et al. 2003). Seed regions, way points and target regions were drawn on FSL's MNI152 T1 and FMRIB58 FA templates and then transferred to subjects' native space, using the parameters obtained through affine registration of the b0 images to the MNI152 T1 template. After tractography, each tract was thresholded at a normalized probability value, and mean FA of each tract was extracted.

The relationship between FA and test performance was analyzed using linear regression. Because FA and neurocognitive performance are both known to improve with age and an association between them could merely arise from their association with age, we also tested whether age-related FA changes mediate age-related changes in test performance using a mediation model (Baron and Kenny 1986). Hierarchical linear regression was performed with age first entered as predictor of test performance, and then FA added as a second predictor. FA was considered to be a partial mediator of test performance when (1) FA was a significant predictor of test performance after adjusting for age; (2) FA partially explained an observed age effect, that is, an association between age and test performance was attenuated when FA was entered into the model. Raw scores of test performances were used.

Statistical tests were conducted in the Statistical Package for the Social Sciences (SPSS), version 11.5.1 (IBM, USA; http://www.spss.com/).

Figure 6.3 Age-related increases in fractional anisotropy.

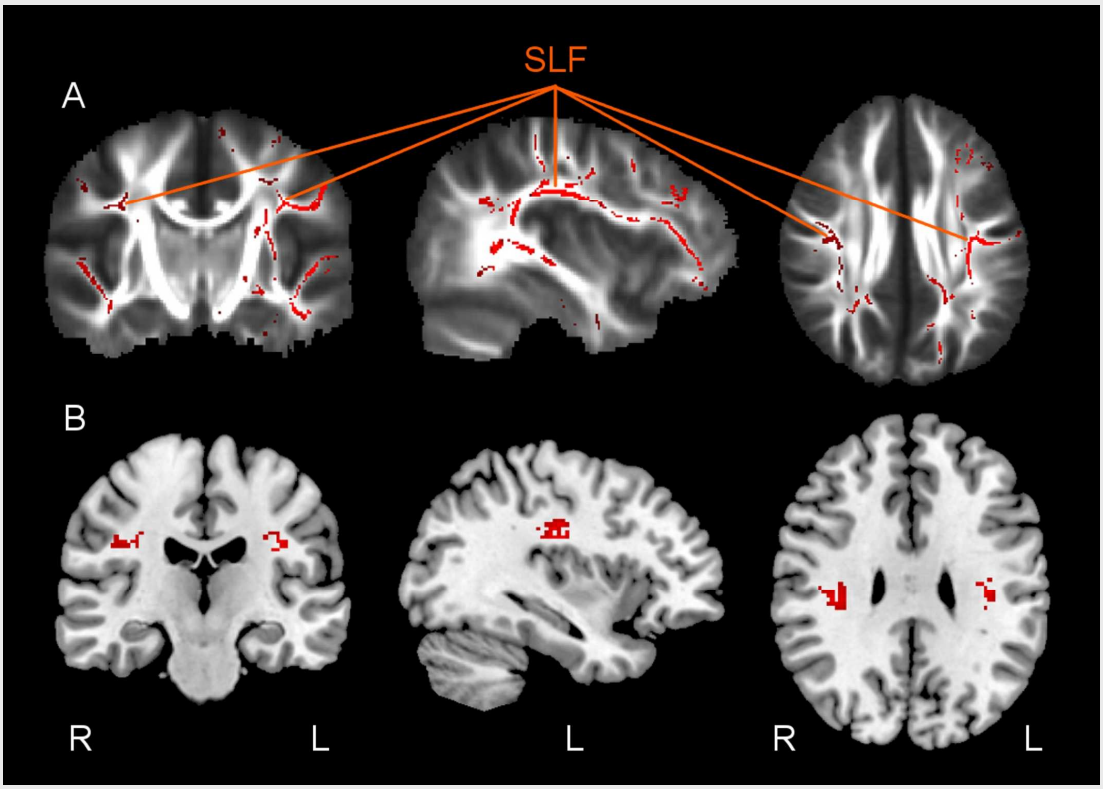

(A) Age-related increases in fractional anisotropy (FA) in 78 healthy subjects 8-21 years old (x = -36, y = -16, z = 31). Significant clusters (red) are overlaid on the mean FA image of all subjects ($P < 0.05$, corrected).

(B) Age-related increases in FA of the bilateral superior longitudinal fasciculus (SLF) in a meta-analysis of studies on healthy adolescent white matter development (x = -36, y = -19, z = 30). Significant clusters (red) are overlaid on an MRIcron template (http://www.mricro.com/mricron) for display purposes ($P < 0.005$, $Z > 1$, > 10 voxels).

6.2.5 Results

6.2.5.1 Analysis of original data

Overall, significant increases in FA with age were observed bilaterally in deep and superficial WM ($P < 0.05$, corrected; see **Figure 6.3A** and **Table 6.1**). In the left hemisphere, a cluster of 13,154 voxels included frontal, parietal, temporal and occipital WM, and association, projection and interhemispheric pathways. In the right hemisphere, a cluster comprised of 2,842 voxels and a cluster of 861 voxels also included parietal, temporal, frontal and occipital WM, and

Table 6.1 White matter clusters showing a positive correlation between age and fractional anisotropy in 78 healthy subjects (8-21 years).

Cluster	Peak-Coordinate (MNI x, y, z)	Cluster Size (voxels)	Hemisphere; Lobe	White Matter Tract
1	-43, -5, -15	13,154	Left; Frontal, Temporal, Parietal, Occipital	ATR/ALIC, CC genu & splenium, CR posterior & superior, CST, EC, F-minor, IFOF, ILF, PLIC, PTR/OR/F-major, SLF/AF (frontal and parietal), Tapetum, UF
2	38, -44, 5	2,842	Right; Parietal, Temporal, Occipital	CC splenium, CR posterior, CST, IC retrolenticular, IFOF & ILF (occipito-temporal), PTR/OR, SLF/AF (temporal)
3	37, -14, 30	861	Right; Parietal, Frontal	SLF (fronto-parietal)
4	-31, -11, -26	345	Left; Temporal	(Parahippocampal WM, anterior; Hippocampal WM)
5	43, -22, 38	234	Right; Parietal	(Postcentral gyrus WM)
6	30, -14, 25	109	Right; Parietal	CR superior, EC, SLF
7	-40, 7, -35	20	Left; Temporal	Temporal pole
8	-39, 6, -26	4	Left; Temporal	UF

AF, arcuate fasciculus; ALIC, anterior limb of the internal capsule; ATR, anterior thalamic radiation; CC, corpus callosum; CR, corona radiata; CST, cortico-spinal tract; EC, external capsule; F, forceps; IFOF, inferior fronto-occipital fasciculus; ILF, inferior longitudinal fasciculus; OR, optic radiation; PLIC, posterior limb of internal capsule; PTR, posterior thalamic radiation; SLF, superior longitudinal fasciculus; UF, uncinate fasciculus; WM, white matter.

association, projection and interhemispheric pathways. No significant decreases in FA with age were observed. Findings were most significant in the left SLF, temporal ILF, frontal IFOF, and frontal ATR ($P < 0.025$, corrected).

An asymmetry in the distribution of FA changes was also reflected in the number of significant voxels per hemisphere: in the left hemisphere a total of 13,523 voxels showed a significant relationship with age, and in the right hemisphere 4,046 voxels. To explore asymmetry in the strength of the age-FA associations, mean FA of the significant voxels in the left hemisphere and the right hemisphere were separately correlated with age. Correlations for the left hemisphere ($r = 0.691$, $P < 0.001$) and the right hemisphere ($r = 0.592$, $P < 0.001$) were significantly different (Steiger procedure; $t = 2.96$, $P = 0.004$).

Table 6.2 Studies included in meta-analysis of diffusion tensor imaging studies on healthy white matter development.

Study	Age		*N*	Sex (% F)	MR Field Strength	Slice Thickness	Diffusion Directions
	Mean±SD	Range					
Asato *et al.* 2010	15.5±4.5	8-28	114	55	3T	4mm	6 (NEX = 14)
Bava *et al.* 2010	17.8±1.4	16-21	22	32	3T	3mm	15 (NEX = 4)
Brauer *et al*. 2010	7.0±1.1 27.8±2.7[a]	6-9 24-32	20	50	3T	1.7mm	60
Giorgio *et al.* 2008	16.0±1.8	13.5-21	42	48	1.5T	2.5mm	60
Qiu *et al.* 2008	10.3±0.5 22.8±2.3[a]	9-12 19-26	51	47	3T	3mm	6 (NEX = 4)

NEX, number of excitations; F, Female.
[a] Mean age for two separate age groups with a bimodal age distribution.

6.2.5.2 Meta-analysis

Seven identified studies met the inclusion criteria for the meta-analysis. One study was excluded because did not report direct age-FA correlations, but a voxel-wise 'developmental timing quotient' (Colby, Van Horn et al. 2010). Another study was excluded because the subjects of that study showed complete overlap with a previous study (Giorgio, Watkins et al. 2008; Giorgio, Watkins et al. 2009). Thus, five studies were included in the meta-analysis (see **Table 6.2**) (Giorgio, Watkins et al. 2008; Qiu, Tan et al. 2008; Asato, Terwilliger et al. 2010; Bava, Thayer et al. 2010; Brauer, Anwander et al. 2011). Asato et al. performed group-comparisons of different age groups, as well as continuous age-FA correlations across all subjects (Asato, Terwilliger et al. 2010). The latter analysis was included in the meta-analysis.

Table 6.3 White matter clusters showing a positive association between age and fractional anisotropy in a meta-analysis of studies on healthy adolescent development.

Cluster	Peak-Coordinate (MNI x, y, z)	Cluster Size (voxels)	*Z*-value	*P*-Value[1] (uncorrected)	White Matter Area/Tract
1	41, -20, 33	79	3.9	*P* < 0.00001	Superior Longitudinal Fasciculus, Right
2	-37, -15, 27	71	3.6	*P* = 0.00001	Superior Longitudinal Fasciculus, Left
3	48, -19, -20	33	3.4	*P* = 0.00008	Inferior Longitudinal Fasciculus, Right
4	-16, 16, -2	22	3.3	*P* = 0.00015	Anterior Limb of Internal Capsule/ Anterior Thalamic Radiation, Left
5	-45, -12, -27	28	3.2	*P* = 0.00033	Inferior Longitudinal Fasciculus, Left
6	12, 2, 5	17	3.1	*P* = 0.00071	Posterior and Anterior Limbs of Internal Capsule/ Anterior Thalamic Radiation, Right
7	-9, 7, 27	11	3.0	*P* = 0.00119	Cingulate/ Corpus Callosum, Left
8	-16, -7, 4	15	2.9	*P* = 0.00171	Posterior Limb of Internal Capsule, Left

Note: Zucker Hillside data not included

[1] *P*-values were obtained with a permutation test.

Meta-analysis of these five studies showed significant FA increases in the fronto-parietal sections of the bilateral SLF, bilateral ILF, bilateral ALIC (mainly in the left hemisphere) containing the ATR, left cingulate/body of the CC, and bilateral PLIC (see **Table 6.3**). It must be noted here that the ILF runs close to the IFOF in this part of the temporal lobe, and therefore this cluster may have included some inferior parts of the IFOF. Of the identified eight clusters, the cluster in the right PLIC and ALIC/ATR, and the cluster in the left cingulate/body of the CC did not correspond to regions found in the original sample. The other six clusters corresponded closely with regions found in the sample. When the results from the sample were included in the meta-analysis, the results were the same regarding location, size and significance of the

clusters, with the exception that the cluster in the left cingulate/body of the CC was no longer significant.

There was no asymmetry observed in the distribution of the significant clusters in the meta-analysis, except for few more significant voxels in the left ALIC as compared to the right ALIC.

Sensitivity analyses showed that the identified WM tracts were consistent across the different studies. The bilateral SLF was highly consistent, independent from any individual study being discarded, and comprised the two largest clusters (see **Figure 6.3B**). The left ILF was no longer significant when the largest study was excluded from the analysis (Asato, Terwilliger et al. 2010), and the right ALIC and PLIC were no longer significant when either the largest study or one study with medium sample size was excluded (Qiu, Tan et al. 2008; Asato, Terwilliger et al. 2010). The left ALIC was no longer significant when either of the two studies with medium sample sizes was excluded (Giorgio, Watkins et al. 2008; Qiu, Tan et al. 2008), as well as the left PLIC when one of these studies was excluded (Qiu, Tan et al. 2008).

6.2.5.3 Neurocognitive correlates of SLF development

As the SLF was the most consistent and robust finding in the original sample and in the meta-analysis, we assessed the relationship between FA of the SLF and neurocognitive domains, which have previously been related to SLF WM integrity: verbal fluency (controlled oral word association test) (Phillips, Clark et al. 2010), reading ability (WRAT-3) (Hoeft, McCandliss et al. 2010), vocabulary (WASI vocabulary score) (Tamnes, Ostby et al. 2010), verbal working memory

(University of Maryland letter-number span) (Karlsgodt, van Erp et al. 2008; Ostby, Tamnes et al. 2011), and spatial working memory (Wechsler Memory Scale 3 spatial span) (Vestergaard, Madsen et al. 2010). The left and right SLF were tracked in each subject with probabilistic tractography (Behrens, Woolrich et al. 2003), by placing a seed region in the frontal part of the SLF (just anterior to the precentral gyrus), a way point in the frontal SLF just posterior to the seed region, a second way point in the middle temporal gyrus (MTG), and an exclusion mask that terminated fibres running anterior to the seed region, inferior to the way point in the MTG or into MTG grey matter. The bilateral SLF of each subject was then thresholded at a normalized probability value of 0.01 (see **Figure 6.4A**). FA-neurocognition relationships could not be assessed in all subjects due to either failure of the probabilistic tractography algorithm (n = 12) and/or missing neurocognitive data (n = 14 for verbal fluency; n = 12 for reading ability, verbal working memory and spatial working memory; n = 18 for vocabulary).

As results were similar for the left and right SLF, results are presented for mean FA of the bilateral SLF. FA of the SLF significantly predicted verbal fluency (beta = 0.436, t = 3.6, P = 0.001; n = 56) and verbal working memory performance (beta = 0.313, t = 2.5, P = 0.018; n = 57). There were trends for FA to predict reading ability (beta = 0.257, t = 2.0, P = 0.053; n = 57) and spatial working memory performance (beta = 0.227, t = 1.7, P = 0.089; n = 57), but not vocabulary (P > 0.1; n = 51). Next, verbal fluency and verbal working memory performance were each entered in a separate mediation model with age and FA as predictor variables. FA of the SLF partially mediated increases in verbal fluency as a function of increasing age: (1) age was a significant predictor of

Figure 6.4 Left superior longitudinal fasciculus as visualized with probabilistic tractography and relationship of its fractional anisotropy with age and verbal fluency

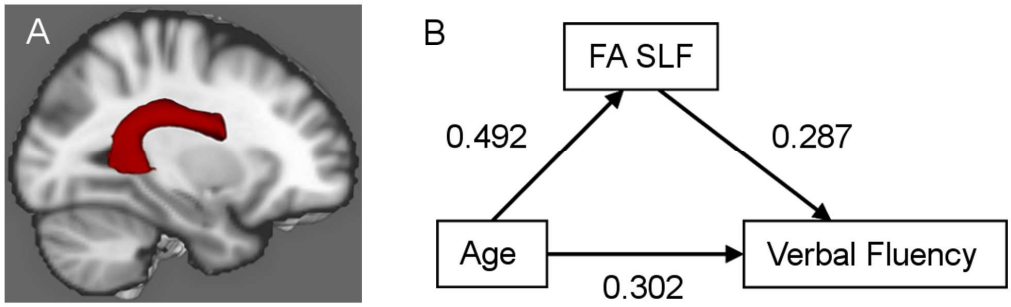

(A) Left superior longitudinal fasciculus (SLF) as visualized with probabilistic tractography; averaged from 66 healthy subjects 8-21 years old, and overlaid on the MNI152 T1 template for display purposes.

(B) Fractional anisotropy (FA) of the bilateral SLF partially mediated an observed relationship between age and verbal fluency. Strength of the relationships is indicated by the standardized regression coefficients ($P < 0.05$). Age and FA of the SLF were both significant predictors of verbal fluency performance, but the coefficient for age was reduced from 0.443 to 0.302 by the presence of the SLF, which in turn was a significant predictor of verbal fluency independent of the age effect.

verbal fluency (beta = 0.443, t = 3.6 , P = 0.001), and this correlation was reduced when FA of the SLF was added to the model (beta = 0.302 t = 2.2, P = 0.030); (2) FA was a significant predictor of verbal fluency independent of the age effect (beta = 0.287, t = 2.1, P = 0.039) (see **Figure 6.4B** and **Figure 6.5**). Age was also a significant predictor of verbal working memory performance (beta = 0.513, t = 4.4, P < 0.001), but FA of the SLF was not a predictor of verbal working memory performance independent of the age effect (beta = 0.071, t = 0.5, P = 0.604).

Because language function has been associated with structural lateralization, we explored the effects of lateralization of the SLF on the examined language-related measures (i.e. verbal fluency, verbal working memory, reading ability, and vocabulary). Lateralization of FA values in the SLF

Figure 6.5 Correlations between fractional anisotropy (FA) of the superior longitudinal fasciculus (SLF), age and verbal fluency in 8-21 year old healthy subjects

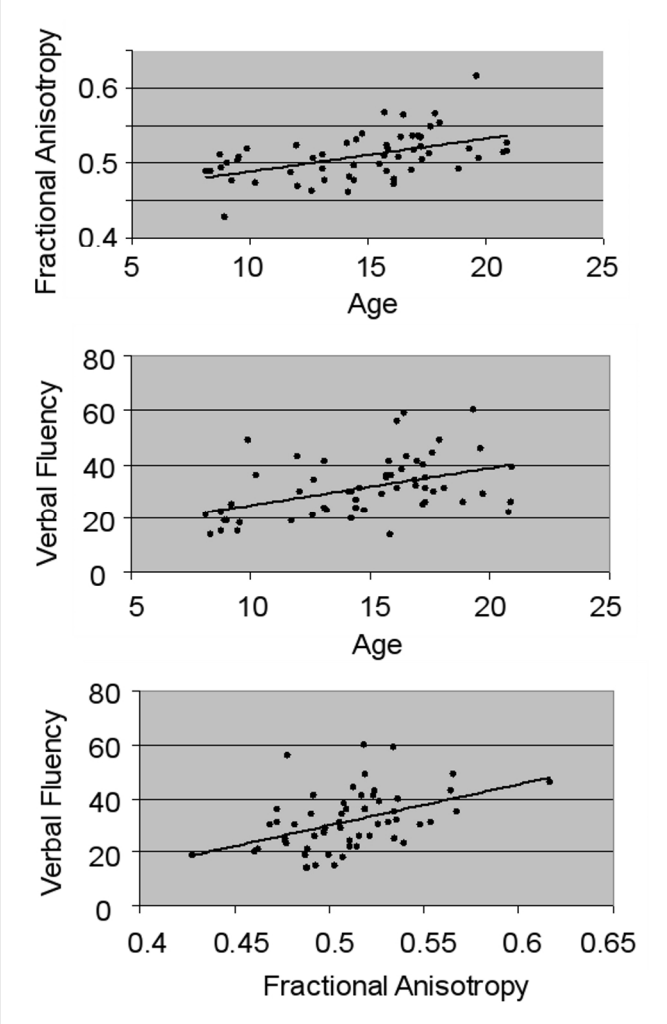

Top panel: age significantly predicted FA of the SLF (beta = 0.492, t = 4.3, *P* < 0.001; n = 56).

Middle panel: age significantly predicted verbal fluency (not adjusted for FA; beta = 0.443, t = 3.6 , *P* = 0.001; n = 56).

Bottom panel: FA was a significant predictor of verbal fluency (not adjusted for age; beta = 0.436, t = 3.6, *P* = 0.001; n = 56).

([FA left SLF – FA right SLF] / [FA left SLF + FA right SLF] / 2) was not significantly associated with these measures (*P* > 0.1).

When the analysis was restricted to right-handed subjects (Edinburgh lateralization index > 0.7) there appeared a trend for lateralization to predict poorer verbal working memory performance (beta = -0.286, *t* = -1.9, *P* = 0.067).

6.2.6 Discussion

This study reports bilateral increases in FA with age in a large sample of healthy children, adolescents and young-adults, with an asymmetric distribution favouring the left hemisphere. This is consistent with previous DTI-TBSS studies that have investigated WM development from childhood into early adulthood, although the identified WM tracts partially vary between the study reported here and other studies (Giorgio, Watkins et al. 2008; Qiu, Tan et al. 2008; Asato, Terwilliger et al. 2010; Bava, Thayer et al. 2010; Brauer, Anwander et al. 2011). This variation in findings may be related to the differences in age range of included subjects, DTI methodology, and inter-individual differences in WM development. A meta-analysis of these studies was therefore performed to identify which fibre tracts show the most pronounced development across adolescence. The meta-analysis identified increases in FA that were most consistent and robust in the bilateral SLF, and less consistent in the bilateral ILF, ALIC/ATR, and posterior PLIC. A left>right asymmetry of age effects on FA was not confirmed by the meta-analysis.

These results concur with findings of DTI studies that have utilized other analysis approaches than TBSS to study healthy WM development. Several DTI tractography studies have also observed FA increases from childhood into early adulthood in the SLF (Lebel, Walker et al. 2008; Giorgio, Watkins et al. 2009; Verhoeven, Sage et al. 2009), ILF (Giorgio, Watkins et al. 2009; Verhoeven, Sage et al. 2009), ALIC (Lebel, Walker et al. 2008), and ATR (Verhoeven, Sage et al. 2009). In conventional VBA studies, the most consistently identified areas of change between childhood and early adulthood were the left SLF and the bilateral PLIC (Ashtari, Cervellione et al. 2007; Snook, Plewes et al. 2007). A

pronounced FA increase in the SLF during adolescence concurs with the cross-sectional analysis by Lebel et al., who calculated that, while FA values of major WM tracts reach their plateau at different age periods, the SLF peaks between 15 and 20 years of age (Lebel, Walker et al. 2008). The uncinate fasciculus and the cingulate were calculated to mature last in early adulthood (Lebel, Walker et al. 2008). Therefore it may be considered unexpected that this study did not identify significant changes in these tracts. This apparent discrepancy may be related to the mean age and age range of the included samples, which focused the present study on detecting FA changes in middle to late adolescence. In a longitudinal follow-up study, Lebel et al. confirmed substantial FA increases in the SLF between 8 and 22 years of age, while the uncinate showed much less FA increases in this period and the cingulate somewhat more increases than the uncinate, but to a lesser extent than the SLF (Lebel and Beaulieu 2011). This observed protracted development of the uncinate fasciculus and cingulate with more gradual FA increases from childhood into early adulthood suggests, together with the results of this study, that adolescence is not a key period in which these tracts undergo most active development.

Neurocognitive correlates of the SLF were tested in the original sample to identify which cognitive functions the SLF serves during healthy development. Among five neurocognitive tests in the domains of language and working memory, FA of the SLF was significantly associated with performance on a verbal fluency test, and partially mediated increases in verbal fluency as a function of increasing age. This finding is in agreement with a previous DTI study in young adults that found an association between SLF WM integrity and verbal fluency (Phillips, Clark et al. 2010). Indeed, there is substantial evidence

from neuroimaging studies that the SLF plays a critical role in human language development. For example, Brauer et al. (2011) found in adults that the SLF connects the language network of Broca's and Wernicke's areas, while in children the language network also included a ventral pathway through the external capsule, suggesting that language development is paralleled by maturation of the SLF. Moreover, in children with dyslexia, improvement in reading skills was predicted by higher FA in the right SLF, compared to children without dyslexia (Hoeft, McCandliss et al. 2010). In this study, higher FA of the SLF predicted better reading ability at trend level, but did not predict vocabulary score, in contrast with a previous DTI study in healthy children (Tamnes, Ostby et al. 2010). Three segments of the dorsal language network have been identified with DTI tractography in healthy adults, consisting of a 'direct' pathway between Wernicke's and Broca's area (i.e. the SLF), and two 'indirect' segments in close proximity to the direct pathway, connecting Broca's area with the inferior parietal lobe (IPL) and the IPL with Wernicke's area (Catani, Allin et al. 2007). The SLF as obtained with the tractography algorithm used in this study most likely comprised the 'direct' pathway, because this pathway runs continuously from frontal to temporal, corresponding with the frontal seed region and temporal way point.

FA of the SLF did not predict spatial working memory performance in this study, contrary to another DTI study in healthy children (Vestergaard, Madsen et al. 2010). However, an association between verbal working memory performance and FA of the SLF was observed, which is consistent with previous DTI studies that have implicated the SLF in verbal working memory performance in healthy children, adolescents and young adults (Karlsgodt, van

Erp et al. 2008; Ostby, Tamnes et al. 2011). Working memory may be served by other components of the SLF than those associated with language (Makris, Kennedy et al. 2005). A detailed tractography study of the SLF in healthy adults identified two subcomponents of the SLF additional to the central core of the SLF (as measured in this study), which connected several parietal and frontal areas including the dorsolateral prefrontal cortex (Makris, Kennedy et al. 2005). In this study, FA of the SLF was no longer a significant predictor of verbal working memory performance after adjusting for age. This is an important dilemma in developmental studies: increases in neurocognitive performance potentially correlate with growth of neural structures simply because of their association with age, yet correcting for age leads to the association with brain structure being co-varied out.

Little effect of lateralization of FA values in the SLF on measures of language function was found. Catani et al. found in healthy adults that leftward lateralization of the reconstructed fibres of the SLF was associated with lower verbal recall score (Catani, Allin et al. 2007). These results indicate that language function is not significantly associated with lateralization of FA in the SLF, while a more symmetric distribution of SLF fibres may be advantageous for remembering words.

The SLF has been implicated in the pathophysiology of schizophrenia, and the results of this study suggest that abnormal development of the SLF during adolescence may play a key role in the pathophysiology of the disorder. In patients with first-episode or recent-onset schizophrenia and patients at clinical high risk for psychosis, reduced FA was identified in the SLF, and correlated with poorer verbal working memory performance in the recent-onset

patients (Karlsgodt, van Erp et al. 2008; Karlsgodt, Niendam et al. 2009; Perez-Iglesias, Tordesillas-Gutierrez et al. 2009). Higher FA values in the SLF have been related to auditory hallucinations in chronic patients (Hubl, Koenig et al. 2004). A key role for the SLF in schizophrenia is consistent with its role in working memory and language, as these faculties are significantly compromised in patients and their relatives (Snitz, Macdonald et al. 2006; Greenwood, Braff et al. 2007). Indeed, it has been proposed that the emergence of language during human evolution has been fundamental to the evolution of schizophrenia (Crow 2000).

A possible limitation of the meta-analysis is the difference in age range between the studies. Nonetheless, despite these differences in age range, all studies included the period of late adolescence/early adulthood. A second limitation is the limited number of TBSS studies that were available for the meta-analysis. A significant strength of our meta-analysis, however, is that original t-statistic maps were available for most of the included studies, thus allowing significantly more accurate results than if estimations had been conducted from only a few reported peak coordinates. The t-statistic images were not available for two studies (Giorgio, Watkins et al. 2008; Bava, Thayer et al. 2010), but in the validation study of ES-SDM (see Chapter 4) it was found that including t-statistic images for as few as 10-20% of the studies greatly enhances the sensitivity of the meta-analysis (Radua, Mataix-Cols et al. 2012).

In conclusion, DTI has provided valuable insights into healthy WM development in adolescence. Findings with TBSS highlight increasing connectivity in the SLF during this period and implicate the SLF as a specific target for neurodevelopmental disorders such as schizophrenia. The functional

correlates of WM changes remain a critically understudied area, especially regarding the cognitive, emotional and behavioural changes that occur in adolescence. Our results confirm the role of the SLF in language development, and to some extent in verbal working memory. Other important future areas of investigation concern those genes that play a role in WM maturation, and how risk genes may contribute to development of WM abnormalities. Large studies applying multi-modal imaging, combined with genomics and comprehensive clinical and neurocognitive assessments can answer these questions. Moreover, longitudinal designs will have greater power to provide more insight into the WM trajectories that may contribute to neurodevelopmental disorders.

6.2.7 Acknowledgements

We would like to acknowledge the essential contributions of Chaya Gopin and Kimberly Cameron to the recruitment and clinical assessments of the participants.

6.3 OVERALL DISCUSSION

An increasingly-used statistical approach to assess the integrity of the white matter tracts consists on projecting the values of the voxels into one-dimensional tracts, and then conducting the comparisons on these tracts (i.e. 'tract-based spatial statistics', TBSS). Unfortunately, the meta-analysis of such studies is not straightforward because the tracts of individual studies show an incomplete overlap.

This chapter described the creation of a TBSS meta-analytic template as well as a new procedure to allow TBSS meta-analyses. Briefly, the latter consists of retrieving a mass number of low-thresholded local peaks from the original t-statistical maps and then incorporating the effect size of these peaks into the ES-SDM algorithms introduced in Chapter 4. Also, a practical application of the method to the study of white matter fractional anisotropy changes during adolescence has been presented, showing considerable promise.

6.4 REFERENCES

Asato, M. R., R. Terwilliger, et al. (2010). "White matter development in adolescence: a DTI study." Cereb Cortex **20**(9): 2122-31.

Ashtari, M., K. L. Cervellione, et al. (2007). "White matter development during late adolescence in healthy males: a cross-sectional diffusion tensor imaging study." Neuroimage **35**(2): 501-10.

Baron, R. M. and D. A. Kenny (1986). "The moderator-mediator variable distinction in social psychological research: conceptual, strategic, and statistical considerations." J Pers Soc Psychol **51**(6): 1173-82.

Bava, S., R. Thayer, et al. (2010). "Longitudinal characterization of white matter maturation during adolescence." Brain Res **1327**: 38-46.

Beaulieu, C. (2002). "The basis of anisotropic water diffusion in the nervous system - a technical review." NMR Biomed **15**(7-8): 435-55.

Behrens, T. E., M. W. Woolrich, et al. (2003). "Characterization and propagation of uncertainty in diffusion-weighted MR imaging." Magn Reson Med **50**(5): 1077-88.

Brauer, J., A. Anwander, et al. (2011). "Neuroanatomical prerequisites for language functions in the maturing brain." Cereb Cortex **21**(2): 459-66.

Catani, M., M. P. Allin, et al. (2007). "Symmetries in human brain language pathways correlate with verbal recall." Proc Natl Acad Sci U S A **104**(43): 17163-8.

Colby, J. B., J. D. Van Horn, et al. (2010). "Quantitative in vivo evidence for broad regional gradients in the timing of white matter maturation during adolescence." Neuroimage **54**(1): 25-31.

Crow, T. J. (2000). "Schizophrenia as the price that homo sapiens pays for language: a resolution of the central paradox in the origin of the species." Brain Res Brain Res Rev **31**(2-3): 118-29.

Galvan, A., T. A. Hare, et al. (2006). "Earlier development of the accumbens relative to orbitofrontal cortex might underlie risk-taking behavior in adolescents." J Neurosci **26**(25): 6885-92.

Giedd, J. N., J. Blumenthal, et al. (1999). "Brain development during childhood and adolescence: a longitudinal MRI study." Nat Neurosci **2**(10): 861-3.

Giorgio, A., K. E. Watkins, et al. (2009). "Longitudinal changes in grey and white matter during adolescence." Neuroimage **49**(1): 94-103.

Giorgio, A., K. E. Watkins, et al. (2008). "Changes in white matter microstructure during adolescence." Neuroimage **39**(1): 52-61.

Greenwood, T. A., D. L. Braff, et al. (2007). "Initial heritability analyses of endophenotypic measures for schizophrenia: the consortium on the genetics of schizophrenia." Arch Gen Psychiatry **64**(11): 1242-50.

Hoeft, F., B. D. McCandliss, et al. (2010). "Neural systems predicting long-term outcome in dyslexia." Proc Natl Acad Sci U S A **108**(1): 361-6.

Hubl, D., T. Koenig, et al. (2004). "Pathways that make voices: white matter changes in auditory hallucinations." Arch Gen Psychiatry **61**(7): 658-68.

Insel, T. R. (2010). "Rethinking schizophrenia." Nature **468**(7321): 187-93.

Karlsgodt, K. H., T. A. Niendam, et al. (2009). "White matter integrity and prediction of social and role functioning in subjects at ultra-high risk for psychosis." Biol Psychiatry **66**(6): 562-9.

Karlsgodt, K. H., T. G. van Erp, et al. (2008). "Diffusion tensor imaging of the superior longitudinal fasciculus and working memory in recent-onset schizophrenia." Biol Psychiatry **63**(5): 512-8.

Lebel, C. and C. Beaulieu (2011). "Longitudinal development of human brain wiring continues from childhood into adulthood." J Neurosci **31**(30): 10937-47.

Lebel, C., L. Walker, et al. (2008). "Microstructural maturation of the human brain from childhood to adulthood." Neuroimage **40**(3): 1044-55.

Makris, N., D. N. Kennedy, et al. (2005). "Segmentation of subcomponents within the superior longitudinal fascicle in humans: a quantitative, in vivo, DT-MRI study." Cereb Cortex **15**(6): 854-69.

Mori, S., S. Wakana, et al. (2005). MRI Atlas of Human White Matter. Amsterdam, Elsevier.

Ostby, Y., C. K. Tamnes, et al. (2011). "Morphometry and connectivity of the fronto-parietal verbal working memory network in development." Neuropsychologia **49**(14): 3854-62.

Paus, T., A. Zijdenbos, et al. (1999). "Structural maturation of neural pathways in children and adolescents: in vivo study." Science **283**(5409): 1908-11.

Perez-Iglesias, R., D. Tordesillas-Gutierrez, et al. (2009). "White matter defects in first episode psychosis patients: a voxelwise analysis of diffusion tensor imaging." Neuroimage **49**(1): 199-204.

Peters, B. D., J. Blaas, et al. (2010). "Diffusion tensor imaging in the early phase of schizophrenia: what have we learned?" J Psychiatr Res **44**(15): 993-1004.

Phillips, O. R., K. A. Clark, et al. (2010). "Topographical relationships between arcuate fasciculus connectivity and cortical thickness." Hum Brain Mapp **32**(11): 1788-801.

Qiu, D., L. H. Tan, et al. (2008). "Diffusion tensor imaging of normal white matter maturation from late childhood to young adulthood: voxel-wise evaluation of mean diffusivity, fractional anisotropy, radial and axial diffusivities, and correlation with reading development." Neuroimage **41**(2): 223-32.

Radua, J. and D. Mataix-Cols (2009). "Voxel-wise meta-analysis of grey matter changes in obsessive-compulsive disorder." Br J Psychiatry **195**(5): 393-402.

Radua, J., D. Mataix-Cols, et al. (2012). "A new meta-analytic method for neuroimaging studies that combines reported peak coordinates and statistical parametric maps." Eur Psychiatry **27**: 605-611.

Radua, J., E. Via, et al. (2011). "Voxel-based meta-analysis of regional white-matter volume differences in autism spectrum disorder versus healthy controls." Psychol Med **41**(7): 1539-50.

Shaw, P., N. Gogtay, et al. (2010). "Childhood psychiatric disorders as anomalies in neurodevelopmental trajectories." Hum Brain Mapp **31**(6): 917-25.

Smith, S. M., M. Jenkinson, et al. (2006). "Tract-based spatial statistics: voxelwise analysis of multi-subject diffusion data." Neuroimage **31**(4): 1487-505.

Smith, S. M. and T. E. Nichols (2009). "Threshold-free cluster enhancement: addressing problems of smoothing, threshold dependence and localisation in cluster inference." Neuroimage **44**(1): 83-98.

Snitz, B. E., A. W. Macdonald, 3rd, et al. (2006). "Cognitive deficits in unaffected first-degree relatives of schizophrenia patients: a meta-analytic review of putative endophenotypes." Schizophr Bull **32**(1): 179-94.

Snook, L., C. Plewes, et al. (2007). "Voxel based versus region of interest analysis in diffusion tensor imaging of neurodevelopment." Neuroimage **34**(1): 243-52.

Tamnes, C. K., Y. Ostby, et al. (2010). "Intellectual abilities and white matter microstructure in development: a diffusion tensor imaging study." Hum Brain Mapp **31**(10): 1609-25.

Verhoeven, J. S., C. A. Sage, et al. (2009). "Construction of a stereotaxic DTI atlas with full diffusion tensor information for studying white matter maturation from childhood to adolescence using tractography-based segmentations." Hum Brain Mapp **31**(3): 470-86.

Vestergaard, M., K. S. Madsen, et al. (2010). "White matter microstructure in superior longitudinal fasciculus associated with spatial working memory performance in children." J Cogn Neurosci **23**(9): 2135-46.

Walterfang, M., D. Velakoulis, et al. (2011). "Understanding aberrant white matter development in schizophrenia: an avenue for therapy?" Expert Rev Neurother **11**(7): 971-87.

CHAPTER 7

Multi-modal meta-analyses

7.1 THEORY

This method was published in *Current Medicinal Chemistry* under the title '*A general approach for combining voxel-based meta-analyses conducted in different neuroimaging modalities*' (Joaquim Radua, Margarita Romeo, David Mataix-Cols and Paolo Fusar-Poli 2012; in Press).

Please find the publisher-authenticated version at:

http://dx.doi.org/10.2174/0929867311320030017

7.2 EXAMPLE: APPLICATION OF THE METHOD

To illustrate the practical uses of the new algorithm, this section describes a multi-modal meta-analysis of structural and functional MRI studies in *first episode of psychosis* (FEP).

This study was published in *Neuroscience & Biobehavioral Reviews* under the title '*Multimodal meta-analysis of structural and functional brain changes in first episode psychosis and the effects of antipsychotic medication*' (Joaquim Radua, Stefan Borgwardt, Alessandra Crescini, David Mataix-Cols, Andreas Meyer-Lindenberg, Philip McGuire and Paolo Fusar-Poli 2012; 36:2325:2333).

The definitive publisher-authenticated version is available online at http://dx.doi.org/10.1016/j.neubiorev.2012.07.012

7.2.1 Introduction

Neuroimaging studies in early psychosis promise to identify core neurobiological alterations at the onset of the disorder (Fusar-Poli, Allen et al. 2008; McGuire, Howes et al. 2008). However, despite the impressive growth of functional and structural studies, neuroimaging has yet to become an established as diagnostic, let alone prognostic, instrument in this area, partly as

a result of significant heterogeneity across the findings from research studies (Fusar-Poli and Broome 2006). These inconsistent and conflicting findings may be the result of inter-study differences in sampling methods, sociodemographic and clinical characteristics, and imaging parameters. In addition, recent evidence has indicated that even brief term treatment with antipsychotics can affect both the function (Fusar-Poli, Broome et al. 2007) and the structure (Smieskova, Fusar-Poli et al. 2009) of the brain during the early phase of the disorder.

To address these issues, we previously conducted meta-analyses of structural and functional neuroimaging studies in the early phase of psychosis or in medication-naïve psychotic subjects (Fusar-Poli, Perez et al. 2007; Fusar-Poli, Borgwardt et al. 2011; Fusar-Poli, Radua et al. 2011). In much of this research, there is an implicit assumption that structural abnormalities are linked to functional abnormalities in the brain regions found so affected, or the functional circuits in which they take part. However, this is not necessarily the case since volumetric changes can occur without clear functional correlates, for example as a consequence of nutritional or hydration status, or other confounds (e.g. (Weinberger and McClure 2002)), and vice versa. To understand the systems-level neurobiology of first episode psychosis (FEP), it is therefore important to know which brain regions, if any, show conjoint abnormalities in both structure and function. There is some evidence from individual studies indicating that reduction of regional grey matter volume (GMV) is associated with an impaired brain function during cognitive tasks during the Ultra High Risk (UHR) phase (Fusar-Poli, Broome et al. 2011). Although some individual multimodal studies in early psychosis are available (Fusar-Poli, Broome et al.

2009; Fusar-Poli, Howes et al. 2009; Fusar-Poli, Howes et al. 2010; Fusar-Poli, Stone et al. 2011), this issue is yet to be addressed across multiple studies, using a meta-analytical approach.

The novel multimodal voxel-based meta-analytical method presented at the beginning of the chapter was applied to overcome this limitation. Specifically, the hypothesis tested in this study was that FEP patients would show both structural and functional alterations in the same brain regions. On the basis of the new multimodal meta-analytical method, structural and functional findings were summarized in a single meta-analytic map, by assessing which brain regions showed *both* structural *and* functional abnormalities in subjects with a FEP. A number of potential confounding factors, including exposure to antipsychotics, were also investigated.

7.2.2. Methods

7.2.2.1 Search strategies

A systematic search strategy was used to identify relevant studies. Two independent researchers (PFP, AC) conducted a two-step literature search. First, a PubMed and Embase search was performed to identify putative studies reporting structural or functional imaging studies in subjects with a FEP. Consistent with the cross-diagnostic approach in the early phases of psychosis (Fusar-Poli, Bechdolf et al. 2012), FEP was defined as including both schizophrenia spectrum psychoses (schizophrenia, schizoaffective, schizophreniform) and affective psychoses (bipolar psychosis and psychotic depression) (Fusar-Poli, Borgwardt et al. 2011; Fusar-Poli, Bechdolf et al.

2012). The search was conducted up to June 2011, with no time span specified for date of publication. The following search terms were used: “psychosis”, “schizophrenia”, “MRI” (magnetic resonance imaging), “fMRI” (functional MRI), “PET” (positron emission tomography), and “SPECT” (single photon emission computed tomography). In a second step the reference lists of the articles included in the review were manually checked for any studies not identified by the computerized literature search. Although there was no language restriction, all the included papers were in English.

7.2.2.2 Selection criteria

Studies were included if they met the following criteria: (a) were reported in an original paper in a peer-reviewed journal, (b) had involved subjects with a FEP and a control group, (c) had employed whole brain structural or functional imaging in both groups. To minimize the heterogeneity of the functional imaging paradigms, only studies employing cognitive tasks were included. Studies not using cognitive paradigms or only reporting region of interests (ROIs) findings were excluded. Similarly, coordinates relative to analyses employing small volume corrections (SVC) in preselected ROIs were not included. Authors of studies where Talairach or Montreal Neurological Institute (MNI) coordinates (necessary for the voxel-level quantitative meta-analysis) were not explicitly reported were contacted to reduce the possibility of a biased sample set. In cases where the same or similar samples were used in separate papers, only data from the analysis of the largest sample were included. Studies were independently ascertained and checked by the two researchers and inclusion

Table 7.2 Description of the studies included in the meta-analysis

			FEP				Controls			Study			
	Assessment instruments	Technique	N	%Females	Age	% Naive	N	%Females	Age	Tesla	Software	FWHM	Statistical threshold
Grey matter volume													
Bergè 2010	PANSS-SCID-SUMD	sMRI	21	43%	25	100%	20	60%	25	NA	SPM5	8	<0.01 unc
Chua 2007	PANSS	sMRI	26	58%	32	100%	38	55%	33	1.5	BAMM	4.4	<0,05(<1FPC)
de Castro-Manglano 2010	CGI-KSADSPL-GAF-HDRS-PANSS	sMRI	26	42%	18	NA	17	47%	18	1.5	SPM2	12	<0,05(FDR)
Douaud 2007	KSADS-PANSS	sMRI	25	28%	16	0%	25	32%	16	1.5	SPM2	8	<0,01
Farrow 2005	PANSS	sMRI	33	33%	18	0%	22	41%	20	1.5	SPM99	12	<0,001(unc)
Janssen 2008	KSADS-PANSS	sMRI	70	27%	16	0%	51	31%	15	1.5	SPM2	12	<0,05(FWE)
Jayakumar 2005	SCID-PANSS	sMRI	18	50%	25	100%	18	50%	26	1.5	SPM2	12	<0,05(FDR)
Job 2002	NA	sMRI	34	32%	21	NA	36	53%	21	1	SPM99	12	<0,05 corr
Venkatasubramanian 2008	PANSS-SCID	sMRI	30	43%	30	100%	27	42%	27	1.5	SPM2	12	<0,005(FDR)
Kasparek 2009	GAF-PANSS-SCID	sMRI	41	0%	24	0%	18	0%	24	1.5	SPM2	12	<0,05(FWE)
Kubicki 2002	BPRS-SCID	sMRI	32	16%	25	0%	18	11%	24	1.5	SPM99	12	<0,05
Lui 2009	GAF-PANSS	sMRI	68	56%	24	100%	68	54%	25	3	SPM2	8	<0,05 corr
Manè 2009	GAF-PANSS-SCID	sMRI	15	20%	26	100%	11	27%	30	1.5	SPM5	8	<0,05(FWE)
Meda 2008	SCID	sMRI	22	36%	25	100%	21	38%	26	1.5	SPM2	8	<0,001 FDR
Meisenzahl 2008	PANSS-SCID	sMRI	93	28%	28	0%	177	30%	31	1.5	SPM2	12	<0,05(FWE)
Molina 2009	PANSS-SCID	sMRI	44	39%	27	0%	40	42%	29	1.5	SPM5	6	< 0,05(FDR)
Morgan 2007	WHO-SCAN	sMRI	73	42%	27	0%	73	42%	27	1.5	AFNI	NA	<0,05
Prasad 2007	SCID	sMRI	15	27%	25	100%	7	57%	25	1.5	SPM2	12	<0,001(unc)
Salgado-Pineda 2003	BPRS-SANS-SAPS	sMRI	13	0%	24	100%	13	0%	23	1.5	SPM99	8	<0,001(unc)
Schaufelberger 2007	PANSS-SCID	sMRI	122	46%	28	2%	94	44%	30	1.5	SPM2	12	<0,05(FEW)
Smesny 2010	SANS-SAPS-SCID	sMRI	13	54%	31	69%	25	60%	35	1.5	SPM8	12	<0,001
Kapaerk 2010	SCID	sMRI	49	0%	24	0%	127	0%	25	1.5	SPM5	12	<0,05
Whitford 2006	PANSS-DASS	sMRI	41	39%	20	0%	47	30%	19	1.5	SPM2	12	<0,05(FWE)
Witthaus 2009	MINI-PANSS-SIPS	sMRI	23	30%	26	74%	29	41%	26	1.5	SPM2	12	<0,05(FWE)
Yoshihara 2008	PANSS-K-SCID-SCID	sMRI	18	50%	16	6%	18	50%	16	1.5	BAMM	NA	<0,001

Table 7.2 Description of the studies included in the meta-analysis (cont)

			FEP				Controls			Study			
	Assessment instruments	Technique	N	%Females	Age	% Naive	N	%Females	Age	Tesla	Software	FWHM	Statistical threshold
Cognitive tasks brain response													
Achim 2007	SANS-SAPS-SCID	fMRI (ViM)	26	31%	23	0%	20	45%	24	1.5	SPM2	8	<0.001(unc)
Ashton 2000	SCID-PANSS	SPECT (VF)	39	NA	NA	100%	39	NA	NA	NA	SPM96	12	<0,001(unc)
Boksman 2005	SANS-SAPS-SCID	fMRI (VF)	10	10%	22	100%	10	10%	23	4	SPM99	8	<0,05 (corr)
Broome 2010	PANSS	fMRI (WM)	10	30%	25	30%	15	27%	25	1.5	XBAM	7.2	<0,05
Broome 2009	PANSS	fMRI (VF)	10	30%	25	30%	15	27%	25	1.5	XBAM	7.2	<0,05
Guerrero-Pedraza 2011	PANSS-SCID	fMRI (WM)	30	30%	26	0%	28	29%	27	1.5	NA	NA	0,05 (corr)
Jones 2004	PANSS	fMRI (VF)	7	14%	28	100%	8	25%	27	1.5	NA	7.2	NA
Keedy 2009	PANSS-SCID	fMRI (At)	9	NA	NA	11%	9	33%	NA	3	AFNI	NA	<0,05
MacDonald III 2005	BPRS-GAS-SANS-SAPS	fMRI (At)	30	30%	27	100%	28	36%	25	1.5	NA	8	<0,01(corr)
Nejad 2011	PANSS-SCAN 2.1	fMRI (WM)	23	22%	26	100%	35	31%	27	3	SPM5	8	0,05 (unc)
Schaufelberger 2005	PANSS	fMRI (VF)	7	57%	30	14%	9	67%	31	1.5	NA	7.2	<0,05(corr)
Scheuerecker 2008	BPRS-CGIS-PANSS-SANS	fMRI (WM)	23	17%	32	100%	23	17%	33	1.5	SPM99	8	<0,001(unc)
Schneider 2007	GAS-HDRS-PANSS-SCID	fMRI (WM)	48	46%	31	0%	57	46%	31	1.5	SPM2	10	0.001
Snitz 2005	BPRS-SANS-SAPS-SCID	fMRI (At)	23	30%	23	100%	24	46%	23	3	NA	8	<0,005(unc)
Strakowski 2008	HDRS-SCID-YMRS	fMRI (At)	16	25%	19	NA	16	44%	20	4	AFNI	NA	<0,05(corr)
Tan 2005	CGIS-GAFS-PANSS-SCID	fMRI (WM)	11	54%	25	0%	11	54%	26	3	NA	8	<0,05
Woodward 2009	GAF-PANSS	fMRI (PS)	15	20%	22	100%	32	59%	27	NA	NA	NA	<0,05
Yoon 2008	BPRS-GAS-SCID-SADSPL-SANS-SAPS	fMRI (At)	25	32%	20	36%	24	46%	22	1.5	SPM2	8	<0,05(FWE)

AFNI: Analysis of Functional NeuroImages; AS: Auditory Stimulation; At: attention; BAMM: Brain Activation and Morphological Mapping; BPRS: Brief Psychiatric Rating Scale; CGI: Clinical Global Impression; CGIS: Clinical Global Impression Schizophrenia; CP: Context Processing; corr: corrected; FDR: False Discovery Rate; FEP: First Episode of Psychosis; fMRI: functional Magnetic Resonance Imaging; FPC: False Positive Cluster; FWE: Family Wise Error; GAF: Global Assessment of Functioning; GAS: Global Assessment Scale; HDRS: Hamilton Depression Rating Scale; KSADS: Kiddie Schedule for Affective Disorders and Schizophrenia; KSADSPL: Kiddie Schedule for Affective Disorders and Schizophrenia Present and Lifetime version; MINI: Mini International Neuropsychiatric Interview; MRI: Magnetic Resonance Imaging; NA: Not Available; PANSS: Positive And Negative Syndrome Scale; PS: processing speed; RI: Response Inhibition; SADS: Schedule for Affective Disorders and Schizophrenia; SADSPL: Schedule for Affective Disorders and Schizophrenia Present and Lifetime version; SANS: Scale for the Assessment of Negative Symptoms; SAPS: Scale for the Assessment of Positive Symptoms; SCAN: Schedules for Clinical Assessment in Neuropsychiatry; SCID: Structured Clinical Interview for DSM-IV; SIPS: Structured Interview for Prodromal Syndromes; sMRI: structural Magnetic Resonance Imaging; SPECT: single photon emission computed tomography; SPM: Statistical Parametric Mapping; SUMD: Scale to assess Unawareness of Mental Disorder; unc: uncorrected; VF: Verbal Fluency; ViM: Visual Memory; WHO: World Health Organization; WM: Working Memory; XBAM: X Brain Activation Mapping; YMRS: Young Mania Rating Scale.

and exclusion criteria were evaluated by consensus. To achieve a high standard of reporting 'Preferred Reporting Items for Systematic Reviews and Meta-Analyses' (PRISMA) guidelines were adopted.

7.2.2.3 Recorded variables

The recorded variables for each article included in the meta-analysis were: assessment instruments, sample size, gender, mean age of participants, imaging package employed, full width at half maximum (FWHM) of the smoothing kernel, magnet intensity and exposure to antipsychotics. The statistical significance of the main findings and the method employed to correct the whole-brain results for multiple comparisons were also recorded. These data are comprehensively reported in the **Table 7.2** to assist the reader in forming an independent view on the following discussion.

7.2.2.4 Standard meta-analyses of structural and functional abnormalities

Separate voxel-based meta-analyses of regional GMV and functional brain response abnormalities were conducted with the effect-size version of SDM (ES-SDM) exposed in Chapter 4 (Radua and Mataix-Cols 2009; Radua and Mataix-Cols 2012; Radua, Mataix-Cols et al. 2012), which has been already used to meta-analyze studies on several neuropsychiatric disorders including schizophrenia and bipolar disorder (Bora, Fornito et al. 2010; Bora, Fornito et al. 2011; Palaniyappan, Balain et al. 2012). Default ES-SDM kernel size and thresholds were used (FWHM=20mm, voxel P=0.005, peak height Z=1, cluster extent=10 voxels) (Radua, Mataix-Cols et al. 2012).

Robustness of the significant results was assessed by means of exploration of the residual heterogeneity, as well as by jack-knife and subgroup analyses. Specifically, the funnel plots of the peaks of maximum heterogeneity were examined in order to check whether findings might had been driven by few or small noisy studies, or to detect any gross abnormality such as studies reporting opposite results (Radua, Mataix-Cols et al. 2012). As regard to the jack-knife analyses, these consisted of systematically repeating the meta-analyses after excluding one study at a time. Finally, separate subgroup analyses were conducted for those studies using 1.5 Tesla (T) scanners, those studies using statistical parametric mapping (SPM) software, those studies using typical smoothing kernels (12mm in VBM, 8mm in fMRI), those studies correcting for multiple comparisons, those studies where most of the patients were males, and in the functional meta-analysis, those studies using MRI scanners and those employing memory tasks.

It must be noted that as shown in **Figure 7.6**, patients may have different functional abnormalities which all would be detected as increases of the blood-oxygen-level dependent (BOLD) response, i.e. “patients > controls”. In this meta-analysis, differences in that direction were understood as either hyperactivations or failures of deactivation.

Figure 7.6 Examples of BOLD response abnormalities which would be detected as an increase of the BOLD response (i.e. patients > controls)

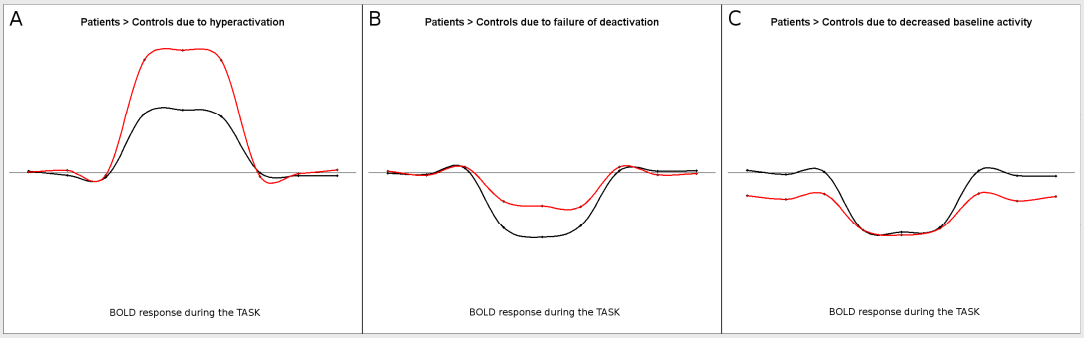

Red curves: simulated BOLD responses in patients. Black curves: simulated BOLD responses in healthy controls.

Note: As shown in the figure, patients may have different functional abnormalities which all would be detected as an increase of the BOLD response, i.e. patients > controls. One abnormality may consist in patients showing stronger activations than controls (i.e. patients hyper-activate, panel A). Conversely, another abnormality may consist in patients showing weaker deactivations than controls (i.e. patients fail to deactivate, panel B). Finally, there is room for more sophisticated abnormalities, such as patients displaying activations whilst controls deactivate, or any of these abnormalities be explained by anomalies of the baseline activity (e.g. panel C).

7.2.2.5 Multimodal analysis of structural and functional response

In order to summarize structural and functional findings in a single meta-analytic map, this study assessed which brain regions showed *both* structural *and* functional abnormalities using the method presented at the beginning of the chapter. It must be noted that our analysis did not aim to detect correlations between structural and functional abnormalities, either in the same or different regions – as it could be the case when a structural damage in a given cortical region produces a functional alteration in another brain region. Rather, the aim of this study was to localize those brain regions which display *both* structural *and* functional abnormalities in FEP. It could be, for instance, that some patients present structural but not functional impairment, whilst other patients show functional but not structural impairment. In that case, the meta-analysis should

detect both structural and functional impairments, and thus signal the region as multi-modally-affected.

7.2.2.6 Meta-regression analysis

The following variables were explored by means of meta-regression: mean age of the patients, and use of antipsychotic medication (percentages of naïve- and drug-free patients). As in previous meta-analyses, in order to minimize the detection of spurious relationships the probability threshold was decreased to 0.0005, abnormalities were required to be detected both in the slope and in one of the extremes of the regressor (e.g. in studies where 0% or where 100% of the patients were receiving medication), and findings in regions other than those detected in the main analyses were discarded (Radua and Mataix-Cols 2009). Finally, regression plots were visually inspected to discard fittings driven by too few studies.

Figure 7.7 Diagram of studies included in the present meta-analysis

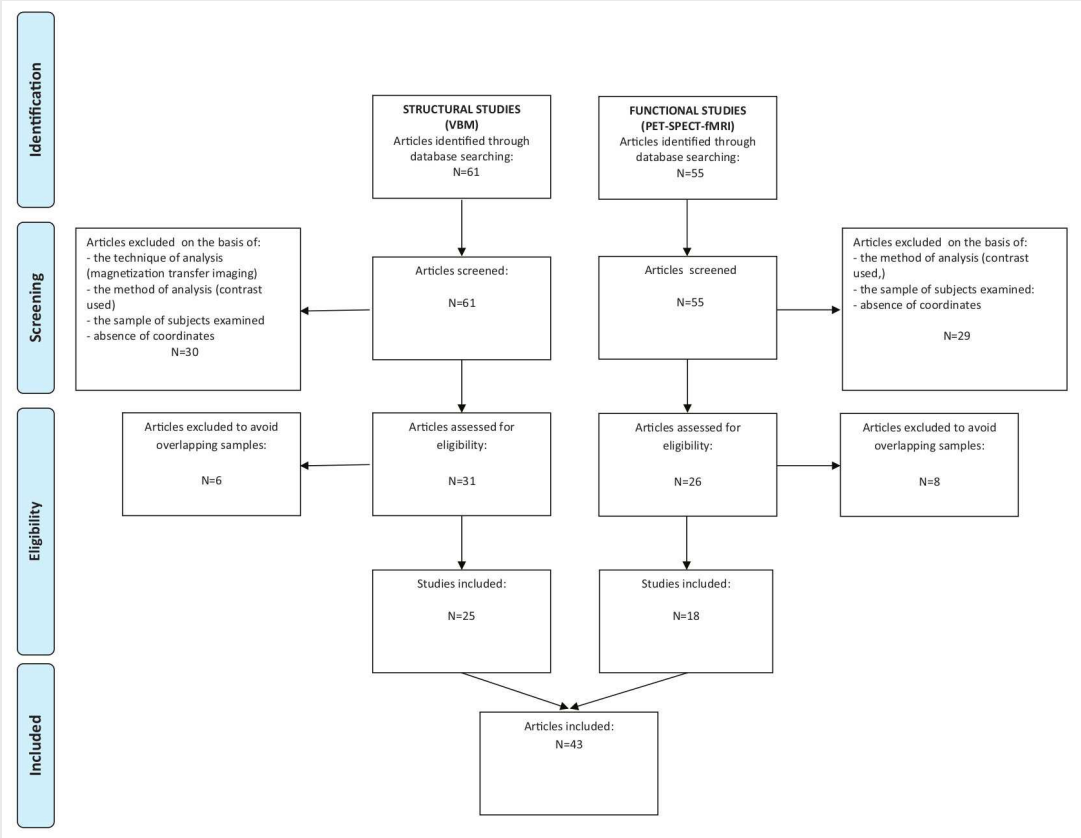

7.2.3. Results

7.2.3.1 Number of studies found

Forty-three studies met inclusion criteria (**Figure 7.7**). Specifically, in the structural meta-analysis 965 FEP subjects (mean age 24, range 15-35 years; 34% females; 76% receiving antipsychotic treatment), matched with 1040 controls (mean age 26, range 15-35 years; 34% females), were included. The cognitive tasks functional imaging cohort included 362 FEP subjects (mean age 26, range 19-36 years; 31% females; 53% receiving antipsychotic treatment), matched with 403 controls (mean age 27, range 23-39 years; 39% females).

Figure 7.8 Separate meta-analyses of structural and functional abnormalities in first psychotic episode

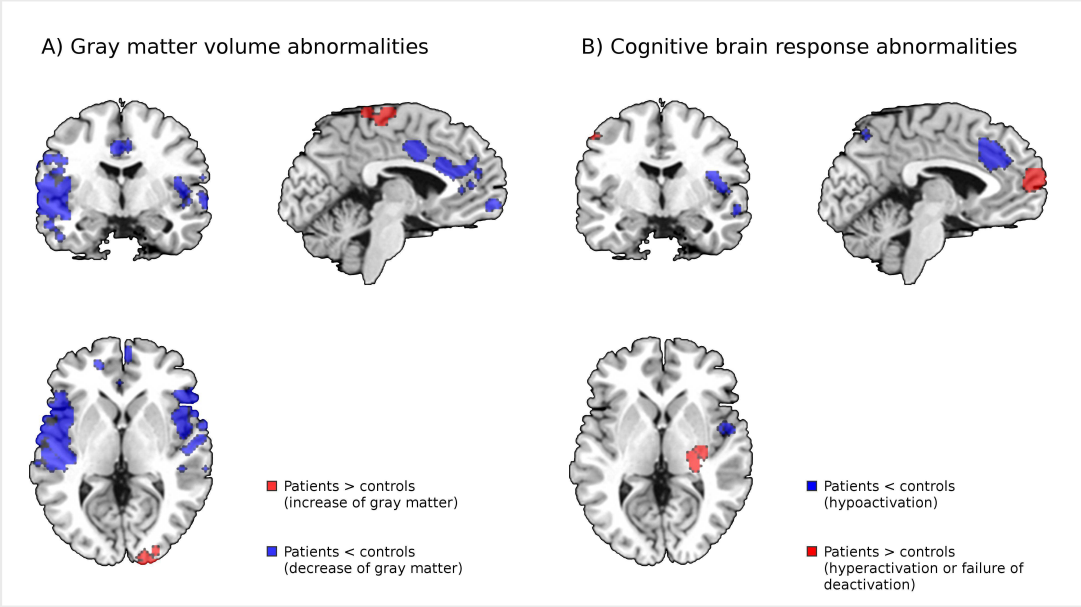

Cognitive tasks according to the clustering based on the MATRICS domains (Fusar-Poli, Deste et al. 2012) were attention (5), processing speed (1), verbal fluency (5), working memory (6), visual memory (1). The vast majority of the studies included in the meta-analysis recruited healthy subjects in the control group. All the contrasts included consisted in pairwise comparisons between patients and well-matched controls. Details of the included studies are presented in the **Table 7.2**.

7.2.3.2 Changes in regional grey matter volume

Patients with a FEP showed large and robust bilateral decreases of GMV in a peri-Sylvian cluster that included the insula, operculum and the superior temporal gyrus, and in the medial frontal and anterior cingulate cortices (**Figure 7.8A** and **Table 7.3**). Patients had relatively greater GMV than controls in the

Table 7.3 Grey matter volume abnormalities in first psychotic episode

	Talairach Coordinates	SDM z-value [(a)]	*P* Value [(b)]	No. of voxels [(c)]	Breakdown (No. of voxels) [(c)]
Increases of GMV (patients > controls)					
Right lingual gyrus	14,-94, -8	1.905	0.00001	306	Right BA 18 (193) Right BA 17 (101)
Left precentral gyrus	-8,-18, 66	1.550	0.0003	111	Left BA 6 (67) Left BA 4 (30) Left BA 3 (14)
Decreases of GMV (patients < controls)					
Left insula / middle and superior temporal / precentral gyri	-42, 6, 8	-4.536	~0	1696	Left BA 13 (347) Left BA 22 (268) Left BA 44 (145) Left BA 9 (142) Left BA 6 (125) Left BA 38 (124) Left BA 21 (123) Left BA 47 (85) Left BA 45 (62) Left BA 41 (58) Left BA 43 (46) Left BA 8 (37) Left BA 46 (33) Left BA 42 (22) Left BA 4 (12) Left BA 40 (10)
Right insula / middle and superior temporal / precentral gyri	46, 2,-10	-4.349	0.0000003	699	Right BA 13 (185) Right BA 22 (124) Right BA 44 (102) Right BA 41 (42) Right BA 47 (41) Right BA 45 (39) Right BA 38 (38) Right BA 21 (32) Right BA 40 (29) Right BA 42 (16)
Medial frontal / anterior cingulate cortices	4, 2, 36	-3.540	0.00006	600	Bilateral BA 24 (222) Bilateral BA 32 (186) Right BA 8 (53) Bilateral BA 10 (51) Bilateral BA 9 (49) Right BA 6 (31)

(a) Voxel probability threshold: p = 0.005
(b) Peak height threshold: z = 1
(c) Cluster extent threshold: 100 voxels. Regions with less than 10 voxels are not reported in the cluster breakdown.

right lingual gyrus and left precentral gyrus. The analyses of robustness showed that all these results were highly replicable (**Table 7.4**).

Table 7.4 Grey matter volume abnormalities in first psychotic episode: robustness analyses

	GMV increase		GMV decrease		
	R lingual gyrus	L precentral gyrus	L insula / temporal gyrus	R insula / temporal gyrus	Medial frontal / anterior cingulate
Jackknife analysis					
All studies but Berge *et al.*	Yes	Yes	Yes	Yes	Yes
All studies but Chua *et al.*	Yes	Yes	Yes	Yes	Yes
All studies but de Castro-Manglano *et al.*	Yes	Yes	Yes	Yes	Yes
All studies but Douaud *et al.*	Yes	Yes	Yes	Yes	Yes
All studies but Farrow *et al.*	Yes	Yes	Yes	Yes	Yes
All studies but Janssen *et al.*	Yes	Yes	Yes	Yes	Yes
All studies but Jayakumar *et al.*	Yes	Yes	Yes	Yes	Yes
All studies but Job *et al.*	Yes	Yes	Yes	Yes	Yes
All studies but Kasparek *et al.*	Yes	Yes	Yes	Yes	Yes
All studies but Kubicki *et al.*	Yes	Yes	Yes	Yes	Yes
All studies but Lui *et al.*	Yes	Yes	Yes	Yes	Yes
All studies but Mane *et al.*	Yes	Yes	Yes	Yes	Yes
All studies but Meda *et al.*	Yes	Yes	Yes	Yes	Yes
All studies but Meisenzah *et al.*l	Yes	Yes	Yes	Yes	Yes
All studies but Molina *et al.*	Yes	Yes	Yes	Yes	Yes
All studies but Morgan *et al.*	Yes	Yes	Yes	Yes	Yes
All studies but Prased *et al.*	Yes	Yes	Yes	Yes	Yes
All studies but Salgado-Pineda *et al.*	Yes	Yes	Yes	Yes	Yes
All studies but Schaufelberger *et al.*	Yes	Yes	Yes	Yes	Yes
All studies but Kasparek *et al.*	Yes	Yes	Yes	Yes	Yes
All studies but Smesny *et al.*	Yes	Yes	Yes	Yes	Yes
All studies but Venkatasubramanian *et al.*	Yes	Yes	Yes	Yes	Yes
All studies but Whitford *et al.*	Yes	Yes	Yes	Yes	Yes
All studies but Witthaus *et al.*	Yes	Yes	Yes	Yes	Yes
All studies but Yoshihara *et al.*	Yes	Yes	Yes	Yes	Yes
	25 out of 25	25 out of 25	25 out of 25	25 out of 25	25 out of 25
Subgroup analyses					
Studies using 1.5T scanners (n = 22, 88%)	Yes	No	Yes	Yes	Yes
Studies using SPM software (n = 22, 88%)	Yes	Yes	Yes	Yes	Yes
Studies applying 12mm FWHM (n = 15, 60%)	Yes	Yes	Yes	Yes	No
Studies correcting for multiple comparisons (n = 18, 72%)	Yes	Yes	Yes	Yes	Yes
Studies where most of the patients were males (n = 22, 88%)	Yes	Yes	Yes	Yes	Yes

Heterogeneity analysis

The heterogeneity analysis showed moderate levels of heterogeneity in bilateral insulae (peaks at 42,10,2 and -50,4,-2), though funnel plots did not reveal that insular findings could be driven by few or small noisy studies. Indeed, as many as 9 and 12 studies (right and left respectively), with both large and small standard errors, had reported GMV decreases in the bilateral peaks of maximum heterogeneity.

7.2.3.3 Changes in regional brain response to cognitive tasks

Patients with a FEP showed functional abnormalities in the right insula / superior temporal gyrus, as well as in the medial frontal / anterior cingulate cortices. However, the basis of the difference in activation varied within these clusters. In the anterior part of the right insula and in the dorsal anterior

Table 7.5 Cognitive tasks brain response abnormalities in first psychotic episode[(d)]

	Talairach Coordinates	SDM z-value [(a)]	*P* Value [(b)]	No. of voxels [(c)]	Breakdown (No. of voxels) [(c)]
Hypoactivations (patients < controls)					
Right anterior insula / middle frontal / superior temporal gyrus	44, 16, 30	-2.590	0.00001	170	Right BA 9 (141) Right BA 6 (23)
	38, 0, 14	-2.202	0.0001	58	Right BA 13 (49)
	54, -2, -6	-1.734	0.002	16	Right BA 22 (10)
Anterior cingulate cortex	4, 26, 32	-1.994	0.0005	174	Bilateral BA 32 (111) Bilateral BA 9 (23) Bilateral BA 6 (21) Bilateral BA 8 (17)
Left precuneus	-18,-72, 50	-1.868	0.001	52	Left BA 7 (49)
Hyperactivations / Failures of deactivation (patients > controls)					
Right basal ganglia / thalamus / posterior insula	28,-20, 4	1.868	0.0001	94	Right thalamus (42) Right putamen (39) Right pallidum (10)
	30,-30, 18	1.458	0.002	21	Right BA 13 (15)
Right inferior frontal / superior temporal gyrus	34, 6,-14	1.547	0.001	21	Right BA 38 (16)
Left precentral gyrus / inferior parietal lobule	-46,-26, 42	1.429	0.002	73	Left BA 2 (47) Left BA 40 (23)
	-50, -2, 48	1.370	0.003	18	Left BA 6 (17)
Medial frontal cortex	-8, 50, 12	1.403	0.002	86	Left BA 10 (63) Left BA 9 (23)

(a) Voxel probability threshold: p = 0.005
(b) Peak height threshold: z = 1
(c) Cluster extent threshold: 10 voxels. Regions with less than 10 voxels are not reported in the cluster breakdown.
(d) A non-significant trend towards functional abnormalities in left insula was also observed (peaks at -46,-26,42 and -42, 12, 28, *Z*=1.43 and -1.64, *P*=0.002 and 0.003)

cingulate cortex there was hypoactivation relative to controls, whereas in the right basal ganglia / thalamus extending to the posterior part of the insula and in the medial frontal cortex, there was a relative reduction in deactivation (**Figure 7.8B** and **Table 7.5**). Patients also showed reductions in deactivation in the right inferior frontal and left precentral gyri, as well as hypoactivation in left precuneus. Also, a non-significant trend towards functional abnormalities in left insula was observed. The analyses of robustness showed that all these results

Table 7.6 Cognitive tasks brain response abnormalities in first psychotic episode: robustness analyses

	Hypoactivions			Hyperactivations / Failures of deactivation			
	R anterior insula	Anterior cingulate	L precuneus	R posterior insula	R inferior frontal	L precentral / inferior parietal	Medial frontal
Jackknife analysis							
All studies but Achim *et al.*	Yes	Yes	Yes	Yes	No	Yes	Yes
All studies but Ashton *et al.*	Yes	Yes	Yes	Yes	Yes	Yes	Yes
All studies but Boksman *et al.*	Yes	Yes	Yes	Yes	Yes	Yes	Yes
All studies but Broome *et al.* 2009	Yes	Yes	Yes	Yes	Yes	Yes	Yes
All studies but Guerrero Pedraza *et al.*	Yes	Yes	Yes	Yes	Yes	Yes	Yes
All studies but Jones *et al.*	Yes	Yes	Yes	Yes	Yes	Yes	Yes
All studies but Keedy *et al.*	Yes	Yes	Yes	Yes	Yes	Yes	Yes
All studies but MacDonald *et al.*	Yes	Yes	Yes	Yes	Yes	Yes	No
All studies but Nejad *et al.*	Yes	Yes	Yes	Yes	Yes	Yes	Yes
All studies but Schaufelberger *et al.*	Yes	Yes	Yes	Yes	Yes	Yes	Yes
All studies but Scheuerecker *et al.*	Yes	Yes	Yes	Yes	Yes	Yes	Yes
All studies but Schneider *et al.*	Yes	Yes	No	No	No	Yes	Yes
All studies but Snitz *et al.*	Yes	Yes	Yes	Yes	Yes	Yes	Yes
All studies but Strakowski *et al.*	Yes	Yes	Yes	Yes	Yes	Yes	Yes
All studies but Tan *et al.*	Yes	Yes	Yes	Yes	Yes	Yes	Yes
All studies but Woodward *et al.*	Yes	Yes	Yes	Yes	Yes	Yes	Yes
All studies but Yoon *et al.*	Yes	Yes	Yes	Yes	Yes	Yes	Yes
	18 out of 18	18 out of 18	17 out of 18	17 out of 18	16 out of 18	18 out of 18	17 out of 18
Subgroup analyses							
Studies using 1.5T scanners (n = 10, 56%)	No	No	No	Yes	No	No	No
Studies using SPM software (n = 7, 39%)	Yes	No	No	Yes	Yes	No	No
Studies applying 7-8mm FWHM (n = 12, 67%)	Yes	Yes	No	No	No	No	Yes
Studies correcting for multiple comparisons (n = 11, 61%)	Yes	No	No	No	No	No	Yes
Studies using MRI scanners (n=17, 94%)	Yes	Yes	Yes	Yes	Yes	Yes	Yes
Studies employing memory tasks (n=8, 44%)	Yes	No[(a)]	Yes	Yes	Yes	Yes	No[(a)]
Studies where most of the patients were males (n = 15, 88%)	Yes	No	Yes	Yes	Yes	Yes	Yes

Heterogeneity analysis

The heterogeneity analysis showed moderate levels of heterogeneity in the anterior cingulate cortex and the superior part of the right insula cluster, though funnel plots did not reveal that insular findings could be driven by few or small noisy studies. Indeed, as many as 6 studies, with both large and small standard errors, had reported hypoactivation in the peak of maximum heterogeneity within the right insula cluster. In the anterior cingulate cortex, heterogeneity seemed to be due to studies finding nearby abnormalities in both directions.

(a) Medial frontal / anterior cingulate cortex could only be detected as a non-significant trend (peaks at -6,42,10 and 6,16,48, *Z*=1.15 and -1.32, *P*=0.009 and 0.013).

were highly replicable, with the possible exception of the abnormalities in right inferior frontal gyrus (**Table 7.6**).

7.2.3.4 Multimodal analysis of grey matter volume and brain response

The multimodal analysis showed conjoint abnormalities (large and robust decreases of GMV together with differences in activation/deactivation), in

Figure 7.9 Multimodal meta-analysis of structural and functional abnormalities in first psychotic episode

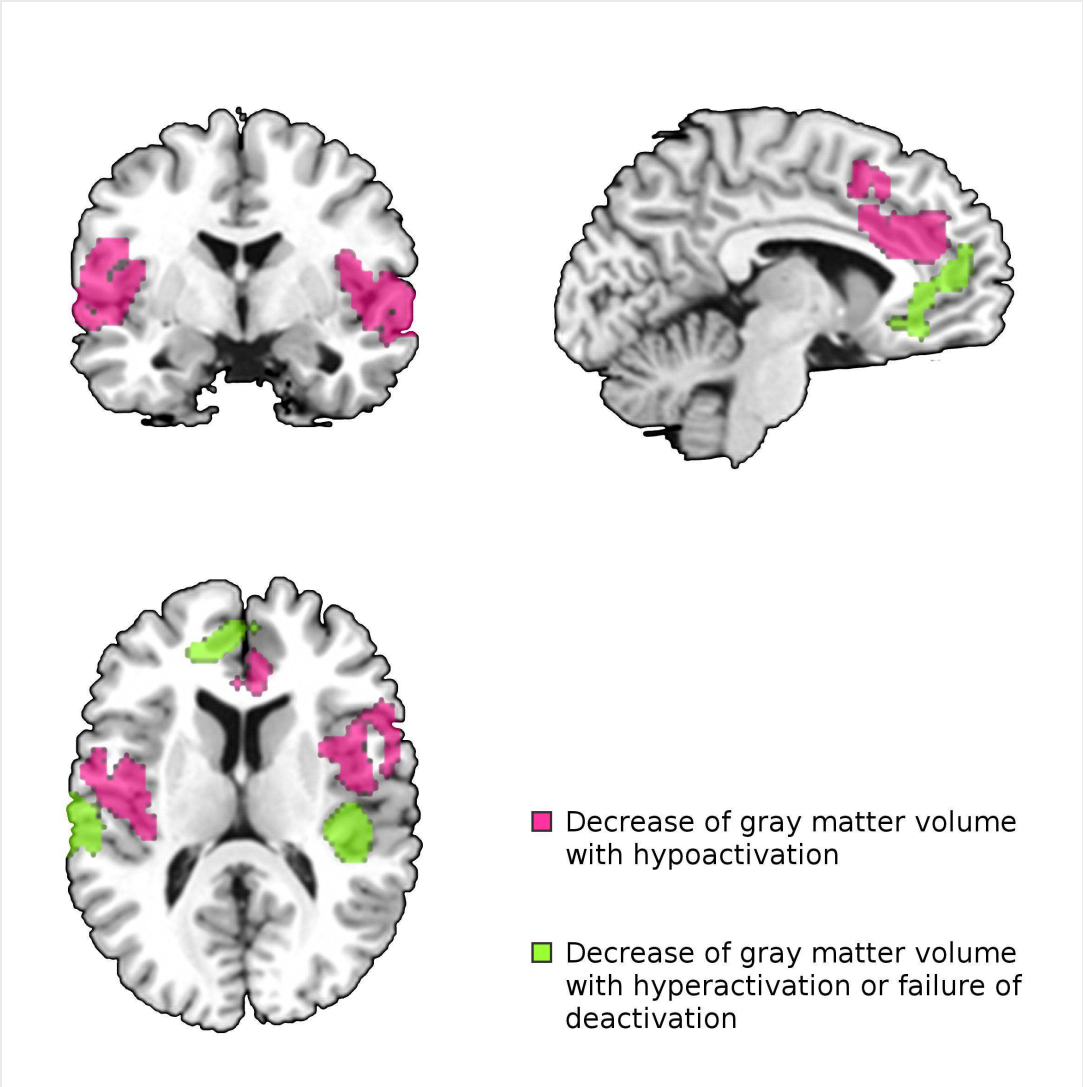

bilateral insulae / superior temporal gyri, as well as in medial frontal / perigenual anterior cingulate cortices. These regions comprised subregions of hypoactivation and subregions of reduced deactivation. Specifically, the anterior parts of the insulae and the dorsal part of the medial frontal / anterior cingulate cortices showed hypoactivation, whereas the posterior parts of the insulae and the ventral part of the medial frontal / anterior cingulate cortices showed reductions in deactivation (**Figure 7.9** and **Table 7.7**).

Table 7.7 Multimodal structural and functional abnormalities in first psychotic episode

	Talairach Coordinates	*P* Value (a,b)	No. of voxels (c)	Breakdown (No. of voxels) (c)
Increases of GM + functional abnormalities				
(none)				
Decreases of GM + hypoactivations				
Anterior part of right insula / superior temporal gyrus	42, 0, 12	~0	439	Right BA 22 (136) Right BA 13 (112) Right BA 44 (47) Right BA 21 (38) Right BA 6 (35) Right BA 9 (31) Right BA 38 (13)
	34, 24, 0	0.0001	44	Right BA 47 (26) Right BA 13 (10)
Anterior part of left insula / superior temporal / precentral gyrus	-40, 12, 34	~0	407	Left BA 13 (126) Left BA 9 (109) Left BA 6 (57) Left BA 22 (57) Left BA 43 (22)
Dorsal part of medial frontal / anterior cingulate gyrus	4, 22, 30	~0	644	Bilateral BA 32 (322) Bilateral BA 24 (95) Bilateral BA 9 (88) Bilateral BA 8 (63) Bilateral BA 6 (43) Right BA 6 (31)
Decreases of GM + hyperactivations / failures of deactivation				
Posterior part of right insula / superior temporal gyrus	34, 4,-12	~0	□Ĥ□Rig	Right BA 38 (41) Right BA 13 (28)
	38,-30, 16	~0	173	Right BA 13 (109) Right BA 41 (59)
	50, 20, 10	0.0001	18	Right BA 45 (12)
	56,-16, 32	0.0002	72	Right BA 4 (30) Right BA 3 (15) Right BA 2 (15)
Posterior part of left superior temporal / postcentral gyrus	-58,-22, 14	0.00005	243	Left BA 42 (106) Left BA 40 (66) Left BA 41 (27) Left BA 22 (25) Left BA 43 (11)
Ventral part of medial frontal / anterior cingulate gyrus	-14, 40, 10	0.0001	117	Bilateral BA 32 (38) Bilateral BA 10 (31) Left BA 9 (27) Left BA 24 (17)

(a) Voxel probability threshold: p = 0.0025
(b) Peak height threshold: p = 0.00025
(c) Cluster extent threshold: 10 voxels. Regions with less than 10 voxels are not reported in the cluster breakdown.

Table 7.8 Grey matter volume abnormalities in first psychotic episode: meta-regression analyses

	Talairach Coordinates	SDM z-value (a)	*P* Value (b)	No. of voxels (c)	Breakdown (No. of voxels) (c)
EFFECTS OF AGE					
Specific GMV decreases in young patients (young patients < old patients and controls)					
Left middle frontal gyrus (within the superior part of the left insula cluster)	-32, 10, 46	-4.121	0.00001	64	Left BA 6 (57)
Specific GMV decreases in old patients (old patients < young patients and controls)					
Right insula	44, -2, 0	-3.527	0.000001	141	Right BA 13 (96) Right BA 22 (18) Right BA 44 (14)
EFFECTS OF ANTIPSYCHOTIC MEDICATION					
Specific GMV decreases in patients having received antipsychotics (non naive patients < naive patients and controls)					
Left middle frontal gyrus (within the superior part of the left insula cluster)	-52, 28, 32	-2.533	0.00002	43	Left BA 9 (25) Left BA 46 (18)
	-52, 12, 36	-2.432	0.00004	50	Left BA 9 (30) Left BA 8 (20)
Medial frontal / anterior cingulate cortices	-4, 16, 30	-2.426	0.00004	90	Bilateral BA 24 (63) Left BA 32 (27)
Specific GMV decreases in patients receiving antipsychotics (medicated patients < medicated patients and controls)					
Medial frontal / anterior cingulate cortices	-4, 16, 30	-3.757	0.000001	179	Left BA 32 (68) Bilateral BA 8 (51) Bilateral BA 24 (37) Bilateral BA 6 (20)
	2, 54, 6	-3.071	0.00005	32	Bilateral BA 10 (32)
Left middle frontal gyrus (within the superior part of the left insula cluster)	-46, 10, 38	-3.077	0.00005	32	Left BA 8 (16) Left BA 9 (14)

(a) Voxel probability threshold: p = 0.0005, for both one intercept and the slope
(b) Peak height threshold: z = 1
(c) Cluster extent threshold: 10 voxels. Regions with less than 10 voxels are not reported in the cluster breakdown.

7.2.3.5 Meta-regression

Meta-regression analyses showed that the GMV in medial frontal / anterior cingulate cortices and left insular clusters were significantly more severely decreased in medicated patients (**Table 7.8**). Indeed, 75% of the studies in

Figure 7.10 Effect size of the differences of grey matter volume between antipsychotic-naïve patients and controls (green bars) and between medicated patients and controls (red bars) in the four peaks of multimodal abnormality in anterior cingulated cortex (ACC) and left insula. No differences between naïve and medicated patients were found in right insula (not shown in the plot).

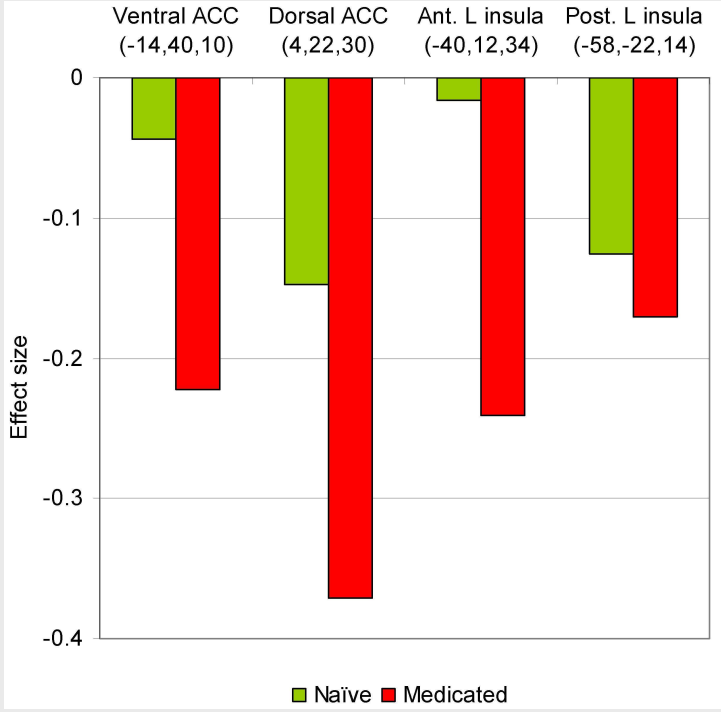

which most of the patients were receiving or had received antipsychotic medication reported some GMV decrease around the regression peaks, whilst only 25% of the studies in which most of the patients were drug-naïve or drug-free reported such abnormalities (**Figure 7.10**). However, antipsychotic-naïve patients still showed significant GMV decrease in medial frontal / anterior cingulate cortices and bilateral insula when compared to healthy controls.

Table 7.9 Cognitive tasks brain response abnormalities in first psychotic episode: meta-regression analyses

	Talairach Coordinates	SDM z-value [(a)]	*P* Value [(b)]	No. of voxels [(c)]	Breakdown (No. of voxels) [(c)]
EFFECTS OF AGE					
(none)					
EFFECTS OF ANTIPSYCHOTIC MEDICATION					
Specific hypoactivations in patients having received antipsychotics (non naive patients < naive patients and controls)					
Right insula	40, 4, -8	-3.340	0.000004	121	Right BA 13 (73) Right claustrum (15)
Specific hypoactivations in patients receiving antipsychotics (medicated patients < medicated patients and controls)					
Right insula	40, 4, -8	-3.506	0.000006	67	Right BA 13 (43) Right claustrum (11)

(a) Voxel probability threshold: p = 0.0005, for both one intercept and the slope
(b) Peak height threshold: z = 1
(c) Cluster extent threshold: 10 voxels. Regions with less than 10 voxels are not reported in the cluster breakdown.

Similarly, meta-regression analyses in the functional dataset showed that abnormalities in right insular cluster were more severe in medicated patients (**Table 7.9**), though these should be taken with caution given the proximity of clusters with opposite findings (hypoactivations vs. hyperactivations / failures of deactivation).

Additional meta-regression findings included a more severe decrease of right insula volume in older patients, and a weaker relationship between younger patients and decreased left insular volume, which was found to be driven by few studies. There were no substantial age differences between medicated and unmedicated samples (medicated patients: 24 years; unmedicated patients: 26 years).

7.2.4. Discussion

This is to our knowledge the first multimodal neuroimaging meta-analysis which combines information from whole brain studies investigating GMV and studies investigating the functional brain response to cognitive tasks to more consistently localize the neural substrates of the FEP. To allow colleagues to apply this multimodal meta-analytic technique to study other neuropsychiatric disorders, this function has been included in the SDM software package (http://www.sdmproject.com/).

The main findings of the present study were that patients with a FEP showed decreases in GMV *and* altered brain response in the medial frontal / perigenual anterior cingulate cortices and in bilateral insulae (**Figure 7.9** and **Table 1**). The changes in functional response were hypoactivations in those subparts of the medial frontal / anterior cingulate cortices and insulae where healthy controls show activations, whilst failures to deactivation in those subparts where healthy controls show deactivations. These results were consistently detected in the several tests conducted to assess the robustness of the findings.

Reduction in anterior cingulate cortex volume has been observed in psychotic disorders in association with impairments in emotional processing and higher executive functions (for a review see Baiano *et al.*(Baiano, David et al. 2007)). The anterior cingulate cortex is crucial for integrating cognitive and emotional processes in support of goal-directed behavior. This functional diversity of the anterior cingulate cortex, which encompasses executive, social cognitive and affective functions, is in line with the findings of abnormal brain

response in the same region, suggesting that alterations in this area may partly explain the difficulties in cognitive and emotional integration that characterize the clinical manifestations of psychosis (Fornito, Yucel et al. 2009). Very similar subdivisions of anterior pericingulate cortex to that observed here have been obtained through examining the connectivity of this region with amygdala (Pezawas, Meyer-Lindenberg et al. 2005), again pointing to a role of these alterations in emotional regulation. However, the exact implication of this region in human cognition and neuropsychiatry disorders is far more complex extending to the processing of effects of errors, conflict, error likelihood, volatility, and reward (Alexander and Brown 2011). The complex neurocognitive profile of medial frontal and anterior cingulate cortices has been recently summarized in a unifying model focusing on a single mechanism, “unexpected non-occurrence”, which reflects the negative component of a prediction error signal for both aversive and rewarding events (Alexander and Brown 2011). Neuropathological research has supported a core role for anterior cingulate cortex dysfunction in psychosis revealing alterations in the cellular and synaptic architecture of the region (Todtenkopf, Vincent et al. 2005). A recent SDM voxel-based meta-analysis confirmed anterior cingulate cortex (and insular) GMV reductions in subjects presenting a FEP, suggesting that the general salience and emotional regulation network is abnormal from the onset of the illness in schizophrenia (Bora, Fornito et al. 2011). Our group has previously showed anterior cingulate cortex alterations are already evident prior the onset of disease during the prodromal phase and play a crucial role in psychosis transition (Borgwardt, McGuire et al. 2008). There is also specific functional imaging evidence indicating abnormal anterior cingulate cortex engagement in

the early phases of psychosis (Boksman, Theberge et al. 2005; Tan, Choo et al. 2005), in subjects at genetic risk for psychosis (Callicott, Egan et al. 2003; Whalley, Simonotto et al. 2006) and in subjects at clinical risk for psychosis (Broome, Matthiasson et al. 2009); for a comprehensive review of anterior cingulate cortex in emerging psychosis see Rothlisberger et al. (2012).

Similarly, involvement of the insular cortex is a common finding in neuroanatomical studies of schizophrenia. The insula is a cortical structure with extensive connections to many areas of the cortex and limbic system, especially amygdala. It integrates external sensory input with the limbic system and is integral to the awareness of the body's state (interoception) (Wylie and Tregellas 2010). Many deficits observed in schizophrenia involve these functions and may relate to insula pathology, including the processing of both visual and auditory emotional information, bodily hallucinations and coenaesthesia, altered pain perception, and neuronal representations of the self. Additional evidence confirms that insula alterations are crucial to the development from a high risk state to frank psychosis (Takahashi, Wood et al. 2009; Fusar-Poli, Radua et al. 2011; Smieskova, Fusar-Poli et al. 2011) and may be secondary to neurofunctional activation of insular areas during experiencing auditory hallucinations (O'Daly, Frangou et al. 2007).

However, the anterior cingulate cortex and the insula play a crucial role in emotional processing and structural and functional alterations in these areas have been consistently demonstrated in a range of anxiety disorders (Paulus and Stein 2006; Milad, Quirk et al. 2007; Radua, van den Heuvel et al. 2010). Thus, our findings may also represent the neural correlates of the high levels of stress and anxiety that are usually associated with the first onset of frank

psychotic symptoms. Of interest, an impact of environmental risk factors linked to social stress, such as urban birth, has recently been shown on the same cingulate subregions identified here (Lederbogen, Kirsch et al. 2011). Furthermore, cingulate-amygdala interactions are altered in genetic variants associated with increased risk of mental illness (although not specifically schizophrenia) in the context of environmental adversity (Pezawas, Meyer-Lindenberg et al. 2005). This interpretation of the findings is consistent with the post-traumatic stress literature suggesting that exposure to traumatic life events is associated with structural abnormalities in various limbic and paralimbic brain regions including the cingulate cortex and the insula, after controlling for genetic factors (Kasai, Yamasue et al. 2008). It is also important to note that the exact specificity of our findings in relation to the development of schizophreniform vs bipolar disorders is mostly unknown (Yu, Cheung et al. 2010).

The mechanistic interpretation of the multimodal findings of this study is highly speculative. On the one hand, if a region has half the grey matter it should have, it could be that it needed half the baseline blood flow, i.e. assuming that each ml of grey matter needs a fixed amount of blood flow. However, if baseline blood flow is low, a relative increase of blood glow may show as an absolute hypo-increase of blood flow, and thus as hypo-activation. On the other hand, a reduction of grey matter could also be accompanied by a compensatory hyperfunctionality of the remaining grey matter, which could involve a higher vascularisation and thus even show as hyper-activation. In any case it is important to remember that BOLD fMRI (which is the modality from which the majority of the data reviewed originates) has no defined zero but contrasts, in the usual approach, two conditions statistically. This means that an

activation or deactivation strongly depends on what the comparator condition is. It is, however, noteworthy that our meta-analysis does depict a differentiation between subgenual and supragenual cingulate compartments, and between anterior and posterior insula, indicating that even though there may not be an easily depictable relationship between grey matter and activation in any given condition, across conditions, our meta-analysis identifies functional subdivisions of the structurally abnormal regions that map onto known neuroanatomy and functional circuits. Interpretations are different if the functional damage is assumed to appear before the decrease in grey matter. In that case, one could hypothesize that hyperfunctionality may lead to a decrease in grey matter by exhaustion, whilst hypo-functionality may lead to the same situation due to some sort of mechanism to avoid neuronal underemployment.

Schizophrenia is associated with 14% increase of striatal dopamine synthesis capacity and antipsychotic treatment is the mainstream clinical approach in the field (Fusar-Poli and Meyer-Lindenberg 2012; Fusar-Poli and Meyer-Lindenberg 2012). Under these premises, GMV abnormalities were found to be significantly more severe in medicated patients (**Figure 7.10**). This result is in line with evidence from imaging studies indicating antipsychotic treatment can influence GMV (Ho, Andreasen et al. 2011) and neural activity (Lui, Li et al. 2010) in psychosis. Recent structural imaging studies have further clarified that antipsychotic exposure can affect GMV even at the onset of the disease, in the early phases of psychosis, influencing the structure of temporal and prefrontal cortex (Smieskova, Fusar-Poli et al. 2009). In line with these findings, functional imaging studies have indicated that short-term or acute antipsychotic treatment can alter the neurophysiological cortical response

during cognitive functioning (Fusar-Poli, Broome et al. 2007). Antipsychotics can reduce frontal cerebral blood flow, and frontal hypoperfusion could be a mechanism underlying smaller brain tissue volumes (Ho, Andreasen et al. 2011). The differences detected can reflect long-lasting changes in brain volume caused by antipsychotic medication but also compensatory processes associated with the underlying disease process. Although a consistent effect of antipsychotic medication was shown in these areas, it did not account for the whole magnitude of GMV alterations. Our data therefore support a model in which antipsychotics target regions of key pathology in early psychosis, but do not necessarily suggest that drug treatment causes these alterations. Indeed, about 25% of the studies in which most of the patients were drug-naïve reported abnormalities in the same brain regions. Our recent voxel-based meta-analysis of VBM studies in drug-naïve subjects at high clinical risk for psychosis or with a confirmed psychosis onset was also associated with GMV decreases in temporo-insular and anterior cingulate cortex regions (Fusar-Poli, Radua et al. 2011). However, it cannot be fully ruled out that antipsychotic medications may cause some of the observed alterations (Knowles, David et al. 2010). Of interest, anterior cingulate cortex function and structure has been reported to be especially sensitive to remedial antipsychotic treatment in psychosis (Lahti, Weiler et al. 2009; Stip, Mancini-Marie et al. 2009). As there is evidence indicating that few weeks of antipsychotic treatment modulate the anterior cingulate cortex response (Lahti, Holcomb et al. 2004; Snitz, MacDonald et al. 2005), the question of the functional significance of dynamic prefrontal changes in the first phases of psychosis may have some potential clinical implications for early interventions.

This study has some limitations. First, whilst voxel-wise meta-analytical methods provide excellent control for false positive results, it is more difficult to avoid false negative results (Radua, Mataix-Cols et al. 2012). We cannot therefore exclude the possibility that we were unable to detect some group differences because of limited statistical power. Indeed, this could be the case for the separate meta-analysis of functional abnormalities, where a lower number of studies could be included and insular/temporal abnormalities only reached statistical significance in the right hemisphere. Second, some of the included VBM studies reported grey matter density rather than volume. Grey matter density might be understood as a type of GMV that has not been corrected by the distorting effects of the normalisation to the stereotactic space; therefore, its inclusion in the meta-analysis is valid (it is also a "volume") although it could add a source of heterogeneity. Other methodological differences such as the use of one or another smoothing kernel (see Table 7.2) may further contribute to this heterogeneity. Third, the included functional imaging studies had employed different cognitive tasks to evoke the brain response of interest, which could result in a source of heterogeneity. However, studies not employing cognitive paradigms were excluded in order to minimize this heterogeneity, and a separate subgroup analysis of only those studies employing memory tasks yielded nearly identical results. In fact, our finding that insular and medial frontal / anterior cingulate cortices were found to be consistently functionally abnormal in FEP is especially remarkable given that the employed tasks have little or no emotional component and do not primarily activate these particular structures. The results may therefore have been quite different if a salience processing task, or an emotional faces task had been

used to provide the fMRI data. Fourth, the meaning of GMV alterations in the adolescent and young adult's is unclear and may have been confounded by factors including other medication types as antidepressants, consumption of alcohol, tobacco or illicit drugs as cannabis, and socioeconomic status. Fifth, it cannot be discarded that the medication effects could be confounded by factors such as duration and severity of psychosis, socioeconomic status or neurocognitive variables. Unfortunately, only few studies reported these data, preventing a covariate analysis. Similarly, only few studies reported the actual medication doses, for what a meta-regression with chlorpromazine equivalents was not feasible. It is also possible that the greater abnormalities in medicated patients could be related to a selection bias of relatively well patients able to be scanned without treatment. Sixth, this study did not aim to detect correlations between structural and functional abnormalities, but rather, to localize those brain regions in which the disorder is associated with both structural and functional abnormalities. Future studies are encouraged in order to investigate the spatial and temporal relationships between the structure and function of the regions detected in this meta-analysis. Finally, our criterion of conjoint functional and structural abnormalities is stringent and regions with meta-analytic support for either functional or structural changes in early psychosis, but not both, should still be considered in the pathophysiology of the illness.

7.2.4.1 Conclusions

Results from our multimodal meta-analysis demonstrate a close relationship between structural and functional brain alterations in subjects with a first

episode of psychosis. In the medial frontal / anterior cingulate cortices, and in the bilateral insulae, patients showed a decrease in grey matter volume as well as abnormal functional response. Some of these changes may be partially related to treatment with antipsychotic medication.

7.3 OVERALL DISCUSSION

Despite the development of several voxel-based meta-analytic methods, the different neuroimaging modalities are still summarized separately, preventing the visualization of the global picture of brain abnormalities in a given neuropsychiatric disorder. This chapter has introduced a novel approach to meta-analytically detect those brain regions that are affected across two or more imaging modalities. Interestingly, this approach may be applied to any type of meta-analytical method, and can be easily implemented in nearly any neuroimaging software library. It is hoped that, with this tool, researchers will be able to provide an advanced description of the brain complexity and thus ultimately increase the level of basic knowledge underlying the major neuropsychiatric disorders.

It must be highlighted that this method does not aim to detect correlations between abnormalities in two modalities, but rather, to localize those brain regions in which the disorder is associated with abnormalities in both modalities.

7.4 REFERENCES

Alexander, W. H. and J. W. Brown (2011). "Medial prefrontal cortex as an action-outcome predictor." Nat Neurosci **14**(10): 1338-44.

Baiano, M., A. David, et al. (2007). "Anterior cingulate volumes in schizophrenia: a systematic review and a meta-analysis of MRI studies." Schizophr Res **93**(1-3): 1-12.

Boksman, K., J. Theberge, et al. (2005). "A 4.0-T fMRI study of brain connectivity during word fluency in first-episode schizophrenia." Schizophr Res **75**(2-3): 247-63.

Bora, E., A. Fornito, et al. (2011). "Neuroanatomical abnormalities in schizophrenia: a multimodal voxelwise meta-analysis and meta-regression analysis." Schizophr Res **127**(1-3): 46-57.

Bora, E., A. Fornito, et al. (2010). "Voxelwise meta-analysis of gray matter abnormalities in bipolar disorder." Biol Psychiatry **67**(11): 1097-1105.

Borgwardt, S. J., P. McGuire, et al. (2008). "Anterior cingulate pathology in the prodromal stage of schizophrenia." Neuroimage **39**(2): 553-554.

Broome, M. R., P. Matthiasson, et al. (2009). "Neural correlates of executive function and working memory in the 'at-risk mental state'." Br J Psychiatry **194**(1): 25-33.

Callicott, J. H., M. F. Egan, et al. (2003). "Abnormal fMRI response of the dorsolateral prefrontal cortex in cognitively intact siblings of patients with schizophrenia." Am J Psychiatry **160**(4): 709-719.

Di, X., S. S. Kannurpatti, et al. (2012). "Calibrating BOLD fMRI Activations with Neurovascular and Anatomical Constraints." Cereb Cortex: in Press, available online 17 February 2012, doi: 10.1093/cercor/bhs001.

Eickhoff, S. B., A. R. Laird, et al. (2009). "Coordinate-based activation likelihood estimation meta-analysis of neuroimaging data: a random-effects approach based on empirical estimates of spatial uncertainty." Hum Brain Mapp **30**(9): 2907-2926.

Etkin, A. and T. D. Wager (2007). "Functional neuroimaging of anxiety: a meta-analysis of emotional processing in PTSD, social anxiety disorder, and specific phobia." Am J Psychiatry **164**(10): 1476-88.

Fornito, A., M. Yucel, et al. (2009). "Anatomical abnormalities of the anterior cingulate cortex in schizophrenia: bridging the gap between neuroimaging and neuropathology." Schizophr Bull **35**(5): 973-993.

Fusar-Poli, P. (2012). "Voxel-wise meta-analysis of fMRI studies in patients at clinical high risk for psychosis." J Psychiatry Neurosci **37**(2): 106-12.

Fusar-Poli, P., P. Allen, et al. (2008). "Neuroimaging studies of the early stages of psychosis: a critical review." Eur Psychiatry **23**(4): 237-44.

Fusar-Poli, P., A. Bechdolf, et al. (2012). "At Risk for Schizophrenic or Affective Psychoses? A Meta-Analysis of DSM/ICD Diagnostic Outcomes in Individuals at High Clinical Risk." Schizophr Bull: in Press, available online 15 May 2012, doi:10.1093/schbul/sbs060.

Fusar-Poli, P., S. Borgwardt, et al. (2011). "Neuroanatomy of vulnerability to psychosis: a voxel-based meta-analysis." Neurosci Biobehav Rev **35**(5): 1175-1185.

Fusar-Poli, P., M. Broome, et al. (2011). "Altered brain function directly related to structural abnormalities in people at ultra high risk of psychosis: longitudinal VBM-fMRI study." Journal of Psychiatric Research **45**(2): 190-8.

Fusar-Poli, P. and M. R. Broome (2006). "Conceptual issues in psychiatric neuroimaging." Curr Opin Psychiatry **19**(6): 608-12.

Fusar-Poli, P., M. R. Broome, et al. (2007). "Effects of acute antipsychotic treatment on brain activation in first episode psychosis: an fMRI study." Eur Neuropsychopharmacol. **17**(6-7): 492-500.

Fusar-Poli, P., M. R. Broome, et al. (2009). "Prefrontal function at presentation directly related to clinical outcome in people at ultrahigh risk of psychosis." Schizophr Bull **37**(1): 189-98.

Fusar-Poli, P., G. Deste, et al. (2012). "Cognitive functioning in prodromal psychosis: A meta-analysis of cognitive functioning in prodromal psychosis." Arch Gen Psychiatry **69**(6): 562-71.

Fusar-Poli, P., O. D. Howes, et al. (2010). "Abnormal frontostriatal interactions in people with prodromal signs of psychosis: a multimodal imaging study." Arch Gen Psychiatry **67**(7): 683-91.

Fusar-Poli, P., O. D. Howes, et al. (2009). "Abnormal prefrontal activation directly related to pre-synaptic striatal dopamine dysfunction in people at clinical high risk for psychosis." Mol Psychiatry **16**(1): 67-75.

Fusar-Poli, P. and A. Meyer-Lindenberg (2012). "Striatal Presynaptic Dopamine in Schizophrenia, Part I: Meta-analysis of Dopamine Active Transporter (DAT) Density." Schizophr Bull: in Press, available online 26 January 2012, doi: 10.1093/schbul/sbr111.

Fusar-Poli, P. and A. Meyer-Lindenberg (2012). "Striatal Presynaptic Dopamine in Schizophrenia, Part II: Meta-Analysis of [18F/11C]-DOPA PET Studies." Schizophr Bull: in Press, available online 26 January 2012, doi: 10.1093/schbul/sbr180.

Fusar-Poli, P., J. Perez, et al. (2007). "Neurofunctional correlates of vulnerability to psychosis: a systematic review and meta-analysis." Neuroscience & Biobehavioral Reviews **31**(4): 465-84.

Fusar-Poli, P., J. Perez, et al. (2007). "Neurofunctional correlates of vulnerability to psychosis: a systematic review and meta-analysis." Neurosci Biobehav Rev **31**(4): 465-484.

Fusar-Poli, P., J. Radua, et al. (2011). "Neuroanatomical maps of psychosis onset: voxelwise meta-analysis of antipsychotic-naive VBM studies." Schizophr Bull: in Press, available online 10 November 2011, doi: 10.1093/schbul/sbr134.

Fusar-Poli, P., J. M. Stone, et al. (2011). "Thalamic glutamate levels as a predictor of cortical response during executive functioning in subjects at high risk for psychosis." Arch Gen Psychiatry **68**(9): 881-90.

Hart, H., J. Radua, et al. (2012). "Meta-analysis of fMRI studies of inhibition and attention in ADHD: exploring task-specific, stimulant medication and age effects." Arch Gen Psychiatry: in Press.

Ho, B. C., N. C. Andreasen, et al. (2011). "Long-term antipsychotic treatment and brain volumes: a longitudinal study of first-episode schizophrenia." Arch Gen Psychiatry **68**(2): 128-137.

Jardri, R., A. Pouchet, et al. (2010). "Cortical activations during auditory verbal hallucinations in schizophrenia: a coordinate-based meta-analysis." Am J Psychiatry **168**(1): 73-81.

Kasai, K., H. Yamasue, et al. (2008). "Evidence for acquired pregenual anterior cingulate gray matter loss from a twin study of combat-related posttraumatic stress disorder." Biol Psychiatry **63**(6): 550-556.

Knowles, E. E., A. S. David, et al. (2010). "Processing speed deficits in schizophrenia: reexamining the evidence." Am J Psychiatry **167**(7): 828-35.

Lahti, A. C., H. H. Holcomb, et al. (2004). "Clozapine but not haloperidol Re-establishes normal task-activated rCBF patterns in schizophrenia within the anterior cingulate cortex." Neuropsychopharmacology **29**(1): 171-178.

Lahti, A. C., M. A. Weiler, et al. (2009). "Modulation of limbic circuitry predicts treatment response to antipsychotic medication: a functional imaging study in schizophrenia." Neuropsychopharmacology **34**(13): 2675-2690.

Lederbogen, F., P. Kirsch, et al. (2011). "City living and urban upbringing affect neural social stress processing in humans." Nature **474**(7352): 498-501.

Lui, S., T. Li, et al. (2010). "Short-term effects of antipsychotic treatment on cerebral function in drug-naive first-episode schizophrenia revealed by

"resting state" functional magnetic resonance imaging." Arch Gen Psychiatry **67**(8): 783-792.

McGuire, P., O. D. Howes, et al. (2008). "Functional neuroimaging in schizophrenia: diagnosis and drug discovery." Trends Pharmacol Sci **29**(2): 91-8.

Milad, M. R., G. J. Quirk, et al. (2007). "A role for the human dorsal anterior cingulate cortex in fear expression." Biol Psychiatry **62**(10): 1191-1194.

Nakao, T., J. Radua, et al. (2011). "Gray matter volume abnormalities in ADHD: voxel-based meta-analysis exploring the effects of age and stimulant medication." Am J Psychiatry **168**(11): 1154-63.

Nichols, T., M. Brett, et al. (2005). "Valid conjunction inference with the minimum statistic." Neuroimage **25**(3): 653-60.

O'Daly, O. G., S. Frangou, et al. (2007). "Brain structural changes in schizophrenia patients with persistent hallucinations." Psychiatry Res **156**(1): 15-21.

Palaniyappan, L., V. Balain, et al. (2012). "Structural correlates of auditory hallucinations in schizophrenia: A meta-analysis." Schizophr Res **137**(1-3): 169-73.

Paulus, M. P. and M. B. Stein (2006). "An insular view of anxiety." Biol Psychiatry **60**(4): 383-387.

Pezawas, L., A. Meyer-Lindenberg, et al. (2005). "5-HTTLPR polymorphism impacts human cingulate-amygdala interactions: a genetic susceptibility mechanism for depression." Nat Neurosci **8**(6): 828-834.

Philip, R. C., M. R. Dauvermann, et al. (2011). "A systematic review and meta-analysis of the fMRI investigation of autism spectrum disorders." Neurosci Biobehav Rev **36**(2): 901-42.

Radua, J. and D. Mataix-Cols (2009). "Voxel-wise meta-analysis of grey matter changes in obsessive-compulsive disorder." Br J Psychiatry **195**(5): 393-402.

Radua, J. and D. Mataix-Cols (2012). "Meta-analytic methods for neuroimaging data explained." Biol Mood Anxiety Disord **2**: 6.

Radua, J., D. Mataix-Cols, et al. (2012). "A new meta-analytic method for neuroimaging studies that combines reported peak coordinates and statistical parametric maps." Eur Psychiatry **27**: 605-611.

Radua, J., O. A. van den Heuvel, et al. (2010). "Meta-analytical comparison of voxel-based morphometry studies in obsessive-compulsive disorder vs other anxiety disorders." Arch Gen Psychiatry **67**(7): 701-711.

Rothlisberger, M., A. Riecher-Rossler, et al. (2012). "Cingulate volume abnormalities in emerging psychosis." Curr Pharm Des **18**(4): 495-504.

Smieskova, R., P. Fusar-Poli, et al. (2009). "The effects of antipsychotics on the brain: what have we learnt from structural imaging of schizophrenia?--a systematic review." Curr.Pharm.Des **15**(22): 2535-2549.

Smieskova, R., P. Fusar-Poli, et al. (2011). "Insular volume abnormalities associated with different transition probabilities to psychosis." Psychol Med **42**(8): 1613-1625.

Snitz, B. E., A. MacDonald, III, et al. (2005). "Lateral and medial hypofrontality in first-episode schizophrenia: functional activity in a medication-naive state and effects of short-term atypical antipsychotic treatment." Am J Psychiatry **162**(12): 2322-2329.

Stip, E., A. Mancini-Marie, et al. (2009). "Increased grey matter densities in schizophrenia patients with negative symptoms after treatment with quetiapine: a voxel-based morphometry study." Int.Clin.Psychopharmacol. **24**(1): 34-41.

Takahashi, T., S. J. Wood, et al. (2009). "Insular cortex gray matter changes in individuals at ultra-high-risk of developing psychosis." Schizophr Res **111**(1-3): 94-102.

Tan, H. Y., W. C. Choo, et al. (2005). "fMRI study of maintenance and manipulation processes within working memory in first-episode schizophrenia." **162**(10): 1849-1858.

Todtenkopf, M. S., S. L. Vincent, et al. (2005). "A cross-study meta-analysis and three-dimensional comparison of cell counting in the anterior cingulate cortex of schizophrenic and bipolar brain." Schizophr Res **73**(1): 79-89.

Turkeltaub, P. E., G. F. Eden, et al. (2002). "Meta-analysis of the functional neuroanatomy of single-word reading: method and validation." Neuroimage **16**(3 Pt 1): 765-780.

Via, E., J. Radua, et al. (2011). "Meta-analysis of gray matter abnormalities in autism spectrum disorder: should Asperger disorder be subsumed under a broader umbrella of autistic spectrum disorder?" Arch Gen Psychiatry **68**(4): 409-18.

Weinberger, D. R. and R. K. McClure (2002). "Neurotoxicity, neuroplasticity, and magnetic resonance imaging morphometry: what is happening in the schizophrenic brain?" Arch Gen Psychiatry **59**(6): 553-558.

Whalley, H. C., E. Simonotto, et al. (2006). "Functional imaging as a predictor of schizophrenia." Biol Psychiatry **60**(5): 454-462.

Wylie, K. P. and J. R. Tregellas (2010). "The role of the insula in schizophrenia." Schizophr Res **123**(2-3): 93-104.

Yu, K., C. Cheung, et al. (2010). "Are Bipolar Disorder and Schizophrenia Neuroanatomically Distinct? An Anatomical Likelihood Meta-analysis." Front Hum Neurosci **4**: 189.

CHAPTER 8

General conclusions and suggestions for future research

8.1 SUMMARY AND CONCLUSIONS

The main types of meta-analytic methods available for neuroimaging studies were reviewed in Chapter 1. Region of interest (ROI) and voxel-based methods each have advantages and disadvantages. Specifically, ROI-based meta-analyses use optimal statistical methods which use effect-sizes and assess the between-study heterogeneity, but they usually have a limited and likely biased inclusion of studies (Ioannidis 2011). Conversely, voxel-based meta-analyses usually have a more exhaustive and unbiased inclusion of studies, but their statistical methods are less accurate. The aim of this thesis was to develop a series of new methods to overcome some of the limitations of the methods that were in existence at the time this thesis was conceived.

8.1.1 The new voxel-based meta-analytic method

This new approach, called *signed differential mapping* (SDM, see Chapter 2), addressed part of the between-study heterogeneity not considered by previous voxel-based meta-analytic methods, by reconstructing positive and negative maps in the same image thus counteracting the effects of studies reporting findings in opposite directions (Radua and Mataix-Cols 2010), and by incorporating meta-regression methods (Radua and Mataix-Cols 2009). Subsequently, the method was modified to allow estimation of more complex linear models such as meta-comparisons of groups, multiple meta-regressions, or inclusion of covariates (see Chapter 3) (Radua, van den Heuvel et al. 2010).

Chapter 4 introduced a newer effect-size version of SDM (ES-SDM) designed with the aim of allowing the combination of studies from which images (statistical parametric maps) are available with studies from which only peak coordinates are reported. This method allows a more exhaustive inclusion of studies, as well as more accurate findings because it weights the calculations by both sample-size and study precision, incorporates effect-sizes and fully addresses between-study heterogeneity (Radua, Mataix-Cols et al. 2012). This is achieved by first using peak coordinates and their statistical values to recreate the statistical parametric maps, and then conducting an image-based meta-analysis.

Figure 8.1 Summary of the main available voxel-based meta-analytic methods.

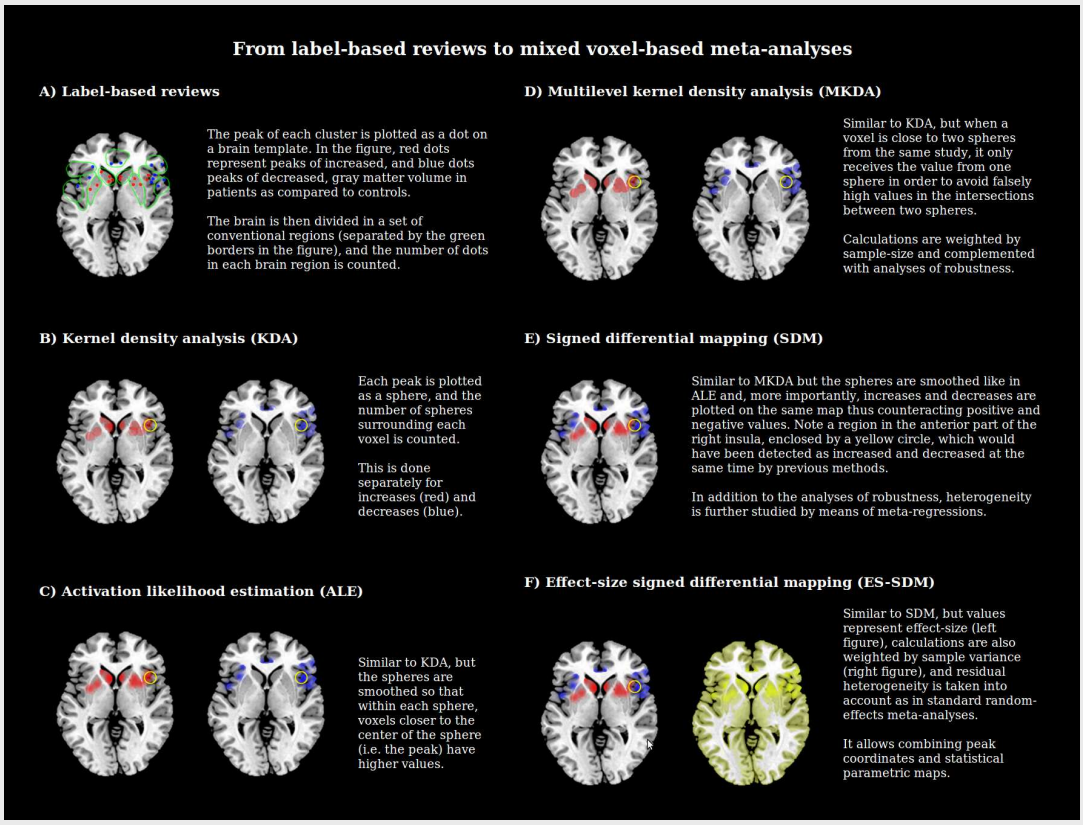

Increases and decreases of grey matter volume are fictitious and have been manually plotted over a MRICroN template to illustrate the main features of the different methods.

In a meta-analysis of the blood oxygen level-dependent (BOLD) response to emotional facial stimuli (Radua, Mataix-Cols et al. 2012), the sensitivity of ES-SDM (55%) was similar to that of SDM (51%) when *only* using peak coordinates. However, the inclusion of the statistical parametric maps led to a gradual and substantial increase of the sensitivity of ES-SDM (73% when the statistical parametric map of one study was included, 87% when the statistical parametric maps of two studies were included, 93% when the statistical parametric maps of three studies were included, etcetera). Therefore, given the potential of this new method, authors are encouraged to make their

Table 8.1 Comparison of the main meta-analytic methods for neuroimaging studies comparing patients and controls.

	ROI-based meta-analysis	Voxel-based meta-analysis			
		KDA / old ALE	MKDA / new ALE	SDM	ES-SDM
Selection of studies					
Exhaustive inclusion of studies	Limited, as information for a given brain region is present in few or no studies	Probable, as far as the included studies investigate the whole brain and not only some ROIs (in which case should be discarded)			More probable, because statistical parametric maps can also be included
Unbiased inclusion of studies	Limited, as information is only available for regions hypothesized a priori	Probable, as far as the included studies do not use different statistical thresholds for different parts of the brain (this is a strict inclusion criterion in SDM and ES-SDM)			
Statistical analyses					
Weighting of the studies	Complete (sample size and study precision)	None	Partial (only sample size)		Complete (sample size and study precision)
Control of the heterogeneity	Residual heterogeneity is correctly included in the analyses	Residual heterogeneity is not controlled and increases and decreases are not counteracted, potentially leading to voxels being detected as increased and decreased at the same time		Residual heterogeneity is not accounted but increases and decreases are counteracted	Residual heterogeneity is correctly included in the weightings
Study of the heterogeneity	Possible, by means of meta-regressions and subgroup analyses	Limited to subgroup analyses		Possible, by means of meta-regressions and subgroup analyses	
Correction for multiple comparisons	Possible	Not possible, questionable or limited to conventional voxel-thresholds cluster-based methods			
Description of the effect sizes	Possible	Not possible	Possible though limited to pseudo-effect sizes based on the proportion of studies reporting significant findings		Possible
Description of relevant non-significant trends	Possible, as the number of ROIs is manageable	Not possible, or limited to the visual inspection of liberally thresholded maps, as the number of voxels is too massive for a more accurate individual inspection			

ALE: activation likelihood estimation; ES-SDM: effect-size signed differential mapping; KDA: kernel density analysis; MKDA: multilevel kernel density analysis; ROI: region of interest; SDM: signed differential mapping

statistical parametric maps widely available to the community on their lab websites or via other means.

Figure 8.1 and Table 8.1 show the main differences between previous methods and SDM / ES-SDM.

8.1.2 The multimodal adaptations

Concurrent innovations of the SDM methods included the possibility of conducting meta-analyses of imaging modalities other than functional magnetic resonance imaging (fMRI) and grey matter volume. Specifically, SDM and especially ES-SDM were adapted for their use with studies voxel-wise and tract-wise investigating white matter volume or water diffusivity (Radua, Via et al. 2010; Peters, Szeszko et al. 2012), thus allowing meta-analyses which were not possible with previous methods (see Chapters 5 and 6).

Finally, a strategy for combining the findings of meta-analyses conducted in different modalities was also developed (Chapter 7). The aim of such approach is to detect key regional abnormalities which show impairments of both grey matter volume and function (or any other combination of modalities) (Radua, Borgwardt et al. 2012; Radua, Romeo et al. 2012). Future clinical studies are encouraged to assess, for each of the regions detected in a multimodal meta-analysis, the clinical significance of structural but not functional impairment, the clinical significance of functional but not structural impairment, and the clinical significance of having both structural and functional impairments. Ultimately, multivariate classifications of this kind may improve diagnostic and/or prognostic classifications.

8.1.3 Main limitations

Although voxel-based meta-analyses minimize the effects of selectively reporting certain regions of interest, they are not totally immune to publication bias, as negative results may still be less likely to be published (what is known as the file drawer problem). Authors of the original papers are strongly encouraged to publish their results even if they perceive them as being disappointing or they do not find differences between patients and controls (Borgwardt, Radua et al. 2012).

Two other relevant limitations of the method, expanded upon in section 8.2, are some spatial imprecision associated to the recreation of clusters, and the lack of a formal correction for multiple comparisons.

8.1.4 Parallel evolution of other meta-analytical methods

It is important to note that, during the timeframe of the current thesis, other methods have also evolved and become progressively more sophisticated, thus dealing with some of their initial limitations.

Activation likelihood estimate (ALE), as well as an evolved-version of *kernel density analysis* (KDA) called *parametric voxel-based meta-analysis* (PVM), introduced computationally fast methods to derive the statistical significance of the results (Costafreda, David et al. 2009; Eickhoff, Bzdok et al. 2011). Furthermore, ALE replaced the false discovery rate (FDR) correction for multiple comparisons by the family-wise error rate (FWE) correction and the

cluster-level significance (Eickhoff, Bzdok et al. 2011) present in multilevel KDA (Wager, Lindquist et al. 2007). Finally, PVM has recently adopted the effect-size approach developed by ES-SDM (Radua, Mataix-Cols et al. 2012), though with some notable differences (Costafreda 2012).

In parallel with the development of these methods, several freely-available website-based databases of neuroimaging data have been made available. These online databases may be classified in three groups, namely: a) sets of original data (e.g. the raw scanner images from several samples of individuals); b) summary statistics from the studies included in one meta-analysis (e.g. the mean±sd ROI volumes); and c) sets of summary statistics of virtually all published studies.

The online sets of original data are composed of the raw and/or pre-processed brain images, along with the demographic and clinical characteristics of each of the many anonymous participants. These databases may be used by researchers to conduct their studies, thus being a useful resource for highly accurate data analyses. It must be noted, however, that analyses derived from these datasets should not be strictly considered 'meta-analyses', as they do not necessarily exhaustively include all available data. Examples of these datasets are BRAINNet (http://www.brainnet.net/), the fMRI Data Center (http://www.fmridc.org/) and OpenfMRI (http://www.openfmri.org/).

Online databases containing the summary statistics from the studies included in particular meta-analyses represent a more interactive (and often complete) alternative to the traditional "supplementary material" that accompanies published meta-analysis. Importantly, these online data may be used by other researchers to conduct updated or secondary analyses.

Outstanding examples of this type of databases are the Bipolar Disorder Neuroimaging Database (http://www.bipolardatabase.org/) and the Major Depressive Disorder Neuroimaging Database (http://www.depressiondatabase.org/) by Kempton and colleagues (Kempton, Geddes et al. 2008; Kempton, Salvador et al. 2011).

Finally, many sets of summary statistics of virtually all published neuroimaging studies exist, allowing a rapid retrieval of specific data in order to facilitate the meta-analytic process. The developers of BrainMap (http://www.brainmap.org/), for instance, have been building and updating an impressive database of neuroimaging findings since 1987 (Laird, Lancaster et al. 2005). Other available databases are the AMAT toolbox (http://www.antoniahamilton.com/amat.html), the Internet Brain Volume Database (http://www.cma.mgh.harvard.edu/ibvd) and the Surface Management System Database (http://sumsdb.wustl.edu/sums/index.jsp).

Two promising online developments, the Brede Database (http://neuro.imm.dtu.dk/services/brededatabase) (Nielsen, Hansen et al. 2004; Nielsen, Kempton et al. 2012) and NeuroSynth (http://www.neurosynth.org/) (Yarkoni, Poldrack et al. 2011), deserve special mentioning. These packages contain a set of summary statistics together with online functions aimed at conducting real-time meta-analyses online. Unfortunately, extraction of coordinates in NeuroSynth from publications is not manually verified, which may bias the results towards those regions that the authors of the original articles want to emphasize in the tables of the manuscripts. However, when the goal is to obtain a very fast and preliminary meta-analysis of the literature, NeuroSynth may be one of the first options.

8.2 SUGGESTIONS FOR FUTURE DEVELOPMENT

8.2.1 Recreation of the study maps

An important aspect of ES-SDM that requires improvement is the recreation of the maps of those studies from which only coordinates are available. Simpler voxel-based meta-analytic methods such as KDA or PVM base these recreations on creating a solid sphere centred at the cluster peak (Wager, Phan et al. 2003). ALE and SDM try to conduct this step more realistically by using a smoothed sphere so that voxels closer to a peak are estimated to have values more similar to that of the peak. ES-SDM further improves this recreation with the use of effect-sizes and a more sophisticated algorithm in which those voxels close to more than one peak have values similar to those of both peaks. However, even ES-SDM recreations may not benefit from all information available.

In the future, voxel-based meta-analytic methods might potentially also incorporate the reported size of the clusters, as well as the shape of the clusters as printed in the two-dimensional figures included in the original manuscripts. Also, recreations might benefit from the knowledge that spheres created by the different local peaks of the same cluster *should* overlap, whilst spheres created by local peaks from different clusters *should not* overlap. Finally, future methods might use a set of aprioristic information, such as the regional distribution of spatial covariance in each neuroimaging modality.

Unfortunately, the implementation of these potential improvements may be hampered by a set of difficulties, which could ultimately introduce more noise, rather than remove noise as intended. For example, visual tasks usually produce large horseshoe-shaped clusters of activation in bilateral fusiform / occipital regions (Surguladze, Radua et al. 2012). With the aim of preserving such cluster size, researchers might try to recreate the cluster with huge spheres (**Figure 8.2A** and **B**). However, this approach could result in erroneously detecting activation in the midline, as shown in **Figure 8.2C**. It must be noted that this type of spatial imprecision may be acceptable when it is the result of smaller spheres, because the distance between the real activation and the meta-analytic findings is in the range of few millimetres; in the example, however, the imprecision is in the range of a several centimetres.

In some cases, the meta-analytic researcher could manually deform the spheres displayed in **Figure 8.2B** so that they reach the specific shapes displayed in the two-dimensional published pictures (probably similar to that in **Figure 8.2A**). However, these adjustments would open the door to a high degree of subjectivity. One researcher might deform one local sphere in one direction; another researcher might prefer to deform another local sphere in the opposite direction; and so on. In other cases, no printed figures would be available to the meta-analytic researcher, for what only aprioristic knowledge about spatial covariance in the specific modality could partially help deform the spheres in the adequate directions.

Figure 8.2 Fictional example of erroneous meta-analytic localization due to the use of huge spheres to recreate huge clusters.

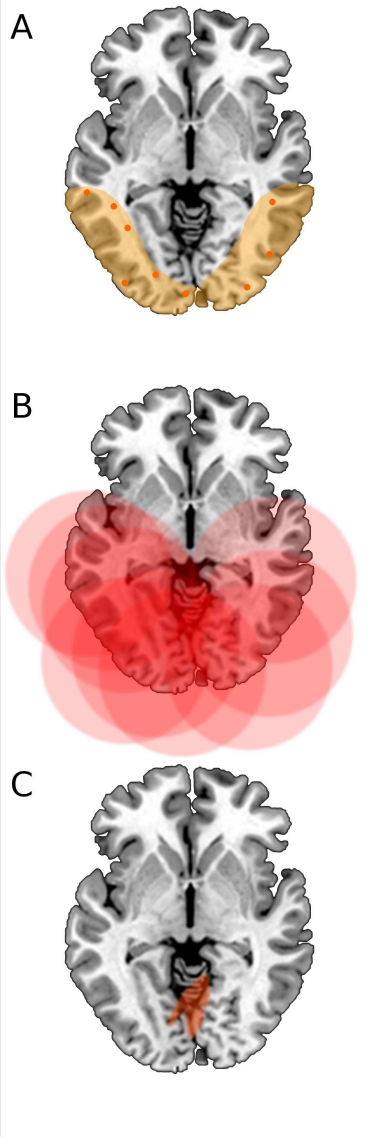

A. Localization of the horseshoe-shaped cluster of activation (pale orange area) and the reported peak coordinates in the different studies included in a meta-analysis (red orange dots).

B. Recreation of the cluster with a huge sphere for the reported peak of each study.

C. Region with higher meta-analytic activation values, which would probably reach statistical significance.

Thus, valid and objective implementation of these potential improvements may probably require a set of sophisticated algorithms which objectively combine cluster sizes, scanned two-dimensional pictures, and specific a priori modal information.

8.2.2 Correction for multiple comparisons

An unsolved issue in ES-SDM, as well as in any voxel-based analysis, is the correction for multiple comparisons.

Voxel-based neuroimaging analyses conduct a statistical test for each of their thousands of voxels, for what applying the standard threshold $P < 0.05$ without correcting for multiple comparisons would lead to a high rate of false positive findings, while conducting a standard Bonferroni correction for multiple comparisons would lead to a huge rate of false negative findings precluding the detection of any true effect.

Several approaches have been developed to deal with this issue. A simple strategy, currently recommended in ES-SDM (Radua, Mataix-Cols et al. 2012), consists in using a more stringent but fixed threshold, namely $P < 0.005$ or $P < 0.001$. Researchers use this stringent threshold with the aim to minimize the number of false positive findings, and thus counteracting the effects of multiple comparisons. However, given that this strategy does not imply a formal correction for multiple comparisons and that it is relatively liberal, results from such strategy are usually known as “uncorrected”.

Other approaches combine standard corrections for multiple comparisons with methods to alleviate their stringency, namely cluster-based statistics (Bullmore, Suckling et al. 1999; Hayasaka and Nichols 2003) and Gaussian random fields (GRF) (Worsley and Friston 1995). These approaches are much more sophisticated and usually preferred, though not free from their own issues.

In its simplest form, cluster-based statistics consist in setting a conventional threshold for the voxels (e.g. $P < 0.05$), grouping the significant voxels in clusters, and estimating the probability associated to the size of each cluster. The idea is that true effects usually involve a substantial amount of voxels and thus form large clusters, which are unlikely to appear by chance – i.e. they are considered statistically significant. Conversely, spurious false positive findings are usually in the form of small clusters, which are likely to appear and thus considered non-significant.

Unfortunately, cluster-based statistics have been found to be biased towards detecting findings in some brain regions while not detecting findings in others (Worsley, Andermann et al. 1999; Good, Johnsrude et al. 2001; Mechelli, Price et al. 2005). Some regions of the brain are large and homogeneous, implying that a large amount of voxels behave like one. In these regions, both true and false positive clusters are large and thus considered statistically significant. On the contrary, some other regions are small and independent from their neighbouring regions, so that both true and false positive clusters are small and discarded. The mask used to define the grey matter may further help the formation of large clusters in some regions while prevent it in other regions.

This issue was partially addressed with the introduction of the GRF theory (Worsley and Friston 1995), which can be applied without including the extent of the clusters (Mechelli, Price et al. 2005). However, this theory assumes the error fields are a reasonable approximation to an underlying continuous random field with a multivariate Gaussian distribution. Moreover, its combination with standard corrections for multiple comparisons such as the

FDR (Benjamini and Yekutieli 2001) has been shown to be inappropriate (Chumbley and Friston 2009).

To sum up, sophisticated methods such as cluster-based statistics and GRF are more elegant and usually preferred, but they have been progressively shown to hide a number of issues. One clear recommendation deriving from the work presented in this thesis is the importance of assessing the reliability of a meta-analysis employing a series of complementary analyses, rather than exclusively relying on any form of ultimately arbitrary p-value.

8.2.3 Further fine-tuning

Finally, there is room for fine-tuning the ES-SDM algorithms and brain templates. Future research, for instance, could aim to improve the treatment of studies with no information in a given voxel, which at the moment are just assumed to have a null effect size. This and other improvements may potentially result in an increase of the sensitivity of the method.

8.3 GENERAL RECOMMENDATIONS FOR META-ANALYTICAL RESEARCHERS

The experience gathered during the development of the methods presented in this thesis, has lead to a series of simple recommendations, which are thought to improve the researchers' confidence in the results of their meta-analyses. In any voxel-based meta-analysis of neuroimaging data, whether employing ES-SDM or any other available method, authors should aim to: 1) only include studies which explored the whole brain; 2) ensure that the same threshold throughout the whole brain was used within each included study; and 3) explore the robustness of the findings with several complementary analyses, for example, sensitivity analyses, quantification of the between-study heterogeneity, funnel plots of the values extracted from the meta-analytic clusters or their peaks, and so on, just like in any standard meta-analysis.

8.4 REFERENCES

Benjamini, Y. and D. Yekutieli (2001). "The Control of the false discovery rate in multiple testing under dependency." Ann Stats **29**(4): 1165-1188.

Borgwardt, S., J. Radua, et al. (2012). "Why are psychiatric imaging methods clinically unreliable? Conclusions and practical guidelines for authors, editors and reviewers." Behav Brain Funct **8**(1): 46.

Bullmore, E. T., J. Suckling, et al. (1999). "Global, voxel, and cluster tests, by theory and permutation, for a difference between two groups of structural MR images of the brain." IEEE Trans Med Imaging **18**(1): 32-42.

Chumbley, J. R. and K. J. Friston (2009). "False discovery rate revisited: FDR and topological inference using Gaussian random fields." Neuroimage **44**(1): 62-70.

Costafreda, S. G. (2012). "Parametric coordinate-based meta-analysis: Valid effect size meta-analysis of studies with differing statistical thresholds." J Neurosci Methods **210**(2): 291-300.

Costafreda, S. G., A. S. David, et al. (2009). "A parametric approach to voxel-based meta-analysis." Neuroimage **46**(1): 115-22.

Eickhoff, S. B., D. Bzdok, et al. (2011). "Activation likelihood estimation meta-analysis revisited." Neuroimage **59**(3): 2349-61.

Good, C. D., I. S. Johnsrude, et al. (2001). "A voxel-based morphometric study of ageing in 465 normal adult human brains." Neuroimage **14**(1 Pt 1): 21-36.

Hayasaka, S. and T. E. Nichols (2003). "Validating cluster size inference: random field and permutation methods." Neuroimage **20**(4): 2343-56.

Ioannidis, J. P. A. (2011). "Excess significance bias in the literature on brain volume abnormalities." Arch Gen Psychiatry **68**(8): 773-780.

Kempton, M. J., J. R. Geddes, et al. (2008). "Meta-analysis, database, and meta-regression of 98 structural imaging studies in bipolar disorder." Arch Gen Psychiatry **65**(9): 1017-1032.

Kempton, M. J., Z. Salvador, et al. (2011). "Structural neuroimaging studies in major depressive disorder. Meta-analysis and comparison with bipolar disorder." Arch Gen Psychiatry **68**(7): 675-690.

Laird, A. R., J. L. Lancaster, et al. (2005). "BrainMap: The social evolution of a functional neuroimaging database." Neuroinformatics **3**(1): 65-78.

Mechelli, A., C. J. Price, et al. (2005). "Voxel-based morphometry of the human brain: methods and applications." Curr Med Imag Rev **1**(2): 105-113.

Nielsen, F. A., L. K. Hansen, et al. (2004). "Mining for associations between text and brain activation in a functional neuroimaging database." Neuroinformatics **2**(4): 369-80.

Nielsen, F. A., M. J. Kempton, et al. (2012). Online open neuroimaging mass meta-analysis with a wiki. SePublica. Heraklion, Greece.

Peters, B. D., P. R. Szeszko, et al. (2012). "White Matter Development in Adolescence: Diffusion Tensor Imaging and Meta-Analytic Results." Schizophr Bull **38**: 1308-1317.

Radua, J., S. Borgwardt, et al. (2012). "Multimodal meta-analysis of structural and functional brain changes in first episode psychosis and the effects of antipsychotic medication." Neurosci Biobehav Rev **36**: 2325:2333.

Radua, J. and D. Mataix-Cols (2009). "Voxel-wise meta-analysis of grey matter changes in obsessive-compulsive disorder." Br J Psychiatry **195**(5): 391-400.

Radua, J. and D. Mataix-Cols (2010). "Heterogeneity of coordinate-based meta-analyses of neuroimaging data: an example from studies in OCD - Authors' reply." Br J Psychiatry **197**(1): 77.

Radua, J., D. Mataix-Cols, et al. (2012). "A new meta-analytic method for neuroimaging studies that combines reported peak coordinates and statistical parametric maps." Eur Psychiatry **27**: 605-611.

Radua, J., M. Romeo, et al. (2012). "A general approach for combining voxel-based meta-analyses conducted in different neuroimaging modalities." Curr Med Chem: in Press.

Radua, J., O. A. van den Heuvel, et al. (2010). "Meta-analytical comparison of voxel-based morphometry studies in obsessive-compulsive disorder vs other anxiety disorders." Arch Gen Psychiatry **67**(7): 701-711.

Radua, J., E. Via, et al. (2010). "Voxel-based meta-analysis of regional white matter volume differences in Autism Spectrum Disorder vs. healthy controls." Psychol Med **41**(7): 1539-1550.

Surguladze, S. A., J. Radua, et al. (2012). "Interaction of catechol O-methyltransferase and serotonin transporter genes modulates effective connectivity in a facial emotion-processing circuitry." Transl Psychiatry **2**: e70.

Wager, T. D., M. Lindquist, et al. (2007). "Meta-analysis of functional neuroimaging data: current and future directions." Soc Cogn Affect Neurosci **2**(2): 150-158.

Wager, T. D., K. L. Phan, et al. (2003). "Valence, gender, and lateralization of functional brain anatomy in emotion: a meta-analysis of findings from neuroimaging." Neuroimage **19**(3): 513-531.

Worsley, K. J., M. Andermann, et al. (1999). "Detecting changes in nonisotropic images." Hum Brain Mapp **8**(2-3): 98-101.

Worsley, K. J. and K. J. Friston (1995). "Analysis of fMRI time-series revisited-again." Neuroimage **2**(3): 173-181.

Yarkoni, T., R. A. Poldrack, et al. (2011). "Large-scale automated synthesis of human functional neuroimaging data." Nat Methods **8**(8): 665-70.

APPENDIX 1

The Signed Differential Mapping software

A1.1 Sample screenshots of the software

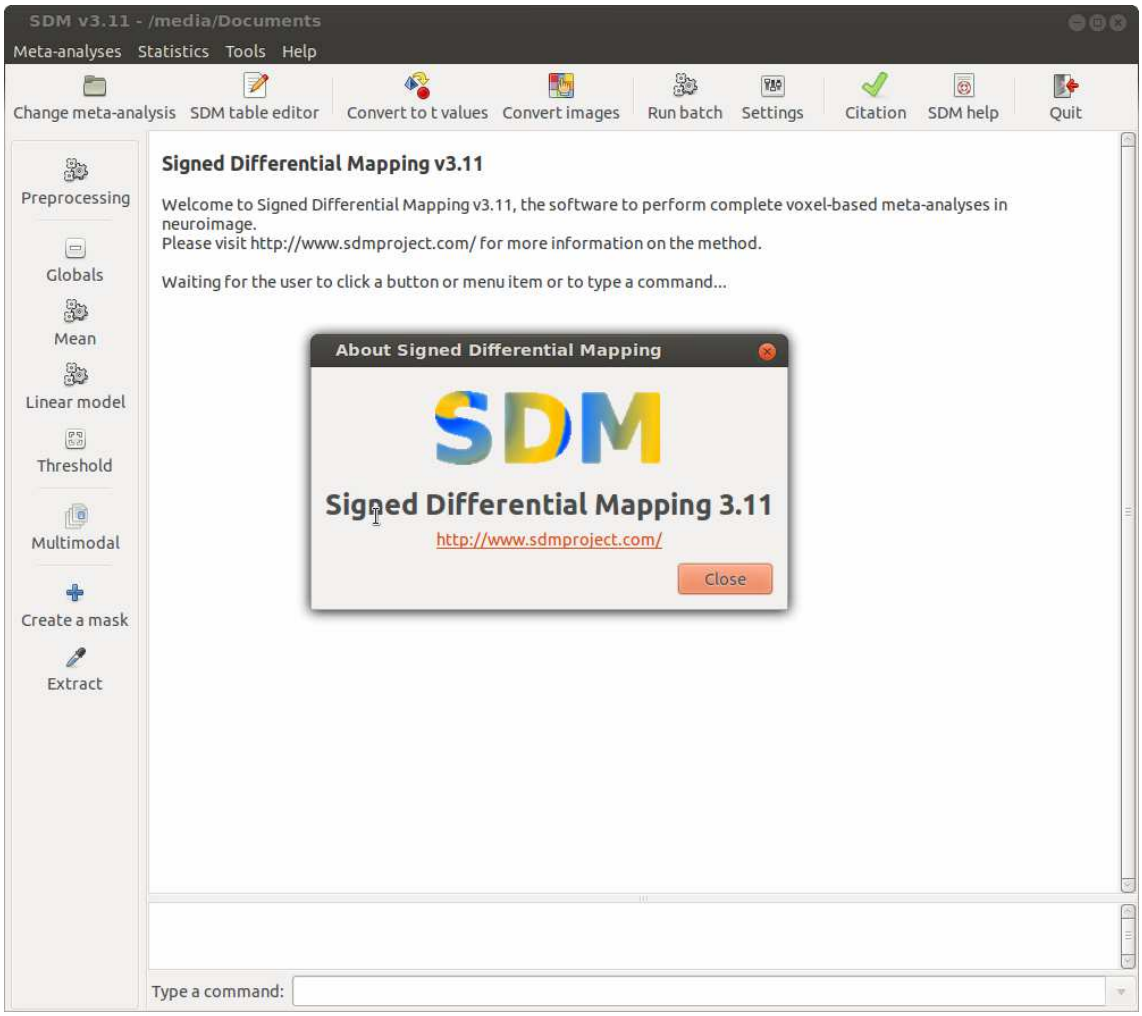

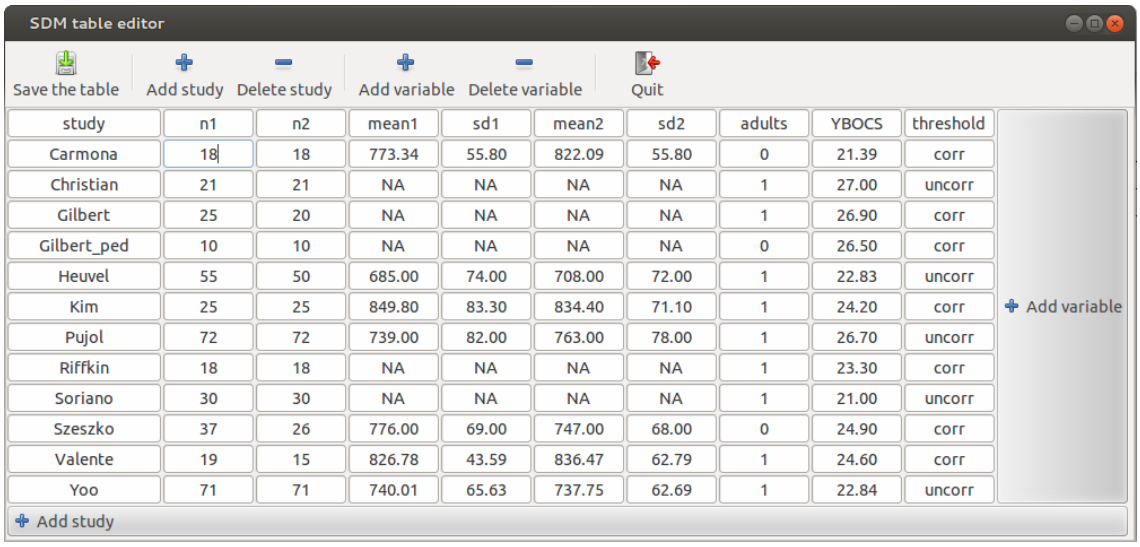

study	n1	n2	mean1	sd1	mean2	sd2	adults	YBOCS	threshold
Carmona	18	18	773.34	55.80	822.09	55.80	0	21.39	corr
Christian	21	21	NA	NA	NA	NA	1	27.00	uncorr
Gilbert	25	20	NA	NA	NA	NA	1	26.90	corr
Gilbert_ped	10	10	NA	NA	NA	NA	0	26.50	corr
Heuvel	55	50	685.00	74.00	708.00	72.00	1	22.83	uncorr
Kim	25	25	849.80	83.30	834.40	71.10	1	24.20	corr
Pujol	72	72	739.00	82.00	763.00	78.00	1	26.70	uncorr
Riffkin	18	18	NA	NA	NA	NA	1	23.30	corr
Soriano	30	30	NA	NA	NA	NA	1	21.00	uncorr
Szeszko	37	26	776.00	69.00	747.00	68.00	0	24.90	corr
Valente	19	15	826.78	43.59	836.47	62.79	1	24.60	corr
Yoo	71	71	740.01	65.63	737.75	62.69	1	22.84	uncorr

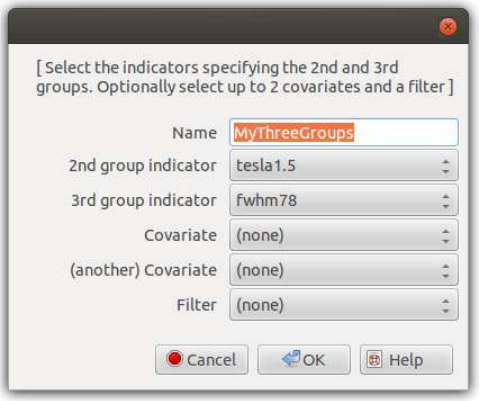

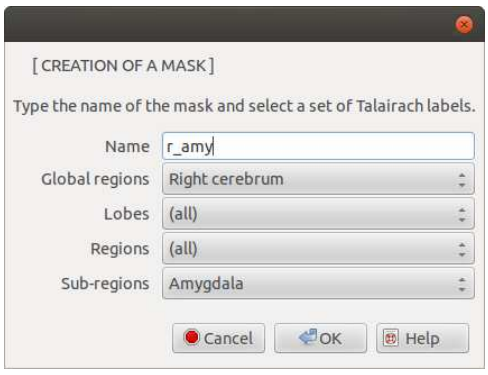

A1.2 *Effect-size* SDM Tutorial

The aim of this tutorial is to show, in a *step by step* basis, how to conduct meta-analyses using SDM software. To this end, you will perform some of the analyses conducted in: *Radua J and Mataix-Cols D. Voxel-wise meta-analysis of grey matter changes in obsessive-compulsive disorder. Br J Psychiatry 2009; 195:393-402.* Note however that these analyses will be conducted with the updated, effect-size-based algorithms (ES-SDM) described in: *Radua J et al. A new meta-analytic method for neuroimaging studies that combines reported peak coordinates and statistical parametric maps. Eur Psychiatry, in Press*. Note also that this tutorial is distributed in the hope that it will be useful, but without any warranty on the accuracy of the text and data.

A1.2.1 Before executing the software

We have invested a lot of time and effort to improve accuracy of SDM method and software. However, calculations might be biased if the following exclusion criterion for peak coordinates is not considered when conducting the searches and contacts with the authors:

> *"While different studies may employ different thresholds, you should ensure that within one study the same threshold was used throughout the whole brain*"

This is of utmost importance because it is not uncommon in neuroimaging studies that some regions (e.g. a priori regions of interest) are more liberally thresholded than the rest of the brain.

A1.2.2 Preparation of the files

Effect-size SDM allows the combination of statistical maps (in NIfTI format, obtained from e.g. SPM or FSL software) and peak coordinates (e.g. reported in the papers). For this tutorial we will only use peak coordinates, and for your convenience, their text files have been already prepared in the folder containing this PDF (if you don't find these files please download the software again from http://www.sdmproject.com/software). Take a look at the names and contents of these text files: coordinates are written in a separate text file for each study, and the filename is just a very short identification of the study (e.g. the name of the first author), plus a dot, plus the stereotactic space of the coordinates ("mni", "mni2tal", or "tal"), plus a dot, plus "txt". These are some of the sample text files:

Carmona.mni.txt
40,39,21,-5.52

Gilbert.mni.txt
-26,40,36,-5.73 6,4,72,-4.28 -48,2,36,-3.64 50,34,20,-5.17 20,26,48,-3.65

Note that each line specifies a coordinate and its *t* statistic. The coordinate is defined by the first three values (e.g. “40,39,21”), and the t statistic by the forth value (e.g. “-5.52”). Note also that the extension of these two sample files is *.mni.txt, for what these coordinates are understood to be in MNI space.

The *t* statistic is a positive number in case that represents a region where patients have more grey matter than controls (or where patients hyper-activate, or where participants activate as compared to baseline, etcetera), while a negative number in case that represents a region where patients have less grey matter than controls (or where patients hypo-activate, or where participants deactivate as compared to baseline, etcetera).

In a real meta-analysis you would have scanned the original papers of these two studies, and noted that they reported z scores instead of t statistics. However, z scores were converted to t statistics using the online converter which may be found at *http://www.sdmproject.com/utilities/?show=Statistics* (this website utility may be easily accessed by pressing the [Convert to t values] button within the SDM software).

In case that the studies had no reported any measure related to effect size (*t* statistic, *z* score, *p* value, etcetera), you should write a “p” for positive peaks (i.e. patients have more grey matter than controls) and an “n” for negative peaks (i.e. patients have less grey matter than controls). The SDM software conducts a pre-analysis to estimate the effect size of these peaks – see *Radua J et al. A new meta-analytic method for neuroimaging studies that combines*

reported peak coordinates and statistical parametric maps. Eur Psychiatry, in Press for details.

IMPORTANT: Statistical maps are preferred to any coordinate text file. In case that such images are obtained, use the [Convert images] button within the SDM software to prepare them for the analysis. Please contact us in case of questions (a contact form may be found at *http://www.sdmproject.com/*).

A1.2.3 Preparation of the SDM software

In this step you should first specify a working folder for the meta-analysis, and second create an SDM table specifying the names of the studies and their sample sizes, as well as optional variables. The latter has been already prepared for you in this tutorial.

➔ Start the SDM software:

Linux users: to start the software click a file called “sdm” in the SDM software folder. If the program does not execute follow the instructions to change file permissions which may be found at http://www.sdmproject.com/software/?show=Linux

Windows users: to start the software click a file called “sdm.exe” in the SDM software folder. If you don't find this file, look for a file called “sdm” whose icon is a green brain.

One or two red warnings might be printed in the screen if you haven’t used this software before: one complaining about the working folder, and another complaining about the MRIcron program.

➔ To specify the working folder for the meta-analysis, click the button [Change folder / meta-analysis] button, look for the folder containing this PDF, and click [Open].

A dialog similar to the following one should appear:

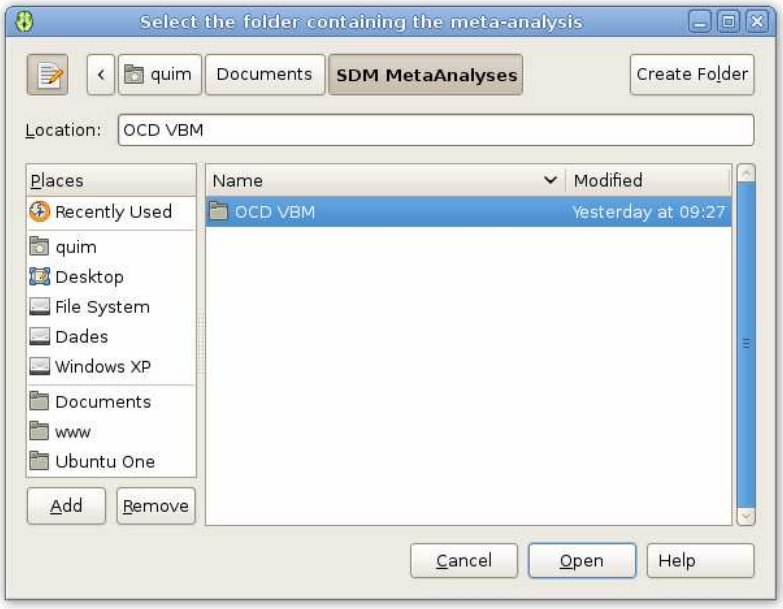

➔ If SDM software did not found MRIcron (or FSLView) program, you can manually specify its location by clicking the [Tools] menu, clicking [Settings], clicking the selection box at the right of [Brain viewer folder], selecting [Other…], looking for the folder which contains the MRIcron or FSLView program (typically something like “C:\Program Files\MRIcroN” in Windows), clicking [Open], and clicking [OK].

A dialog similar to the following one should appear:

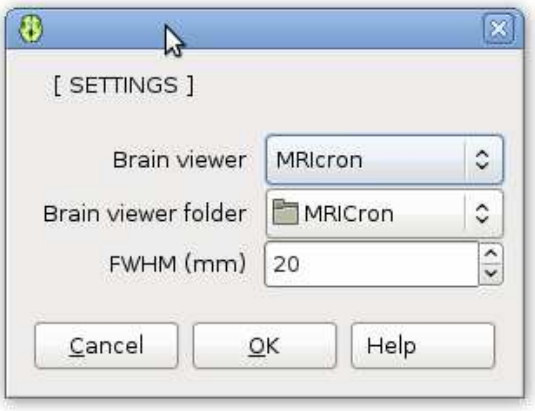

➔ To create or edit the SDM table, click the button [SDM table editor] button.

A window similar to the following one should appear:

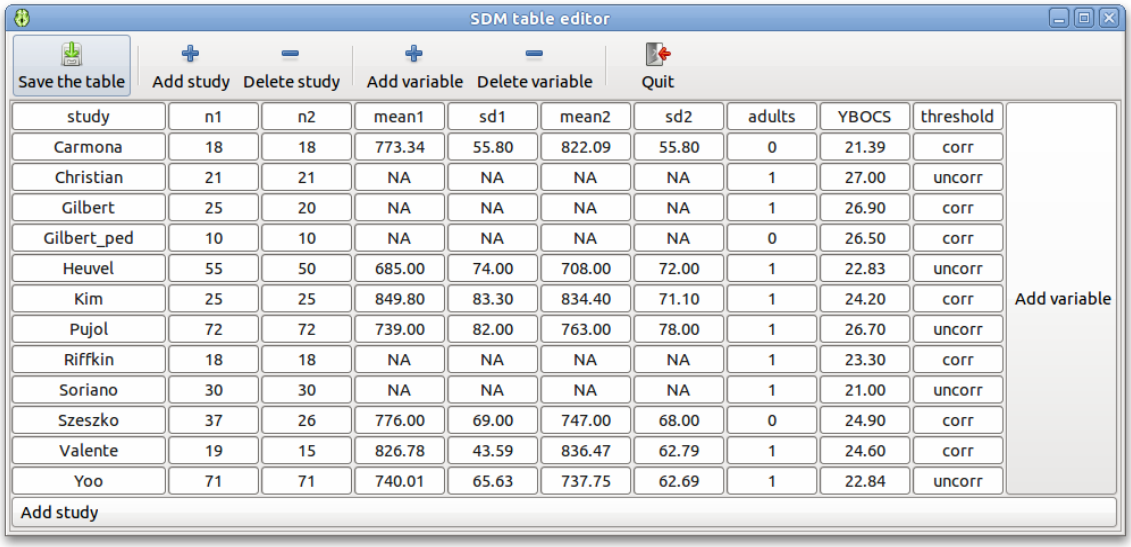

study	n1	n2	mean1	sd1	mean2	sd2	adults	YBOCS	threshold
Carmona	18	18	773.34	55.80	822.09	55.80	0	21.39	corr
Christian	21	21	NA	NA	NA	NA	1	27.00	uncorr
Gilbert	25	20	NA	NA	NA	NA	1	26.90	corr
Gilbert_ped	10	10	NA	NA	NA	NA	0	26.50	corr
Heuvel	55	50	685.00	74.00	708.00	72.00	1	22.83	uncorr
Kim	25	25	849.80	83.30	834.40	71.10	1	24.20	corr
Pujol	72	72	739.00	82.00	763.00	78.00	1	26.70	uncorr
Riffkin	18	18	NA	NA	NA	NA	1	23.30	corr
Soriano	30	30	NA	NA	NA	NA	1	21.00	uncorr
Szeszko	37	26	776.00	69.00	747.00	68.00	0	24.90	corr
Valente	19	15	826.78	43.59	836.47	62.79	1	24.60	corr
Yoo	71	71	740.01	65.63	737.75	62.69	1	22.84	uncorr

Each row in the SDM table specifies one study. In this example, the first column sets the identification of the study (exactly the same than in the text files), the second column specifies the size of the patients' sample ("n1"), the third column the size of the controls' sample ("n2"), the 4^{th}-7^{th} columns optional global grey matter values, the 8^{th}-9^{th} columns optional variables, and the 10^{th} column a special optional variable called "threshold", which may be used to specify the threshold type (e.g. "uncorrected" vs "corrected") used in each study.

A1.2.4 “Globals” analysis

Prior to the voxel-based meta-analysis, you will conduct an analysis of the global grey matter volumes. To this end, the following variables must be defined in the SDM table: “n1” and “n2” (sample size of the patients’ and the controls’ groups), “mean1” and “mean2” (global grey matter means), and “sd1” and “sd2” (global grey matter standard deviations).

➔ To conduct the “globals” analysis, click the button [Globals], and click [OK] twice.

A dialog similar to the following one should appear:

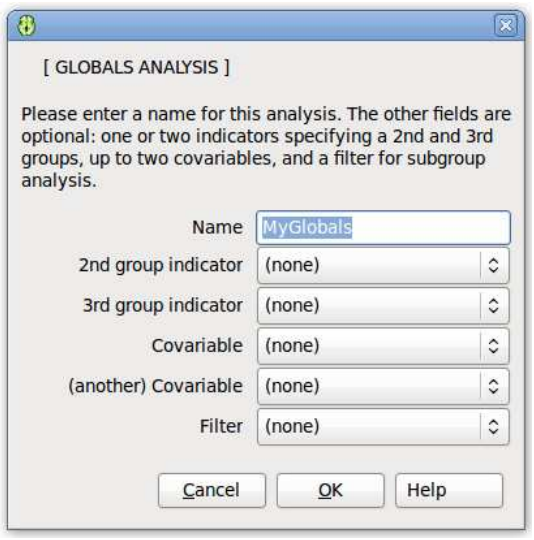

This will create and automatically open a web-like file called “globals_MyGlobals.htm” with many standard meta-analytic measures for global grey matter. The most important are the mean (Hedge’s δ along with its

corresponding Z and *P* values and the confidence interval) and the analysis of heterogeneity (τ and its corresponding Q and *P* values).

Note that you could have selected indicators for subgroup comparisons, covariates, and a filter for subgroup analysis. If one variable is selected, the program will create a coefficient called “0” which estimates the global grey matter volume at the minimum value of the variable, a coefficient called “1” which estimates the global grey matter volume at the maximum value of the variable, and a coefficient called “1m0” which estimates the difference in global grey matter volume between the maximum and the minimum values of the variable. If two variables are selected, “10” means the maximum value of the first variable and the minimum of the second, while “01” means the minimum value of the first variable and the maximum of the second. In this case, the two-variable Q statistic is also computed, with a meaning similar to the F of an ANOVA.

A1.2.5 Pre-processing

In this step SDM will use the coordinates’ text files to recreate the effect-size brain maps of the original studies. Voxels from these brain maps will be then randomly permuted to create Monte Carlo brain maps, useful for estimating the null distributions of the subsequent analyses.

➔ To pre-process the studies, click the button [Preprocessing], select the [VBM - gray matter] template, and click [OK].

A dialog similar to the following one should appear:

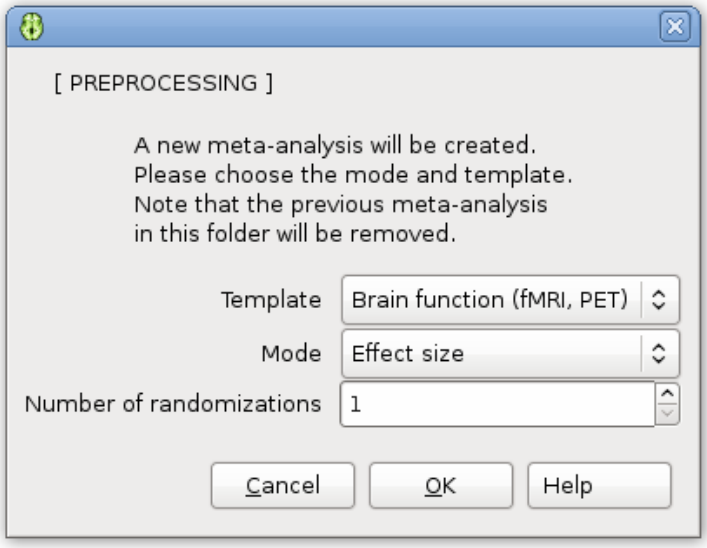

This will create a system file called “sdm_main.sdm” which contains the maps of the studies, a system file called “sdm_nd.sdm” which contains the null distributions of subsequent analyses, and a set of “sdm_r*.sdm” system files which contain the Monte Carlo maps. Notice that you specified only 1 randomization, but in a real meta-analysis several randomizations are recommended.

For checking purposes, this procedure will also create a set of “pp_*.nii.gz” NIfTI files which contain the recreated maps, and a web-like file called “pp.htm” which will be automatically opened. You should check that the absolute maximum and minimum peaks reported in the summary of “pp.htm”

approximately correspond to those reported in the original manuscripts. Pay special attention to check the side (left vs. right).

Note: It is highly recommended to use the new effect-size SDM algorithms. In case that you wish to use the original SDM algorithms you should indicate so by selecting the [Original, old method] mode in the preprocessing dialog.

A1.2.6 Mean analysis

Now it's time to conduct the mean analysis, which is usually the main outcome of a meta-analysis. In this tutorial, the mean analysis represents the weighted mean differences in regional grey matter between patients with OCD and healthy controls.

➔ To conduct the mean analysis, click the button [Mean], specify a name for this analysis (we will call it “mean”) and click [OK].

A dialog similar to the following one should appear:

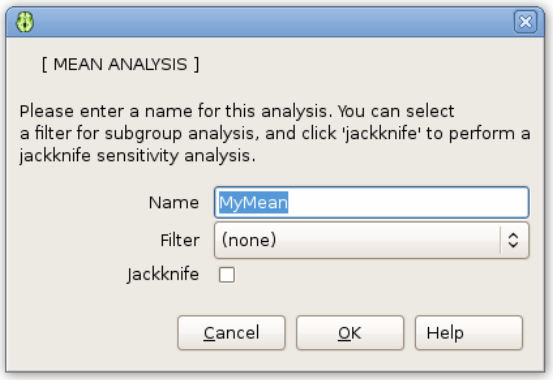

This will create the mean and the between-study heterogeneity (QH) maps within the “sdm_main.sdm” file, the null distribution for these maps within the “sdm_nd.sdm” file, and new web-like files called “mean_z.htm” and “mean_QH_z.htm” with the statistical thresholds obtained after calculating the mean and the heterogeneity in each set of Monte Carlo maps.

➔ To threshold and see the results, click the button [Threshold], click [OK], select the “mean_z” map, and click [OK].

A dialog similar to the following one should appear:

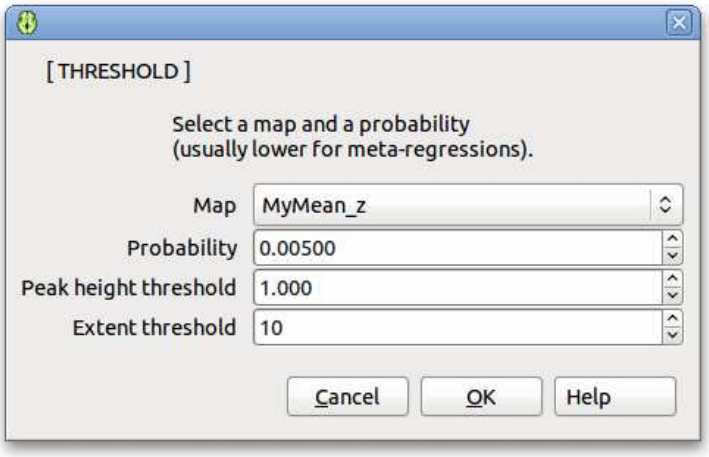

This will create and automatically open a web-like file called something like “mean_z_p0.00500_1.000_10.htm” with many statistics, coordinates and brain regional breakdowns, and will also start the MRIcron or FSLView program to visually inspect them. The following images will be also created:

- mean_p0.00500_pos.nii.gz (a NIfTI file of positive statistically significant differences)
- mean_p0.00500_pos_p.nii.gz (a NIfTI file of the p-values of the positive differences)
- mean_p0.00500_pos_logp.nii.gz (a NIfTI file of the minus log10 p-values of the positive differences)

- mean_p0.00500_neg.nii.gz (a NIfTI file of negative statistically significant differences).

- mean_p0.00500_neg_p.nii.gz (a NIfTI file of the p-values of the negative differences)

- mean_p0.00500_neg_logp.nii.gz (a NIfTI file of the minus log10 p-values of the negative differences)

Important: Please notice that the *p* values of SDM *z* scores have been found using randomizations, and they are usually much different from the *p* values associated to standard *z* scores!

A1.2.7 Visual inspection of heterogeneity

The new effect-size SDM algorithms allow a visual inspection of the brain regions with more inter-study heterogeneity. To obtain a map of the heterogeneity (in which Q_H statistics have been converted into *z* scores), click the button [Threshold], click [OK], and select the "mean_QH_z" map.

This map should be only taken for guidance, e.g. to know which brain regions are more heterogeneous. Its exact values, however, should be taken with caution as the recreation of maps from peak coordinates might result in highly inflated statistics.

Important: It is strongly recommended to extract values from relevant peaks (see later), and inspect their funnel plots with Excel, R or any other program that you use for standard meta-analyses. Note however that studies with null *z* scores (i.e. because no peak coordinates were reported in the proximity of the voxel) will all be in a straight line, thus creating "artificially ugly" plots!

A1.2.8 Subgroup analysis of adult samples

This is similar to the mean analysis, with the exception that you will specify the "adults" filter in order that only studies with adult samples are included in the analysis.

➔ To conduct the subgroup analysis, click the button [Mean], specify a name for this analysis (we will call it "adults"), select the "adults" filter, and click [OK].

➔ To threshold and see the results, click the button [Threshold], click [OK], select the "adults_z" map, and click [OK].

Tip: Please notice that you will be able to threshold any time any result from previous analyses, you do not have to conduct the calculations again!

A1.2.9 Jackknife sensitivity analysis

This is again similar to the mean analysis, with the exception that you will select the “Jackknife” option.

➔ To conduct the jackknife analysis, click the button [Mean] button, specify a name for this analysis (we will call it “mean” again), select the “Jackknife” option, and click [OK].

A dialog similar to the following one should appear:

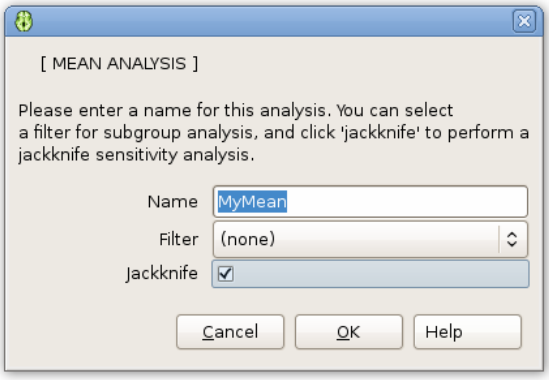

The software will repeat the mean analysis several times, including each time all the studies but one. The names of the resulting maps will be “mean”, plus “JK”, plus the name of the discarded study. E.g. the analysis including all the studies but “Carmona” will be called “meanJKCarmona”.

➔ To threshold and see the results, click the [Threshold] button, click [OK], select one of the maps (e.g. “meanJKCarmona_z”), and click [OK].

A1.2.10 Meta-regression by YBOCS

The last analysis will be a weighted regression of voxel values across the studies by the YBOCS of the corresponding patients’ samples.

➔ To conduct the regression analysis, click the button [Linear model], select [Meta-regression] and click [OK], specify a name for this analysis (e.g. “ybocs”), select “YBOCS” as the regressor, and click [OK].

A dialog similar to the following one should appear:

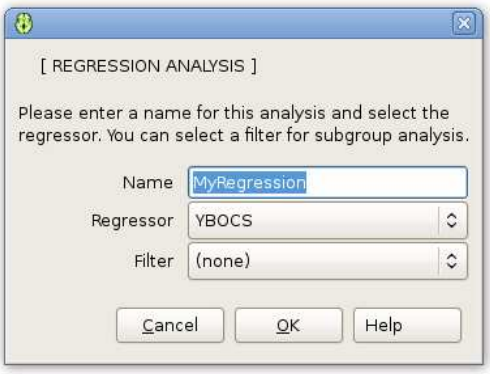

This will create three maps: “ybocs_1” (differences between patients with maximum YBOCS and healthy controls), “ybocs_0” (differences between patients with minimum YBOCS and healthy controls), and “ybocs_1m0”

(differences between patients with maximum YBOCS and patients with minimum YBOCS).

➔ To threshold and see the results, click the button [Threshold] button, click [OK], select one of the analyses (e.g. “ybocs_1_z”), specify a conservative probability, and click [OK].

Please remember that statistical significance of these meta-regressions should be taken with caution.

A1.2.11 Extraction of values

Extraction of values is useful for creating graphics such as funnel or meta-regression plots with Microsoft Excel, R or similar software, either for creating a figure for the publication, or for visually inspecting the heterogeneity or publication bias. You should first create a mask which includes the voxel or region from where you want to extract the values, and then extract these values using the mask. In this tutorial you will extract values from the voxel (20,14,0), located in right lentiform nucleus.

a) Creation of the mask

- To create the mask, click the [Create a mask] button, click [OK], specify a name for the mask (e.g. “rLentif”), type the coordinate (X = 20, Y = 14, Z = 0), and click [OK].

A dialog similar to the following one should appear:

This will create a file called “mask_rLentif.sdm” which contains the mask. Note that you can copy this file to the folder of another meta-analysis in order to avoid creating it again.

b) Extraction of values

- To extract the values using this mask, click the [Extract] button, select "rLentif", and click [Open].

A dialog similar to the following one should appear:

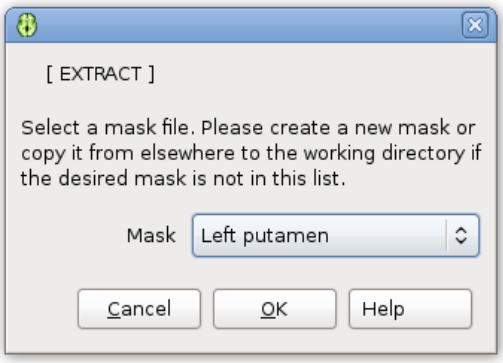

This will create and automatically open a web-like file called "extract_rLentif.htm" with the grey matter values of each map in this voxel.

APPENDIX 2

The Signed Differential Mapping project website

A2.1 Screenshot of the home page

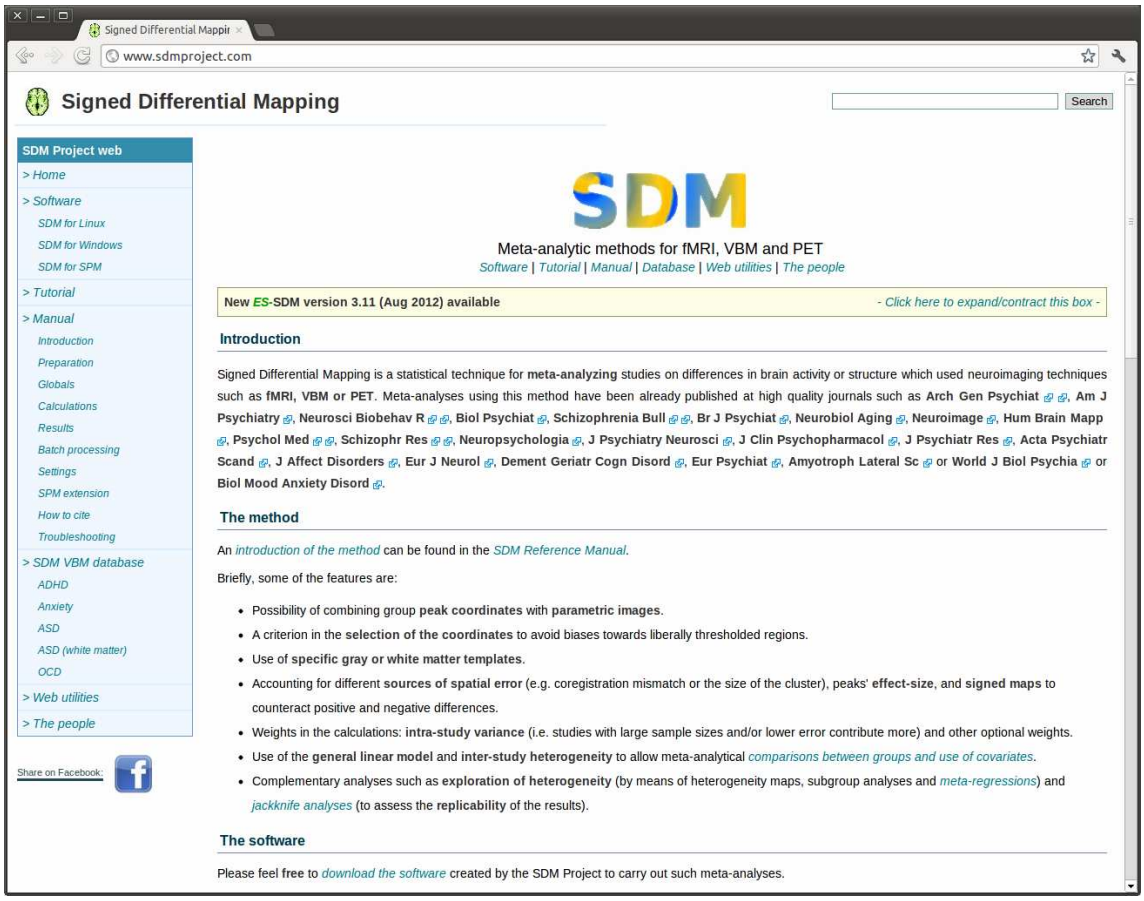

A2.2 Screenshots of the software downloads

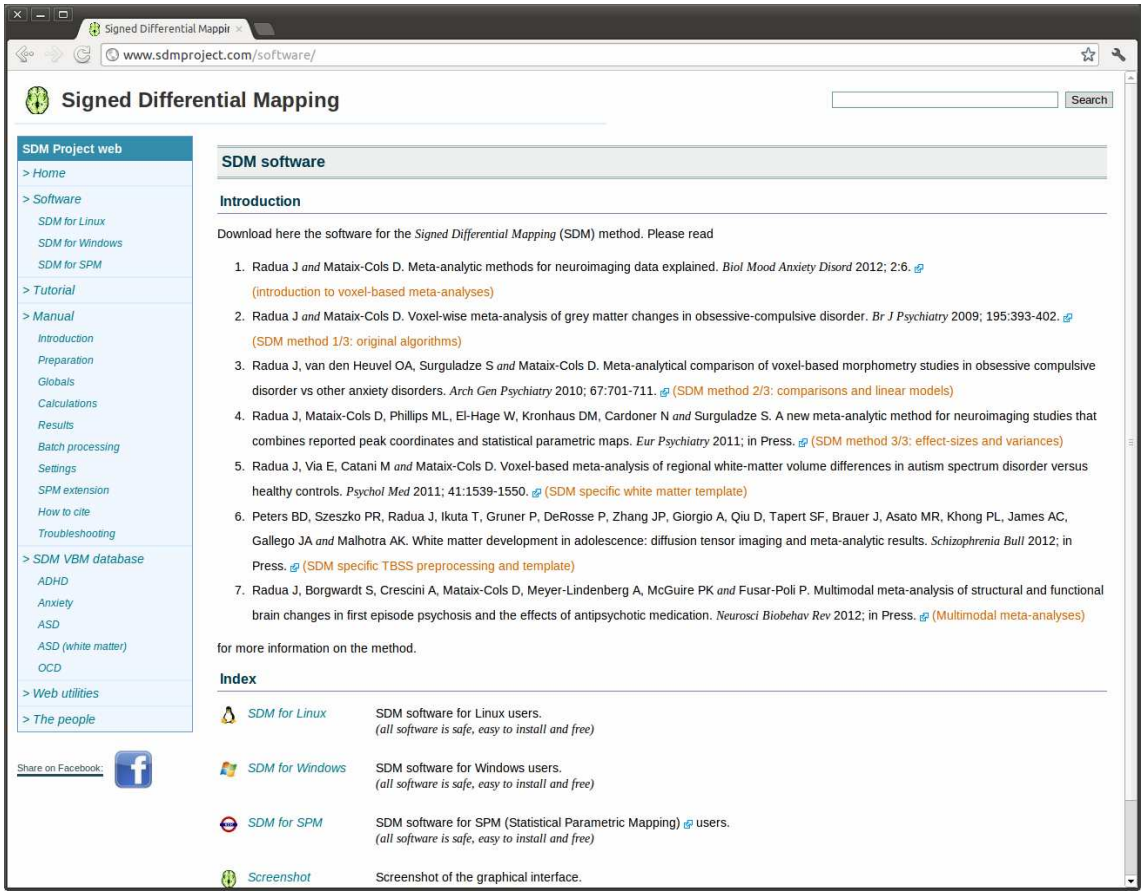

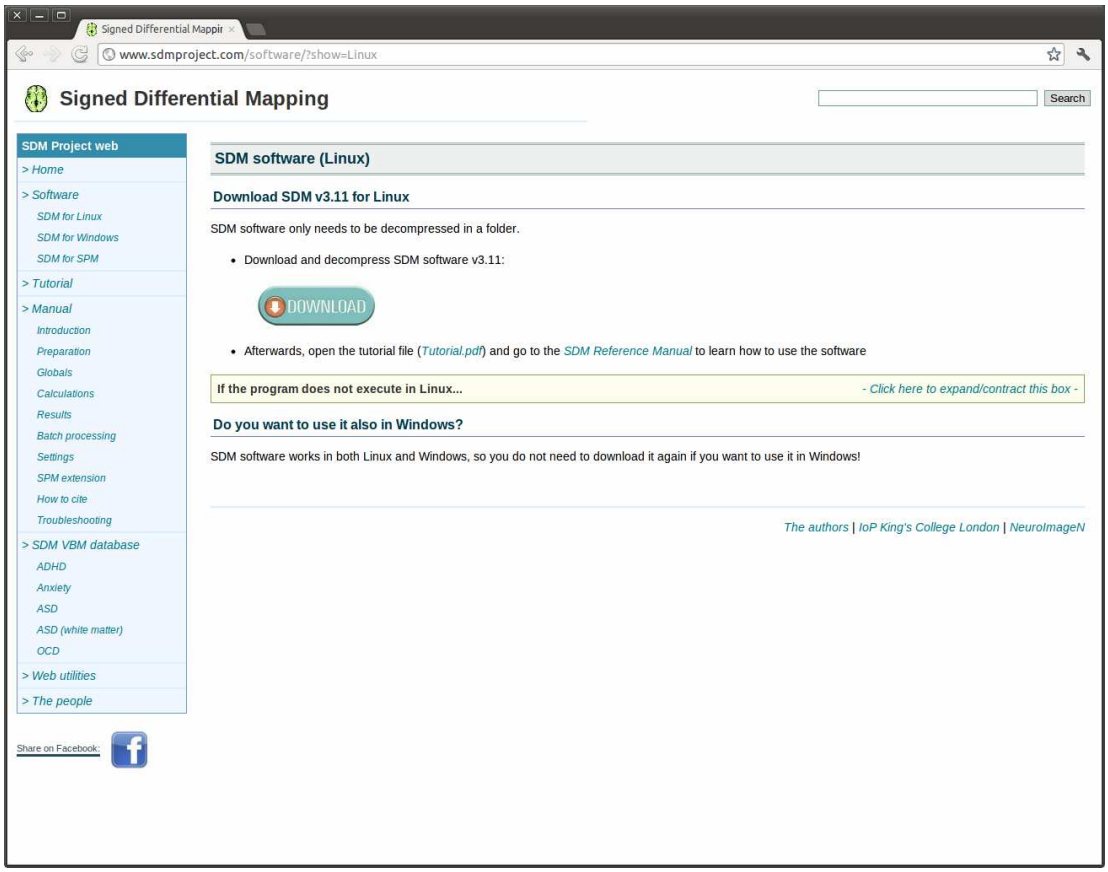
Signed Differential Mappir
www.sdmproject.com/software/?show=Linux
Signed Differential Mapping
Search
SDM Project web
> Home
> Software
SDM for Linux
SDM for Windows
SDM for SPM
> Tutorial
> Manual
Introduction
Preparation
Globals
Calculations
Results
Batch processing
Settings
SPM extension
How to cite
Troubleshooting
> SDM VBM database
ADHD
Anxiety
ASD
ASD (white matter)
OCD
> Web utilities
> The people
Share on Facebook:
SDM software (Linux)
Download SDM v3.11 for Linux
SDM software only needs to be decompressed in a folder.
Download and decompress SDM software v3.11:
DOWNLOAD
Afterwards, open the tutorial file (Tutorial.pdf) and go to the SDM Reference Manual to learn how to use the software
If the program does not execute in Linux...
- Click here to expand/contract this box -
Do you want to use it also in Windows?
SDM software works in both Linux and Windows, so you do not need to download it again if you want to use it in Windows!
The authors | IoP King's College London | NeuroImageN

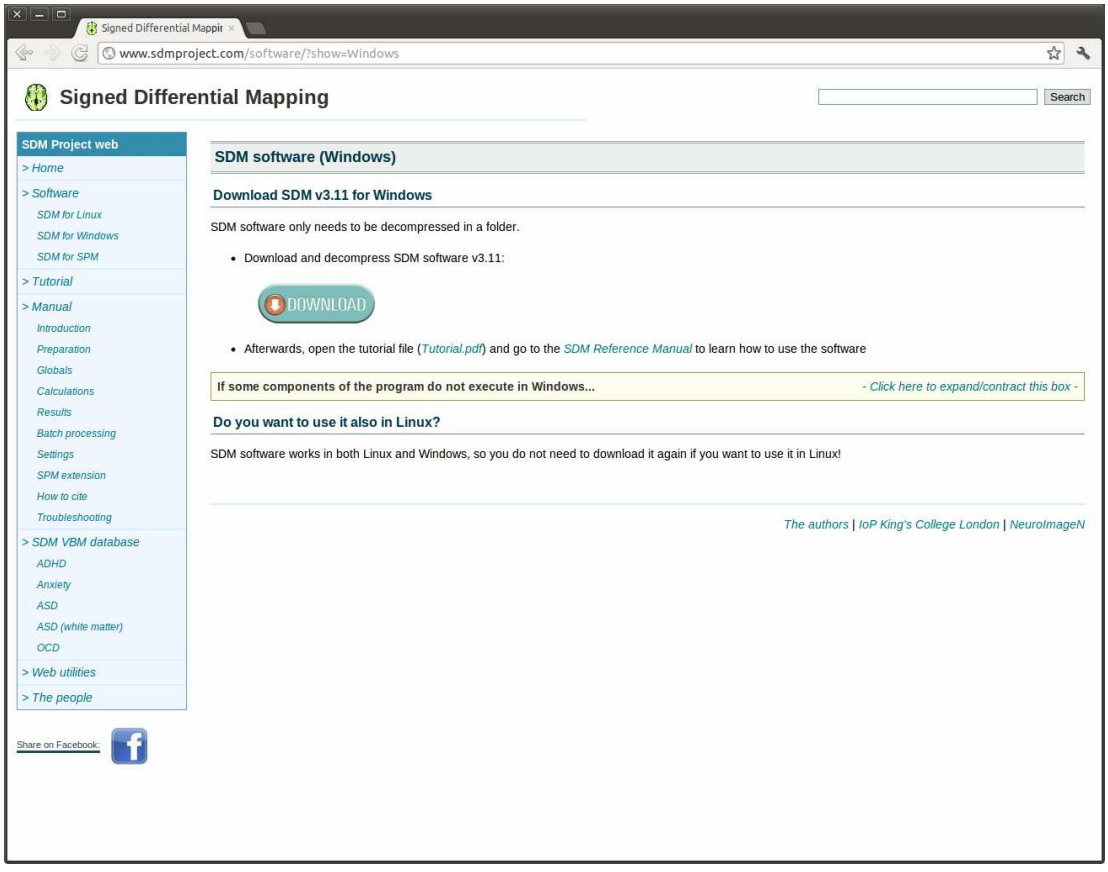
Signed Differential Mappir
www.sdmproject.com/software/?show=Windows
Signed Differential Mapping
Search
SDM Project web
> Home
> Software
SDM for Linux
SDM for Windows
SDM for SPM
> Tutorial
> Manual
Introduction
Preparation
Globals
Calculations
Results
Batch processing
Settings
SPM extension
How to cite
Troubleshooting
> SDM VBM database
ADHD
Anxiety
ASD
ASD (white matter)
OCD
> Web utilities
> The people
Share on Facebook:
SDM software (Windows)
Download SDM v3.11 for Windows
SDM software only needs to be decompressed in a folder.
Download and decompress SDM software v3.11:
DOWNLOAD
Afterwards, open the tutorial file (Tutorial.pdf) and go to the SDM Reference Manual to learn how to use the software
If some components of the program do not execute in Windows...
- Click here to expand/contract this box -
Do you want to use it also in Linux?
SDM software works in both Linux and Windows, so you do not need to download it again if you want to use it in Linux!
The authors | IoP King's College London | NeuroImageN

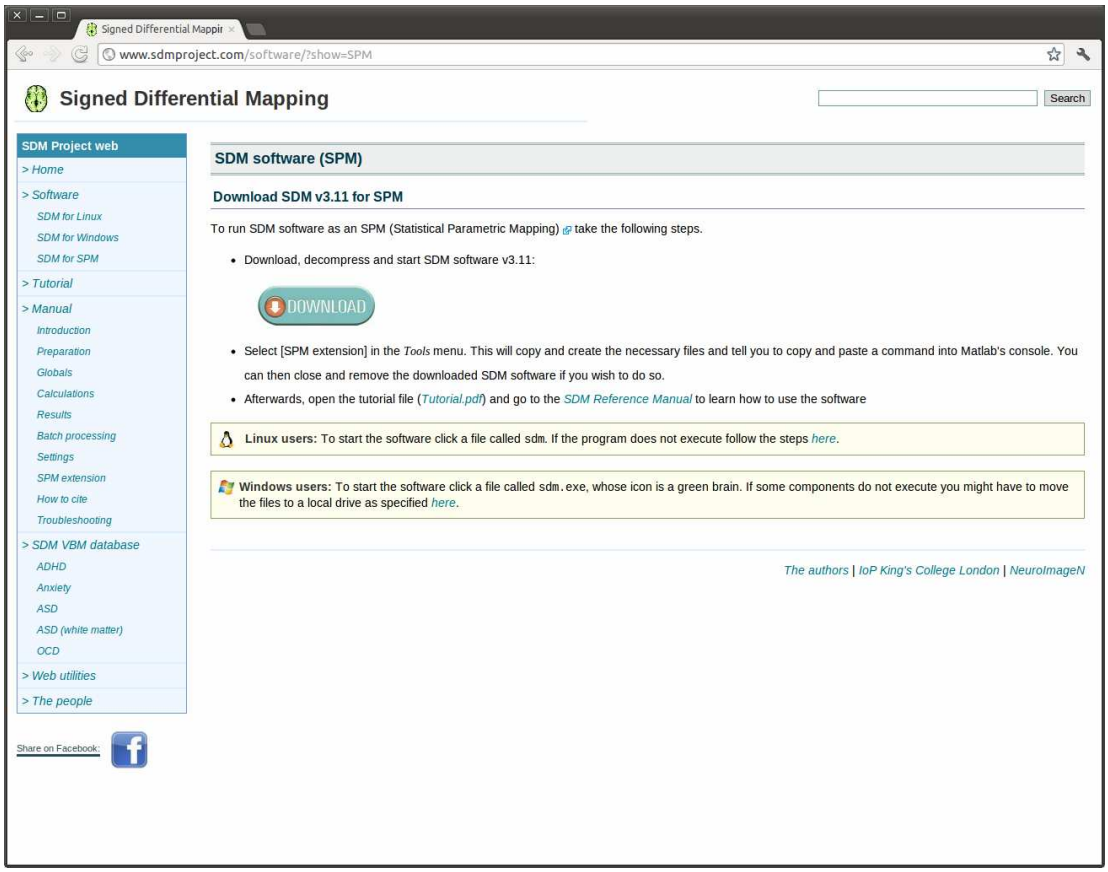
Signed Differential Mappir
www.sdmproject.com/software/?show=SPM
Signed Differential Mapping
Search
SDM Project web
> Home
> Software
SDM for Linux
SDM for Windows
SDM for SPM
> Tutorial
> Manual
Introduction
Preparation
Globals
Calculations
Results
Batch processing
Settings
SPM extension
How to cite
Troubleshooting
> SDM VBM database
ADHD
Anxiety
ASD
ASD (white matter)
OCD
> Web utilities
> The people
Share on Facebook:
SDM software (SPM)
Download SDM v3.11 for SPM
To run SDM software as an SPM (Statistical Parametric Mapping) take the following steps.
Download, decompress and start SDM software v3.11:
DOWNLOAD
Select [SPM extension] in the Tools menu. This will copy and create the necessary files and tell you to copy and paste a command into Matlab's console. You can then close and remove the downloaded SDM software if you wish to do so.
Afterwards, open the tutorial file (Tutorial.pdf) and go to the SDM Reference Manual to learn how to use the software
Linux users: To start the software click a file called sdm. If the program does not execute follow the steps here.
Windows users: To start the software click a file called sdm.exe, whose icon is a green brain. If some components do not execute you might have to move the files to a local drive as specified here.
The authors | IoP King's College London | NeuroImageN

A2.3 Screenshots of the manual

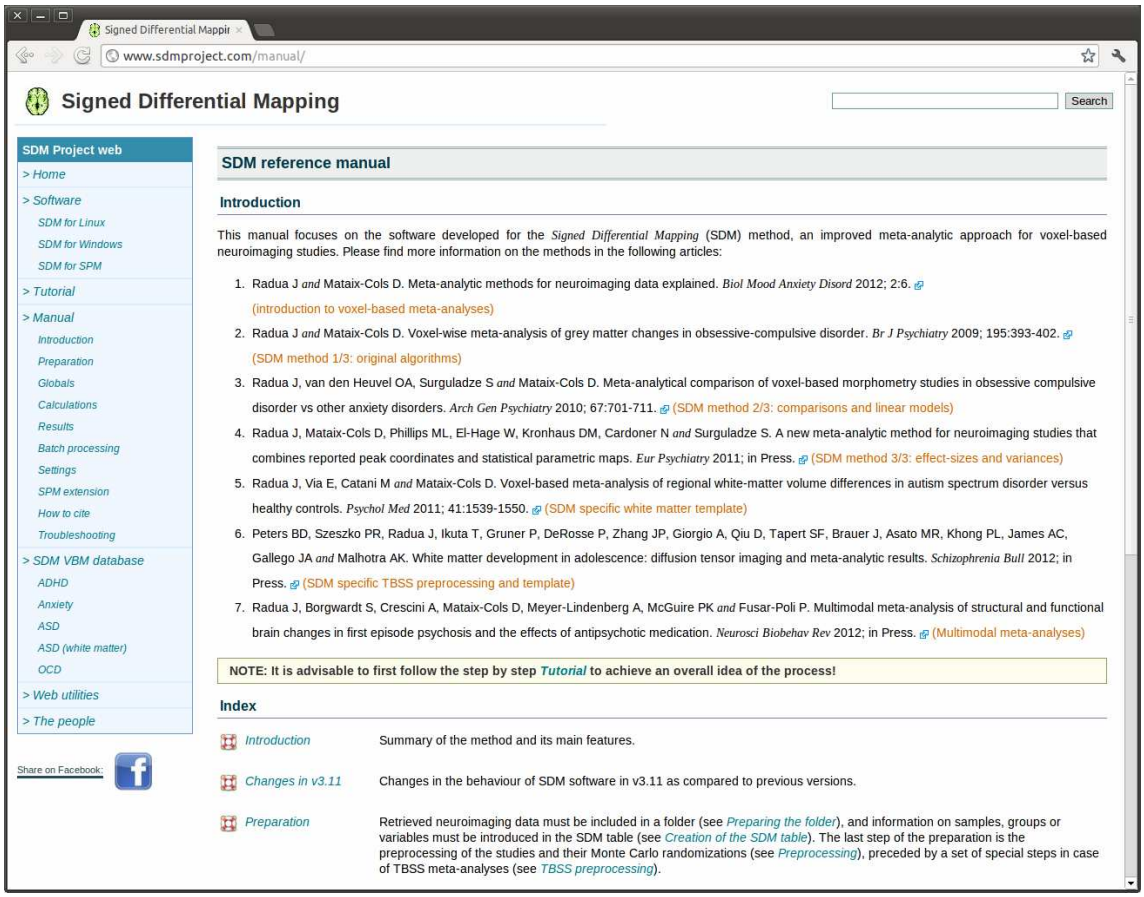

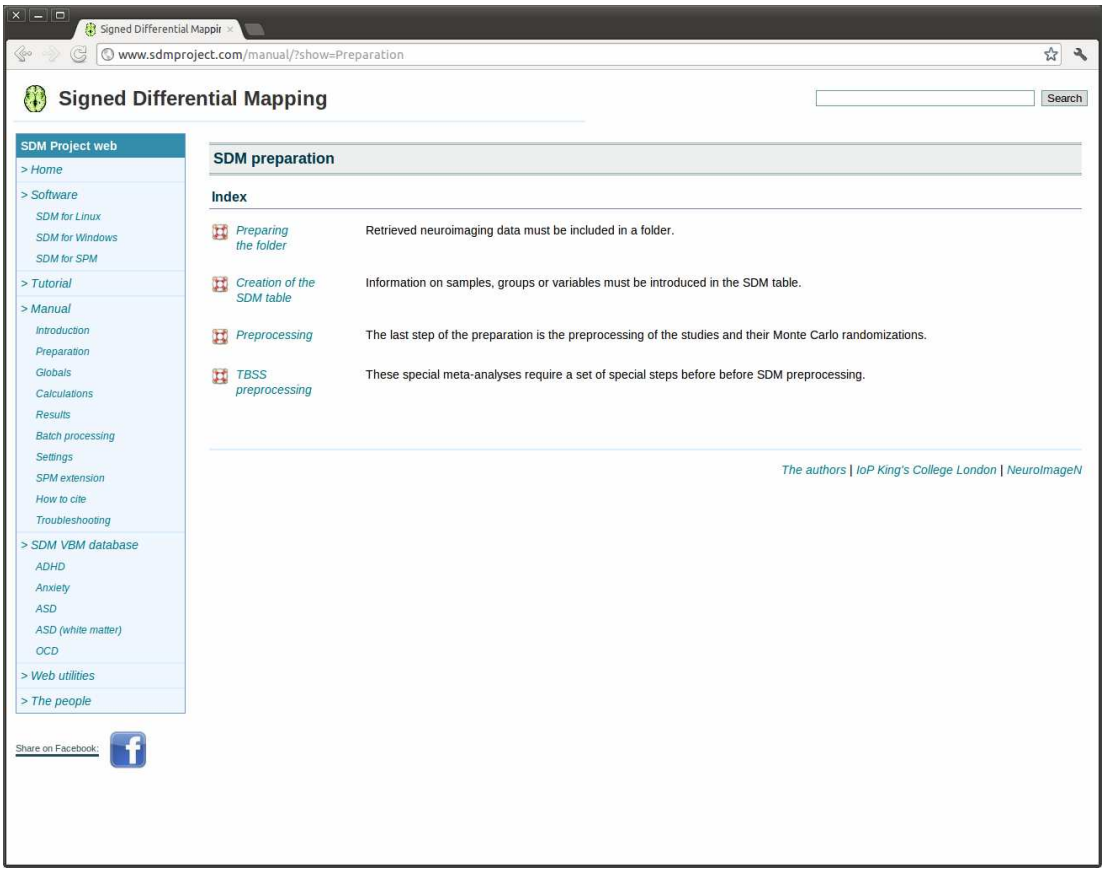
Signed Differential Mappir
www.sdmproject.com/manual/?show=Preparation
Signed Differential Mapping
Search
SDM Project web
> Home
> Software
SDM for Linux
SDM for Windows
SDM for SPM
> Tutorial
> Manual
Introduction
Preparation
Globals
Calculations
Results
Batch processing
Settings
SPM extension
How to cite
Troubleshooting
> SDM VBM database
ADHD
Anxiety
ASD
ASD (white matter)
OCD
> Web utilities
> The people
Share on Facebook:
SDM preparation
Index
Preparing the folder
Retrieved neuroimaging data must be included in a folder.
Creation of the SDM table
Information on samples, groups or variables must be introduced in the SDM table.
Preprocessing
The last step of the preparation is the preprocessing of the studies and their Monte Carlo randomizations.
TBSS preprocessing
These special meta-analyses require a set of special steps before before SDM preprocessing.
The authors | IoP King's College London | NeuroImageN

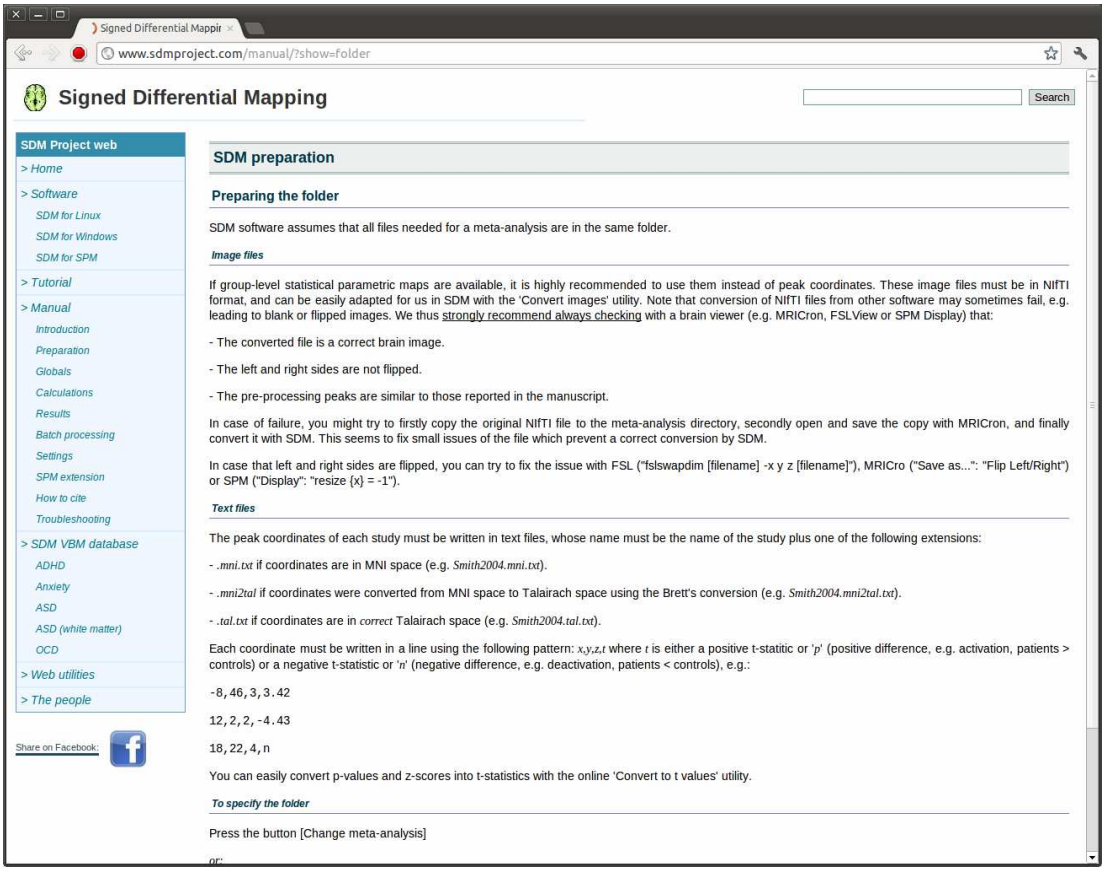
Signed Differential Mappir
www.sdmproject.com/manual/?show=folder
Signed Differential Mapping
Search
SDM Project web
> Home
> Software
SDM for Linux
SDM for Windows
SDM for SPM
> Tutorial
> Manual
Introduction
Preparation
Globals
Calculations
Results
Batch processing
Settings
SPM extension
How to cite
Troubleshooting
> SDM VBM database
ADHD
Anxiety
ASD
ASD (white matter)
OCD
> Web utilities
> The people
Share on Facebook:
SDM preparation
Preparing the folder
SDM software assumes that all files needed for a meta-analysis are in the same folder.
Image files
If group-level statistical parametric maps are available, it is highly recommended to use them instead of peak coordinates. These image files must be in NIfTI format, and can be easily adapted for us in SDM with the 'Convert images' utility. Note that conversion of NIfTI files from other software may sometimes fail, e.g. leading to blank or flipped images. We thus strongly recommend always checking with a brain viewer (e.g. MRICron, FSLView or SPM Display) that:
- The converted file is a correct brain image.
- The left and right sides are not flipped.
- The pre-processing peaks are similar to those reported in the manuscript.
In case of failure, you might try to firstly copy the original NIfTI file to the meta-analysis directory, secondly open and save the copy with MRICron, and finally convert it with SDM. This seems to fix small issues of the file which prevent a correct conversion by SDM.
In case that left and right sides are flipped, you can try to fix the issue with FSL ("fslswapdim [filename] -x y z [filename]"), MRICro ("Save as...": "Flip Left/Right") or SPM ("Display": "resize {x} = -1").
Text files
The peak coordinates of each study must be written in text files, whose name must be the name of the study plus one of the following extensions:
- .mni.txt if coordinates are in MNI space (e.g. Smith2004.mni.txt).
- .mni2tal if coordinates were converted from MNI space to Talairach space using the Brett's conversion (e.g. Smith2004.mni2tal.txt).
- .tal.txt if coordinates are in correct Talairach space (e.g. Smith2004.tal.txt).
Each coordinate must be written in a line using the following pattern: x,y,z,t where t is either a positive t-statitic or 'p' (positive difference, e.g. activation, patients > controls) or a negative t-statistic or 'n' (negative difference, e.g. deactivation, patients < controls), e.g.:
-8,46,3,3.42
12,2,2,-4.43
18,22,4,n
You can easily convert p-values and z-scores into t-statistics with the online 'Convert to t values' utility.
To specify the folder
Press the button [Change meta-analysis]
or:

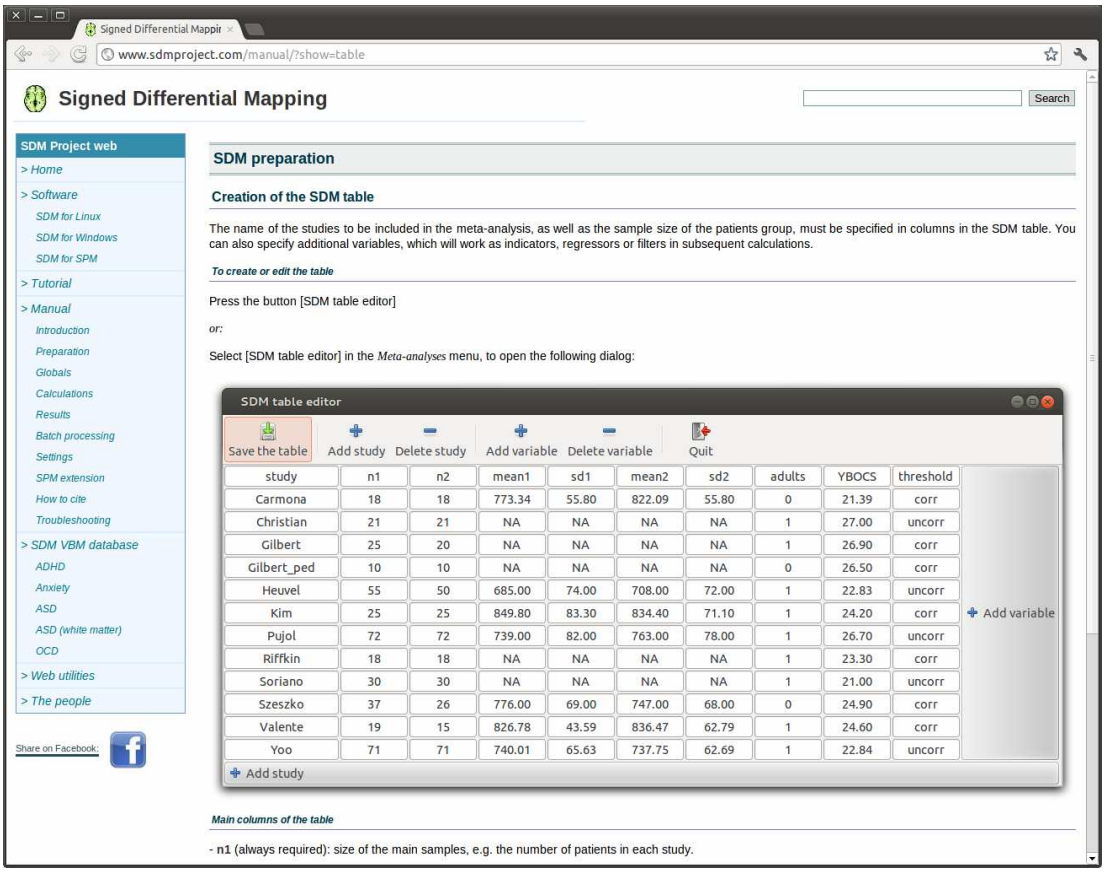
Signed Differential Mappir
www.sdmproject.com/manual/?show=table
Signed Differential Mapping
Search
SDM Project web
> Home
> Software
SDM for Linux
SDM for Windows
SDM for SPM
> Tutorial
> Manual
Introduction
Preparation
Globals
Calculations
Results
Batch processing
Settings
SPM extension
How to cite
Troubleshooting
> SDM VBM database
ADHD
Anxiety
ASD
ASD (white matter)
OCD
> Web utilities
> The people
Share on Facebook:
SDM preparation
Creation of the SDM table
The name of the studies to be included in the meta-analysis, as well as the sample size of the patients group, must be specified in columns in the SDM table. You can also specify additional variables, which will work as indicators, regressors or filters in subsequent calculations.
To create or edit the table
Press the button [SDM table editor]
or:
Select [SDM table editor] in the Meta-analyses menu, to open the following dialog:
SDM table editor
Save the table
Add study
Delete study
Add variable
Delete variable
Quit
study n1 n2 mean1 sd1 mean2 sd2 adults YBOCS threshold
Carmona 18 18 773.34 55.80 822.09 55.80 0 21.39 corr
Christian 21 21 NA NA NA NA 1 27.00 uncorr
Gilbert 25 20 NA NA NA NA 1 26.90 corr
Gilbert_ped 10 10 NA NA NA NA 0 26.50 corr
Heuvel 55 50 685.00 74.00 708.00 72.00 1 22.83 uncorr
Kim 25 25 849.80 83.30 834.40 71.10 1 24.20 corr
Pujol 72 72 739.00 82.00 763.00 78.00 1 26.70 uncorr
Riffkin 18 18 NA NA NA NA 1 23.30 corr
Soriano 30 30 NA NA NA NA 1 21.00 uncorr
Szeszko 37 26 776.00 69.00 747.00 68.00 0 24.90 corr
Valente 19 15 826.78 43.59 836.47 62.79 1 24.60 corr
Yoo 71 71 740.01 65.63 737.75 62.69 1 22.84 uncorr
Add variable
Add study
Main columns of the table
- n1 (always required): size of the main samples, e.g. the number of patients in each study.

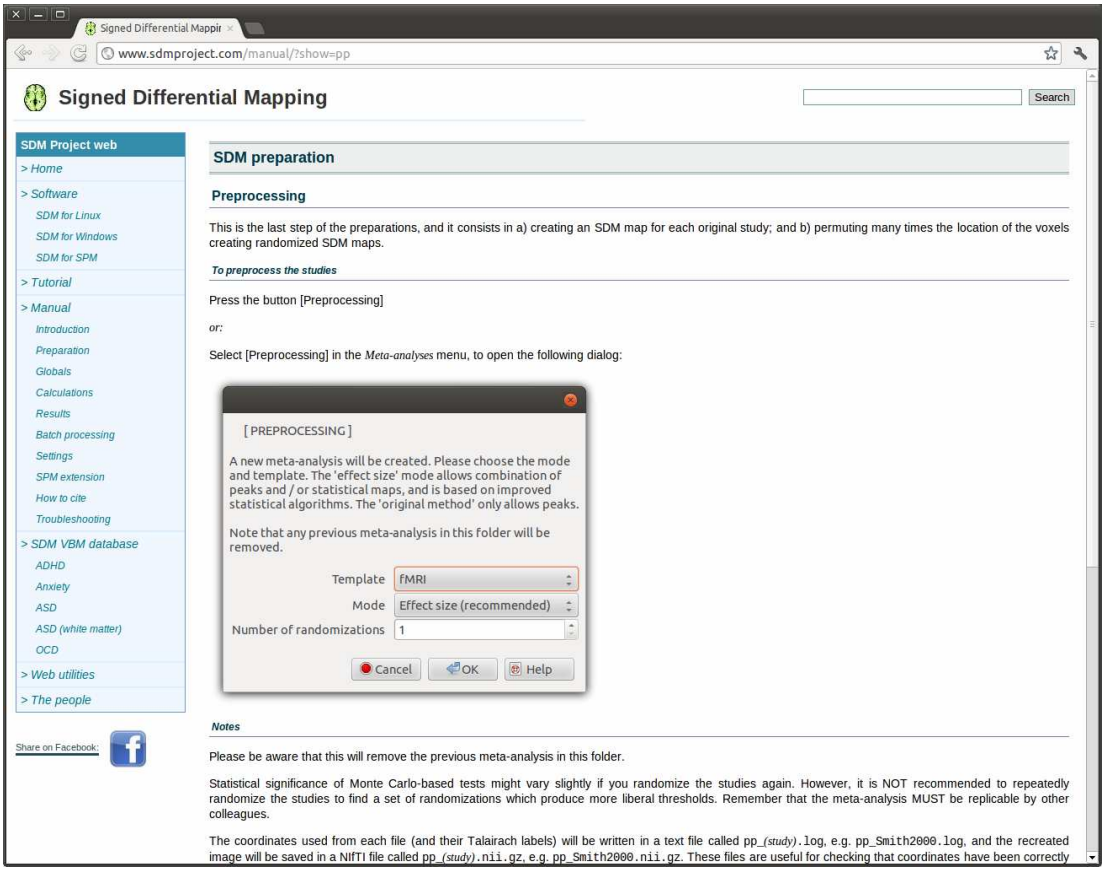
Signed Differential Mappir
www.sdmproject.com/manual/?show=pp
Signed Differential Mapping
Search
SDM Project web
> Home
> Software
SDM for Linux
SDM for Windows
SDM for SPM
> Tutorial
> Manual
Introduction
Preparation
Globals
Calculations
Results
Batch processing
Settings
SPM extension
How to cite
Troubleshooting
> SDM VBM database
ADHD
Anxiety
ASD
ASD (white matter)
OCD
> Web utilities
> The people
Share on Facebook:
SDM preparation
Preprocessing
This is the last step of the preparations, and it consists in a) creating an SDM map for each original study; and b) permuting many times the location of the voxels creating randomized SDM maps.
To preprocess the studies
Press the button [Preprocessing]
or:
Select [Preprocessing] in the Meta-analyses menu, to open the following dialog:
[PREPROCESSING]
A new meta-analysis will be created. Please choose the mode and template. The 'effect size' mode allows combination of peaks and / or statistical maps, and is based on improved statistical algorithms. The 'original method' only allows peaks.
Note that any previous meta-analysis in this folder will be removed.
Template
fMRI
Mode
Effect size (recommended)
Number of randomizations
1
Cancel
OK
Help
Notes
Please be aware that this will remove the previous meta-analysis in this folder.
Statistical significance of Monte Carlo-based tests might vary slightly if you randomize the studies again. However, it is NOT recommended to repeatedly randomize the studies to find a set of randomizations which produce more liberal thresholds. Remember that the meta-analysis MUST be replicable by other colleagues.
The coordinates used from each file (and their Talairach labels) will be written in a text file called pp_(study).log, e.g. pp_Smith2000.log, and the recreated image will be saved in a NIfTI file called pp_(study).nii.gz, e.g. pp_Smith2000.nii.gz. These files are useful for checking that coordinates have been correctly

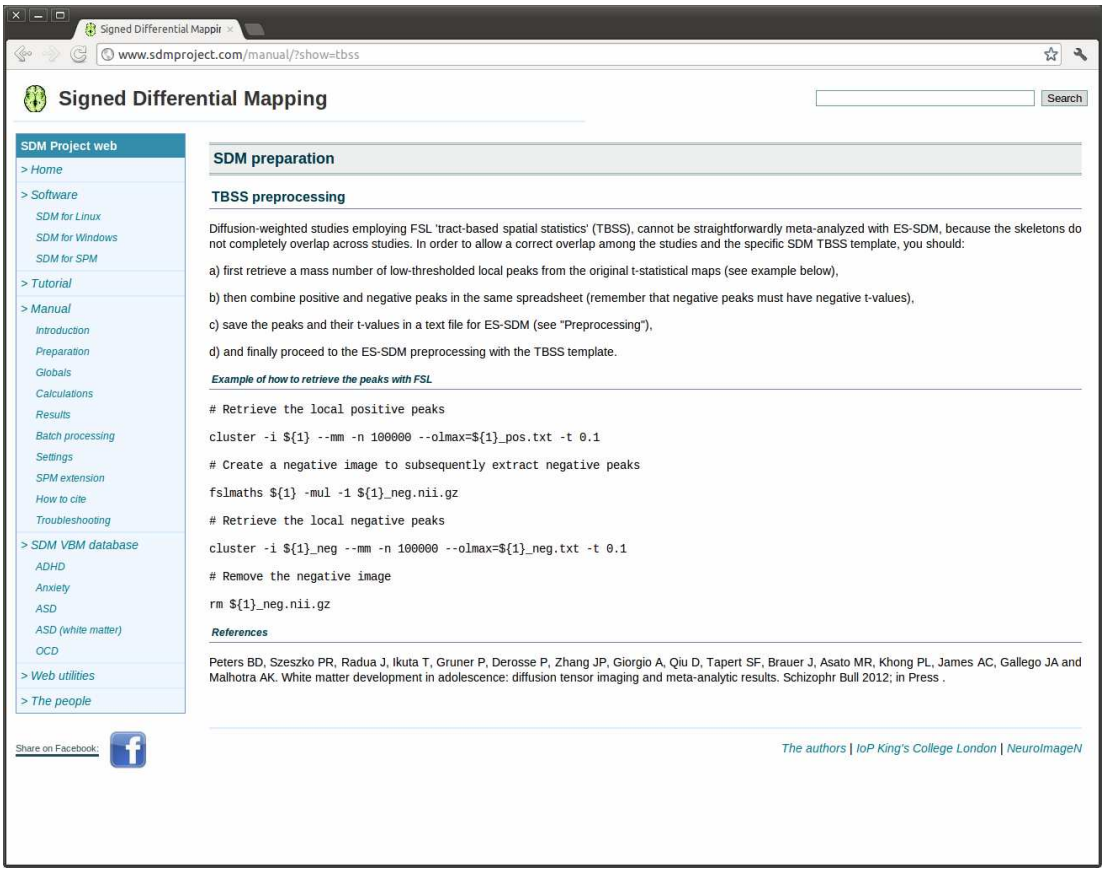
Signed Differential Mappir
www.sdmproject.com/manual/?show=tbss
Signed Differential Mapping
Search
SDM Project web
> Home
> Software
SDM for Linux
SDM for Windows
SDM for SPM
> Tutorial
> Manual
Introduction
Preparation
Globals
Calculations
Results
Batch processing
Settings
SPM extension
How to cite
Troubleshooting
> SDM VBM database
ADHD
Anxiety
ASD
ASD (white matter)
OCD
> Web utilities
> The people
Share on Facebook:
SDM preparation
TBSS preprocessing
Diffusion-weighted studies employing FSL 'tract-based spatial statistics' (TBSS), cannot be straightforwardly meta-analyzed with ES-SDM, because the skeletons do not completely overlap across studies. In order to allow a correct overlap among the studies and the specific SDM TBSS template, you should:
a) first retrieve a mass number of low-thresholded local peaks from the original t-statistical maps (see example below),
b) then combine positive and negative peaks in the same spreadsheet (remember that negative peaks must have negative t-values),
c) save the peaks and their t-values in a text file for ES-SDM (see "Preprocessing"),
d) and finally proceed to the ES-SDM preprocessing with the TBSS template.
Example of how to retrieve the peaks with FSL
Retrieve the local positive peaks
cluster -i ${1} --mm -n 100000 --olmax=${1}_pos.txt -t 0.1
Create a negative image to subsequently extract negative peaks
fslmaths ${1} -mul -1 ${1}_neg.nii.gz
Retrieve the local negative peaks
cluster -i ${1}_neg --mm -n 100000 --olmax=${1}_neg.txt -t 0.1
Remove the negative image
rm ${1}_neg.nii.gz
References
Peters BD, Szeszko PR, Radua J, Ikuta T, Gruner P, Derosse P, Zhang JP, Giorgio A, Qiu D, Tapert SF, Brauer J, Asato MR, Khong PL, James AC, Gallego JA and Malhotra AK. White matter development in adolescence: diffusion tensor imaging and meta-analytic results. Schizophr Bull 2012; in Press .
The authors | IoP King's College London | NeuroImageN

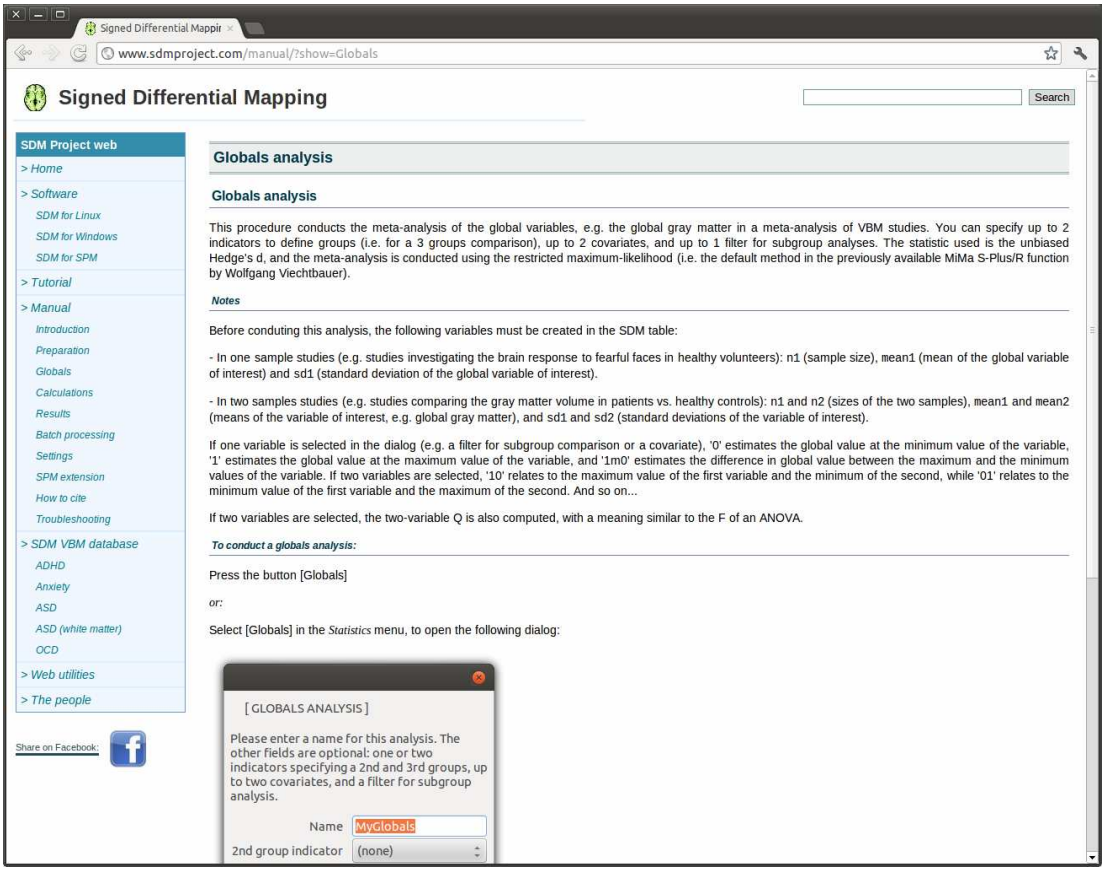
Signed Differential Mappir
www.sdmproject.com/manual/?show=Globals
Signed Differential Mapping
Search
SDM Project web
> Home
> Software
SDM for Linux
SDM for Windows
SDM for SPM
> Tutorial
> Manual
Introduction
Preparation
Globals
Calculations
Results
Batch processing
Settings
SPM extension
How to cite
Troubleshooting
> SDM VBM database
ADHD
Anxiety
ASD
ASD (white matter)
OCD
> Web utilities
> The people
Share on Facebook:
Globals analysis
Globals analysis
This procedure conducts the meta-analysis of the global variables, e.g. the global gray matter in a meta-analysis of VBM studies. You can specify up to 2 indicators to define groups (i.e. for a 3 groups comparison), up to 2 covariates, and up to 1 filter for subgroup analyses. The statistic used is the unbiased Hedge's d, and the meta-analysis is conducted using the restricted maximum-likelihood (i.e. the default method in the previously available MiMa S-Plus/R function by Wolfgang Viechtbauer).
Notes
Before conduting this analysis, the following variables must be created in the SDM table:
- In one sample studies (e.g. studies investigating the brain response to fearful faces in healthy volunteers): n1 (sample size), mean1 (mean of the global variable of interest) and sd1 (standard deviation of the global variable of interest).
- In two samples studies (e.g. studies comparing the gray matter volume in patients vs. healthy controls): n1 and n2 (sizes of the two samples), mean1 and mean2 (means of the variable of interest, e.g. global gray matter), and sd1 and sd2 (standard deviations of the variable of interest).
If one variable is selected in the dialog (e.g. a filter for subgroup comparison or a covariate), '0' estimates the global value at the minimum value of the variable, '1' estimates the global value at the maximum value of the variable, and '1m0' estimates the difference in global value between the maximum and the minimum values of the variable. If two variables are selected, '10' relates to the maximum value of the first variable and the minimum of the second, while '01' relates to the minimum value of the first variable and the maximum of the second. And so on...
If two variables are selected, the two-variable Q is also computed, with a meaning similar to the F of an ANOVA.
To conduct a globals analysis:
Press the button [Globals]
or:
Select [Globals] in the Statistics menu, to open the following dialog:
[GLOBALS ANALYSIS]
Please enter a name for this analysis. The other fields are optional: one or two indicators specifying a 2nd and 3rd groups, up to two covariates, and a filter for subgroup analysis.
Name
MyGlobals
2nd group indicator
(none)

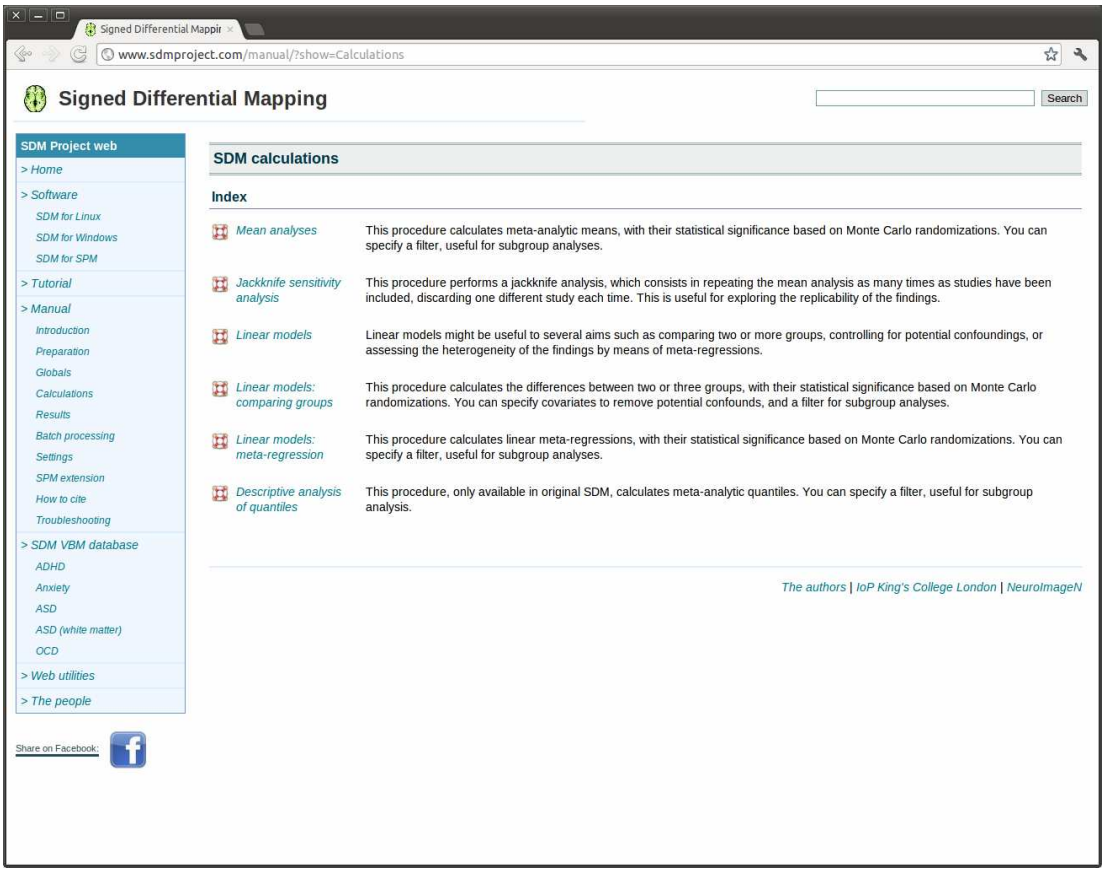
Signed Differential Mappir
www.sdmproject.com/manual/?show=Calculations
Signed Differential Mapping
Search
SDM Project web
> Home
> Software
SDM for Linux
SDM for Windows
SDM for SPM
> Tutorial
> Manual
Introduction
Preparation
Globals
Calculations
Results
Batch processing
Settings
SPM extension
How to cite
Troubleshooting
> SDM VBM database
ADHD
Anxiety
ASD
ASD (white matter)
OCD
> Web utilities
> The people
Share on Facebook:
SDM calculations
Index
Mean analyses
This procedure calculates meta-analytic means, with their statistical significance based on Monte Carlo randomizations. You can specify a filter, useful for subgroup analyses.
Jackknife sensitivity analysis
This procedure performs a jackknife analysis, which consists in repeating the mean analysis as many times as studies have been included, discarding one different study each time. This is useful for exploring the replicability of the findings.
Linear models
Linear models might be useful to several aims such as comparing two or more groups, controlling for potential confoundings, or assessing the heterogeneity of the findings by means of meta-regressions.
Linear models: comparing groups
This procedure calculates the differences between two or three groups, with their statistical significance based on Monte Carlo randomizations. You can specify covariates to remove potential confounds, and a filter for subgroup analyses.
Linear models: meta-regression
This procedure calculates linear meta-regressions, with their statistical significance based on Monte Carlo randomizations. You can specify a filter, useful for subgroup analyses.
Descriptive analysis of quantiles
This procedure, only available in original SDM, calculates meta-analytic quantiles. You can specify a filter, useful for subgroup analysis.
The authors | IoP King's College London | NeuroImageN

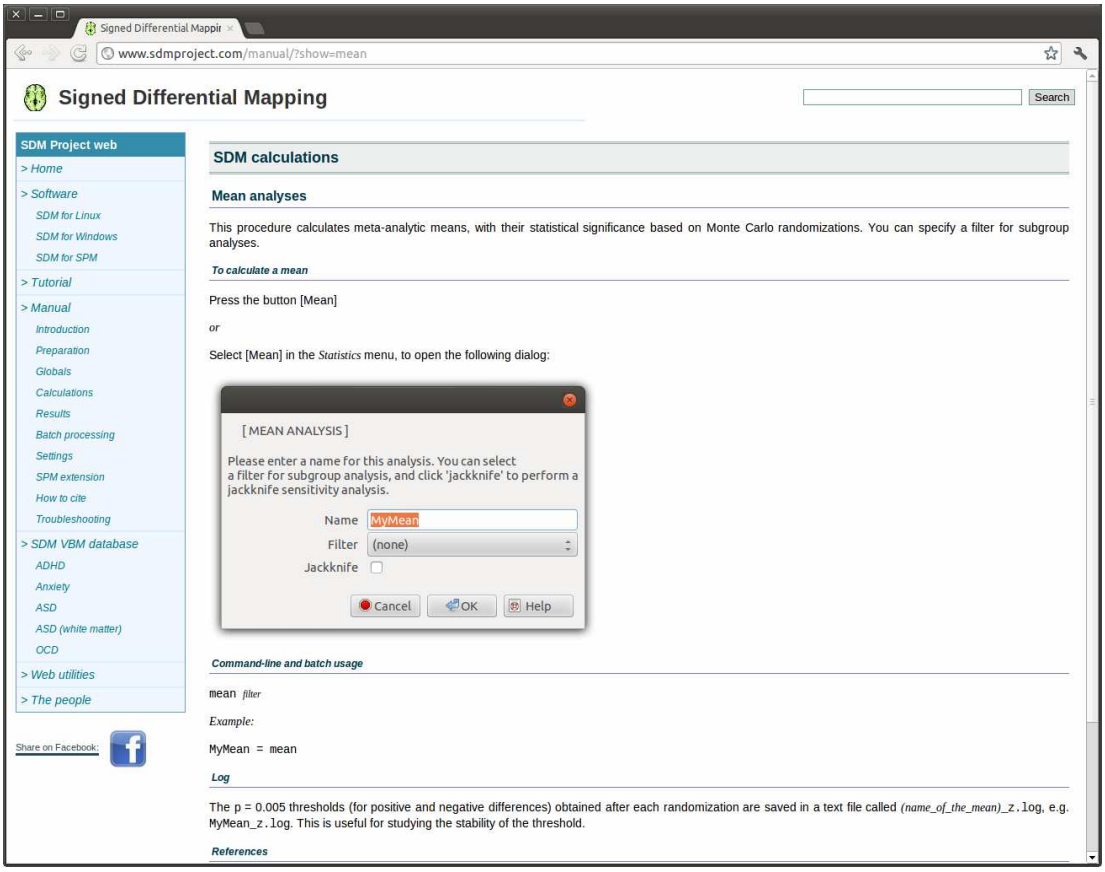
Signed Differential Mappir
www.sdmproject.com/manual/?show=mean
Signed Differential Mapping
Search
SDM Project web
> Home
> Software
SDM for Linux
SDM for Windows
SDM for SPM
> Tutorial
> Manual
Introduction
Preparation
Globals
Calculations
Results
Batch processing
Settings
SPM extension
How to cite
Troubleshooting
> SDM VBM database
ADHD
Anxiety
ASD
ASD (white matter)
OCD
> Web utilities
> The people
Share on Facebook:
SDM calculations
Mean analyses
This procedure calculates meta-analytic means, with their statistical significance based on Monte Carlo randomizations. You can specify a filter for subgroup analyses.
To calculate a mean
Press the button [Mean]
or
Select [Mean] in the Statistics menu, to open the following dialog:
[MEAN ANALYSIS]
Please enter a name for this analysis. You can select a filter for subgroup analysis, and click 'jackknife' to perform a jackknife sensitivity analysis.
Name
MyMean
Filter
(none)
Jackknife
Cancel
OK
Help
Command-line and batch usage
mean filter
Example:
MyMean = mean
Log
The p = 0.005 thresholds (for positive and negative differences) obtained after each randomization are saved in a text file called (name_of_the_mean)_z.log, e.g. MyMean_z.log. This is useful for studying the stability of the threshold.
References

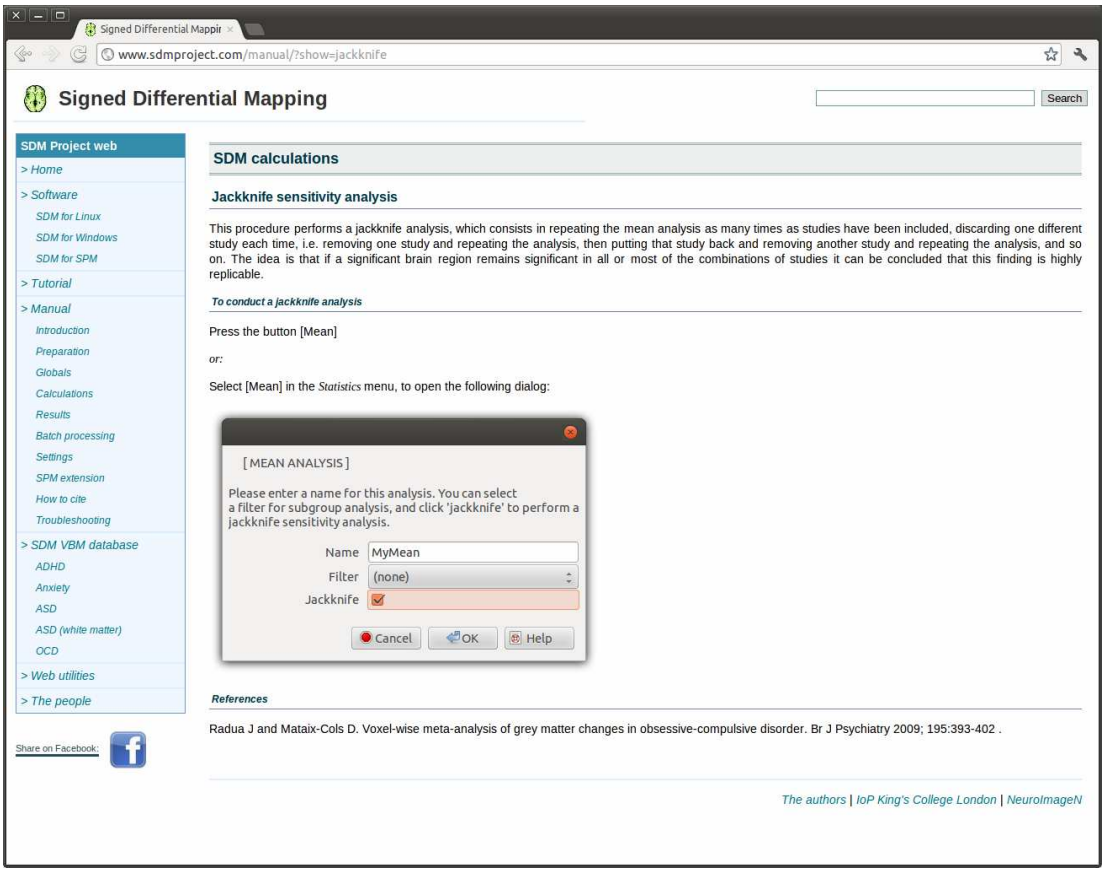
Signed Differential Mappir
www.sdmproject.com/manual/?show=jackknife
Signed Differential Mapping
Search
SDM Project web
> Home
> Software
SDM for Linux
SDM for Windows
SDM for SPM
> Tutorial
> Manual
Introduction
Preparation
Globals
Calculations
Results
Batch processing
Settings
SPM extension
How to cite
Troubleshooting
> SDM VBM database
ADHD
Anxiety
ASD
ASD (white matter)
OCD
> Web utilities
> The people
Share on Facebook:
SDM calculations
Jackknife sensitivity analysis
This procedure performs a jackknife analysis, which consists in repeating the mean analysis as many times as studies have been included, discarding one different study each time, i.e. removing one study and repeating the analysis, then putting that study back and removing another study and repeating the analysis, and so on. The idea is that if a significant brain region remains significant in all or most of the combinations of studies it can be concluded that this finding is highly replicable.
To conduct a jackknife analysis
Press the button [Mean]
or:
Select [Mean] in the Statistics menu, to open the following dialog:
[MEAN ANALYSIS]
Please enter a name for this analysis. You can select a filter for subgroup analysis, and click 'jackknife' to perform a jackknife sensitivity analysis.
Name
MyMean
Filter
(none)
Jackknife
Cancel
OK
Help
References
Radua J and Mataix-Cols D. Voxel-wise meta-analysis of grey matter changes in obsessive-compulsive disorder. Br J Psychiatry 2009; 195:393-402 .
The authors | IoP King's College London | NeuroImageN

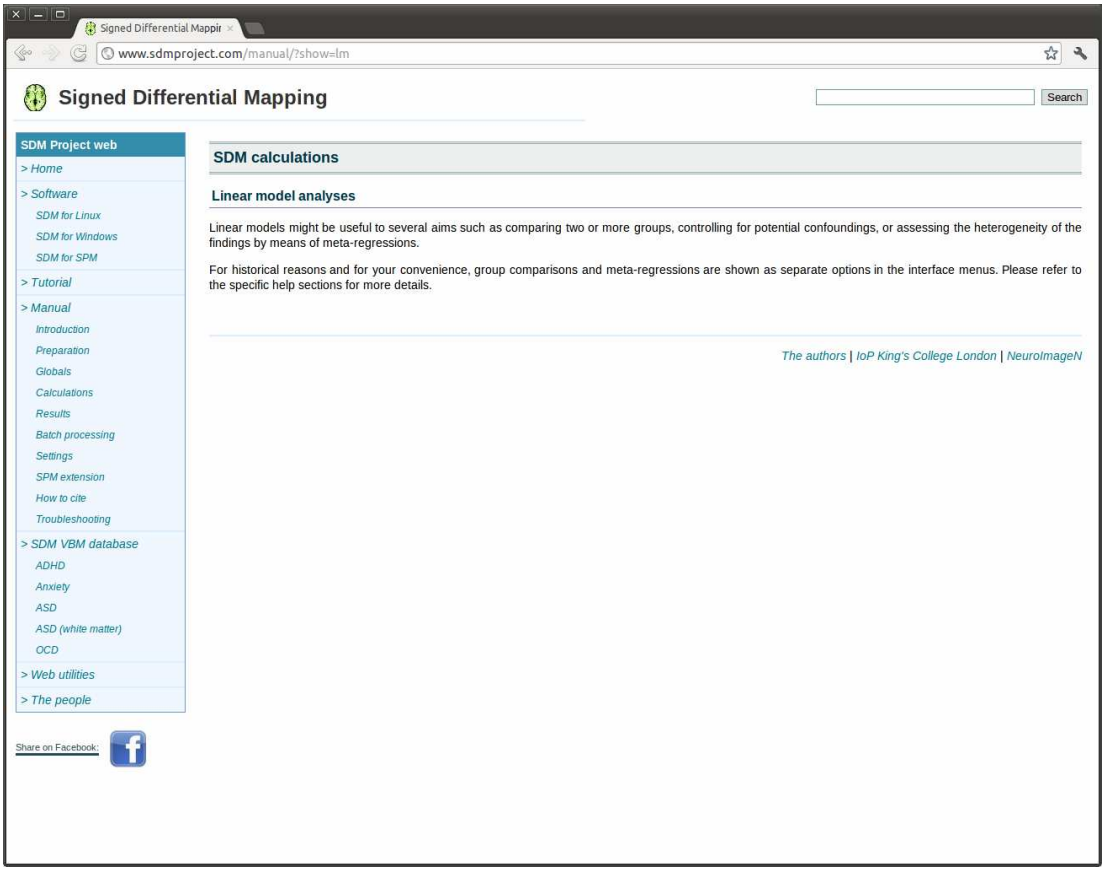
Signed Differential Mappir
www.sdmproject.com/manual/?show=lm
Signed Differential Mapping
Search
SDM Project web
> Home
> Software
SDM for Linux
SDM for Windows
SDM for SPM
> Tutorial
> Manual
Introduction
Preparation
Globals
Calculations
Results
Batch processing
Settings
SPM extension
How to cite
Troubleshooting
> SDM VBM database
ADHD
Anxiety
ASD
ASD (white matter)
OCD
> Web utilities
> The people
Share on Facebook:
SDM calculations
Linear model analyses
Linear models might be useful to several aims such as comparing two or more groups, controlling for potential confoundings, or assessing the heterogeneity of the findings by means of meta-regressions.
For historical reasons and for your convenience, group comparisons and meta-regressions are shown as separate options in the interface menus. Please refer to the specific help sections for more details.
The authors | IoP King's College London | NeuroImageN

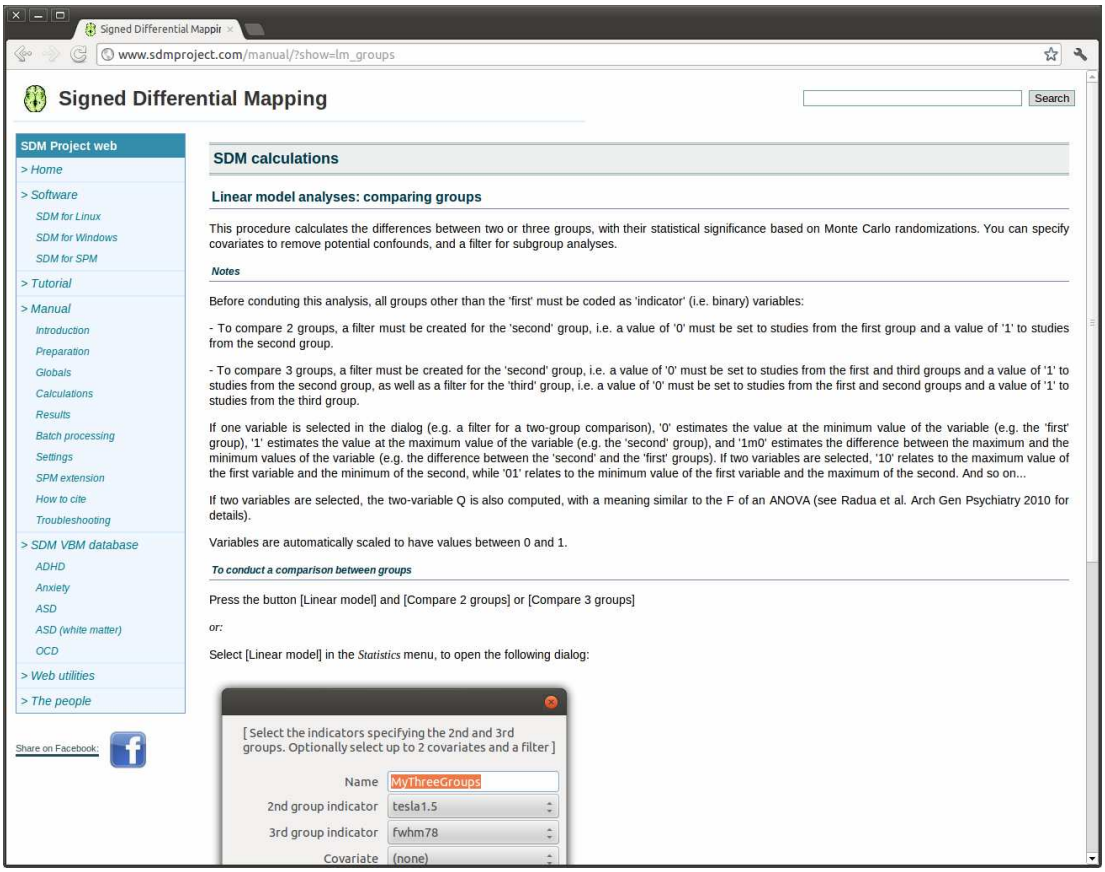
Signed Differential Mappir
www.sdmproject.com/manual/?show=lm_groups
Signed Differential Mapping
Search
SDM Project web
> Home
> Software
SDM for Linux
SDM for Windows
SDM for SPM
> Tutorial
> Manual
Introduction
Preparation
Globals
Calculations
Results
Batch processing
Settings
SPM extension
How to cite
Troubleshooting
> SDM VBM database
ADHD
Anxiety
ASD
ASD (white matter)
OCD
> Web utilities
> The people
Share on Facebook:
SDM calculations
Linear model analyses: comparing groups
This procedure calculates the differences between two or three groups, with their statistical significance based on Monte Carlo randomizations. You can specify covariates to remove potential confounds, and a filter for subgroup analyses.
Notes
Before conduting this analysis, all groups other than the 'first' must be coded as 'indicator' (i.e. binary) variables:
- To compare 2 groups, a filter must be created for the 'second' group, i.e. a value of '0' must be set to studies from the first group and a value of '1' to studies from the second group.
- To compare 3 groups, a filter must be created for the 'second' group, i.e. a value of '0' must be set to studies from the first and third groups and a value of '1' to studies from the second group, as well as a filter for the 'third' group, i.e. a value of '0' must be set to studies from the first and second groups and a value of '1' to studies from the third group.
If one variable is selected in the dialog (e.g. a filter for a two-group comparison), '0' estimates the value at the minimum value of the variable (e.g. the 'first' group), '1' estimates the value at the maximum value of the variable (e.g. the 'second' group), and '1m0' estimates the difference between the maximum and the minimum values of the variable (e.g. the difference between the 'second' and the 'first' groups). If two variables are selected, '10' relates to the maximum value of the first variable and the minimum of the second, while '01' relates to the minimum value of the first variable and the maximum of the second. And so on...
If two variables are selected, the two-variable Q is also computed, with a meaning similar to the F of an ANOVA (see Radua et al. Arch Gen Psychiatry 2010 for details).
Variables are automatically scaled to have values between 0 and 1.
To conduct a comparison between groups
Press the button [Linear model] and [Compare 2 groups] or [Compare 3 groups]
or:
Select [Linear model] in the Statistics menu, to open the following dialog:
[Select the indicators specifying the 2nd and 3rd groups. Optionally select up to 2 covariates and a filter]
Name
MyThreeGroups
2nd group indicator
tesla1.5
3rd group indicator
fwhm78
Covariate
(none)

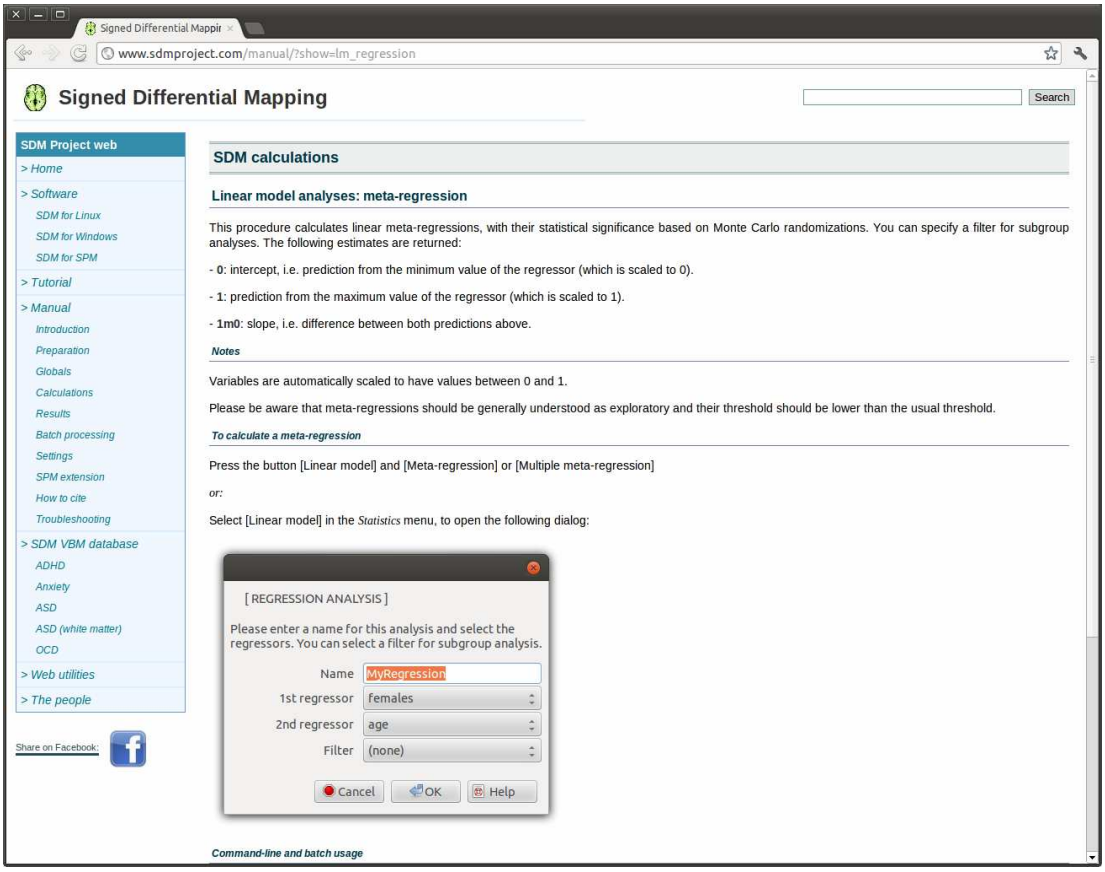
Signed Differential Mappir
www.sdmproject.com/manual/?show=lm_regression
Signed Differential Mapping
Search
SDM Project web
> Home
> Software
SDM for Linux
SDM for Windows
SDM for SPM
> Tutorial
> Manual
Introduction
Preparation
Globals
Calculations
Results
Batch processing
Settings
SPM extension
How to cite
Troubleshooting
> SDM VBM database
ADHD
Anxiety
ASD
ASD (white matter)
OCD
> Web utilities
> The people
Share on Facebook:
SDM calculations
Linear model analyses: meta-regression
This procedure calculates linear meta-regressions, with their statistical significance based on Monte Carlo randomizations. You can specify a filter for subgroup analyses. The following estimates are returned:
- 0: intercept, i.e. prediction from the minimum value of the regressor (which is scaled to 0).
- 1: prediction from the maximum value of the regressor (which is scaled to 1).
- 1m0: slope, i.e. difference between both predictions above.
Notes
Variables are automatically scaled to have values between 0 and 1.
Please be aware that meta-regressions should be generally understood as exploratory and their threshold should be lower than the usual threshold.
To calculate a meta-regression
Press the button [Linear model] and [Meta-regression] or [Multiple meta-regression]
or:
Select [Linear model] in the Statistics menu, to open the following dialog:
[REGRESSION ANALYSIS]
Please enter a name for this analysis and select the regressors. You can select a filter for subgroup analysis.
Name
MyRegression
1st regressor
females
2nd regressor
age
Filter
(none)
Cancel
OK
Help
Command-line and batch usage

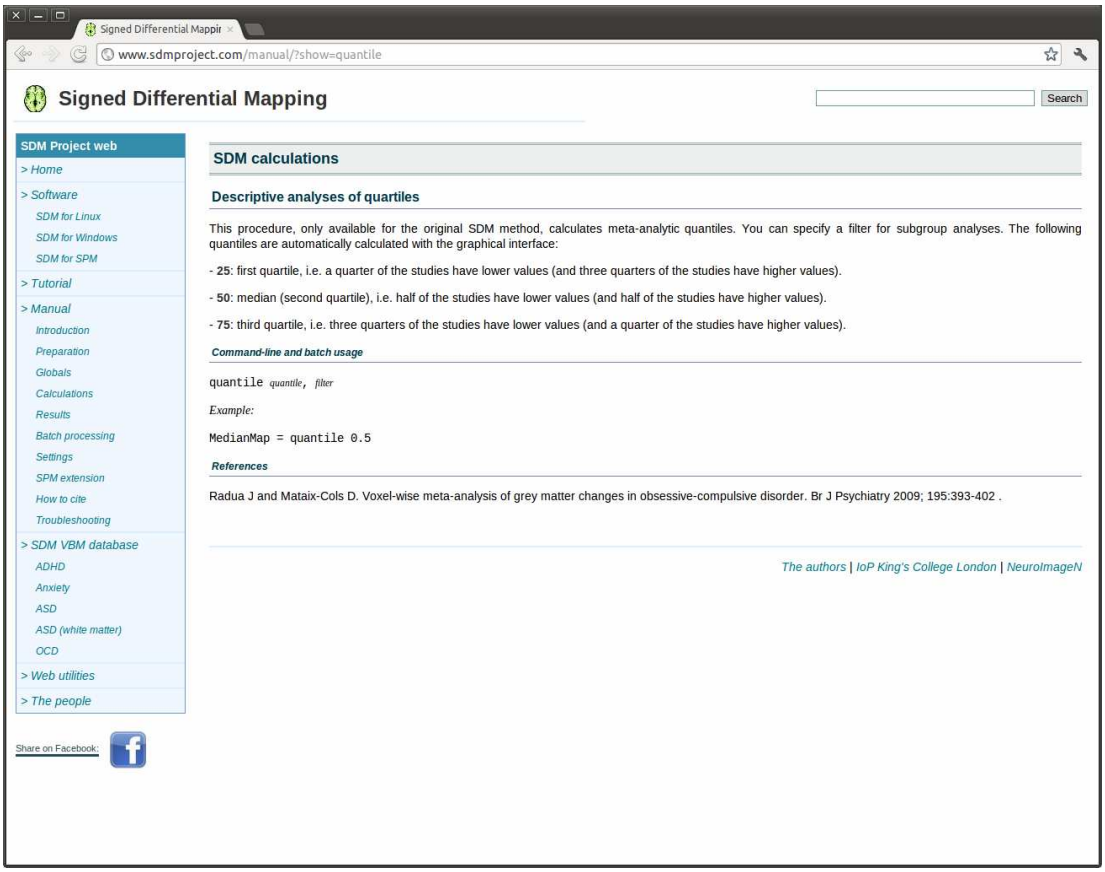
Signed Differential Mappir
www.sdmproject.com/manual/?show=quantile
Signed Differential Mapping
Search
SDM Project web
> Home
> Software
SDM for Linux
SDM for Windows
SDM for SPM
> Tutorial
> Manual
Introduction
Preparation
Globals
Calculations
Results
Batch processing
Settings
SPM extension
How to cite
Troubleshooting
> SDM VBM database
ADHD
Anxiety
ASD
ASD (white matter)
OCD
> Web utilities
> The people
Share on Facebook:
SDM calculations
Descriptive analyses of quartiles
This procedure, only available for the original SDM method, calculates meta-analytic quantiles. You can specify a filter for subgroup analyses. The following quantiles are automatically calculated with the graphical interface:
- 25: first quartile, i.e. a quarter of the studies have lower values (and three quarters of the studies have higher values).
- 50: median (second quartile), i.e. half of the studies have lower values (and half of the studies have higher values).
- 75: third quartile, i.e. three quarters of the studies have lower values (and a quarter of the studies have higher values).
Command-line and batch usage
quantile quantile, filter
Example:
MedianMap = quantile 0.5
References
Radua J and Mataix-Cols D. Voxel-wise meta-analysis of grey matter changes in obsessive-compulsive disorder. Br J Psychiatry 2009; 195:393-402 .
The authors | IoP King's College London | NeuroImageN

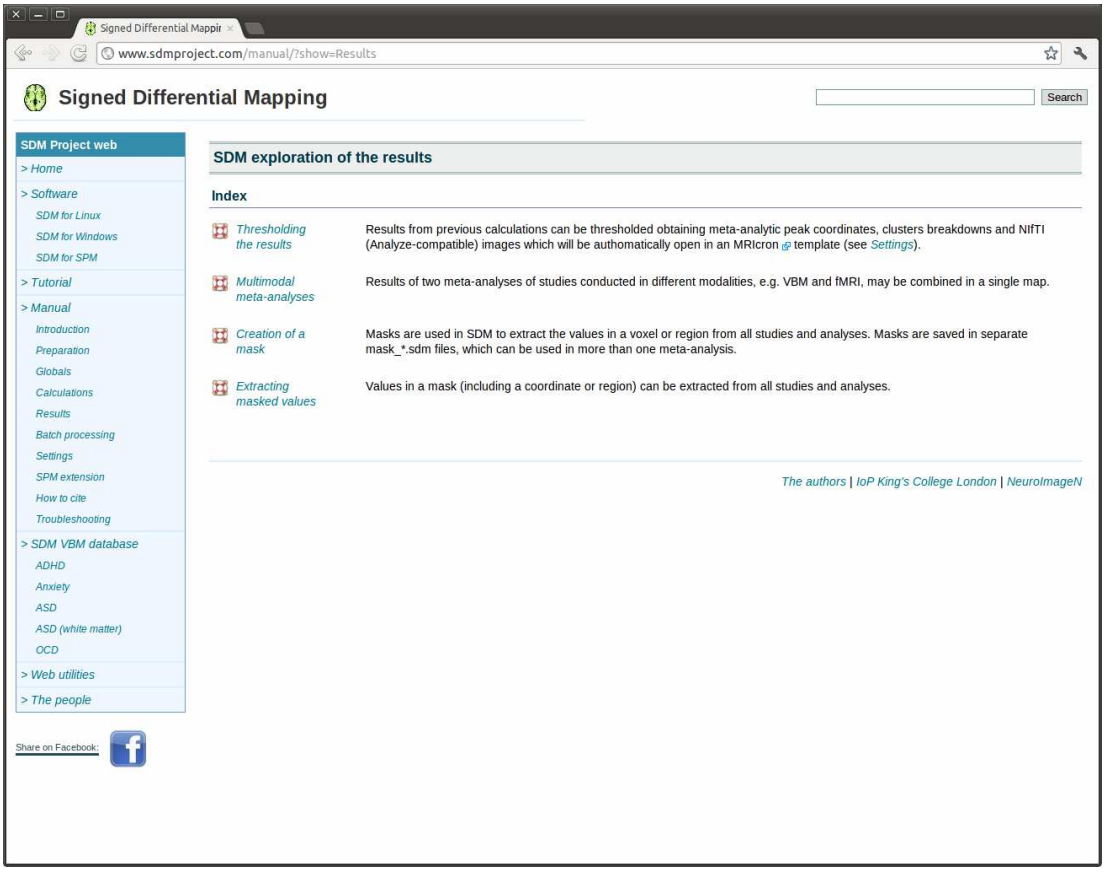
Signed Differential Mappir
www.sdmproject.com/manual/?show=Results
Signed Differential Mapping
Search
SDM Project web
> Home
> Software
SDM for Linux
SDM for Windows
SDM for SPM
> Tutorial
> Manual
Introduction
Preparation
Globals
Calculations
Results
Batch processing
Settings
SPM extension
How to cite
Troubleshooting
> SDM VBM database
ADHD
Anxiety
ASD
ASD (white matter)
OCD
> Web utilities
> The people
Share on Facebook:
SDM exploration of the results
Index
Thresholding the results
Results from previous calculations can be thresholded obtaining meta-analytic peak coordinates, clusters breakdowns and NIfTI (Analyze-compatible) images which will be authomatically open in an MRIcron template (see Settings).
Multimodal meta-analyses
Results of two meta-analyses of studies conducted in different modalities, e.g. VBM and fMRI, may be combined in a single map.
Creation of a mask
Masks are used in SDM to extract the values in a voxel or region from all studies and analyses. Masks are saved in separate mask_*.sdm files, which can be used in more than one meta-analysis.
Extracting masked values
Values in a mask (including a coordinate or region) can be extracted from all studies and analyses.
The authors | IoP King's College London | NeuroImageN

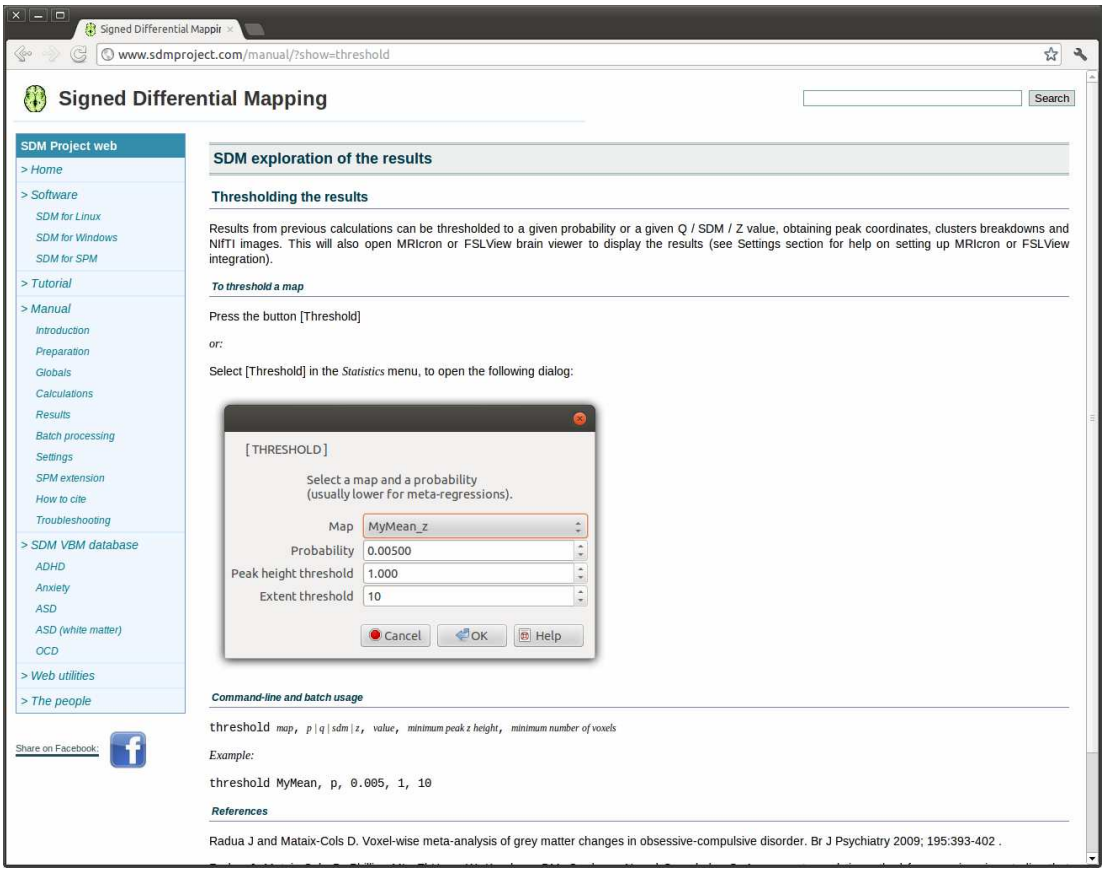
Signed Differential Mappir
www.sdmproject.com/manual/?show=threshold
Signed Differential Mapping
Search
SDM Project web
> Home
> Software
SDM for Linux
SDM for Windows
SDM for SPM
> Tutorial
> Manual
Introduction
Preparation
Globals
Calculations
Results
Batch processing
Settings
SPM extension
How to cite
Troubleshooting
> SDM VBM database
ADHD
Anxiety
ASD
ASD (white matter)
OCD
> Web utilities
> The people
Share on Facebook:
SDM exploration of the results
Thresholding the results
Results from previous calculations can be thresholded to a given probability or a given Q / SDM / Z value, obtaining peak coordinates, clusters breakdowns and NifTI images. This will also open MRIcron or FSLView brain viewer to display the results (see Settings section for help on setting up MRIcron or FSLView integration).
To threshold a map
Press the button [Threshold]
or:
Select [Threshold] in the Statistics menu, to open the following dialog:
[THRESHOLD]
Select a map and a probability
(usually lower for meta-regressions).
Map
MyMean_z
Probability
0.00500
Peak height threshold
1.000
Extent threshold
10
Cancel
OK
Help
Command-line and batch usage
threshold map, p | q | sdm | z, value, minimum peak z height, minimum number of voxels
Example:
threshold MyMean, p, 0.005, 1, 10
References
Radua J and Mataix-Cols D. Voxel-wise meta-analysis of grey matter changes in obsessive-compulsive disorder. Br J Psychiatry 2009; 195:393-402 .

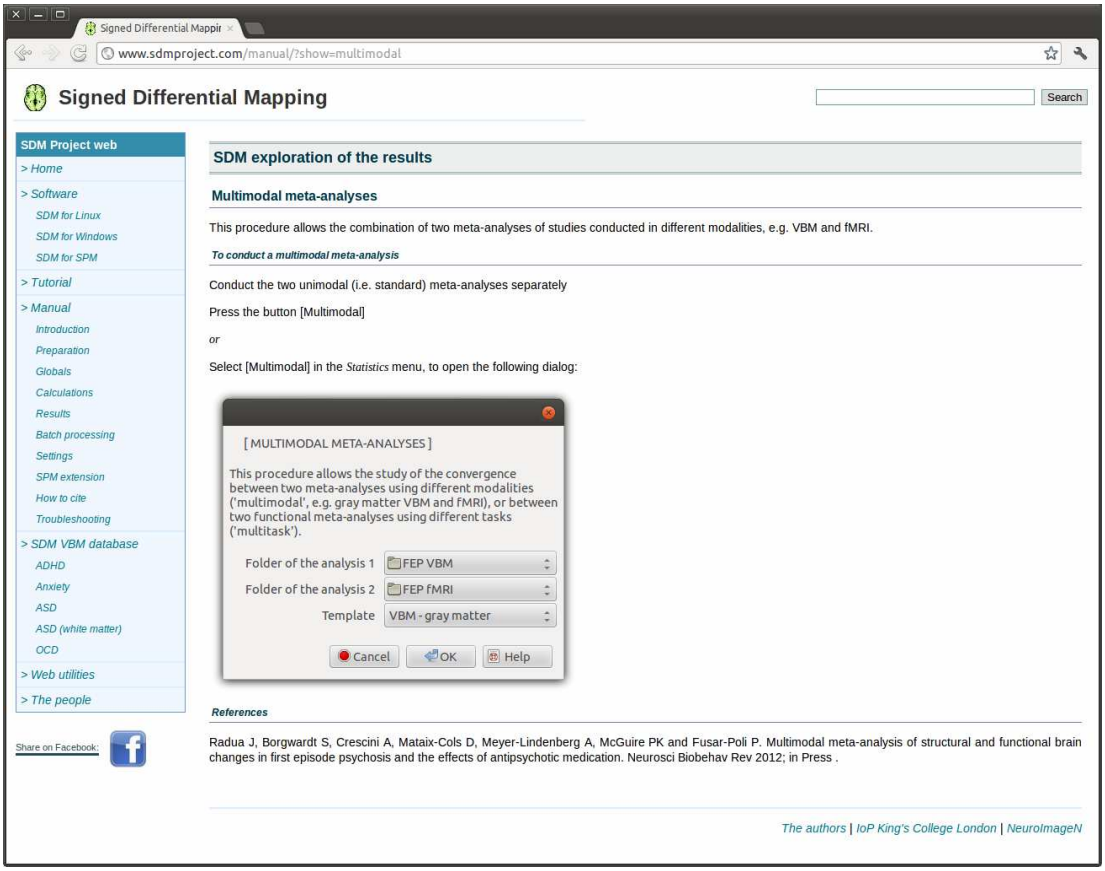
Signed Differential Mappir
www.sdmproject.com/manual/?show=multimodal
Signed Differential Mapping
Search
SDM Project web
> Home
> Software
SDM for Linux
SDM for Windows
SDM for SPM
> Tutorial
> Manual
Introduction
Preparation
Globals
Calculations
Results
Batch processing
Settings
SPM extension
How to cite
Troubleshooting
> SDM VBM database
ADHD
Anxiety
ASD
ASD (white matter)
OCD
> Web utilities
> The people
Share on Facebook:
SDM exploration of the results
Multimodal meta-analyses
This procedure allows the combination of two meta-analyses of studies conducted in different modalities, e.g. VBM and fMRI.
To conduct a multimodal meta-analysis
Conduct the two unimodal (i.e. standard) meta-analyses separately
Press the button [Multimodal]
or
Select [Multimodal] in the Statistics menu, to open the following dialog:
[MULTIMODAL META-ANALYSES]
This procedure allows the study of the convergence between two meta-analyses using different modalities ('multimodal', e.g. gray matter VBM and fMRI), or between two functional meta-analyses using different tasks ('multitask').
Folder of the analysis 1
FEP VBM
Folder of the analysis 2
FEP fMRI
Template
VBM - gray matter
Cancel
OK
Help
References
Radua J, Borgwardt S, Crescini A, Mataix-Cols D, Meyer-Lindenberg A, McGuire PK and Fusar-Poli P. Multimodal meta-analysis of structural and functional brain changes in first episode psychosis and the effects of antipsychotic medication. Neurosci Biobehav Rev 2012; in Press .
The authors | IoP King's College London | NeuroImageN

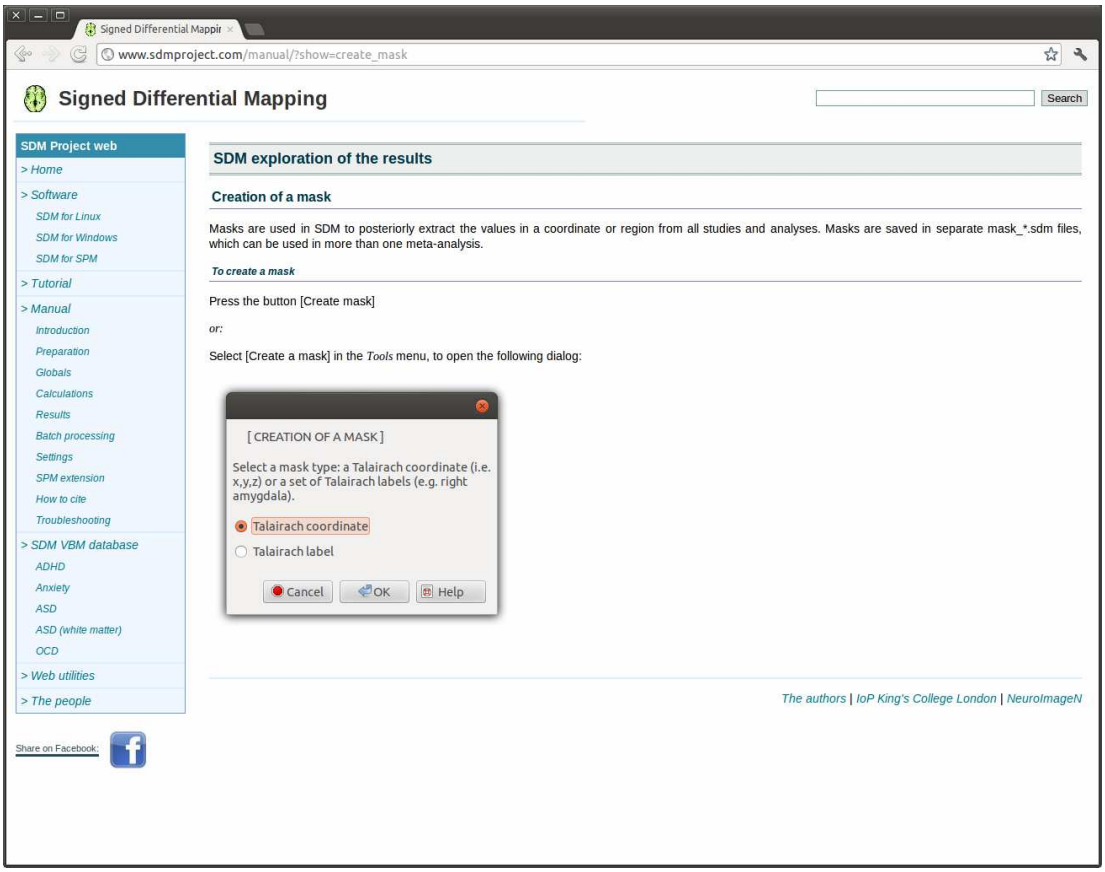
Signed Differential Mappir
www.sdmproject.com/manual/?show=create_mask
Signed Differential Mapping
Search
SDM Project web
> Home
> Software
SDM for Linux
SDM for Windows
SDM for SPM
> Tutorial
> Manual
Introduction
Preparation
Globals
Calculations
Results
Batch processing
Settings
SPM extension
How to cite
Troubleshooting
> SDM VBM database
ADHD
Anxiety
ASD
ASD (white matter)
OCD
> Web utilities
> The people
Share on Facebook:
SDM exploration of the results
Creation of a mask
Masks are used in SDM to posteriorly extract the values in a coordinate or region from all studies and analyses. Masks are saved in separate mask_*.sdm files, which can be used in more than one meta-analysis.
To create a mask
Press the button [Create mask]
or:
Select [Create a mask] in the Tools menu, to open the following dialog:
[CREATION OF A MASK]
Select a mask type: a Talairach coordinate (i.e. x,y,z) or a set of Talairach labels (e.g. right amygdala).
Talairach coordinate
Talairach label
Cancel
OK
Help
The authors | IoP King's College London | NeuroImageN

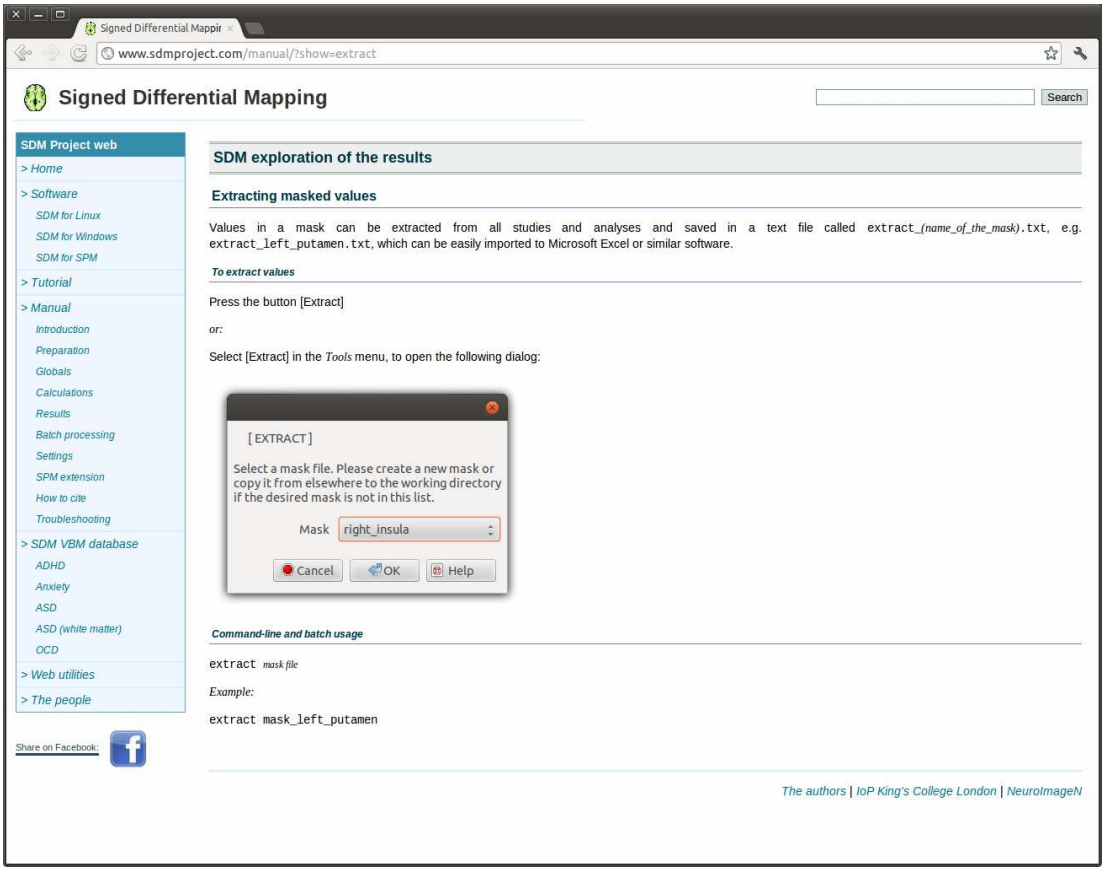
Signed Differential Mappir
www.sdmproject.com/manual/?show=extract
Signed Differential Mapping
Search
SDM Project web
> Home
> Software
SDM for Linux
SDM for Windows
SDM for SPM
> Tutorial
> Manual
Introduction
Preparation
Globals
Calculations
Results
Batch processing
Settings
SPM extension
How to cite
Troubleshooting
> SDM VBM database
ADHD
Anxiety
ASD
ASD (white matter)
OCD
> Web utilities
> The people
Share on Facebook:
SDM exploration of the results
Extracting masked values
Values in a mask can be extracted from all studies and analyses and saved in a text file called extract_(name_of_the_mask).txt, e.g. extract_left_putamen.txt, which can be easily imported to Microsoft Excel or similar software.
To extract values
Press the button [Extract]
or:
Select [Extract] in the Tools menu, to open the following dialog:
[EXTRACT]
Select a mask file. Please create a new mask or copy it from elsewhere to the working directory if the desired mask is not in this list.
Mask
right_insula
Cancel
OK
Help
Command-line and batch usage
extract mask file
Example:
extract mask_left_putamen
The authors | IoP King's College London | NeuroImageN

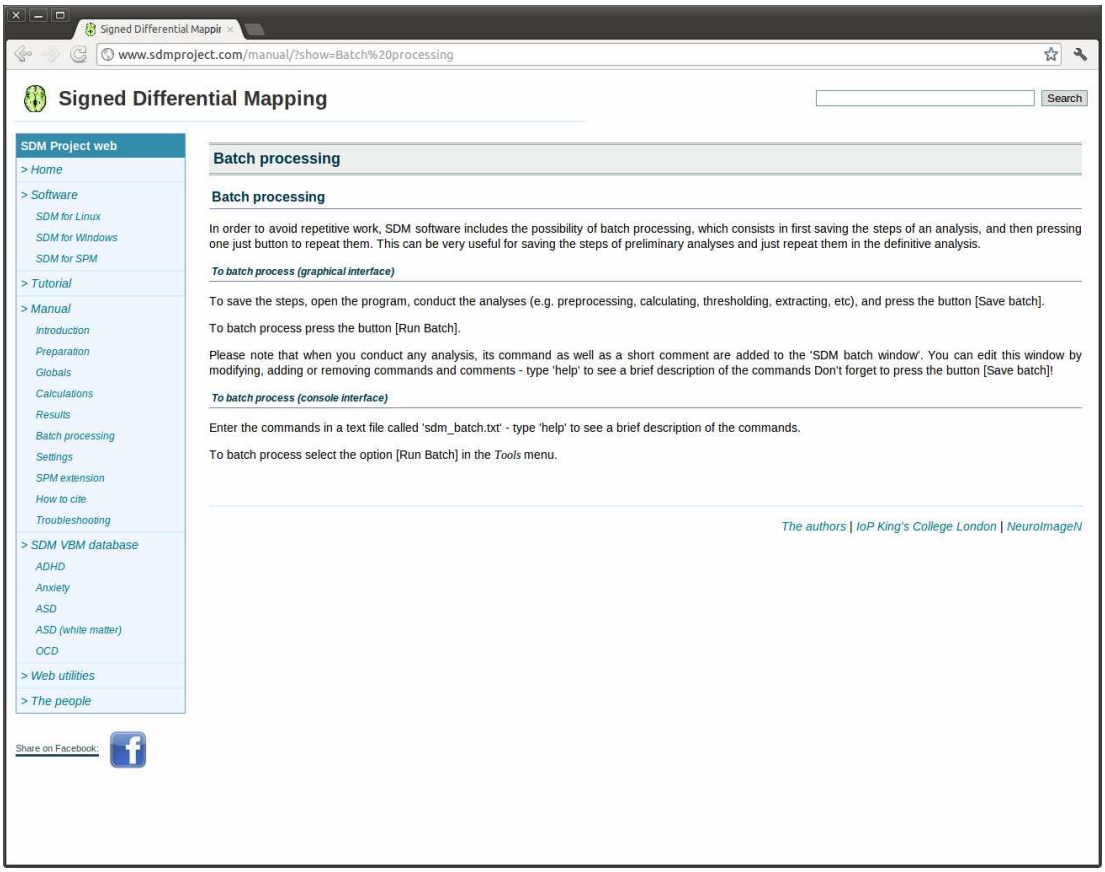
Signed Differential Mappir
www.sdmproject.com/manual/?show=Batch%20processing
Signed Differential Mapping
Search
SDM Project web
> Home
> Software
SDM for Linux
SDM for Windows
SDM for SPM
> Tutorial
> Manual
Introduction
Preparation
Globals
Calculations
Results
Batch processing
Settings
SPM extension
How to cite
Troubleshooting
> SDM VBM database
ADHD
Anxiety
ASD
ASD (white matter)
OCD
> Web utilities
> The people
Share on Facebook:
Batch processing
Batch processing
In order to avoid repetitive work, SDM software includes the possibility of batch processing, which consists in first saving the steps of an analysis, and then pressing one just button to repeat them. This can be very useful for saving the steps of preliminary analyses and just repeat them in the definitive analysis.
To batch process (graphical interface)
To save the steps, open the program, conduct the analyses (e.g. preprocessing, calculating, thresholding, extracting, etc), and press the button [Save batch].
To batch process press the button [Run Batch].
Please note that when you conduct any analysis, its command as well as a short comment are added to the 'SDM batch window'. You can edit this window by modifying, adding or removing commands and comments - type 'help' to see a brief description of the commands Don't forget to press the button [Save batch]!
To batch process (console interface)
Enter the commands in a text file called 'sdm_batch.txt' - type 'help' to see a brief description of the commands.
To batch process select the option [Run Batch] in the Tools menu.
The authors | IoP King's College London | NeuroImageN

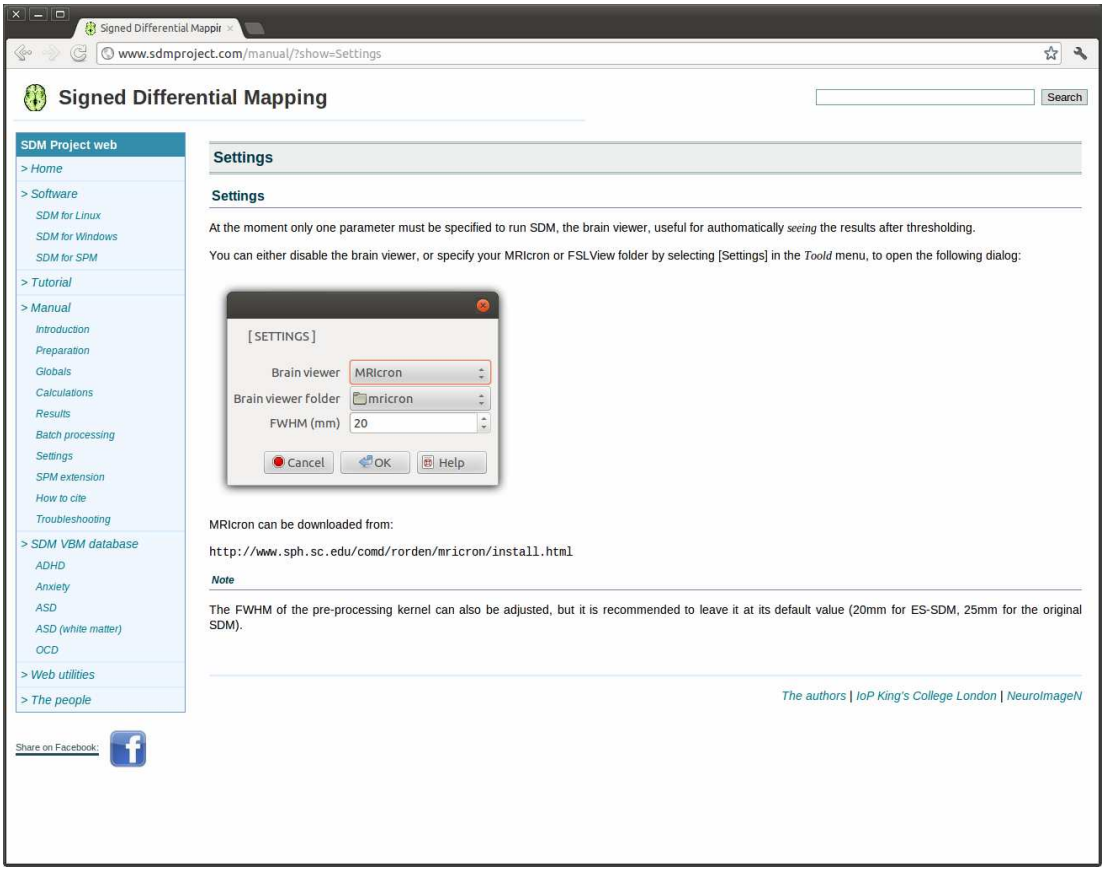
Signed Differential Mappir
www.sdmproject.com/manual/?show=Settings
Signed Differential Mapping
Search
SDM Project web
> Home
> Software
SDM for Linux
SDM for Windows
SDM for SPM
> Tutorial
> Manual
Introduction
Preparation
Globals
Calculations
Results
Batch processing
Settings
SPM extension
How to cite
Troubleshooting
> SDM VBM database
ADHD
Anxiety
ASD
ASD (white matter)
OCD
> Web utilities
> The people
Share on Facebook:
Settings
Settings
At the moment only one parameter must be specified to run SDM, the brain viewer, useful for authomatically seeing the results after thresholding.
You can either disable the brain viewer, or specify your MRIcron or FSLView folder by selecting [Settings] in the Toold menu, to open the following dialog:
[SETTINGS]
Brain viewer
MRIcron
Brain viewer folder
mricron
FWHM (mm)
20
Cancel
OK
Help
MRIcron can be downloaded from:
http://www.sph.sc.edu/comd/rorden/mricron/install.html
Note
The FWHM of the pre-processing kernel can also be adjusted, but it is recommended to leave it at its default value (20mm for ES-SDM, 25mm for the original SDM).
The authors | IoP King's College London | NeuroImageN

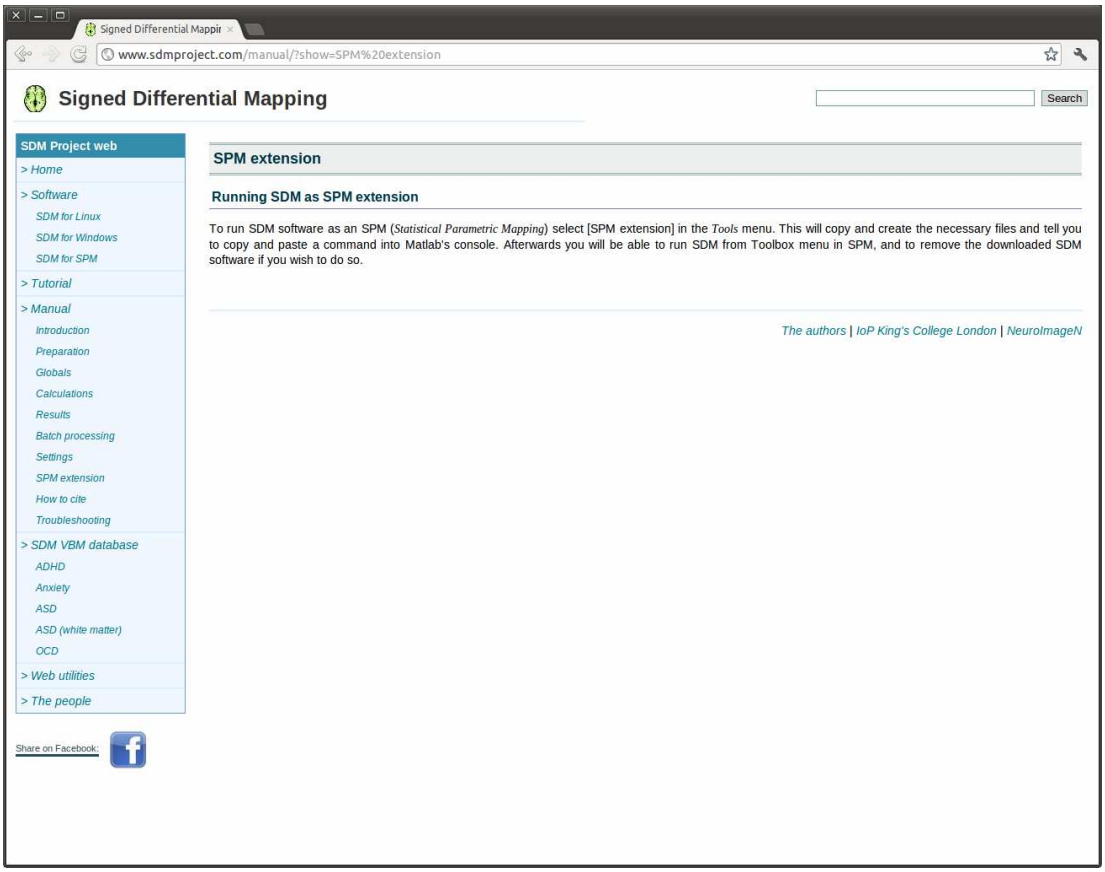
Signed Differential Mappir
www.sdmproject.com/manual/?show=SPM%20extension
Signed Differential Mapping
Search
SDM Project web
> Home
> Software
SDM for Linux
SDM for Windows
SDM for SPM
> Tutorial
> Manual
Introduction
Preparation
Globals
Calculations
Results
Batch processing
Settings
SPM extension
How to cite
Troubleshooting
> SDM VBM database
ADHD
Anxiety
ASD
ASD (white matter)
OCD
> Web utilities
> The people
Share on Facebook:
SPM extension
Running SDM as SPM extension
To run SDM software as an SPM (Statistical Parametric Mapping) select [SPM extension] in the Tools menu. This will copy and create the necessary files and tell you to copy and paste a command into Matlab's console. Afterwards you will be able to run SDM from Toolbox menu in SPM, and to remove the downloaded SDM software if you wish to do so.
The authors | IoP King's College London | NeuroImageN

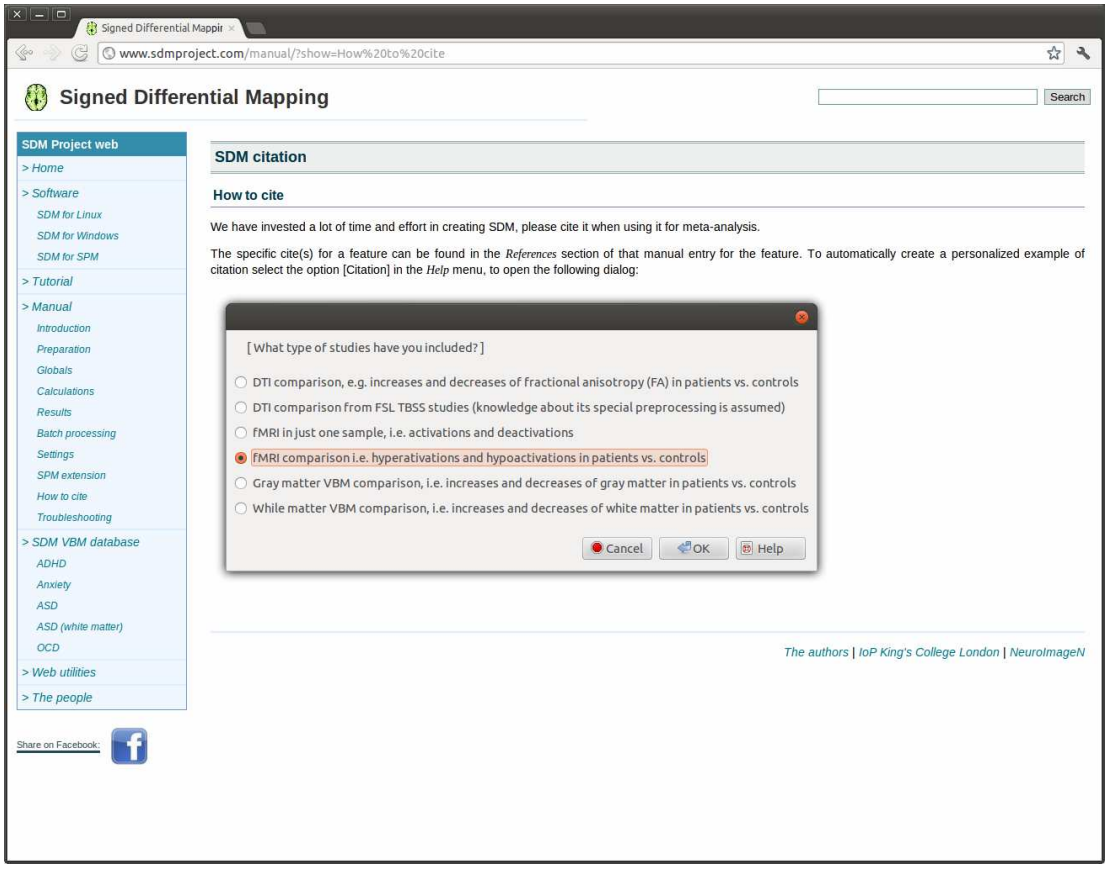
Signed Differential Mappir
www.sdmproject.com/manual/?show=How%20to%20cite
Signed Differential Mapping
Search
SDM Project web
> Home
> Software
SDM for Linux
SDM for Windows
SDM for SPM
> Tutorial
> Manual
Introduction
Preparation
Globals
Calculations
Results
Batch processing
Settings
SPM extension
How to cite
Troubleshooting
> SDM VBM database
ADHD
Anxiety
ASD
ASD (white matter)
OCD
> Web utilities
> The people
Share on Facebook:
SDM citation
How to cite
We have invested a lot of time and effort in creating SDM, please cite it when using it for meta-analysis.
The specific cite(s) for a feature can be found in the References section of that manual entry for the feature. To automatically create a personalized example of citation select the option [Citation] in the Help menu, to open the following dialog:
[What type of studies have you included?]
DTI comparison, e.g. increases and decreases of fractional anisotropy (FA) in patients vs. controls
DTI comparison from FSL TBSS studies (knowledge about its special preprocessing is assumed)
fMRI in just one sample, i.e. activations and deactivations
fMRI comparison i.e. hyperativations and hypoactivations in patients vs. controls
Gray matter VBM comparison, i.e. increases and decreases of gray matter in patients vs. controls
While matter VBM comparison, i.e. increases and decreases of white matter in patients vs. controls
Cancel
OK
Help
The authors | IoP King's College London | NeuroImageN

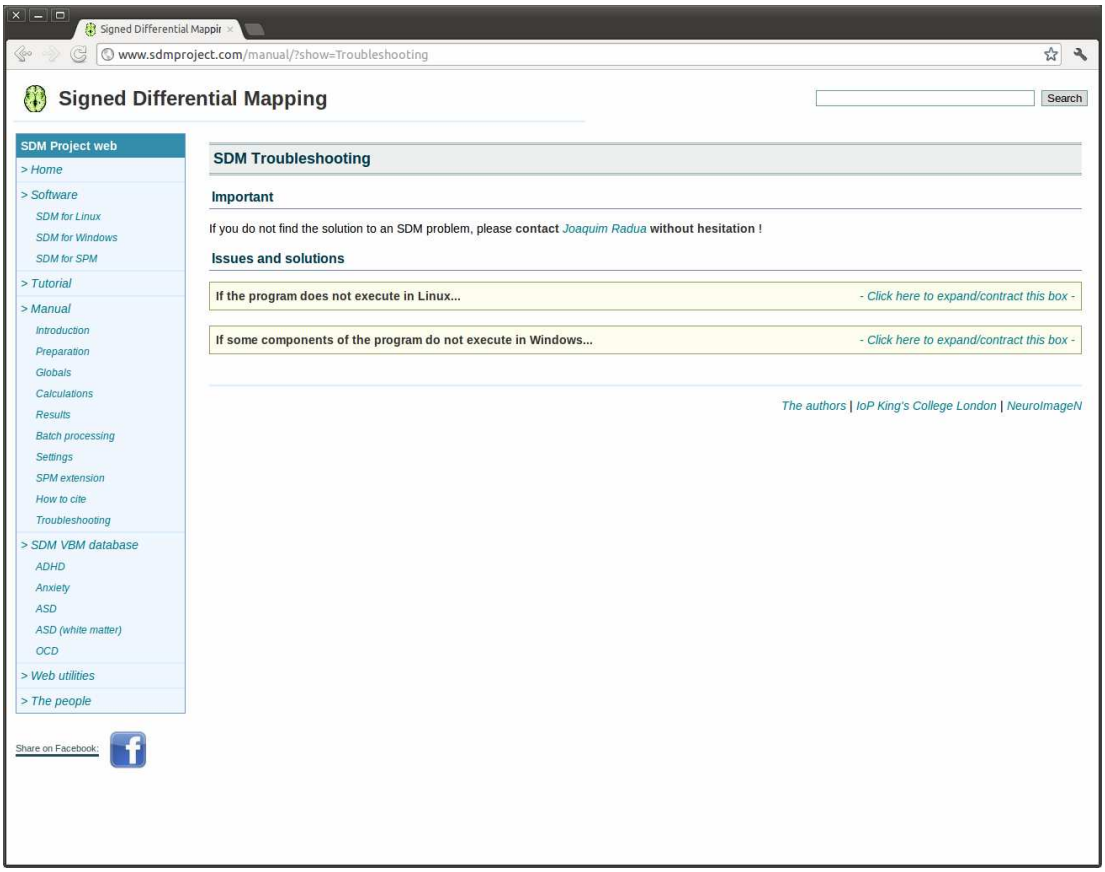
Signed Differential Mappir
www.sdmproject.com/manual/?show=Troubleshooting
Signed Differential Mapping
Search
SDM Project web
> Home
> Software
SDM for Linux
SDM for Windows
SDM for SPM
> Tutorial
> Manual
Introduction
Preparation
Globals
Calculations
Results
Batch processing
Settings
SPM extension
How to cite
Troubleshooting
> SDM VBM database
ADHD
Anxiety
ASD
ASD (white matter)
OCD
> Web utilities
> The people
Share on Facebook:
SDM Troubleshooting
Important
If you do not find the solution to an SDM problem, please contact Joaquim Radua without hesitation !
Issues and solutions
If the program does not execute in Linux...
- Click here to expand/contract this box -
If some components of the program do not execute in Windows...
- Click here to expand/contract this box -
The authors | IoP King's College London | NeuroImageN

A2.1 Sample screenshots of the database

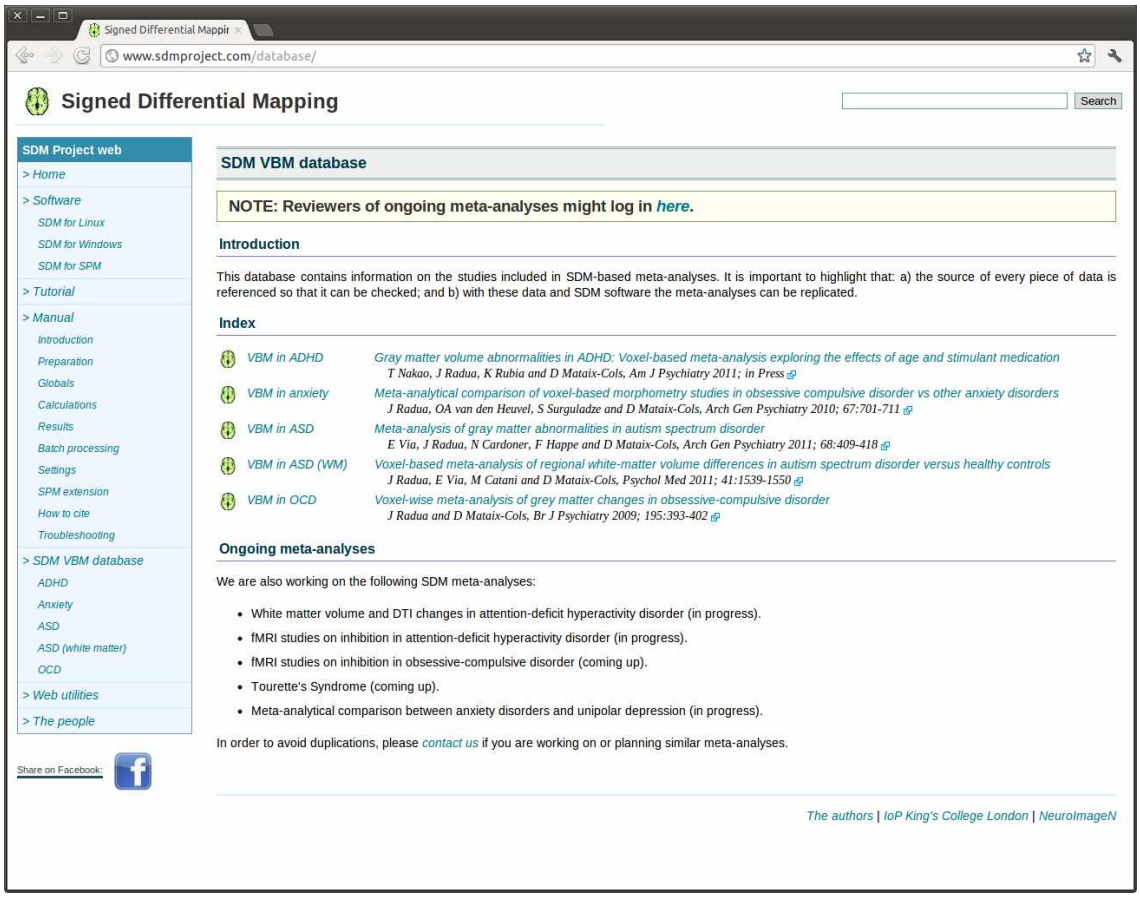

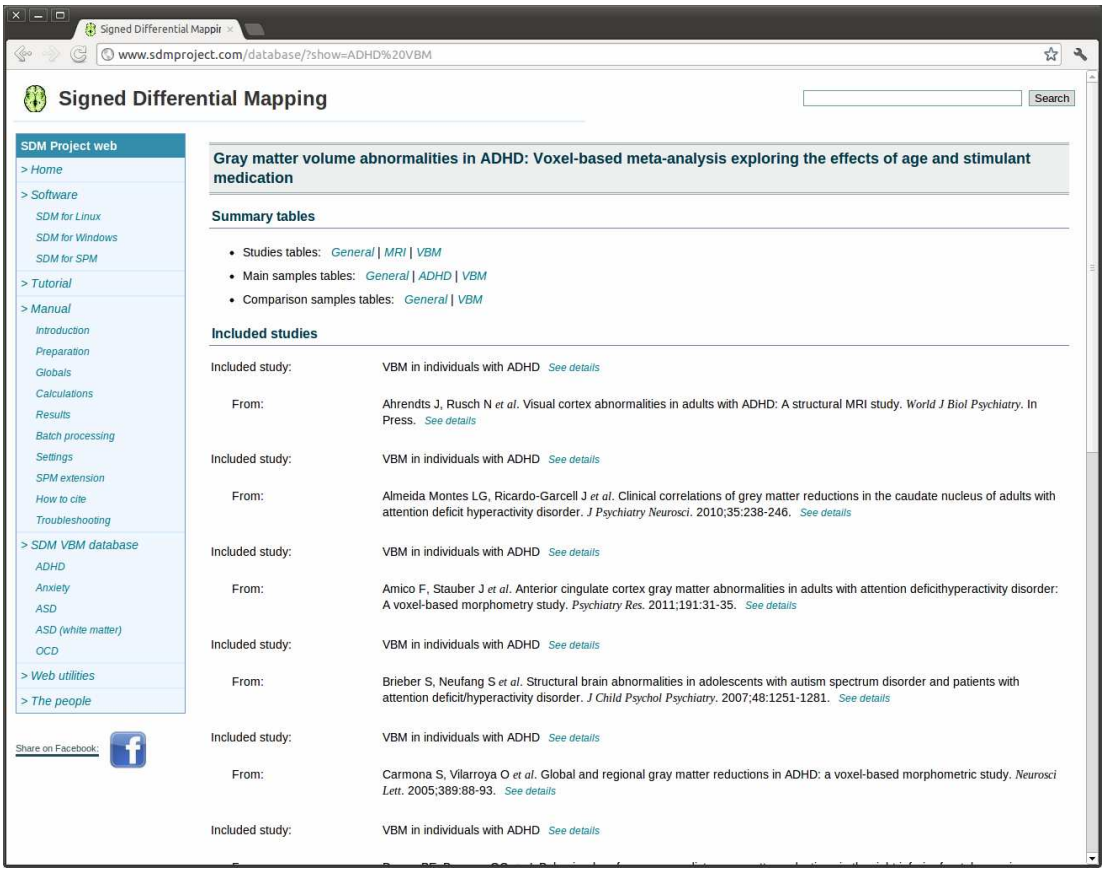
Signed Differential Mappir
www.sdmproject.com/database/?show=ADHD%20VBM
Signed Differential Mapping
Search
SDM Project web
> Home
> Software
SDM for Linux
SDM for Windows
SDM for SPM
> Tutorial
> Manual
Introduction
Preparation
Globals
Calculations
Results
Batch processing
Settings
SPM extension
How to cite
Troubleshooting
> SDM VBM database
ADHD
Anxiety
ASD
ASD (white matter)
OCD
> Web utilities
> The people
Share on Facebook:
Gray matter volume abnormalities in ADHD: Voxel-based meta-analysis exploring the effects of age and stimulant medication
Summary tables
Studies tables: General | MRI | VBM
Main samples tables: General | ADHD | VBM
Comparison samples tables: General | VBM
Included studies
Included study: VBM in individuals with ADHD See details
From: Ahrendts J, Rusch N et al. Visual cortex abnormalities in adults with ADHD: A structural MRI study. World J Biol Psychiatry. In Press. See details
Included study: VBM in individuals with ADHD See details
From: Almeida Montes LG, Ricardo-Garcell J et al. Clinical correlations of grey matter reductions in the caudate nucleus of adults with attention deficit hyperactivity disorder. J Psychiatry Neurosci. 2010;35:238-246. See details
Included study: VBM in individuals with ADHD See details
From: Amico F, Stauber J et al. Anterior cingulate cortex gray matter abnormalities in adults with attention deficithyperactivity disorder: A voxel-based morphometry study. Psychiatry Res. 2011;191:31-35. See details
Included study: VBM in individuals with ADHD See details
From: Brieber S, Neufang S et al. Structural brain abnormalities in adolescents with autism spectrum disorder and patients with attention deficit/hyperactivity disorder. J Child Psychol Psychiatry. 2007;48:1251-1281. See details
Included study: VBM in individuals with ADHD See details
From: Carmona S, Vilarroya O et al. Global and regional gray matter reductions in ADHD: a voxel-based morphometric study. Neurosci Lett. 2005;389:88-93. See details
Included study: VBM in individuals with ADHD See details

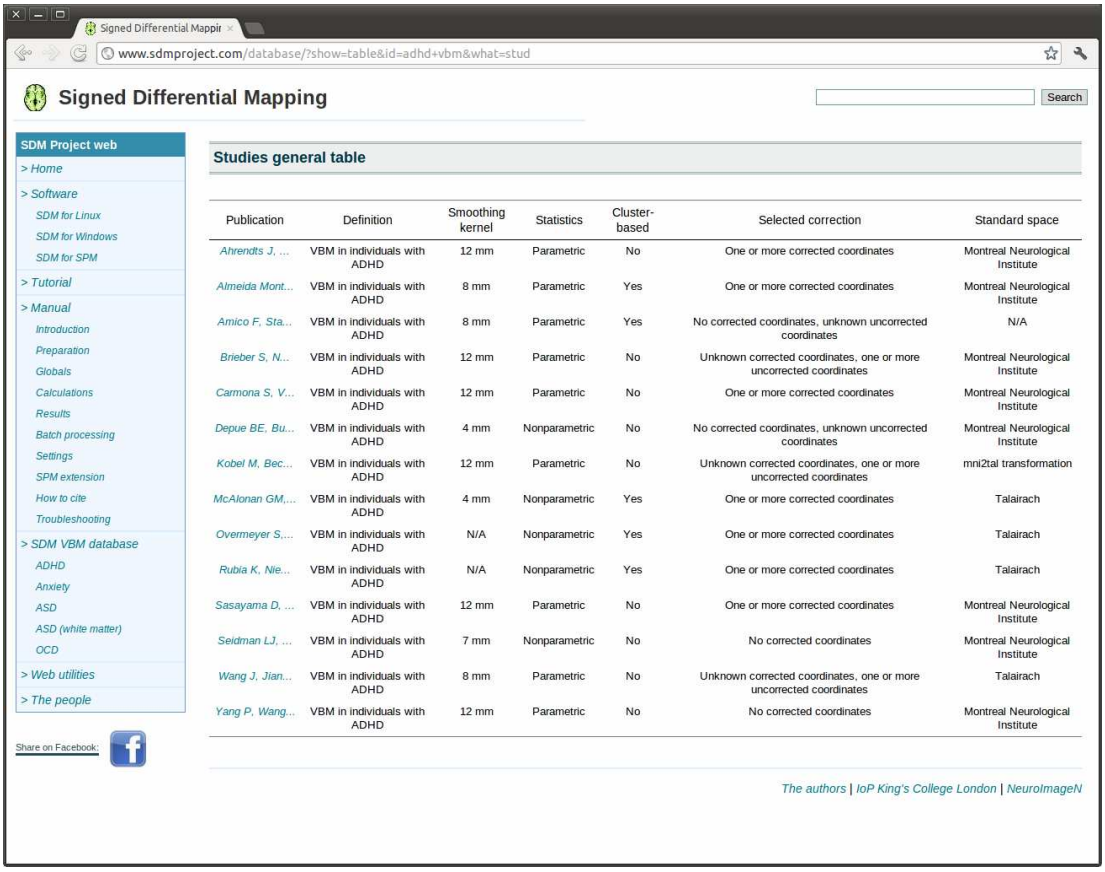
Signed Differential Mappir
www.sdmproject.com/database/?show=table&id=adhd+vbm&what=stud
Signed Differential Mapping
Search
SDM Project web
> Home
> Software
SDM for Linux
SDM for Windows
SDM for SPM
> Tutorial
> Manual
Introduction
Preparation
Globals
Calculations
Results
Batch processing
Settings
SPM extension
How to cite
Troubleshooting
> SDM VBM database
ADHD
Anxiety
ASD
ASD (white matter)
OCD
> Web utilities
> The people
Share on Facebook:
Studies general table
Publication | Definition | Smoothing kernel | Statistics | Cluster-based | Selected correction | Standard space
Ahrendts J, ... | VBM in individuals with ADHD | 12 mm | Parametric | No | One or more corrected coordinates | Montreal Neurological Institute
Almeida Mont... | VBM in individuals with ADHD | 8 mm | Parametric | Yes | One or more corrected coordinates | Montreal Neurological Institute
Amico F, Sta... | VBM in individuals with ADHD | 8 mm | Parametric | Yes | No corrected coordinates, unknown uncorrected coordinates | N/A
Brieber S, N... | VBM in individuals with ADHD | 12 mm | Parametric | No | Unknown corrected coordinates, one or more uncorrected coordinates | Montreal Neurological Institute
Carmona S, V... | VBM in individuals with ADHD | 12 mm | Parametric | No | One or more corrected coordinates | Montreal Neurological Institute
Depue BE, Bu... | VBM in individuals with ADHD | 4 mm | Nonparametric | No | No corrected coordinates, unknown uncorrected coordinates | Montreal Neurological Institute
Kobel M, Bec... | VBM in individuals with ADHD | 12 mm | Parametric | No | Unknown corrected coordinates, one or more uncorrected coordinates | mni2tal transformation
McAlonan GM,... | VBM in individuals with ADHD | 4 mm | Nonparametric | Yes | One or more corrected coordinates | Talairach
Overmeyer S,... | VBM in individuals with ADHD | N/A | Nonparametric | Yes | One or more corrected coordinates | Talairach
Rubia K, Nie... | VBM in individuals with ADHD | N/A | Nonparametric | Yes | One or more corrected coordinates | Talairach
Sasayama D, ... | VBM in individuals with ADHD | 12 mm | Parametric | No | One or more corrected coordinates | Montreal Neurological Institute
Seidman LJ, ... | VBM in individuals with ADHD | 7 mm | Nonparametric | No | No corrected coordinates | Montreal Neurological Institute
Wang J, Jian... | VBM in individuals with ADHD | 8 mm | Parametric | No | Unknown corrected coordinates, one or more uncorrected coordinates | Talairach
Yang P, Wang... | VBM in individuals with ADHD | 12 mm | Parametric | No | No corrected coordinates | Montreal Neurological Institute
The authors | IoP King's College London | NeuroImageN

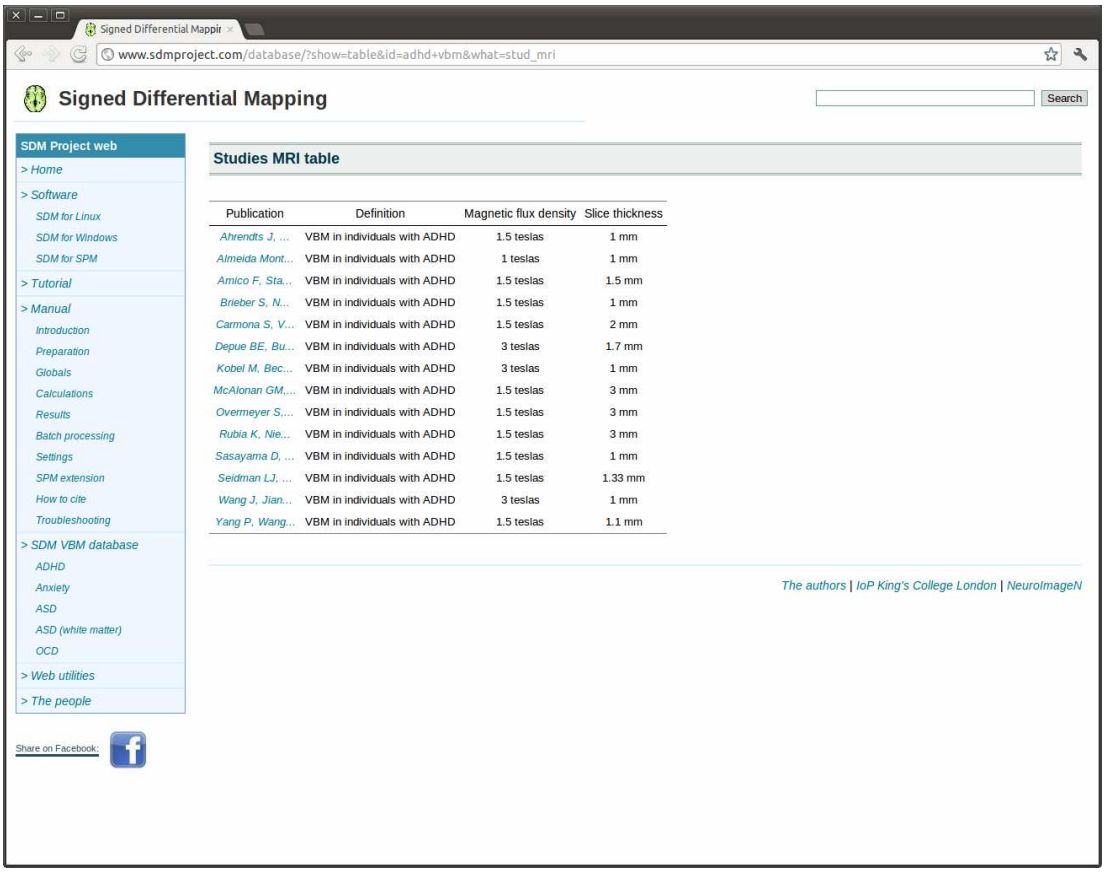
Signed Differential Mappir
www.sdmproject.com/database/?show=table&id=adhd+vbm&what=stud_mri
Signed Differential Mapping
Search
SDM Project web
> Home
> Software
SDM for Linux
SDM for Windows
SDM for SPM
> Tutorial
> Manual
Introduction
Preparation
Globals
Calculations
Results
Batch processing
Settings
SPM extension
How to cite
Troubleshooting
> SDM VBM database
ADHD
Anxiety
ASD
ASD (white matter)
OCD
> Web utilities
> The people
Share on Facebook:
Studies MRI table
Publication | Definition | Magnetic flux density | Slice thickness
Ahrendts J, ... | VBM in individuals with ADHD | 1.5 teslas | 1 mm
Almeida Mont... | VBM in individuals with ADHD | 1 teslas | 1 mm
Amico F, Sta... | VBM in individuals with ADHD | 1.5 teslas | 1.5 mm
Brieber S, N... | VBM in individuals with ADHD | 1.5 teslas | 1 mm
Carmona S, V... | VBM in individuals with ADHD | 1.5 teslas | 2 mm
Depue BE, Bu... | VBM in individuals with ADHD | 3 teslas | 1.7 mm
Kobel M, Bec... | VBM in individuals with ADHD | 3 teslas | 1 mm
McAlonan GM,... | VBM in individuals with ADHD | 1.5 teslas | 3 mm
Overmeyer S,... | VBM in individuals with ADHD | 1.5 teslas | 3 mm
Rubia K, Nie... | VBM in individuals with ADHD | 1.5 teslas | 3 mm
Sasayama D, ... | VBM in individuals with ADHD | 1.5 teslas | 1 mm
Seidman LJ, ... | VBM in individuals with ADHD | 1.5 teslas | 1.33 mm
Wang J, Jian... | VBM in individuals with ADHD | 3 teslas | 1 mm
Yang P, Wang... | VBM in individuals with ADHD | 1.5 teslas | 1.1 mm
The authors | IoP King's College London | NeuroImageN

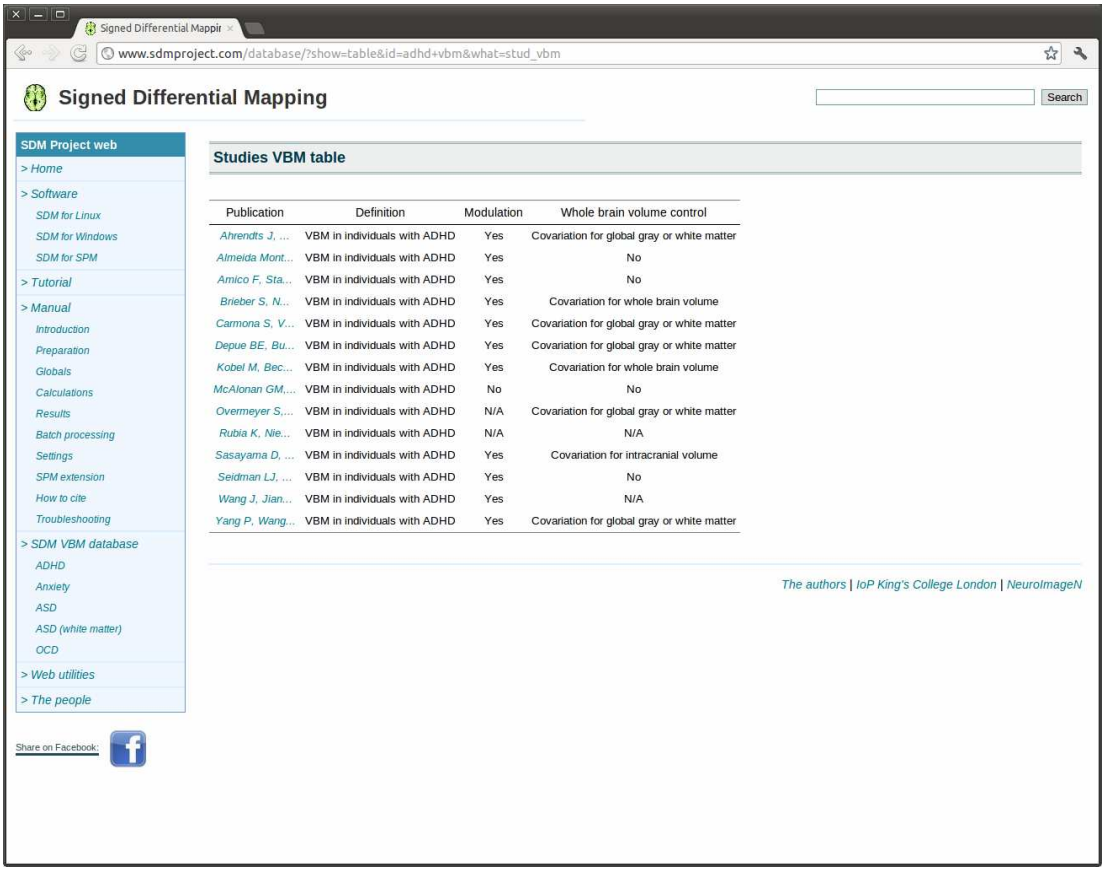
Signed Differential Mappir
www.sdmproject.com/database/?show=table&id=adhd+vbm&what=stud_vbm
Signed Differential Mapping
Search
SDM Project web
> Home
> Software
SDM for Linux
SDM for Windows
SDM for SPM
> Tutorial
> Manual
Introduction
Preparation
Globals
Calculations
Results
Batch processing
Settings
SPM extension
How to cite
Troubleshooting
> SDM VBM database
ADHD
Anxiety
ASD
ASD (white matter)
OCD
> Web utilities
> The people
Share on Facebook:
Studies VBM table
Publication | Definition | Modulation | Whole brain volume control
Ahrendts J, ... | VBM in individuals with ADHD | Yes | Covariation for global gray or white matter
Almeida Mont... | VBM in individuals with ADHD | Yes | No
Amico F, Sta... | VBM in individuals with ADHD | Yes | No
Brieber S, N... | VBM in individuals with ADHD | Yes | Covariation for whole brain volume
Carmona S, V... | VBM in individuals with ADHD | Yes | Covariation for global gray or white matter
Depue BE, Bu... | VBM in individuals with ADHD | Yes | Covariation for global gray or white matter
Kobel M, Bec... | VBM in individuals with ADHD | Yes | Covariation for whole brain volume
McAlonan GM,... | VBM in individuals with ADHD | No | No
Overmeyer S,... | VBM in individuals with ADHD | N/A | Covariation for global gray or white matter
Rubia K, Nie... | VBM in individuals with ADHD | N/A | N/A
Sasayama D, ... | VBM in individuals with ADHD | Yes | Covariation for intracranial volume
Seidman LJ, ... | VBM in individuals with ADHD | Yes | No
Wang J, Jian... | VBM in individuals with ADHD | Yes | N/A
Yang P, Wang... | VBM in individuals with ADHD | Yes | Covariation for global gray or white matter
The authors | IoP King's College London | NeuroImageN

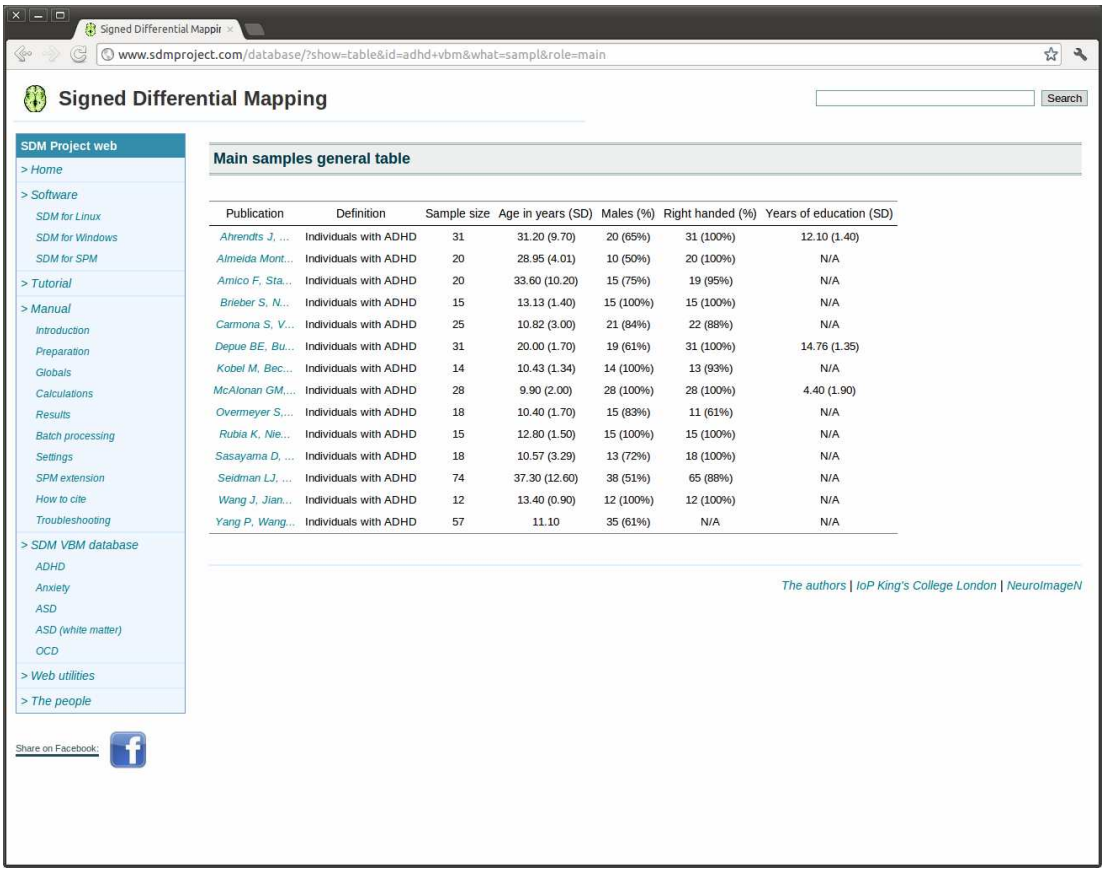

Publication	Definition	Sample size	Age in years (SD)	Males (%)	Right handed (%)	Years of education (SD)
Ahrendts J, ...	Individuals with ADHD	31	31.20 (9.70)	20 (65%)	31 (100%)	12.10 (1.40)
Almeida Mont...	Individuals with ADHD	20	28.95 (4.01)	10 (50%)	20 (100%)	N/A
Amico F, Sta...	Individuals with ADHD	20	33.60 (10.20)	15 (75%)	19 (95%)	N/A
Brieber S, N...	Individuals with ADHD	15	13.13 (1.40)	15 (100%)	15 (100%)	N/A
Carmona S, V...	Individuals with ADHD	25	10.82 (3.00)	21 (84%)	22 (88%)	N/A
Depue BE, Bu...	Individuals with ADHD	31	20.00 (1.70)	19 (61%)	31 (100%)	14.76 (1.35)
Kobel M, Bec...	Individuals with ADHD	14	10.43 (1.34)	14 (100%)	13 (93%)	N/A
McAlonan GM,...	Individuals with ADHD	28	9.90 (2.00)	28 (100%)	28 (100%)	4.40 (1.90)
Overmeyer S,...	Individuals with ADHD	18	10.40 (1.70)	15 (83%)	11 (61%)	N/A
Rubia K, Nie...	Individuals with ADHD	15	12.80 (1.50)	15 (100%)	15 (100%)	N/A
Sasayama D, ...	Individuals with ADHD	18	10.57 (3.29)	13 (72%)	18 (100%)	N/A
Seidman LJ, ...	Individuals with ADHD	74	37.30 (12.60)	38 (51%)	65 (88%)	N/A
Wang J, Jian...	Individuals with ADHD	12	13.40 (0.90)	12 (100%)	12 (100%)	N/A
Yang P, Wang...	Individuals with ADHD	57	11.10	35 (61%)	N/A	N/A

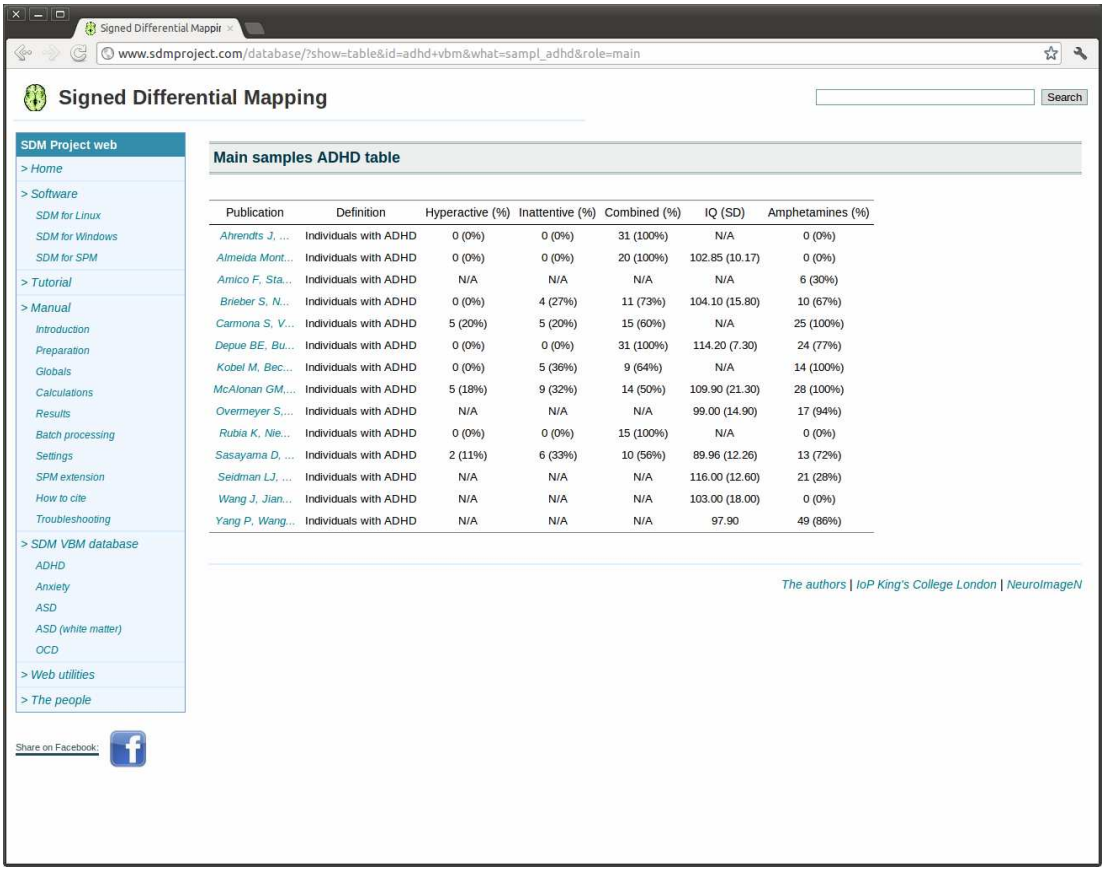

Publication	Definition	Hyperactive (%)	Inattentive (%)	Combined (%)	IQ (SD)	Amphetamines (%)
Ahrendts J, ...	Individuals with ADHD	0 (0%)	0 (0%)	31 (100%)	N/A	0 (0%)
Almeida Mont...	Individuals with ADHD	0 (0%)	0 (0%)	20 (100%)	102.85 (10.17)	0 (0%)
Amico F, Sta...	Individuals with ADHD	N/A	N/A	N/A	N/A	6 (30%)
Brieber S, N...	Individuals with ADHD	0 (0%)	4 (27%)	11 (73%)	104.10 (15.80)	10 (67%)
Carmona S, V...	Individuals with ADHD	5 (20%)	5 (20%)	15 (60%)	N/A	25 (100%)
Depue BE, Bu...	Individuals with ADHD	0 (0%)	0 (0%)	31 (100%)	114.20 (7.30)	24 (77%)
Kobel M, Bec...	Individuals with ADHD	0 (0%)	5 (36%)	9 (64%)	N/A	14 (100%)
McAlonan GM,...	Individuals with ADHD	5 (18%)	9 (32%)	14 (50%)	109.90 (21.30)	28 (100%)
Overmeyer S,...	Individuals with ADHD	N/A	N/A	N/A	99.00 (14.90)	17 (94%)
Rubia K, Nie...	Individuals with ADHD	0 (0%)	0 (0%)	15 (100%)	N/A	0 (0%)
Sasayama D, ...	Individuals with ADHD	2 (11%)	6 (33%)	10 (56%)	89.96 (12.26)	13 (72%)
Seidman LJ, ...	Individuals with ADHD	N/A	N/A	N/A	116.00 (12.60)	21 (28%)
Wang J, Jian...	Individuals with ADHD	N/A	N/A	N/A	103.00 (18.00)	0 (0%)
Yang P, Wang...	Individuals with ADHD	N/A	N/A	N/A	97.90	49 (86%)

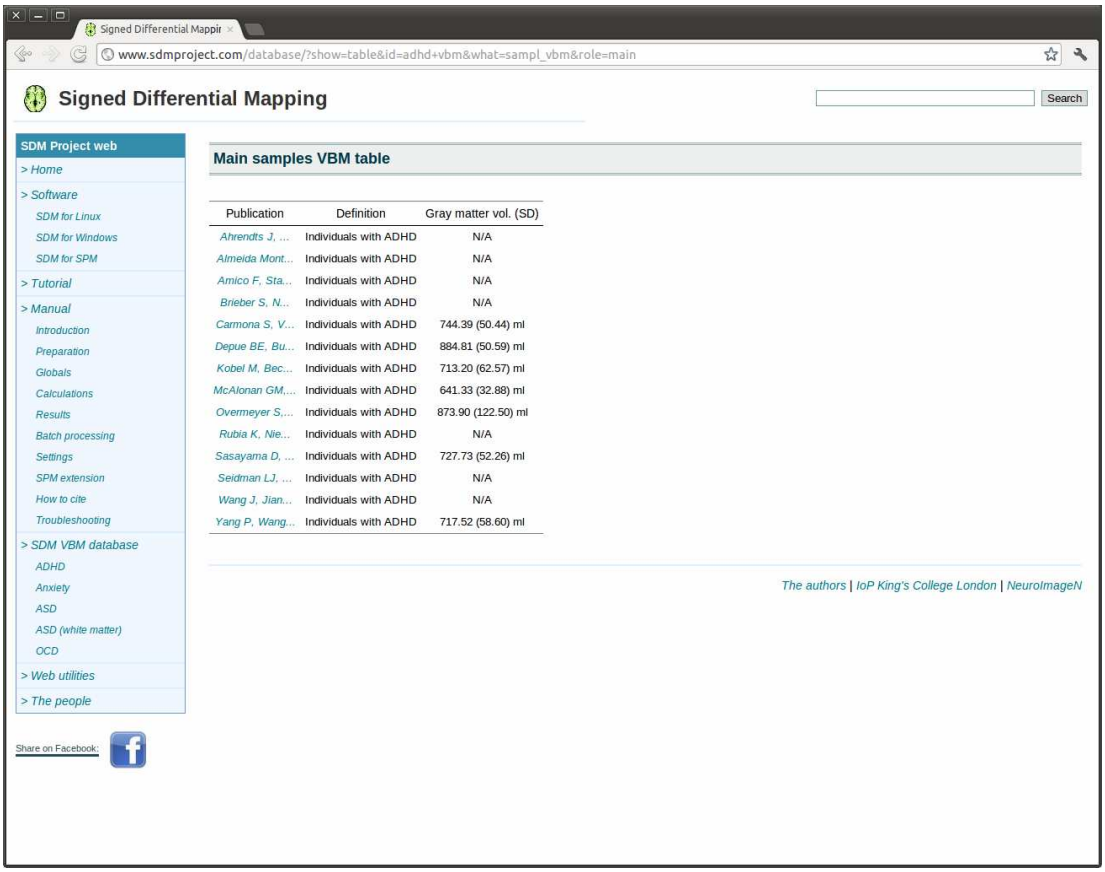
Signed Differential Mappir
www.sdmproject.com/database/?show=table&id=adhd+vbm&what=sampl_vbm&role=main
Signed Differential Mapping
Search
SDM Project web
> Home
> Software
SDM for Linux
SDM for Windows
SDM for SPM
> Tutorial
> Manual
Introduction
Preparation
Globals
Calculations
Results
Batch processing
Settings
SPM extension
How to cite
Troubleshooting
> SDM VBM database
ADHD
Anxiety
ASD
ASD (white matter)
OCD
> Web utilities
> The people
Share on Facebook:
Main samples VBM table
Publication | Definition | Gray matter vol. (SD)
Ahrendts J, ... | Individuals with ADHD | N/A
Almeida Mont... | Individuals with ADHD | N/A
Amico F, Sta... | Individuals with ADHD | N/A
Brieber S, N... | Individuals with ADHD | N/A
Carmona S, V... | Individuals with ADHD | 744.39 (50.44) ml
Depue BE, Bu... | Individuals with ADHD | 884.81 (50.59) ml
Kobel M, Bec... | Individuals with ADHD | 713.20 (62.57) ml
McAlonan GM,... | Individuals with ADHD | 641.33 (32.88) ml
Overmeyer S,... | Individuals with ADHD | 873.90 (122.50) ml
Rubia K, Nie... | Individuals with ADHD | N/A
Sasayama D, ... | Individuals with ADHD | 727.73 (52.26) ml
Seidman LJ, ... | Individuals with ADHD | N/A
Wang J, Jian... | Individuals with ADHD | N/A
Yang P, Wang... | Individuals with ADHD | 717.52 (58.60) ml
The authors | IoP King's College London | NeuroImageN

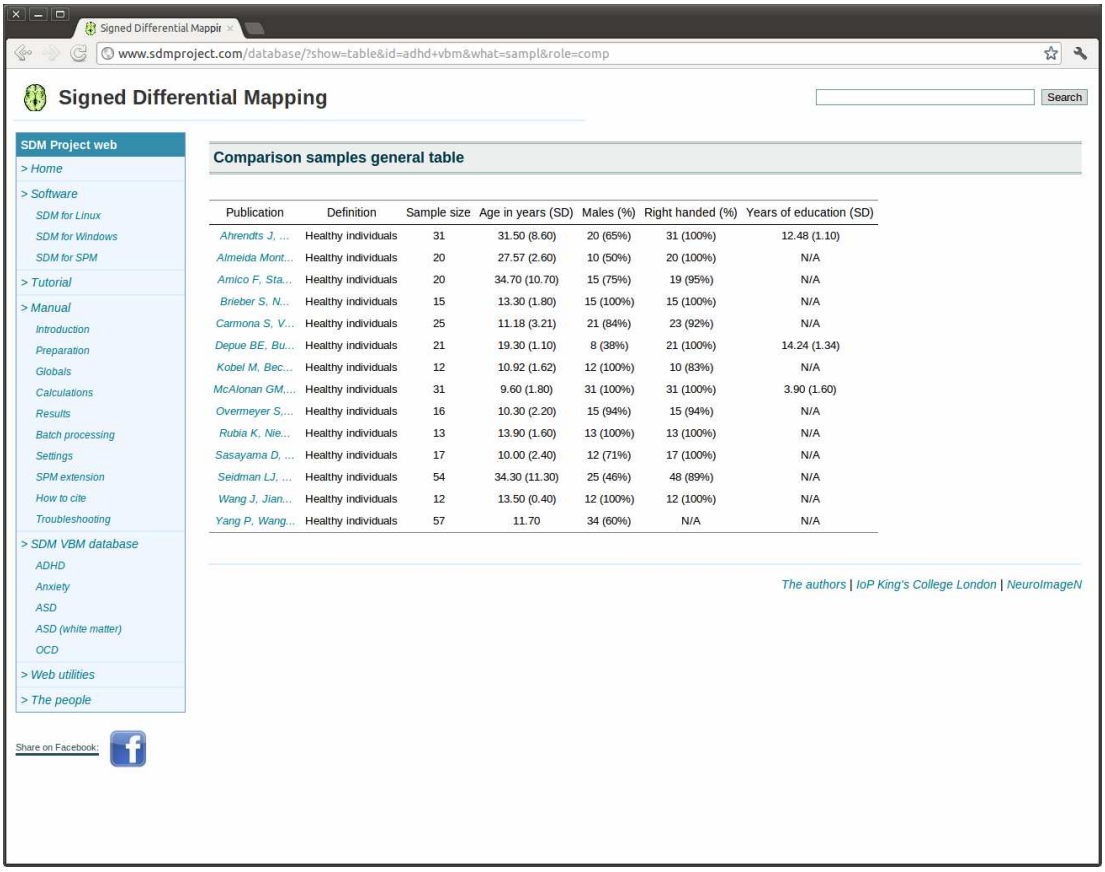
Signed Differential Mappir
www.sdmproject.com/database/?show=table&id=adhd+vbm&what=sampl&role=comp
Signed Differential Mapping
Search
SDM Project web
> Home
> Software
SDM for Linux
SDM for Windows
SDM for SPM
> Tutorial
> Manual
Introduction
Preparation
Globals
Calculations
Results
Batch processing
Settings
SPM extension
How to cite
Troubleshooting
> SDM VBM database
ADHD
Anxiety
ASD
ASD (white matter)
OCD
> Web utilities
> The people
Share on Facebook:
Comparison samples general table
Publication | Definition | Sample size | Age in years (SD) | Males (%) | Right handed (%) | Years of education (SD)
Ahrendts J, ... | Healthy individuals | 31 | 31.50 (8.60) | 20 (65%) | 31 (100%) | 12.48 (1.10)
Almeida Mont... | Healthy individuals | 20 | 27.57 (2.60) | 10 (50%) | 20 (100%) | N/A
Amico F, Sta... | Healthy individuals | 20 | 34.70 (10.70) | 15 (75%) | 19 (95%) | N/A
Brieber S, N... | Healthy individuals | 15 | 13.30 (1.80) | 15 (100%) | 15 (100%) | N/A
Carmona S, V... | Healthy individuals | 25 | 11.18 (3.21) | 21 (84%) | 23 (92%) | N/A
Depue BE, Bu... | Healthy individuals | 21 | 19.30 (1.10) | 8 (38%) | 21 (100%) | 14.24 (1.34)
Kobel M, Bec... | Healthy individuals | 12 | 10.92 (1.62) | 12 (100%) | 10 (83%) | N/A
McAlonan GM,... | Healthy individuals | 31 | 9.60 (1.80) | 31 (100%) | 31 (100%) | 3.90 (1.60)
Overmeyer S,... | Healthy individuals | 16 | 10.30 (2.20) | 15 (94%) | 15 (94%) | N/A
Rubia K, Nie... | Healthy individuals | 13 | 13.90 (1.60) | 13 (100%) | 13 (100%) | N/A
Sasayama D, ... | Healthy individuals | 17 | 10.00 (2.40) | 12 (71%) | 17 (100%) | N/A
Seidman LJ, ... | Healthy individuals | 54 | 34.30 (11.30) | 25 (46%) | 48 (89%) | N/A
Wang J, Jian... | Healthy individuals | 12 | 13.50 (0.40) | 12 (100%) | 12 (100%) | N/A
Yang P, Wang... | Healthy individuals | 57 | 11.70 | 34 (60%) | N/A | N/A
The authors | IoP King's College London | NeuroImageN

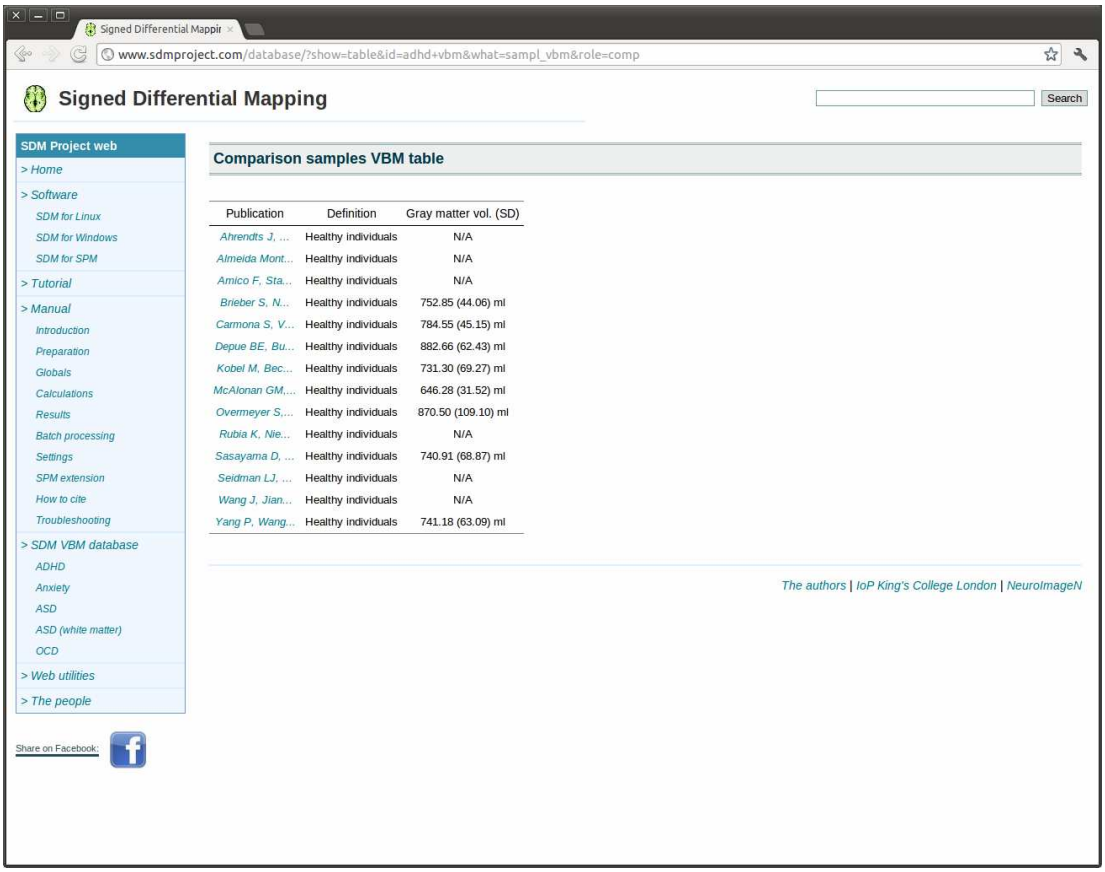
Signed Differential Mappir
www.sdmproject.com/database/?show=table&id=adhd+vbm&what=sampl_vbm&role=comp
Signed Differential Mapping
Search
SDM Project web
> Home
> Software
SDM for Linux
SDM for Windows
SDM for SPM
> Tutorial
> Manual
Introduction
Preparation
Globals
Calculations
Results
Batch processing
Settings
SPM extension
How to cite
Troubleshooting
> SDM VBM database
ADHD
Anxiety
ASD
ASD (white matter)
OCD
> Web utilities
> The people
Share on Facebook:
Comparison samples VBM table
Publication | Definition | Gray matter vol. (SD)
Ahrendts J, ... | Healthy individuals | N/A
Almeida Mont... | Healthy individuals | N/A
Amico F, Sta... | Healthy individuals | N/A
Brieber S, N... | Healthy individuals | 752.85 (44.06) ml
Carmona S, V... | Healthy individuals | 784.55 (45.15) ml
Depue BE, Bu... | Healthy individuals | 882.66 (62.43) ml
Kobel M, Bec... | Healthy individuals | 731.30 (69.27) ml
McAlonan GM,... | Healthy individuals | 646.28 (31.52) ml
Overmeyer S,... | Healthy individuals | 870.50 (109.10) ml
Rubia K, Nie... | Healthy individuals | N/A
Sasayama D, ... | Healthy individuals | 740.91 (68.87) ml
Seidman LJ, ... | Healthy individuals | N/A
Wang J, Jian... | Healthy individuals | N/A
Yang P, Wang... | Healthy individuals | 741.18 (63.09) ml
The authors | IoP King's College London | NeuroImageN

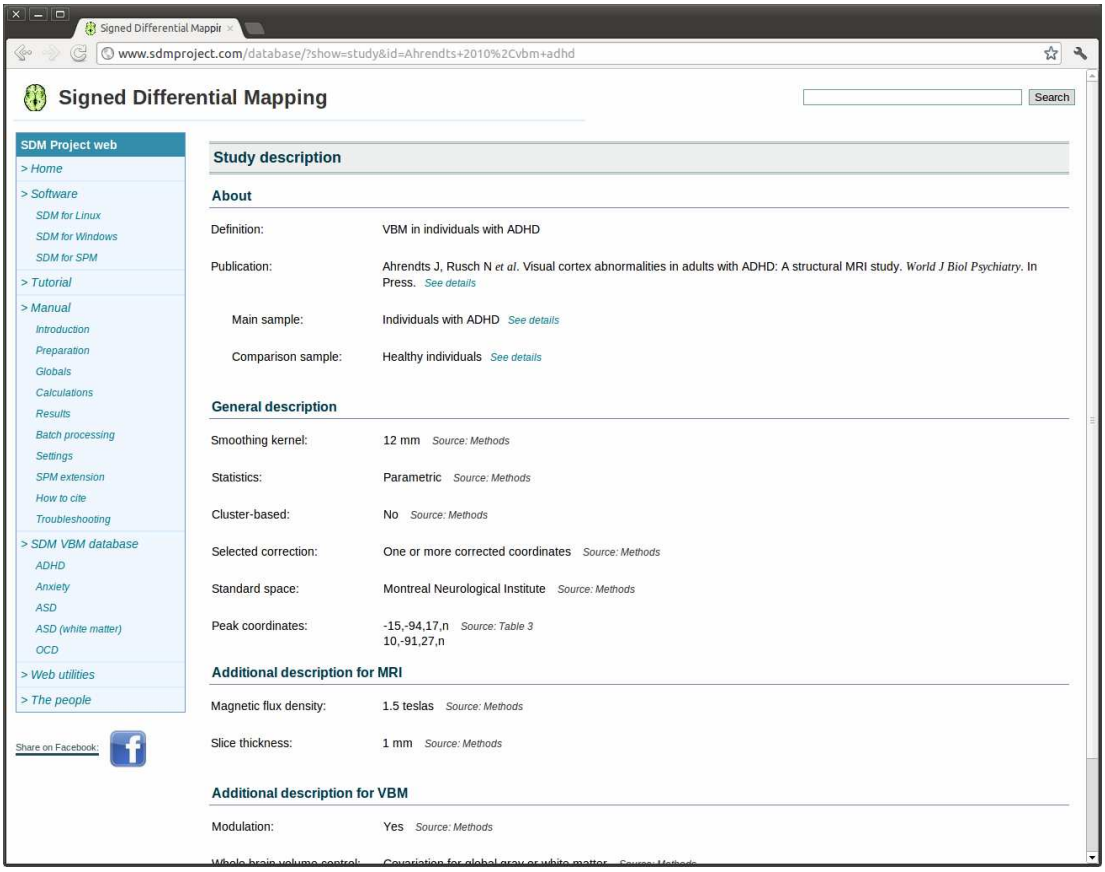
Signed Differential Mappir
www.sdmproject.com/database/?show=study&id=Ahrendts+2010%2Cvbm+adhd
Signed Differential Mapping
Search
SDM Project web
> Home
> Software
SDM for Linux
SDM for Windows
SDM for SPM
> Tutorial
> Manual
Introduction
Preparation
Globals
Calculations
Results
Batch processing
Settings
SPM extension
How to cite
Troubleshooting
> SDM VBM database
ADHD
Anxiety
ASD
ASD (white matter)
OCD
> Web utilities
> The people
Share on Facebook:
Study description
About
Definition: VBM in individuals with ADHD
Publication: Ahrendts J, Rusch N et al. Visual cortex abnormalities in adults with ADHD: A structural MRI study. World J Biol Psychiatry. In Press. See details
Main sample: Individuals with ADHD See details
Comparison sample: Healthy individuals See details
General description
Smoothing kernel: 12 mm Source: Methods
Statistics: Parametric Source: Methods
Cluster-based: No Source: Methods
Selected correction: One or more corrected coordinates Source: Methods
Standard space: Montreal Neurological Institute Source: Methods
Peak coordinates: -15,-94,17,n Source: Table 3
10,-91,27,n
Additional description for MRI
Magnetic flux density: 1.5 teslas Source: Methods
Slice thickness: 1 mm Source: Methods
Additional description for VBM
Modulation: Yes Source: Methods

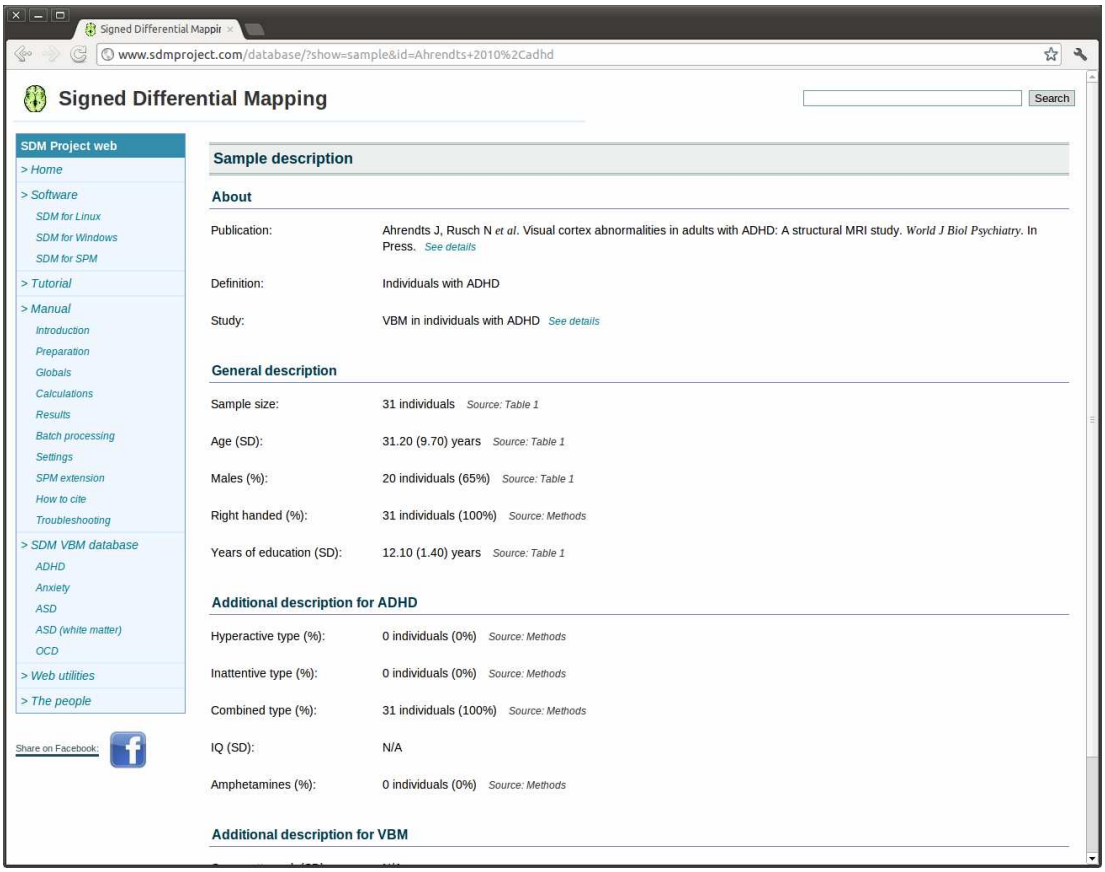
Signed Differential Mappir
www.sdmproject.com/database/?show=sample&id=Ahrendts+2010%2Cadhd
Signed Differential Mapping
Search
SDM Project web
> Home
> Software
SDM for Linux
SDM for Windows
SDM for SPM
> Tutorial
> Manual
Introduction
Preparation
Globals
Calculations
Results
Batch processing
Settings
SPM extension
How to cite
Troubleshooting
> SDM VBM database
ADHD
Anxiety
ASD
ASD (white matter)
OCD
> Web utilities
> The people
Share on Facebook:
Sample description
About
Publication: Ahrendts J, Rusch N et al. Visual cortex abnormalities in adults with ADHD: A structural MRI study. World J Biol Psychiatry. In Press. See details
Definition: Individuals with ADHD
Study: VBM in individuals with ADHD See details
General description
Sample size: 31 individuals Source: Table 1
Age (SD): 31.20 (9.70) years Source: Table 1
Males (%): 20 individuals (65%) Source: Table 1
Right handed (%): 31 individuals (100%) Source: Methods
Years of education (SD): 12.10 (1.40) years Source: Table 1
Additional description for ADHD
Hyperactive type (%): 0 individuals (0%) Source: Methods
Inattentive type (%): 0 individuals (0%) Source: Methods
Combined type (%): 31 individuals (100%) Source: Methods
IQ (SD): N/A
Amphetamines (%): 0 individuals (0%) Source: Methods
Additional description for VBM

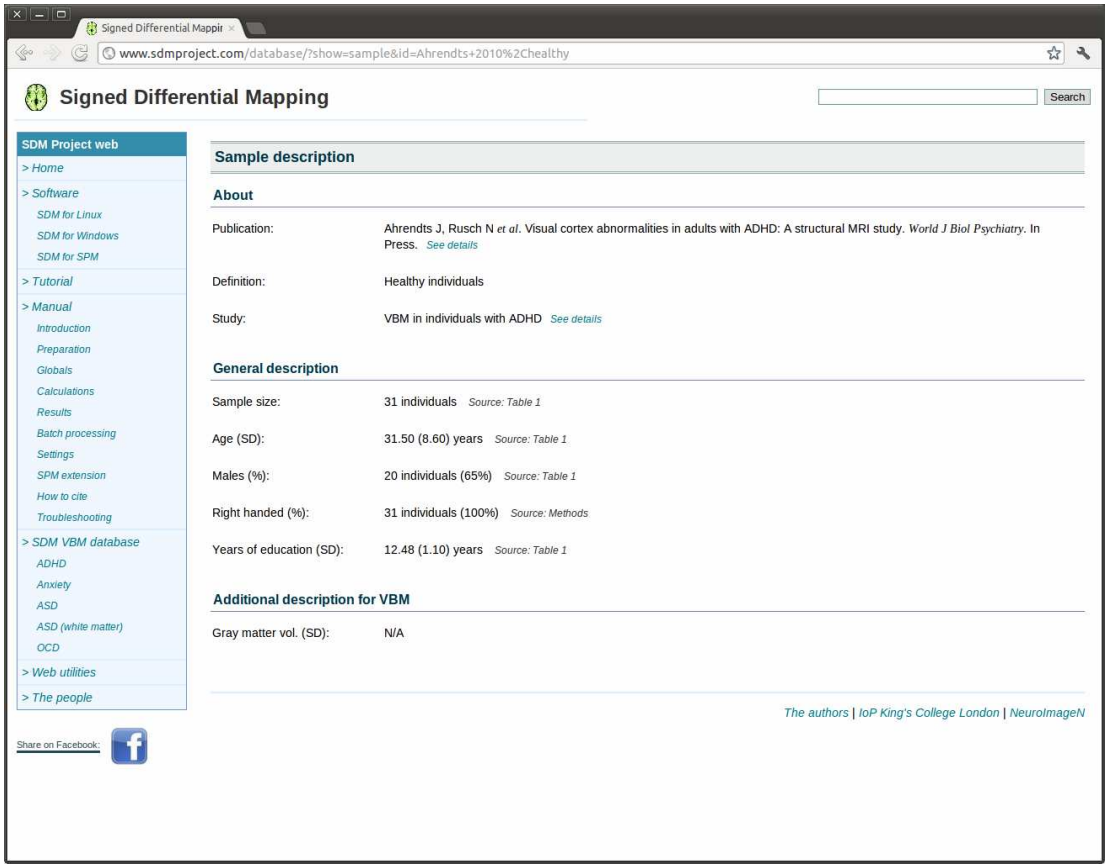
Signed Differential Mappir
www.sdmproject.com/database/?show=sample&id=Ahrendts+2010%2Chealthy
Signed Differential Mapping
Search
SDM Project web
> Home
> Software
SDM for Linux
SDM for Windows
SDM for SPM
> Tutorial
> Manual
Introduction
Preparation
Globals
Calculations
Results
Batch processing
Settings
SPM extension
How to cite
Troubleshooting
> SDM VBM database
ADHD
Anxiety
ASD
ASD (white matter)
OCD
> Web utilities
> The people
Share on Facebook:
Sample description
About
Publication: Ahrendts J, Rusch N et al. Visual cortex abnormalities in adults with ADHD: A structural MRI study. World J Biol Psychiatry. In Press. See details
Definition: Healthy individuals
Study: VBM in individuals with ADHD See details
General description
Sample size: 31 individuals Source: Table 1
Age (SD): 31.50 (8.60) years Source: Table 1
Males (%): 20 individuals (65%) Source: Table 1
Right handed (%): 31 individuals (100%) Source: Methods
Years of education (SD): 12.48 (1.10) years Source: Table 1
Additional description for VBM
Gray matter vol. (SD): N/A
The authors | IoP King's College London | NeuroImageN

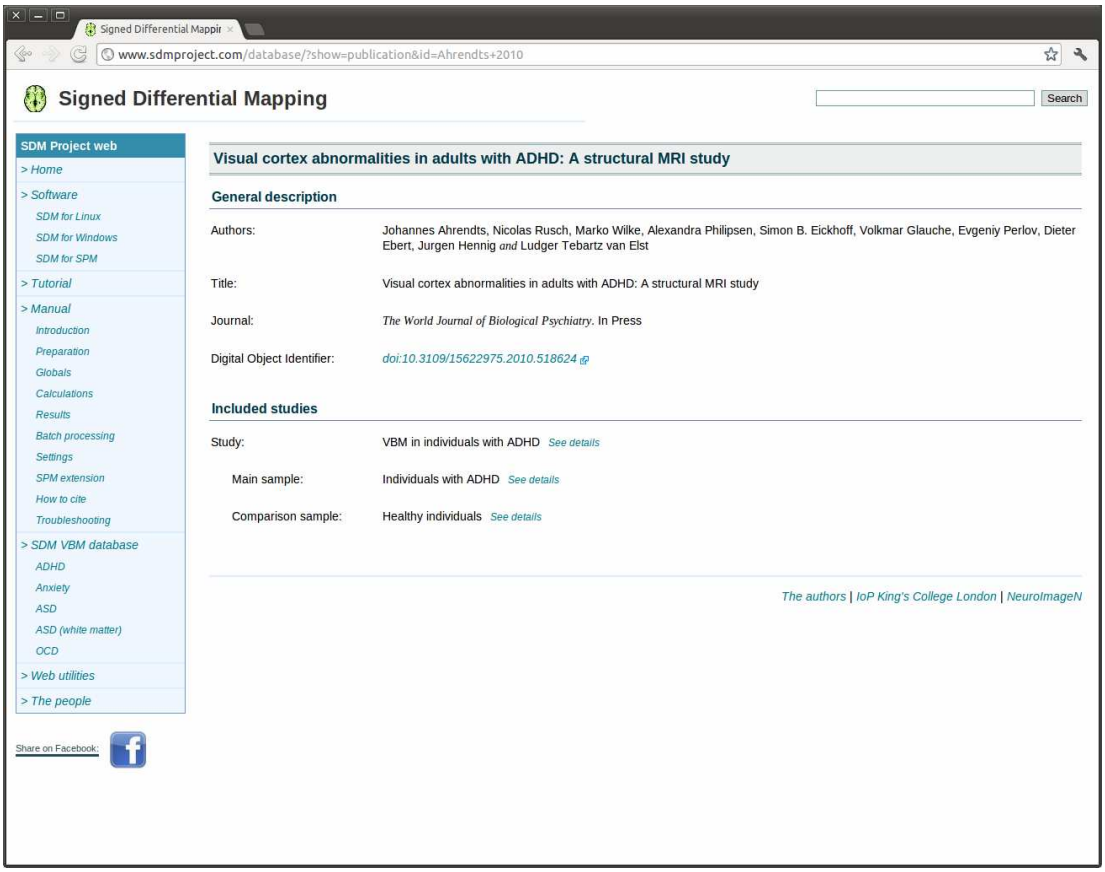
Signed Differential Mappir
www.sdmproject.com/database/?show=publication&id=Ahrendts+2010
Signed Differential Mapping
Search
SDM Project web
> Home
> Software
SDM for Linux
SDM for Windows
SDM for SPM
> Tutorial
> Manual
Introduction
Preparation
Globals
Calculations
Results
Batch processing
Settings
SPM extension
How to cite
Troubleshooting
> SDM VBM database
ADHD
Anxiety
ASD
ASD (white matter)
OCD
> Web utilities
> The people
Share on Facebook:
Visual cortex abnormalities in adults with ADHD: A structural MRI study
General description
Authors:
Johannes Ahrendts, Nicolas Rusch, Marko Wilke, Alexandra Philipsen, Simon B. Eickhoff, Volkmar Glauche, Evgeniy Perlov, Dieter Ebert, Jurgen Hennig and Ludger Tebartz van Elst
Title:
Visual cortex abnormalities in adults with ADHD: A structural MRI study
Journal:
The World Journal of Biological Psychiatry. In Press
Digital Object Identifier:
doi:10.3109/15622975.2010.518624
Included studies
Study:
VBM in individuals with ADHD See details
Main sample:
Individuals with ADHD See details
Comparison sample:
Healthy individuals See details
The authors | IoP King's College London | NeuroImageN

A2.5 Screenshots of other sections

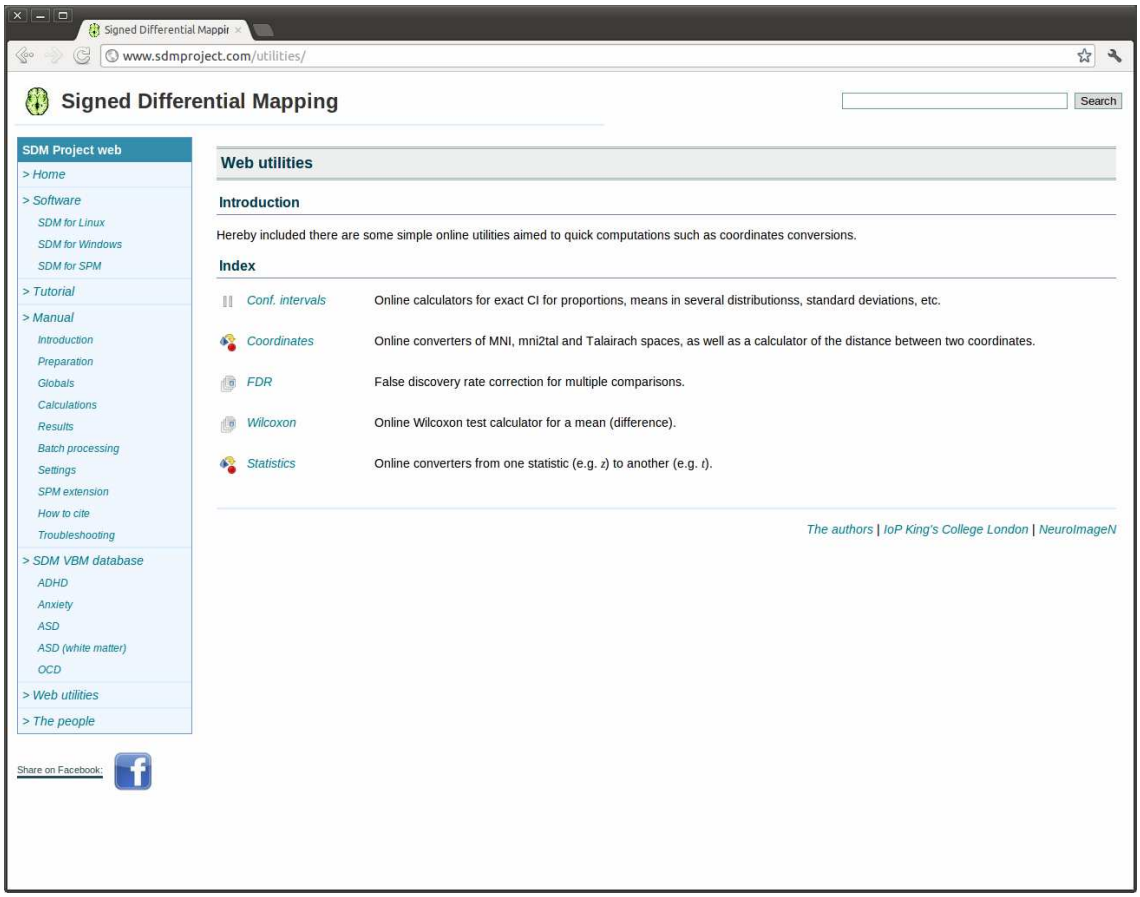

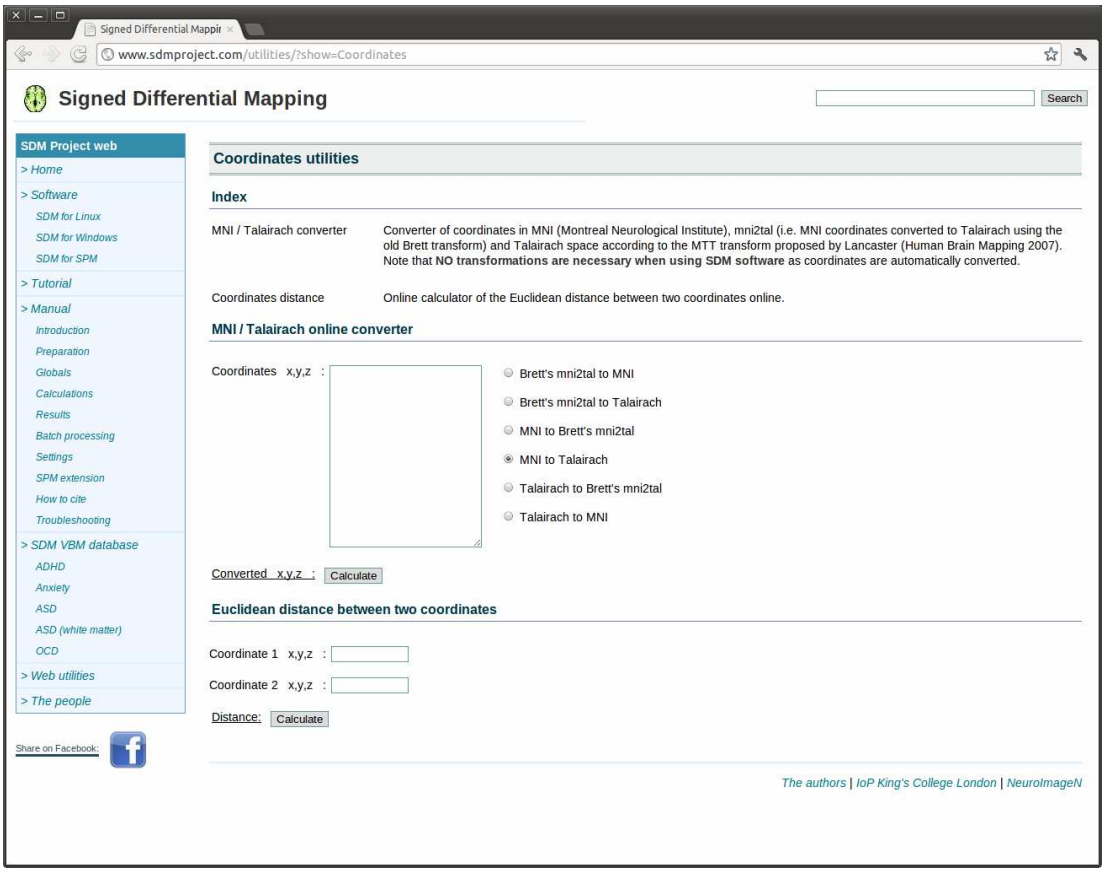
Signed Differential Mappir
www.sdmproject.com/utilities/?show=Coordinates
Signed Differential Mapping
Search
SDM Project web
> Home
> Software
SDM for Linux
SDM for Windows
SDM for SPM
> Tutorial
> Manual
Introduction
Preparation
Globals
Calculations
Results
Batch processing
Settings
SPM extension
How to cite
Troubleshooting
> SDM VBM database
ADHD
Anxiety
ASD
ASD (white matter)
OCD
> Web utilities
> The people
Share on Facebook:
Coordinates utilities
Index
MNI / Talairach converter
Converter of coordinates in MNI (Montreal Neurological Institute), mni2tal (i.e. MNI coordinates converted to Talairach using the old Brett transform) and Talairach space according to the MTT transform proposed by Lancaster (Human Brain Mapping 2007). Note that NO transformations are necessary when using SDM software as coordinates are automatically converted.
Coordinates distance
Online calculator of the Euclidean distance between two coordinates online.
MNI / Talairach online converter
Coordinates x,y,z :
Brett's mni2tal to MNI
Brett's mni2tal to Talairach
MNI to Brett's mni2tal
MNI to Talairach
Talairach to Brett's mni2tal
Talairach to MNI
Converted x,y,z :
Calculate
Euclidean distance between two coordinates
Coordinate 1 x,y,z :
Coordinate 2 x,y,z :
Distance:
Calculate
The authors | IoP King's College London | NeuroImageN

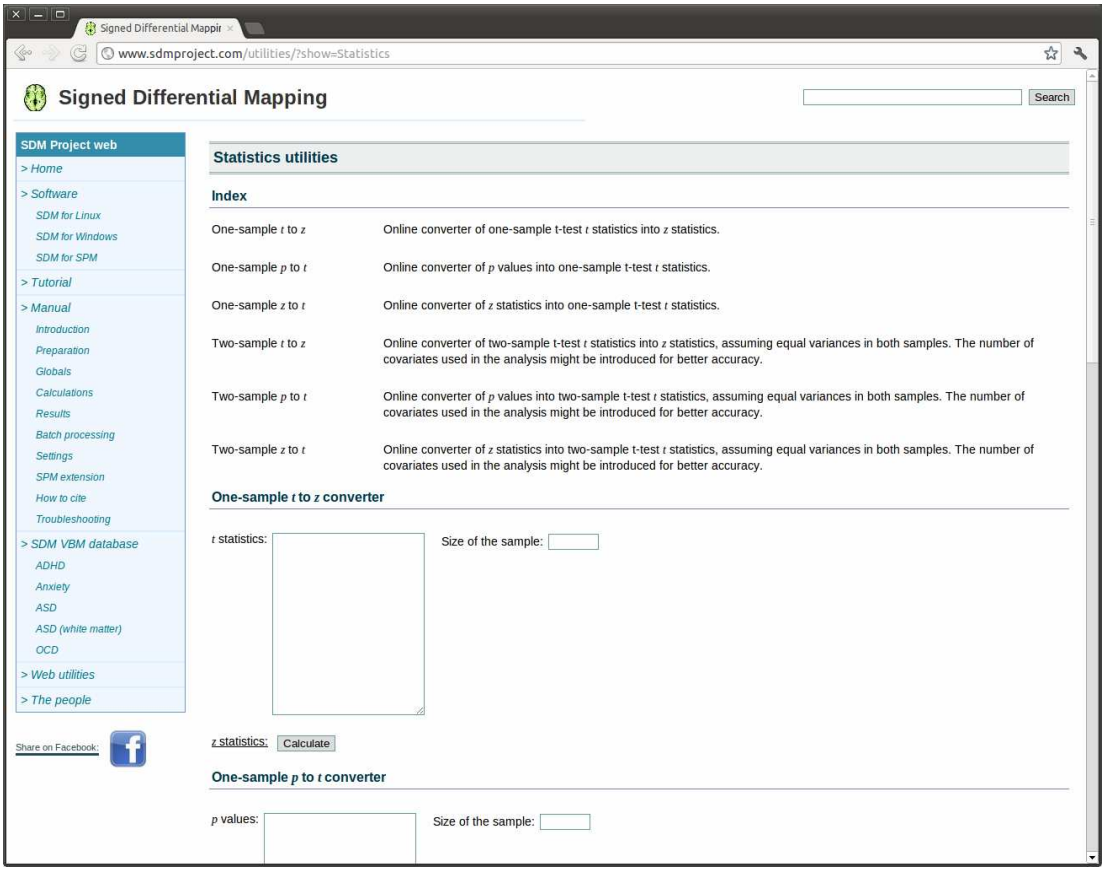
Signed Differential Mappir
www.sdmproject.com/utilities/?show=Statistics
Signed Differential Mapping
Search
SDM Project web
> Home
> Software
SDM for Linux
SDM for Windows
SDM for SPM
> Tutorial
> Manual
Introduction
Preparation
Globals
Calculations
Results
Batch processing
Settings
SPM extension
How to cite
Troubleshooting
> SDM VBM database
ADHD
Anxiety
ASD
ASD (white matter)
OCD
> Web utilities
> The people
Share on Facebook:
Statistics utilities
Index
One-sample t to z
Online converter of one-sample t-test t statistics into z statistics.
One-sample p to t
Online converter of p values into one-sample t-test t statistics.
One-sample z to t
Online converter of z statistics into one-sample t-test t statistics.
Two-sample t to z
Online converter of two-sample t-test t statistics into z statistics, assuming equal variances in both samples. The number of covariates used in the analysis might be introduced for better accuracy.
Two-sample p to t
Online converter of p values into two-sample t-test t statistics, assuming equal variances in both samples. The number of covariates used in the analysis might be introduced for better accuracy.
Two-sample z to t
Online converter of z statistics into two-sample t-test t statistics, assuming equal variances in both samples. The number of covariates used in the analysis might be introduced for better accuracy.
One-sample t to z converter
t statistics:
Size of the sample:
z statistics:
Calculate
One-sample p to t converter
p values:
Size of the sample:

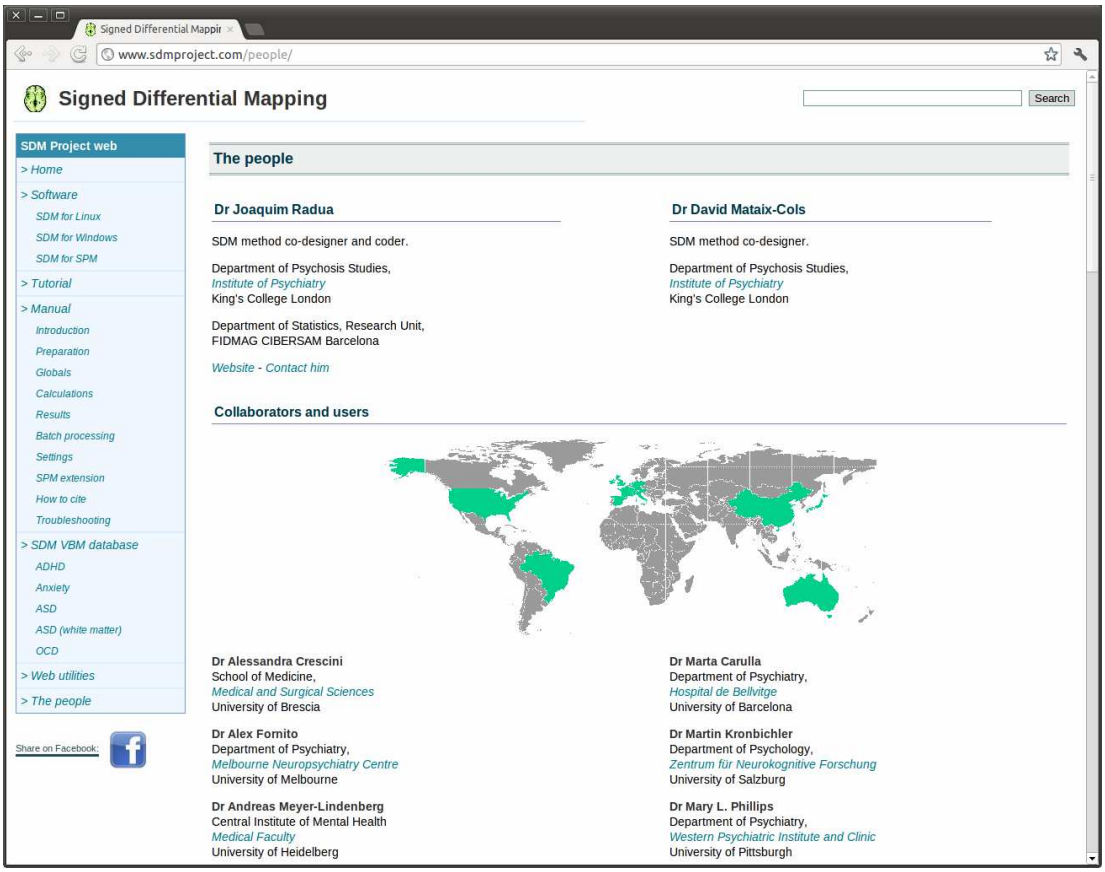
Signed Differential Mappir
www.sdmproject.com/people/
Signed Differential Mapping
Search
SDM Project web
> Home
> Software
SDM for Linux
SDM for Windows
SDM for SPM
> Tutorial
> Manual
Introduction
Preparation
Globals
Calculations
Results
Batch processing
Settings
SPM extension
How to cite
Troubleshooting
> SDM VBM database
ADHD
Anxiety
ASD
ASD (white matter)
OCD
> Web utilities
> The people
Share on Facebook:
The people
Dr Joaquim Radua
SDM method co-designer and coder.
Department of Psychosis Studies,
Institute of Psychiatry
King's College London
Department of Statistics, Research Unit,
FIDMAG CIBERSAM Barcelona
Website - Contact him
Dr David Mataix-Cols
SDM method co-designer.
Department of Psychosis Studies,
Institute of Psychiatry
King's College London
Collaborators and users
Dr Alessandra Crescini
School of Medicine,
Medical and Surgical Sciences
University of Brescia
Dr Alex Fornito
Department of Psychiatry,
Melbourne Neuropsychiatry Centre
University of Melbourne
Dr Andreas Meyer-Lindenberg
Central Institute of Mental Health
Medical Faculty
University of Heidelberg
Dr Marta Carulla
Department of Psychiatry,
Hospital de Bellvitge
University of Barcelona
Dr Martin Kronbichler
Department of Psychology,
Zentrum für Neurokognitive Forschung
University of Salzburg
Dr Mary L. Phillips
Department of Psychiatry,
Western Psychiatric Institute and Clinic
University of Pittsburgh